



Addressing the Challenges of Crude Oil Processing Utilising Chemometric Approaches

By
Frederick J. Stubbins

*A thesis submitted for the degree of
Doctor of Engineering at Newcastle University*

Biopharmaceutical Bioprocessing Technology Centre
School of Chemical Engineering and Advanced Materials

November, 2017

Abstract

Throughout the hydrocarbon supply chain, process optimisation is driven by the desire to maximise profit margins. In the global refining marketplace, the biggest cost is crude oil and to improve margins increasing use of non-conventional crude oils (also called opportunity crudes) lowers the cost of the crude blend. Opportunity crudes are selected based on market forces, for example in North America, the production booms in shale oil and tar sands have provided ample amounts of new low-cost oils which refineries are buying and processing.

However, as these oils are new to the marketplace many refineries have never processed them before which brings about challenges. These are mainly a lack of understanding of the quality of the crude oil being processed (shale oils for example can come from many thousands of wells) and how these oils interact with the more conventional refinery feedstocks (such as Brent or West Texas Intermediate).

The Eng.D project was carried out in collaboration with Intertek Group plc, a multinational corporate organisation consisting of more than 42,000 employees in over 1,000 locations in over 100 countries across the globe, and was aimed at developing solutions to address crude oil processing problems. The issues covered over the course of the project fall into the areas of: enhancing understanding of crude oil quality, addressing issues of hydrocarbon blend stability because of blending and better utilisation of process data to promote efficiency and facilitate process troubleshooting.

As such, the Eng.D project was firstly concerned with developing a robust chemometric model, based on Near Infrared spectra, for use in a major Asian refinery. Once built and tuned this model was ultimately used to predict physical properties (such as density, sulphur content and distillation properties) of every crude oil delivery and also online in the refinery for frequent prediction of crude oil blend properties.

The second project was then aimed at solving refinery issues of the deposition of undesirable material (such as wax and asphaltenes) in pipes and process units. The research carried out during the course of the Eng.D project resulted in a patented approach to characterise these issues and provide refineries strategies to mitigate the problems. This approach is not just limited to crude oils but can be applied to any blended hydrocarbon streams and detects the precipitation of undesirable material using Near Infrared spectroscopy and microscopy. This

approach has now been applied to solving problems of blending crude oils in refineries and offshore, heavy fuel oils, shale oils and marine fuels.

Finally, the application of smart data analytics in an upstream installation was investigated. The objective of this application was to provide a customer with process troubleshooting for a historical recurring pump failure issue. To achieve this, the root cause of the issue first needed to be identified and then a solution developed.

Publications

Patents

- I. Frederick Stubbins, John Wade, Paul Winstone

Method and System for Analysing a Blend of Two or More Hydrocarbon Feed Streams

GB Patent 2931790

WO2015087049 A1

Conference Papers

- I. Frederick Stubbins, Colin Stewart

Optimising Refinery Crude Blends to Minimise Organic Deposition

Presented at the Haverly MUGI Conference, Edinburgh, April 2014

- II. Frederick Stubbins, Colin Stewart

Quality Tracking, Property Predictions and the Intertek Organic Deposition Programme

Presented at the 4th Opportunity Crudes Conference, Houston, September 2014

- III. Frederick Stubbins

Toolbox to Deal with Changing Crudes

Presented at the 5th Opportunity Crudes Conference, Houston, October 2016

- IV. Frederick Stubbins

The Hydrocarbon Supply Chain – Assuring Quality

Presented at the Crude Oil Quality Association, Houston, October 2016

Article

I. Frederick Stubbins

Optimising the Value of Big Data

Oil Review Middle East, Volume 19, Issue 5, 2016

II. Frederick Stubbins

*Near Infrared Spectra Prediction of Hydrocarbon Streams to
Benefit Refiners*

Oil Review Middle East, Volume 19, Issue 7, 2016

Acknowledgements

I would like to express my sincerest gratitude to the following people all of which have contributed to my thesis and engaged with me during my Eng.D programme.

I would like to say a very large thank you to my academic supervisor's Dr Chris J. O'Malley and Prof. Elaine B. Martin for supporting throughout the course of the programme.

My heartfelt gratitude also goes out to my industrial supervisors John Wade and Paul Winstone. John passed away before the thesis was completed but his lessons in life and business will never leave me.

I would also like to thank my current manager at Intertek Colin Stewart who challenges me on a daily basis and I trust will continue to do so for the foreseeable future!

I would like to express my gratitude to the team at Intertek who I work closely with on a daily basis, Harvey Henderson, Daniel Thom, Iain Fairclough and Megan Finlay.

Financial support from both the EPSRC (Grant Number EP/GO 37620/1) and Intertek Group plc. is sincerely appreciated.

To my friends and family, my parents John and Christine thank you for all your support throughout my 28 years on this planet. To my mates Matthew and Andy, thanks for all your help and advice – whether it was wanted or not!

Finally, to my partner Laurie, you have always stood by me when I needed you (which is always) and I look forward to many more happy years together.

Contents

Chapter 1. Introduction.....	2
1.1 Intertek.....	2
1.2 PT5Technology	3
1.3 Objectives	4
1.4 Contributions	4
1.5 Thesis Overview	4
Chapter 2. Literature Review.....	7
2.1 Formation	7
2.2 Composition	8
2.3 Exploration and Production	10
2.3.1 Enhanced Oil Recovery (EOR)	12
2.4 Refining	13
2.5 Primary Reference Data.....	16
2.5.1 ASTM D2892/D5236 – Distillation Curve	16
2.5.2 ASTM D5002 - Density	17
2.5.3 ASTM D4294 - Sulphur	18
2.6 Spectroscopy.....	19
2.7 Near Infrared	20
2.8 Applications of Infrared Spectroscopy in the Hydrocarbon Processing Industry	21
2.9 Gas Chromatography	25
2.9.1 Nuclear Magnetic Resonance	27
2.10 Organic Deposition.....	28
2.11 Background to the problem	28
2.12 Refining Economics	29
2.12.1 Net Cash Margin.....	29
2.12.2 Margin Improvement Strategy?.....	31
2.13 Asphaltenes.....	31
2.14 Oil compatibility model and SARA relationship	33
2.15 Investigating asphaltene precipitation and behaviour	34
2.16 Techniques for Dealing with Aggregation	41
2.17 Oil in Water Emulsions	42
2.18 Modelling	43
2.18.1 Pre-processing	43

2.18.2 Principal Component Analysis	44
2.18.3 Partial Least Squares	50
2.18.4 Nearest Neighbour.....	51
Chapter 3. Refinery Crude Oil Quality Monitoring	54
3.1 Introduction	55
3.2 Methodology.....	55
3.2.1 NIR Spectra in PT5	57
3.2.2 PT5Technology - Chemometric Modelling Process	58
3.3 PT5Technology Aggregate Plots.....	60
3.3.1 Finding properties for spectra.....	63
3.3.2 Sparse Data.....	68
3.4 Treatment of outliers	69
3.5 Case Study 1 – PT5Technology in an Asian Refinery	71
3.5.1 Utilising the Aggregate Plot	72
3.6 Crude Type XX Analysis	75
3.7 Net Back Calculations	83
3.8 Conclusion.....	84
Chapter 4. Blended Hydrocarbon Stability.....	86
4.1 Introduction	88
4.2 Methodology.....	88
4.2.1 Observing Organic Deposition by Spectral Inflection	93
4.2.2 Neat Crude Tracking	94
4.2.3 Neat Crude Stability and Instability Assessments.....	96
4.2.4 Generating Blend Stability / Instability Coefficients by Experimentation.....	98
4.3 Blending and regression fitting.....	99
4.3.1 N-1 Factor Blend	99
4.3.2 Comparison of Methodologies	101
4.4 Condensate Testing of Crude Blends	102
4.4.1 Blend Feasibility Report.....	103
4.4.2 Experimental Results from Blend Titration.....	105
4.4.3 Blend Evaluation Report	106
4.5 Case Study 2: Assessment of Heavy Fuel Oil Blending in a Refinery.....	108
4.5.1 Methodology.....	109
4.5.2 NIR Spectroscopy.....	110
4.5.3 Microscopy	110

4.5.4 Physical Property Testing	111
4.5.5 Microscopy	112
4.5.6 Neat HFO Blend Tests.....	116
4.5.7 HVN Titrations (Instantaneous) - Observations	119
4.5.8 HVN Titrations (Time Dependent) - Observations	119
4.5.9 Reference Crude Titrations.....	119
4.5.10 Conclusions	119
4.5.11 Recommended action:	121
4.5.12 Part 1 – Characterisation and Feasibility Phase.....	122
4.5.13 Methodology.....	123
4.5.14 Results	125
4.5.15 Microscopy	127
4.5.16 Part 2 – Additive Efficacy Assessments.....	129
4.5.17 Physical Properties	130
4.5.18 Results	130
4.5.19 Blend 1 (DL242838/DL243169)	132
4.5.20 Blend 2 (DL242840/DL243094)	133
4.5.21 Additive	134
4.5.22 Conclusions	135
Chapter 5. Troubleshooting Upstream Process Issues with Data Analytics.....	137
5.1 Case Study 4: Offshore Data Analysis	138
5.1.1 Data Pre-Processing.....	140
5.1.2 Univariate Analysis – Pump A	140
5.1.3 Univariate Analysis – Pump B	151
5.2 General Observations and Future analysis	156
5.2.1 Axial Displacement	156
5.2.2 Lean fluid periods.....	157
5.2.3 Density.....	157
5.2.4 Torque and pump power.....	157
5.3 Multivariate Data Analysis.....	158
5.3.1 Data Cleansing.....	158
5.3.2 Investigation of Variables.....	158
5.3.3 Interpolation during Data Export.....	158
5.3.4 Variable Statistics	160
5.3.5 Variable Histograms	161

5.3.6 Variable Autocorrelation	162
5.3.7 Comparison of Variables	165
5.3.8 Partial least squares regression	167
5.4 Part 3 – Dimensionality Reduction by Principal Component Analysis	168
5.4.1 Pump A PCA	169
5.4.2 Pump B PCA	174
5.4.3 Linking Univariate with Multivariate.....	177
5.5 Conclusions	178
5.5.1 Future directions	179
Chapter 6. Conclusion	181
Chapter 7. Future Work.....	185
References	189
Appendix A - Additional Heavy Fuel Oil Assessment Results.....	195
7.1 1% Sulphur HFO	195
7.2 1.8% Sulphur HFO	196
7.3 1.8% Used Sulphur HFO.....	197
7.4 3% Sulphur HFO	198
Appendix B – Additional Marine Fuel Blending Results	200
7.5 Blend 3 (DL242837/DL243017)	200
Appendix C - Algorithms	202
7.6 Principal Components Analysis	202
7.7 Principal Components Analysis	203

Index of Figures

Figure 1-1: Global Exploration and Production business line locations	3
Figure 2-1: Showing an anticline trap (a) and a fault trap (b) taken from Burg et al. (1997)	8
Figure 2-2: A representation of the chemical forms of Paraffin's, Naphthenes and Aromatics taken from Naskar (2015).....	9
Figure 2-3: SARA separation taken from Lundanes and Greibrokk (1994)	10
Figure 2-4: A seismic survey taken from Grace (2007)	11
Figure 2-5: Showing an oil drilling rig (a) and a schematic of drilling (b) taken from Grace (2007)	12
Figure 2-6: Refinery flowsheet taken from Kraus (1996)	14
Figure 2-7: showing the fraction temperatures and chain lengths taken from Energia (2010)	15
Figure 2-8: The spectrum of light taken from NG (2012)	19
Figure 2-9: Different Crude Oil Spectra Baselines	21
Figure 2-10: Showing the comparison of errors for several models used to predict the composition of gasoline taken from Balabin et al. (2007)	25
Figure 2-11: A representation of the GC equipment taken from Sheffield Hallam (2010).....	26
Figure 2-12: A plot comparing margins of refineries in Europe, FSU and Africa taken from Wood-Mackenzie (2012a)	30
Figure 2-13: Showing NCM in \$/bbl. for a selection of major European refineries taken from Wood-Mackenzie (2012a)	31
Figure 2-14: Showing NCM in \$/bbl. of major European Refiners taken from Wood-Mackenzie (2012a).....	31
Figure 2-15: Solvents and precipitants for asphaltenes taken from Wiehe and Kennedy (2000b)	32
Figure 2-16: A hypothetical asphaltene molecule taken from Aurdal et al., (1998)	32
Figure 2-17: Physical model of a petroleum system, showing the SARA balance taken from Wiehe and Kennedy (2000b).....	34
Figure 2-18: Showing a typical Vapour Pressure Osmometer setup taken from UCI (2016)..	35
Figure 2-19: VPO determined molar masses in Athabasca bitumen taken from Gawrys and Kilpatrick (2004)	36
Figure 2-20: SARA Fractions Methodology taken from Lundanes and Greibrokk (1994)	38
Figure 2-21: A Plot Showing the Shift in Principal Component Scores of a Crude Oil Sample during Depressurisation taken from Aske (2002b)	40
Figure 2-22: PCA Example 1	45

Figure 2-23: First Principal Component.....	45
Figure 2-24: Second Principal Component	46
Figure 2-25: Projection to Principal Component 1 taken from Richardson (2009)	47
Figure 2-26: Bivariate Scores plot (PC1 v PC2) taken from Richardson (2009).....	48
Figure 2-27: Bivariate loadings plot (PC1 v PC2) taken from Richardson (2009)	48
Figure 2-28: Bivariate Scores Applied to a Refinery Dataset	49
Figure 2-29: Showing modelling errors for different methods used to build a gasoline model taken from Balabin et al. (2012).....	52
Figure 3-1 - Typical Spectrometers (courtesy of ABB 2017)	56
Figure 3-2 - Laboratory Crude Oil Sample Handling and Spectrometer	57
Figure 3-3 - Hydrocarbon absorption in Near Infra-Red radiation	58
Figure 3-4 - Link Spectrum to Properties.....	58
Figure 3-5 - NIR as Information Vector.....	59
Figure 3-6 - Same Sample have Same Spectrum	59
Figure 3-7 - Same Spectra Same Properties	60
Figure 3-8: Simple sample spectra	61
Figure 3-9: Simple Aggregate	62
Figure 3-10 – Spectral Plane with Boxes of sample families.....	63
Figure 3-11 - PT5Technology Prediction - Database Search.....	64
Figure 3-12 - Topological Modelling Using Nearest Neighbours.....	65
Figure 3-13 - Topological Modelling Using Artificial Nearest Neighbours	66
Figure 3-14 - Effect of R-Sphere.....	67
Figure 3-15 - Change of property with distance.....	68
Figure 3-16 - Prediction and Model Update.....	70
Figure 3-17: Case Study Crude Spectra	73
Figure 3-18: PT5 Aggregate Plots of all Example Crudes showing API gravity aggregate (a) and 565°C+ aggregate (b).....	74
Figure 3-19: Showing PT5 Aggregate plot (a) and a physical properties correlation (b)	75
Figure 3-20: PT5Crude Aggregate Plot of Crude Type XX showing cluster and difference ..	76
Figure 3-21: TBP Curves for all four crude samples	77
Figure 3-22: Showing Average TBP v Sample_03	78
Figure 3-23: the difference between the average and Sample_03.....	78
Figure 3-24: TBP curves from PT5 prediction.....	79
Figure 4-1: Binary Crude Blend Exhibiting linear behaviour	90
Figure 4-2: Linear Blend Aggregate.....	90

Figure 4-3: Transmitted Light Microscopy 100% Crude A (a), 50% Crude A (b), 0% Crude A (c).....	91
Figure 4-4: Binary Crude Blend Exhibiting Non-Linear Behaviour	91
Figure 4-5: 8,000 Region of NIR Spectra Showing Non-Linearity	92
Figure 4-6: Linear Blend Aggregate.....	92
Figure 4-7: Transmitted Light Microscopy 100% Crude A (a), 50% Crude A (b), 0% Crude A (c).....	93
Figure 4-8: Showing inflection point.....	94
Figure 4-9 - Crude Tracking on PT5 Aggregate.....	94
Figure 4-10 - Aggregate plot of instability observed from blend titrations.....	96
Figure 4-11: Determination of Insolubility Number and Solubility Blending Number for Forties and Souedie Crude Oils taken from Wiehe, Kennedy and Dickakian (2001)	97
Figure 4-12 - Example Blend Recipe Feasibility Report	104
Figure 4-13 - Example Experimental Results from Matrix Blend Algorithm.....	105
Figure 4-14 - Example Blend Evaluation Report	106
Figure 4-15: HFO Laser Microscopy 1% Sulphur HFO (a), 1.8% Sulphur HFO (b), 1.8% Sulphur Used HFO (c) and 3% Sulphur HFO (d)	112
Figure 4-16: HFO Microscopy with Transmitted Light on 1% Sulphur HFO (a), 1.8% Sulphur HFO (b), 1.8% Sulphur Used HFO (c) and 3% Sulphur HFO (d)	113
Figure 4-17: 1.8% Used Sulphur HFO with 50% HVN at time 0 hrs (a) and time 72 hours (b)	114
Figure 4-18: Cross Polar Microscopy 1% Sulphur HFO (a), 1.8% Sulphur HFO (b), 1.8% Sulphur Used HFO (c) and 3% Sulphur HFO (d)	115
Figure 4-19: Showing full spectra for 1.8% Sulphur Blend (a) and 9000 wavenumber region (b)	117
Figure 4-20: Showing full spectra for 20% HVN titration (a) and 9000 wavenumber region (b)	118
Figure 4-21: Comparison of physical properties to average	120
Figure 4-22: Showing the an inflection point.....	124
Figure 4-23: Linear Spectral Blending	125
Figure 4-24: Blend 1 (a) and Blend 2 (b) aggregate plots	126
Figure 4-25: Blend 1- MDO in HFO at 0% (a), 30% (b), 60% (c) and 90% (d).....	127
Figure 4-26: Blend 2 - MDO in HFO	128
Figure 4-27: Showing blends with additive (a) and (c) and without additive (b) and (d).....	132
Figure 4-28: Showing blends with additive (a) and (c) and without additive (b) and (d).....	133

Figure 4-29: Neat Additive.....	134
Figure 5-1: Process Flow Diagram.....	138
Figure 5-2: Pump Schematic	139
Figure 5-3: Pump A throughout time period 1	142
Figure 5-4: Pump A throughout period 4	143
Figure 5-5: Pump A throughout Period 5	145
Figure 5-6: Axial Displacement	146
Figure 5-7: Buffer Tank Level.....	146
Figure 5-8 Flow Rate and Torque	147
Figure 5-9: Inlet Temperature vs DP.....	149
Figure 5-10: Axial Displacement of MPP B through time period 1.....	152
Figure 5-11: Axial displacement of MPPB throughout time period 4	153
Figure 5-12: Pump B event 1 period 4	154
Figure 5-13: Buffer tank level through event 1	154
Figure 5-14: Flow and Torque through event 1.....	155
Figure 5-15: Pump B event 2 period 4 Torque and DP over the venturi.....	155
Figure 5-16: Venturi DP vs Torque.....	156
Figure 5-17: Example of Interpolation histogram	159
Figure 5-18: Close examination of interpolation.....	160
Figure 5-19: Example frequency histogram	162
Figure 5-20: Example Autocorrelation plot.....	163
Figure 5-21: Autocorrelation plot for buffer tank percentage in pump A.....	164
Figure 5-22: Inlet Temperature (left) and axial vibration (right)	165
Figure 5-23: heatmap of mean Pearson's correlation coefficient across the longer time periods (1, 4, 5)	166
Figure 5-24: PLS Loadings for each pump's non-temperature sensors against the pump's Z-axis displacement as an objective function.	168
Figure 5-25: Variance explained by the Principal Components fitted to the dataset.	169
Figure 5-26: Plotting the individual time points by their position each principle component, coloured by the period of origin.	170
Figure 5-27: Bar plots of how each sensor value contributes to the first 3 principal components in the PCAs with (above) and without (below) temperature sensors.	171
Figure 5-28: Operating Regions PCA	173
Figure 5-29: Variance explained by the Principal Components fitted to the dataset with temperature sensors (a) and without temperature sensors and period 5 (b)	174

Figure 5-30: Plotting the individual time points by their position each principle component, coloured by the period of origin.	175
Figure 5-31: Bar plots of how each sensor value contributes to the first 3 principal components in the PCAs where period 5 is included and excluded.	176
Figure 5-32: Projecting the data values of an event noticed in the technical analysis event 2 in period 5 for Pump A	177
Figure 5-33: Projecting the data values of an event noticed in the technical analysis (event 1 in period 5 for Pump A	178
Figure 7-1: Forties Pipeline System (FPS) North Sea taken from Subsea (2017)	185
Figure 7-2: North Sea Fields Aggregate Plot	187
Figure A-1: 1% Sulphur HFO - 5% HVN	195
Figure A-2: 1% Sulphur HFO - 10% HVN	195
Figure A-3: 1% Sulphur HFO - 50% HVN	195
Figure A-4: 1.8% Sulphur HFO - 5% HVN	196
Figure A-5: 1.8% Sulphur HFO - 10% HVN	196
Figure A-6: 1.8% Sulphur HFO - 50% HVN	196
Figure A-7: 1.8% Used Sulphur HFO - 5% HVN	197
Figure A-8: 1.8% Used Sulphur HFO - 10% HVN (left) and (right).....	197
Figure A-9: 3% Sulphur HFO - 5% HVN	198
Figure A-10: 3% Sulphur HFO - 10% HVN	198
Figure A-11: 3% Sulphur HFO - 50% HVN	198
Figure B-1: Marine Fuel Blends	200

Index of Tables

Table 1: Food Consumption in the UK (g/person/week) taken from Richardson (2009)	47
Table 3-1: Database Structure	64
Table 3-2: Database Management	69
Table 3-3: Four samples of type XX with their API, Sulphur and the cut 565°C+ from TBP	72
Table 3-4: Property Prediction Statistics	79
Table 3-5: Aggregate Distance Matrix	80
Table 3-6: Difference between prediction and laboratory analysis expressed as a percentage of method reproducibility R.....	82
Table 3-7: Simple Refinery Netbacks	83
Table 3-8: Complex Refinery Netbacks	83
Table 4-1: Example Blend Experiment	98
Table 4-2: Stability testing for variation in crude ratios.....	101
Table 4-3: Laboratory Results, condensate Matrix	103
Table 4-4: Showing the Full set of blend tested	109
Table 4-5: HFO Physical Properties	111
Table 4-6: Percentages of Reference Crude (RC) around the point of instability.....	119
Table 4-7: Physical Properties for Samples.....	123
Table 4-8: Physical Properties for Samples.....	130
Table 4-9: Summary table	131
Table 5-1: Summary of histogram observations	162
Table 7-1: Showing properties measured for the FPS Application on Whole crude (Left) and Light Ends (Right).....	186

Index of Definitions

American Petroleum Institute	API
American Petroleum Institute Gravity	°API
American Society for Testing and Materials	ASTM
Artificial Neural Network	ANN
Artificial Neural Network Multilayer Perceptron	ANN - MLP
Assurance, Testing, Inspection and Certification	ATIC
Atmospheric Pressure Photoionisation	APPI
Barrel (Typically used for crude oil, Volume = 42 US Gallons)	BBL
Binding Resins	BR
Carbon Dioxide	CO ₂
Crude Distillation Unit	CDU
Enhanced Oil Recovery	EOR
Equations of State	EOS
Exploration and Production	E&P
Final Boiling Point	FBP
Former Soviet Union	FSU
Forties Pipeline System	FPS
Fourier Transform Infrared (spectroscopy)	FTIR
Fourier Transform Ion Cyclotron Resonance Mass Spectrometry	FT-ICR MS
Freeze Fracture and Transmission Electron Microscopy	FF-TEM
Gas Chromatography	GC
Hierarchical Partial Least Squares (regression)	H - PLS
High Performance Liquid Chromatography	HPLC
High Sulphur Fuel Oil	HSFO
Infrared	IR
Instability Coefficient	IC
Initial Boiling Point	IBP
Intertek Proprietary Chemometric Modelling Technology	PT5
K Nearest Neighbours	KNN
Knock Index	KI
Latent Variable	LV
Light Virgin Naphtha	LVN
Linear Discriminant Analysis	LDA
Linear Predictive Coding	LPC
Linear Solvation Energy Relation	LSER
Low Sulphur Fuel Oil	LSFO
Mid InfraRed	MIR
Motor Octane Number	MON
Multi-Block Partial Least Squares (regression)	MB-PLS
MultiLayer Perceptron	MLP
Multiple Linear Regression	MLR
Multiplicative Scatter Correction	MSC
Near InfraRed	NIR
Net Cash Margin	NCM
Neural Network	NN

Nuclear Magnetic Resonance	NMR
Octane Number	ON
Open Column Chromatography	OPC
Order Derivative	OrD
Organic Deposition	OD
Oxides of Carbon	CO _x
Oxides of Nitrogen	NO _x
Oxides of Sulphur	SO _x
Partial Least Squares (regression)	PLS
Polynomial Partial Least Squares (regression)	Poly - PLS
Partial Least Squares Discriminant Analysis	PLS - DA
Pour Point	PP
Principal Component	PC
Principal Component Analysis	PCA
Process Assurance Group	PAG
Pulse-Field Gradient Spin Echo Nuclear Magnetic Resonance	PFG-SE NMR
Principal Component Regression	PCR
Probabilistic Neural Network	PNN
Quadratic Discriminant Analysis	QDA
Regularised Discriminant Analysis	RDA
Refinery Gross Margin	RGM
Refractive Index	RI
Research Octane Number	RON
Residual Asphaltenes	RA
Root Mean Squared Error of Cross Validation	RMSECV
Root Mean Squared Error of Prediction	RMSEP
Saturates Aromatics, Resins and Asphaltenes	SARA
Serial PLS	S-PLS
Simulated Distillation	SimDis
Small Angle Neutron Scattering	SANS
Soft Independent Modelling of Class Analogy	SIMCA
Spline Partial Least Squares (regression)	Spline - PLS
Stability Coefficient	SC
Standard Error of Prediction	SEP
Standard Normal Variance	SNV
Statistical Association Fluid Theory for Potentials of Variable Range	SAFT - VR
Support Vector Machines	SVM
TetraHydroFuran	THF
Total Acid Number	TAN
Transmission Electron Microscope	TEM
TriChloroEthylene	TCE
True Boiling Point	TBP
Vapour Pressure Osmometry	VPO
Wavelet Neural Network	WNN

Chapter 1:

Introduction

Chapter 1. Introduction

Throughout the hydrocarbon supply chain, process optimisation is driven by the desire to maximise profit margins. In the global refining marketplace, the biggest cost is crude oil and to improve margins increasing use of non-conventional crude oils such as shale oils or tar sands high (also called opportunity crudes) lowers the cost of the crude blend. Opportunity crudes are selected based on market forces, for example in North America, the production booms in shale oil and tar sands have provided ample amounts of new low-cost oils which refineries are buying and processing.

However, as these oils are new to the marketplace and many refineries have never processed them before it brings about challenges including: lack of understanding of the quality of the crude oil being processed (shale oils for example can come from many thousands of wells) and how these oils interact with the more conventional refinery feedstocks (such as Brent or West Texas Intermediate).

1.1 Intertek

Intertek Group plc are a multinational corporate organisation consisting of more than 42,000 employees in over 1,000 locations in over 100 countries across the globe.

Through their global network of state-of-the-art facilities and industry-leading technical expertise Intertek provides innovative and bespoke Assurance, Testing, Inspection and Certification (ATIC) services to customers in a variety of sectors including food, pharmaceuticals, electrical, automotive and oil and gas. (Intertek, 2016).

The Exploration and Production (E&P) division is one of Intertek's oil and gas focussed business lines and primarily deals with upstream operations, the locations of the E&P division globally are shown in Figure 1-1.

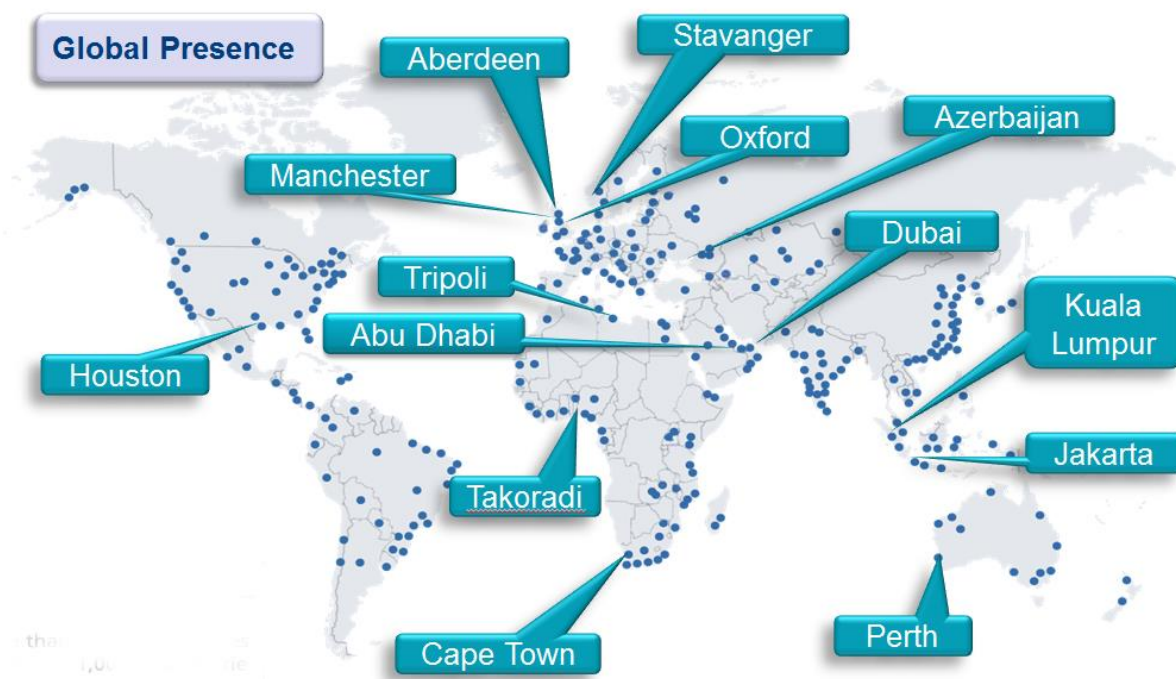


Figure 1-1: Global Exploration and Production business line locations

The E&P business line is itself split into four sub business lines: Upstream Services, Production and Integrity Assurance, Calibration and Metering and Production Support.

The Production Support sub business line is responsible for activities including hydrocarbon characterisation, pipeline allocation, crude oil assay, oil condition monitoring and deposits analysis. Because of the nature of its business, the Production Support sub business line supports the deployment of Intertek's chemometric modelling software 'PT5Technology' on a global basis.

1.2 PT5Technology

PT5 measurement technology (PT5Technology) is used across the entire crude oil supply chain, including crude oil production, pipelines, refining and biofuel blending activities. The combined topological modelling and near infrared analysis combination supports quality control and control systems, enhances production yields and helps customers run their business more efficiently and profitably.

PT5 software is combined with on-line near infrared (NIR) analysis to provide rapid product analysis, exploiting real time property measurement for improved control and optimisation. When Intertek's PT5 software is combined with on-line NIR Analysis, accurate and real-time data is available for online composition measurement and quality assurance on platforms and pipelines, fiscal allocation and hydrocarbon accounting for shared pipeline system, well-stream

allocations, multiphase meter validation and distillation column reconciliation. The technology can be used across the whole spectrum, including MIR (Mid Infra-Red), NIR (Near Infra-Red), Nuclear Magnetic Resonance (NMR) and Gas Chromatography (GC).

1.3 Objectives

This Eng.D project has been focused on working in collaboration with the industrial partner Intertek to develop commercially viable solutions to provide customers in the hydrocarbon-processing sector with the following:

1. Develop a methodology for rapid identification of crude oil composition both online and offline.
2. Implement a tool to facilitate optimisation of crude blending performance utilising the information from objective 1.
3. Develop an approach to characterise the stability and compatibility of blended hydrocarbon streams
4. Apply data analytics approaches to solve historical hydrocarbon processing issues

1.4 Contributions

My contribution has been to firstly critique and improve existing chemometric approaches for helping refineries understand and predict the quality of crude oils from Near Infrared (NIR) spectra. Using this information has helped refineries to inform crude processing and process control decisions.

Secondly, as a consequence of the research, a process was developed to assess the compatibility of blended crude oils. This is of critical importance to the industry because blending incompatible crude oils can elicit precipitation of problematic material such as wax and asphaltene. These can contribute to heat exchanger and distillation column fouling, block pipes and storage tank offtakes to name a few of the multitude of undesirable effects.

Finally, further development of the data analytics approach of the industrial partner to solving client specific issues has shown exciting outcomes including maximisation of refinery fractions and improving process stability.

1.5 Thesis Overview

This thesis is designed to build up the story of the work, to take the reader on the research journey and ultimately present the achievements of the project in a series of case studies.

As such an initial literature review draws attention to literature relevant to the research and covers the oil & gas industry in general as well as the principles of oil refining. It then drills down to the chemistry of crude oil stability and the economic drivers to develop a solution. Finally, it looks at spectroscopic techniques for hydrocarbon characterisation and modelling techniques for both chemometric and process data analysis

The first case study then explores the contributions of the thesis to the field of chemometrics. It describes the refinement of the modelling tool and then demonstrates its application within an Asian refinery.

The thesis then goes on to describe the development and application of an innovative methodology, patented during the course of the Eng.D project, for describing and predicting the stability of blended crude oils. The benefits of the research and development are then contextualised in two case studies, one that looks at the blending of heavy fuel oil in refineries and another which looks at challenges of fuel blending in the maritime sector.

Finally, the thesis presents a study of the application of multivariate statistics to an offshore facility and talks through an example of the application of data analytics to resolve a historical pump failure problem.

Chapter 2:

Literature Review

Chapter 2. Literature Review

In this section different themes from the literature, relevant to the industry and the research will be explored. Examples of the application of various techniques to the characterisation of hydrocarbon process streams, as well as non oil and gas applications will be explored with the intention of drawing out the strengths and weaknesses of the methodologies used in the research.

As this project is predominantly focussed in the oil and gas industry, an overview of crude oil formation, exploration, production and refining will be examined. Crude oil is the key resource in the world today, almost everyone comes into contact with a crude oil derivative product on a daily basis, whether it is in the form of plastics, fuels or paints and as such the price of oil is an important factor, which affects daily lives.

A voracious appetite for crude oil from rapidly growing economies such as China and India was driving the price up. However, due to the shale oil boom, weaker than anticipated global demand, and the refusal of OPEC countries (particularly Saudi Arabia) to cut production means that the price of oil has fallen dramatically since the start of the project in 2011.

This literature review draws attention to key areas relevant to the research and covers the oil & gas industry in general as well as the principles of oil refining. It then drills down to the chemistry of crude oil stability and the economic drivers to develop a solution. Finally, it looks at spectroscopic techniques for hydrocarbon characterisation and modelling techniques for both chemometric and process data analysis

2.1 Formation

Crude oil is formed from prehistoric flora and fauna falling to the beds of lakes and warm shallow seas. This was mixed with the mud and sediments forming anaerobic conditions. As a consequence of the conditions, the organic material did not decompose in the normal manner by aerobic bacteria.

Over a period of many years, more layers of mud and sediment build up burying the material deeper. As more weight pressed down the heat and pressure increased, this caused a transformation of the material into Kerogen (a collection of organic compounds found in

sedimentary rock). with the addition of more heat and pressure the Kerogen was then altered into liquid and gaseous hydrocarbons by a process called catagenesis (Braun and Burnham, 1993).

To trap oil after it has formed it is necessary for three conditions to exist. First of all a rock rich in organic matter has to have been buried deep enough to have experienced the intense heat and pressure required for the formation of oil. Secondly, a porous rock must be in place, which can act as a reservoir for the oil to accumulate. Finally, a non-porous rock must sit over the porous and act as a cap to stop the oil seeping out of the reservoir. Shown in Figure 2-1 are two types of traps that occur to create oil reservoirs. The first (Figure 2-1a) is an anticline trap; this is caused by ripples in the earth's plate due to tectonic movement. The ripples are called anticlines at the crest and synclines at the trough (Grace, 2007). Figure 2-1b is a fault trap, this is caused by tectonic plate shearing (Burg, Selverstone and Molnar, 1997).

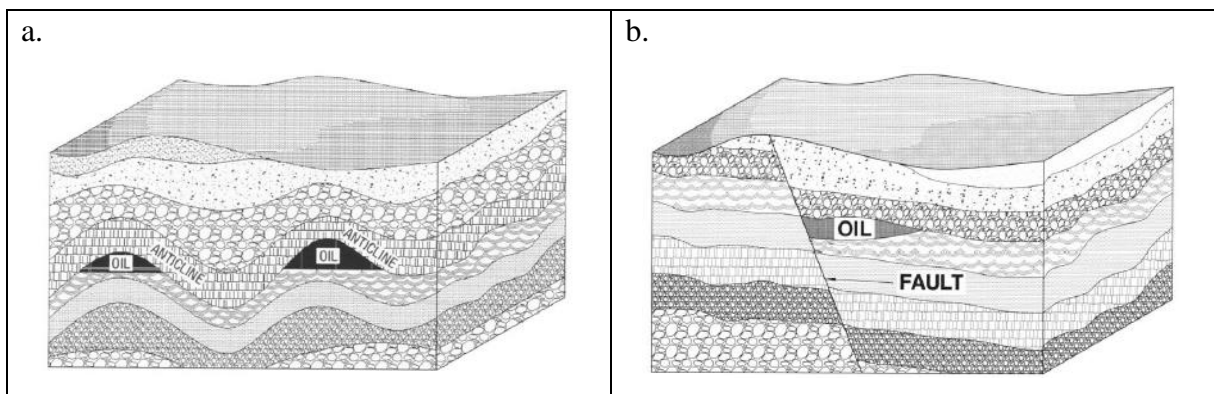


Figure 2-1: Showing an anticline trap (a) and a fault trap (b) taken from Burg *et al.* (1997)

2.2 Composition

The precise chemical composition of petroleum can vary with location and the age of the field in additions to any variations that occur with the depth of the individual well (Speight, 2001). It is also possible that two wells that are adjacent to each other may produce oil that is of varying composition. However all crude oils contain at least some of the following components: Hydrocarbons, nitrogen compounds, oxygen compounds, sulphur compounds and metallic constituents (Speight, 2001).

Speight (2001) also states that the consideration of the atomic hydrogen-carbon ratio, sulphur content, and API gravity are no longer adequate to the task of determining refining behaviour. This is in strong agreement with the research work carried out in this project, a large constituent of which is aimed at providing refiners with more information in a shorter time space to allow

for improved process optimisation. As will be seen in a case study later on, the measurement of API gravity and Sulphur measurements of both neat crudes and blends are the predominant metrics used by refineries for quality monitoring and economic optimisation, as they are quick, simple and cheap tests.

Although crude oil is composed of a plethora of components including inorganic components such as salts and metals (such as vanadium, nickel and iron), by far the most abundant and useful constituent of crude oils are the hydrocarbons, for convenience these can be divided into three groups (paraffin's, naphthenes and aromatics) (Speight, 2001) and are shown in Figure 2-2:

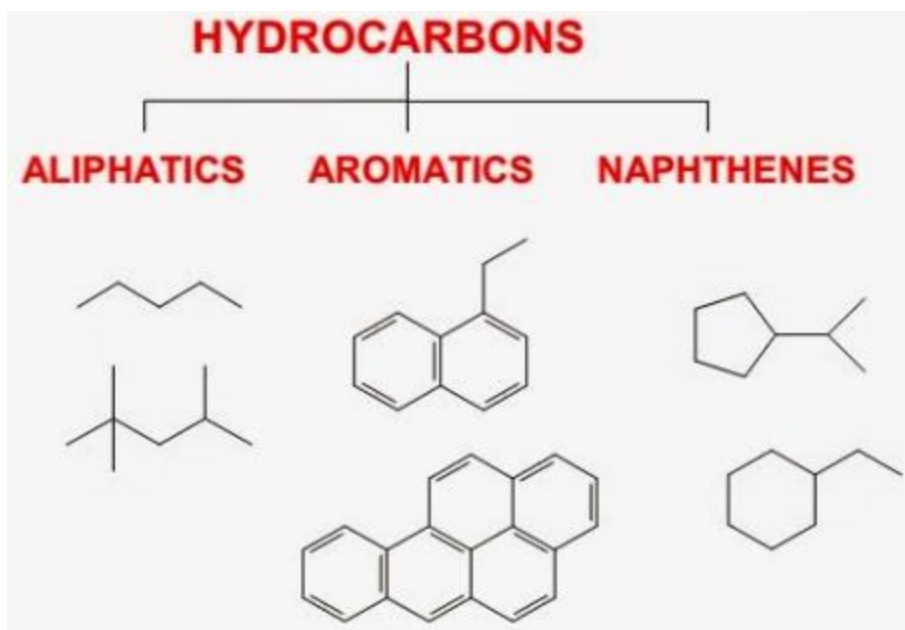


Figure 2-2: A representation of the chemical forms of Paraffin's, Naphthenes and Aromatics taken from Naskar (2015)

1. *Paraffin's* - Saturated hydrocarbons with straight or branched chains, but without any ring structure.
2. *Naphthenes* - Saturated hydrocarbons containing one or more rings, each of which may have one or more paraffinic side chains (more correctly known as *alicyclic hydrocarbons*).
3. *Aromatics* Hydrocarbons containing one or more aromatic nuclei, such as benzene, naphthalene, and phenanthrene ring systems, which may be linked up with (substituted) naphthene rings and/or paraffinic side chains.

A variant of this classifies crude oils depending on the characteristics of the distillation residues and whether it is asphalt-base, paraffin base or mixed base. (Guthrie, 1960).

However the above classifications do not work well for heavy oils (Speight, 2016) and does not describe all the constituents which must be considered when describing crude oil blending

behaviour (particularly with respect to crude oil stability) and as a consequence a four group classification of crude oils is more widely used.

This model, named SARA, is discussed in more detail in section 2.14 and includes Saturates (S) as an umbrella term covering paraffin's and naphthenes. Aromatics (A), Resins (R) which are a solubility group of molecules with both polar and non-polar constituent, miscible with heptane and Asphaltenes (A) which are the most polar fraction of crude oil, soluble in toluene and insoluble in heptane. In this process, the oil is first deasphalted to obtain asphaltenes + SAR fraction. This is then separated by HPLC using either bonded phase columns or a combination of silica and bonded phase columns (Lundanes and Greibrokk, 1994).

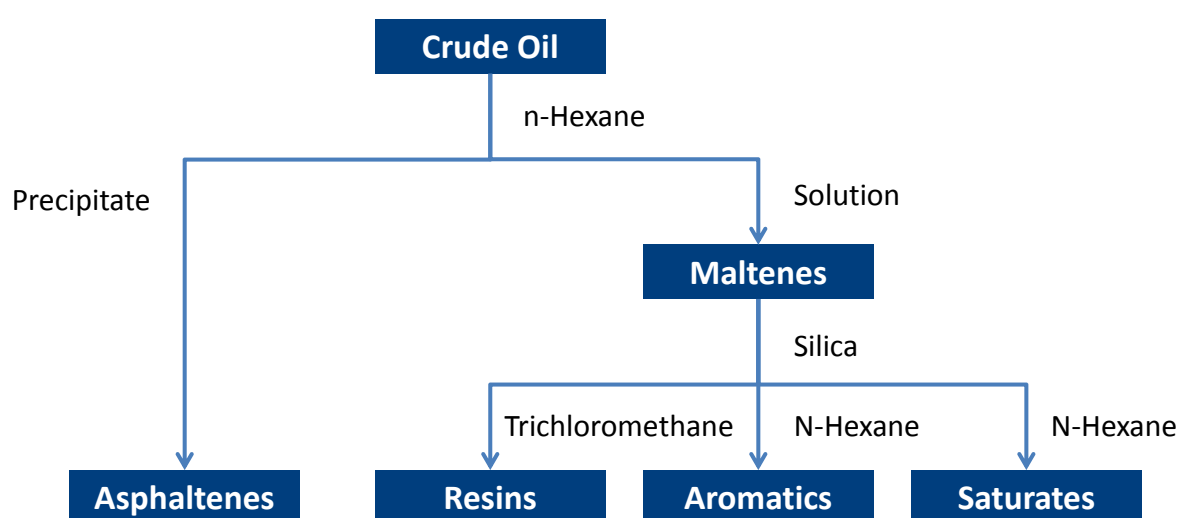


Figure 2-3: SARA separation taken from Lundanes and Greibrokk (1994)

2.3 Exploration and Production

Petroleum exploration is the domain of geologists and geophysicists. It is not economically viable to drill holes in the ground and hope to strike lucky, although this has been historically undertaken by both large and small energy companies, a practice known as 'wildcatting'. The normal practice before drilling, however, is to carry out full and proper geographical surveys.

It is a well understood fact that there are locations in the world where oil is more prevalent. Indeed, there are parts of the world (such as Casper, Wyoming) where oil seeps to the surface, drilling in that area found a vast oil field, which is still producing to this day. In other places visible mounds where the earth has been pushed up by the pressure of subterranean oil (such as tea pot dome, Wyoming) has also yielded oil strikes (Grace, 2007).

However, in locations where oil is not so obvious, surveys are carried out. Figure 2-4 is a diagram of the undertaking of a seismic survey to find the location of oil. The fundamentals of the seismic survey are straightforward, an explosion on the surface sends shocks rippling through the rock strata, and these are deflected off the different layers of rock and are detected by instruments on the surface of the earth. The time taken for the echo to be detected and the intensity of the signal are then recorded.

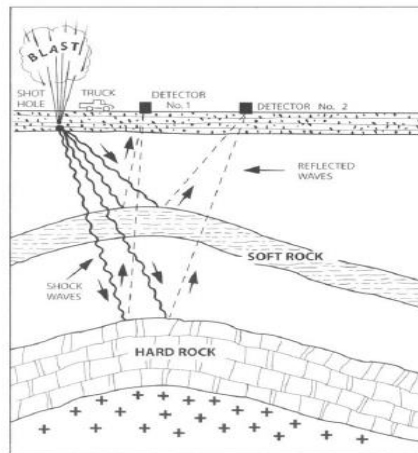


Figure 2-4: A seismic survey taken from Grace (2007)

Once the oil has been located, it then has to be reached by drilling. Figure 2-5 shows a picture of a drilling rig (left) and a schematic of the process (right). This particular example is a land drilling rig however; the principles of both exploration and drilling at sea are the same. Basic drilling has not changed for over 100 years; the only advancements made are in what is known as ‘directional drilling.’

Directional drilling involves directing the drill bit whilst drilling. In this way, it can pass through faults that can otherwise separate wells. This has been revolutionary in allowing more oil to be extracted from previously depleted wells. Other methodologies employed for enhancing well recovery are performed post drilling and known as enhanced oil recovery (EOR) techniques and can be generally classified as either thermal injection or gas recovery; these are discussed in more detail in 2.3.1.

There are many problems that can arise during the drilling process such as leakage of oil during drilling due to the lack of a proper seal (Ibrahim, 2007). The latest proposed method of drilling is to use laser drilling. This method will eliminate the current problems with conventional drilling, and is also less expensive than current methods. It has also found widespread and very successful use in other industries (Ibrahim, 2007).

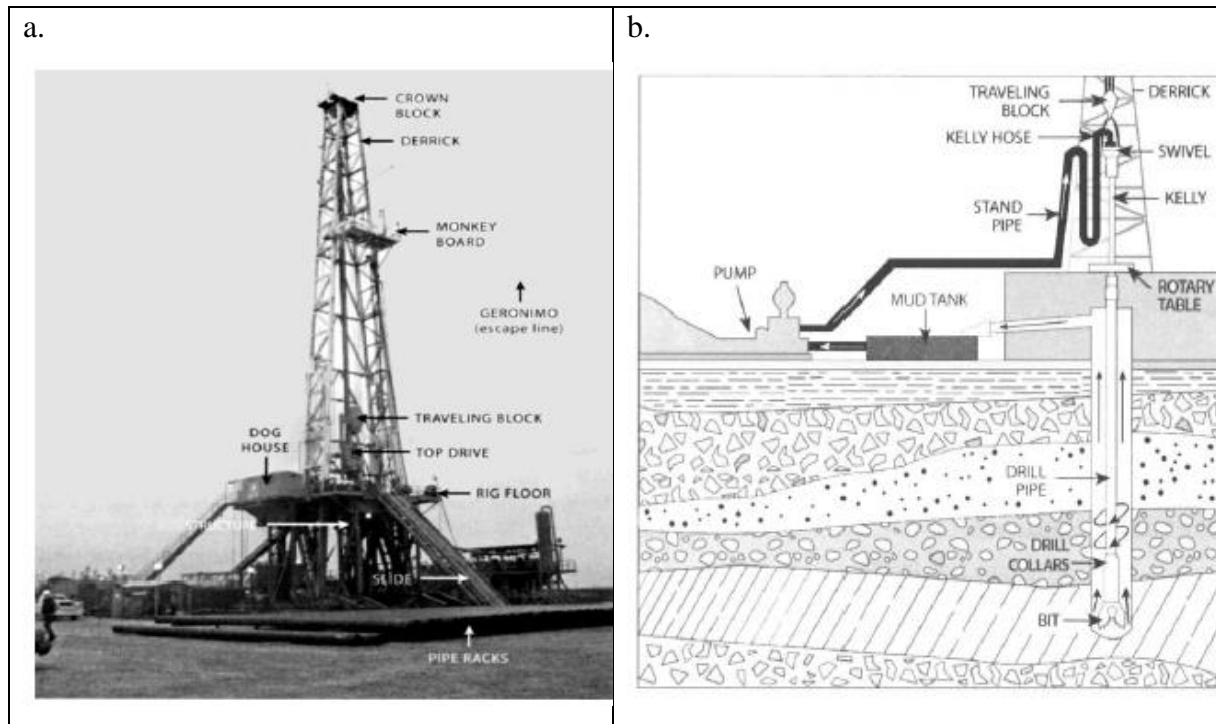


Figure 2-5: Showing an oil drilling rig (a) and a schematic of drilling (b) taken from Grace (2007)

Another new proposal reported is water jet drilling which has similar advantages to laser drilling. It has also been postulated that the two methodologies are combined, using laser drilling to start the hole and then following it up with water jet drilling to widen it. (Ibrahim, 2007).

2.3.1 *Enhanced Oil Recovery (EOR)*

Directional drilling is not the only methodology that has allowed greater well production to be possible. Other post drilling EOR strategies are utilised to maximise well recovery, these were defined by Islam (2000) as a recovery scheme that uses the injection of fluids not normally present in the reservoir.

Most EOR techniques are based on oil viscosity reduction and/or improvement of the mobility ratio by increasing the displacement phase viscosity or by reducing oil viscosity and/or interfacial tension between injected fluid and oil (Ibrahim, 2007).

Three main categories of EOR that have been successful to varying degrees are (Koottungal, 2004; Ibrahim, 2007; Alvarado and Manrique, 2010):

- Thermal recovery - Involves the introduction of heat, such as the injection of steam to lower the viscosity or thin the heavy viscous oil, and so improve its ability to flow

through the reservoir. Thermal techniques account for over 50% of US EOR production and enjoy extensive popularity throughout the Canadian tar sands fields.

- Gas injection - Uses gases such as natural gas, nitrogen, or carbon dioxide that expand in a reservoir to push additional oil to a production wellbore, or other gases that dissolve in the oil to lower its viscosity and improve its flow rate.
- Chemical Injection – Widely used in the 1980's but has been in decline ever since. Chemical injection strategies involve flooding wells with manufactured compounds, usually polymeric in nature, to increase well production. This is achieved by adding the polymer to waterflood (a technique for maintaining well pressure by injecting water into the well to displace the oil) fluids alter viscosity and thus increase pore mobility and waterflood characteristics.

2.4 Refining

Refineries come in many sizes and complexities, however even the 'simplest' of refineries still has upstream and downstream processing. The heart of a refinery is the crude distillation unit (CDU). Figure 2-6 shows a simplified refinery flow sheet. It can be seen that the crude from the tank farm flows into the CDU where it undergoes fractionation. The majority of these fractions then undergo additional downstream processing to turn them into more valuable refined products.

An expanded view of the CDU is shown in Figure 2-7 complete with the temperatures of the fractions (also known as 'cut points) and the chain lengths that come off at each cut.

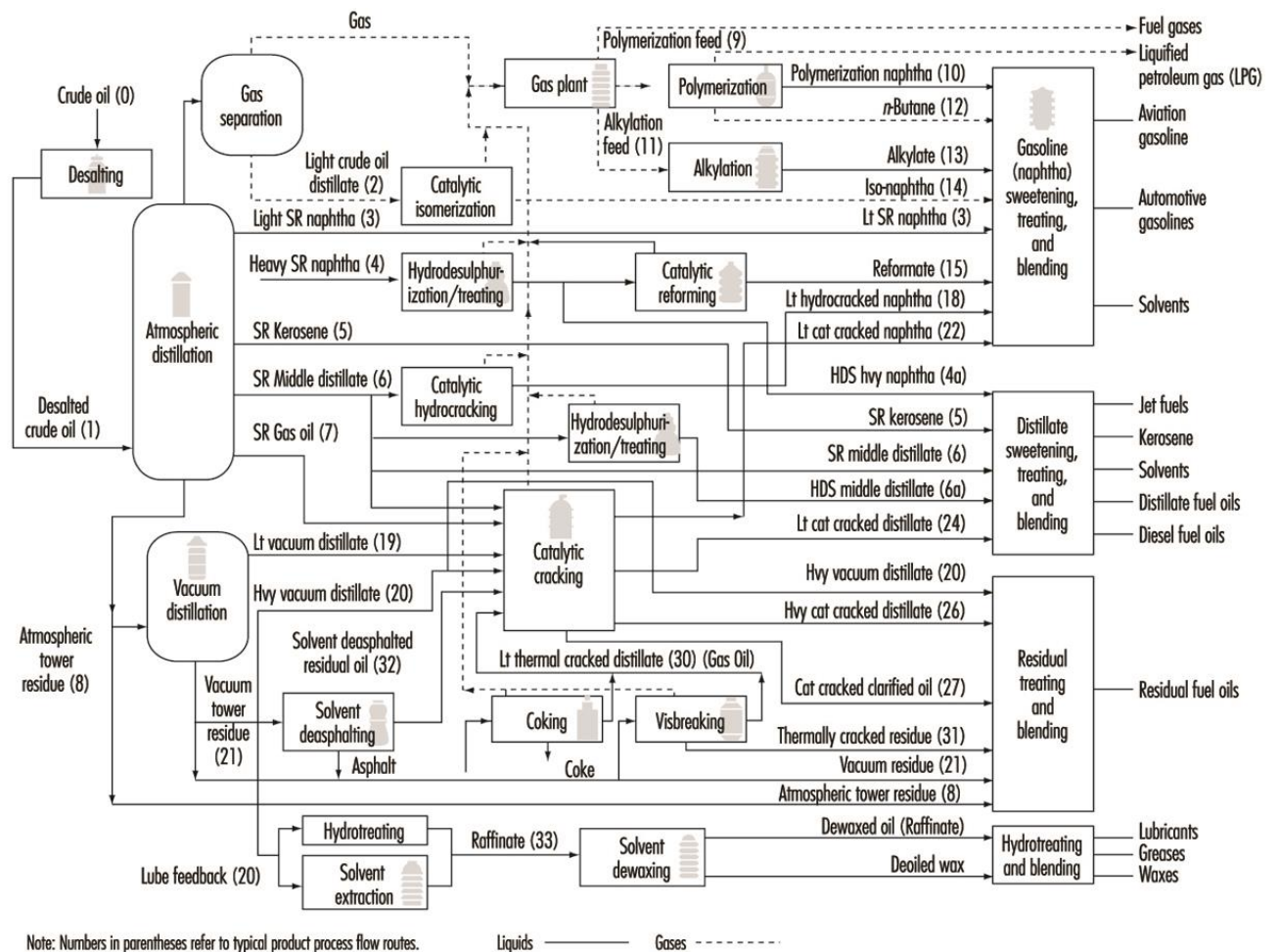


Figure 2-6: Refinery flowsheet taken from Kraus (1996)

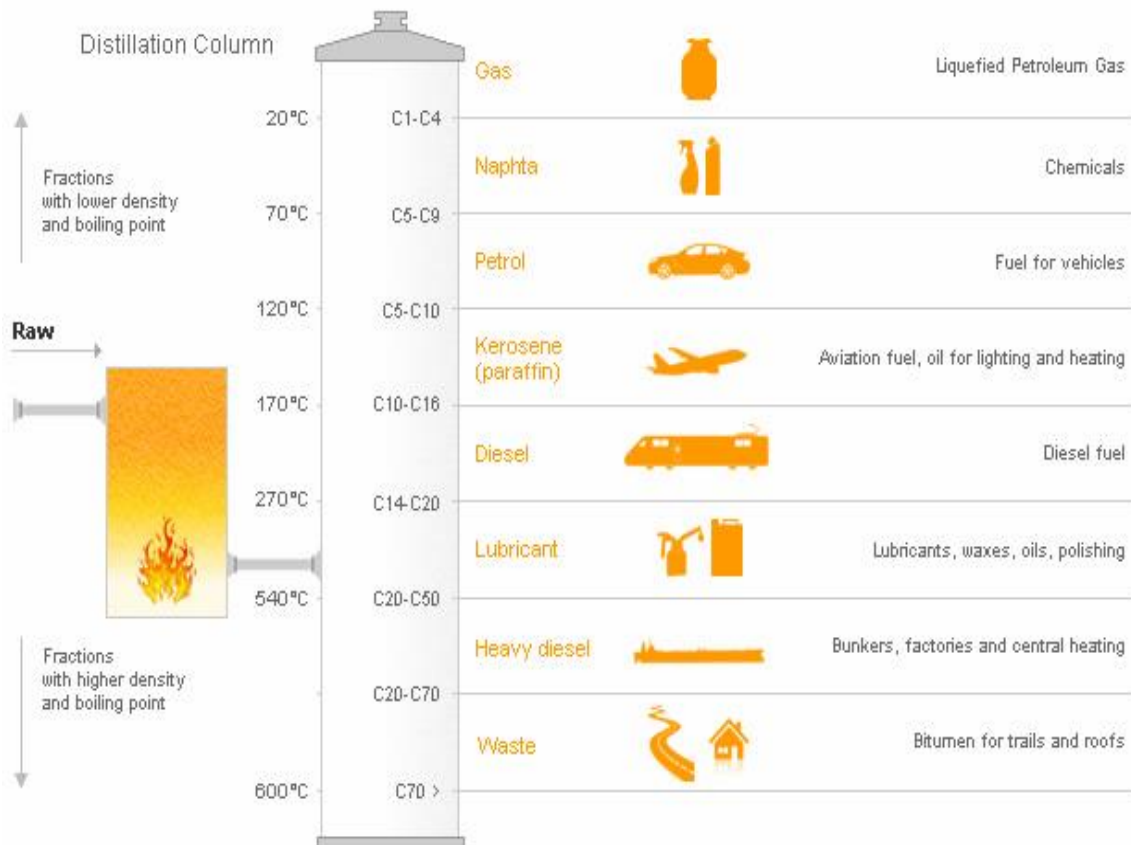


Figure 2-7: showing the fraction temperatures and chain lengths taken from Energia (2010)

Refineries can be optimised (both in terms of design and operation) to process crudes in a variety of ways. The refineries of North America tend to be optimised to produce light distillate products such as gasoline, whereas European refineries tend to be orientated towards the production of middle distillates such as Diesel and Jet fuel (Energia, 2010). In addition, older refineries tend to be optimised to produce more gasoline due to the fact that it is only relatively recently that diesel cars have made diesel a more popular commercial fuel.

A conference paper by (Blanco *et al.* 2005) discusses crude oil processing and planning throughout the whole supply chain. It also covers the important issue of optimizing refinery blending processes. Refinery blending is essential to refinery economics because by having an effective blending model the refinery can be operated at the best possible margin.

For example, light sweet (those with less than 0.5 weight percent sulphur) crudes (such as Brent or Arab Light) command a higher price than heavier sour crudes (such as those from Venezuela or the Canadian Tar Sands). Thus to keep down costs and maximise margins crudes are blended before the CDU. The object of the blend optimisation is to minimise the cost of the blend whilst still meeting current refinery operating constraints (such as Sulphur, API, TBP etc.).

Extensive work has been carried out on the subject of scheduling refinery crude oil operations and processing. Mouret (2010) produced an extensive Ph.D. dissertation on the subject of scheduling refinery operations, in the thesis the problem of scheduling refinery processes is approached by using both linear and non-linear mixed integer procedures.

Blending of crude oils to maximise refinery economics is a key theme for the Eng.D project. The organic deposition work was sparked by the identified need to develop a methodology to assess stability of blended crude oils. This is becoming more important with the increased amount of low cost (but also not well understood) opportunity oils in the marketplace such as U.S. shale oils and Canadian tar sands.

2.5 Primary Reference Data

No two crude oils are the same, each has unique molecular and chemical characteristics resulting in crucial differences in crude oil quality. These in turn have an effect on the valuation of each individual crude.

The physical testing results of the individual fractions contained within each crude provide extensive detailed analysis data for refiners, oil traders and producers. The data also helps producers design new refineries to maximise product output and or type according to the feedstock provided.

Existing refineries can determine if a new crude feedstock is compatible, or if the crude could cause yield, quality, production, environmental and other problems. Feedstock assay data is used for detailed refinery engineering, client marketing purposes and an important tool in the refining process.

To generate the data used within the chemometric models, ASTM methodologies for crude oil analysis are applied to generate the primary reference data. The case studies presented later focus primarily on distillation data, density and sulphur content so those will now be described.

2.5.1 *ASTM D2892/D5236 – Distillation Curve*

Used to produce True Boiling Point (TBP) curve for the determination of the %wt or %vol against temperature curve and also to produce fractions for further analysis. This distillation corresponds very closely to the type of fractionation obtained in a refinery.

The method is split over two stages, firstly the atmospheric (D2892) still is charged with crude oil and then distilled up to 350°C. The residue from this distillation is then taken and charged to the high vacuum (D5236) still where it is then taken to 565°C.

Combining the two methods then gives a full distillation profile of the crude oils which can be used for optimisation. It will be seen in the later case study however that the crossover can create variability in the dataset and make this region difficult to model. This can be seen in the below table where the reproducibility in wt% over this the crossover (circa. 350°C) is higher than the other fractions until 565°C+ is reached, this also has a high reproducibility as the amount of residue in a crude oil can vary dramatically depending on its molecular composition

Method	Cut	ASTM Reproducibility (wt%)
D2892	W_IBP-45	1.3
	W_45-60	1.3
	W_60-75	1.3
	W_75-90	1.3
	W_90-105	1.3
	W_105-120	1.3
	W_120-135	1.3
	W_135-165	1.3
	W_165-200	1.3
	W_200-250	1.4
	W_250-300	1.4
	W_300-350	1.4
D5236	W_350-400	2.7
	W_400-450	2.5
	W_450-500	2
	W_500-550	2
	W_550-565	2
	W_565°C+	2.9

2.5.2 ASTM D5002 - Density

Price for crude and processing needs are usually initially based on density. Used in conjunction with other analysis density can be used to give approximate hydrocarbon composition and heat of combustion.

The ASTM method uses a digital densitometer and stipulates the results must be reported in grams per centimetre cubed (g/cm^3) to 4 decimal place accuracy. Density is a quick and simple test for crude oil quality and is subject to the following reproducibility:

$$0.00412 * X \quad (2-1)$$

Where X is the average of two results. To critique modelling data this is taken as the average of the laboratory data and the prediction generate by the chemometric model for the same sample.

2.5.3 *ASTM D4294 - Sulphur*

High sulphur content in petroleum products may be undesirable as it can be corrosive and create an environmental hazard when burned. For these reasons, sulphur limitations are specified in the quality control of fuels, solvents etc. Hydrogen sulphide deactivates catalysts; feed pretreating can be used to remove these materials.

A hydrotreater is used to convert organic sulphur and nitrogen compounds to hydrogen sulphide and ammonia, which are then removed from the system with the unreacted hydrogen. The hydrogen required is obtained from the catalytic reformer. Sulphur is removed to reduce or eliminate corrosion during refining, handling or in the use of various products. To produce products with an acceptable odour and specification and to improve burning characteristics of fuel oils.

In the laboratory Sulphur is measured using X-Ray Diffraction (XRD) and is subject to the following reproducibility

$$1.9182 * ((X * 10,000) ^ 0.6446) / 10000 \quad (2-2)$$

Where X is once again the average of two results. To critique modelling data this is taken as the average of the laboratory data and the prediction generate by the chemometric model for the same sample.

2.6 Spectroscopy

Shown in Figure 2-8 is the spectrum of light. It clearly shows the well-known groups of the electromagnetic spectrum including microwaves, X-Rays, UV and Infrared.

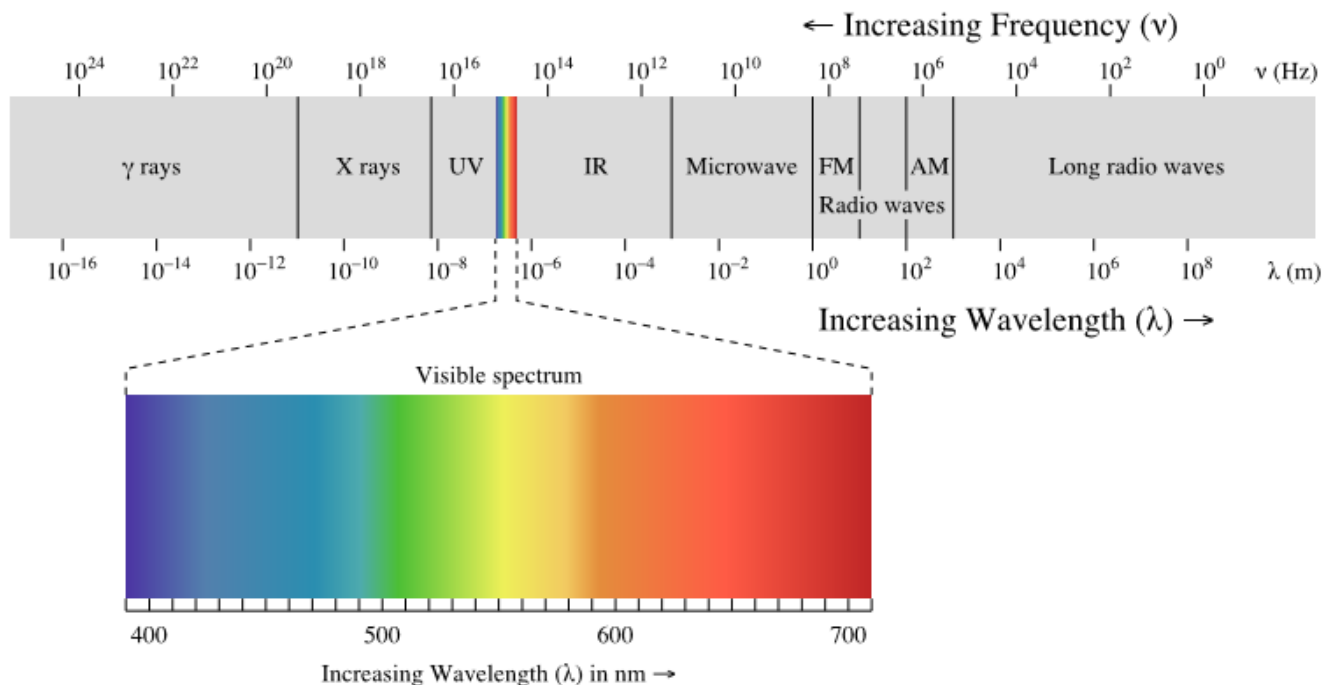


Figure 2-8: The spectrum of light taken from NG (2012)

Typically, areas of the electromagnetic spectrum are expressed in terms of the distance between the peaks of the waves; in the diagram this is shown in meters, it can also be expressed in terms of frequency or the number of waves per second (for which the units are Hertz).

In chemometric applications different regions are described in terms of wavenumber or the number of waves per centimetre (give units of cm^{-1}). This is primarily for convenience because wavenumber is directly proportional to photon energy as shown below.

If wavenumber (ν') is equal to reciprocal wavelength (λ):

$$\nu' = \frac{1}{\lambda} \quad (2-3)$$

The energy of a photon (E) is equal to Planck's constant (h) multiplied by frequency (f):

$$E = hf \quad (2-4)$$

And the relationship between velocity (v), frequency and wavelength is:

$$v = f\lambda \quad (2-5)$$

By substituting the velocity of a photon as the speed of light (c) the equation becomes:

$$c = f\lambda \quad (2-6)$$

Rearranging:

$$f = \frac{c}{\lambda} \quad (2-7)$$

And substituting back into Equation (2-4):

$$E = hc \times \frac{1}{\lambda} \quad (2-8)$$

$$E = hcv' \quad (2-9)$$

2.7 Near Infrared

The Near Infrared Region covers the 4000cm^{-1} to $12,820\text{cm}^{-1}$ region (780nm to 2500nm) and contains regions known as the combination region and overtone regions. NIR has been used in the hydrocarbon processing industry for decades, primarily for fuels blending (Rohrback, 1991). The attraction of NIR is due to its strong response to functional groups such as methylinic, olefinic or aromatic C-H stretching vibrations that are independent of the molecule (Kelly and Callis, 1990; Aske *et al.*, 2001).

Near Infrared is a particular focus of this thesis because it has the ability to describe changes in both the chemical composition of a hydrocarbon stream (Blanco *et al.*, 2000; Chung and Ku, 2000) and the physical composition of a hydrocarbon stream (Gossen, MacGregor and Pelton, 1993; Pasikatan *et al.*, 2003). This has a twofold implication for the analysis of crude oils, that the chemical changes in blended oils change and therefore so do the spectra, and also that if any

non-linear behaviour occurs (such as particle flocculation) that this should also be picked out in the spectra.

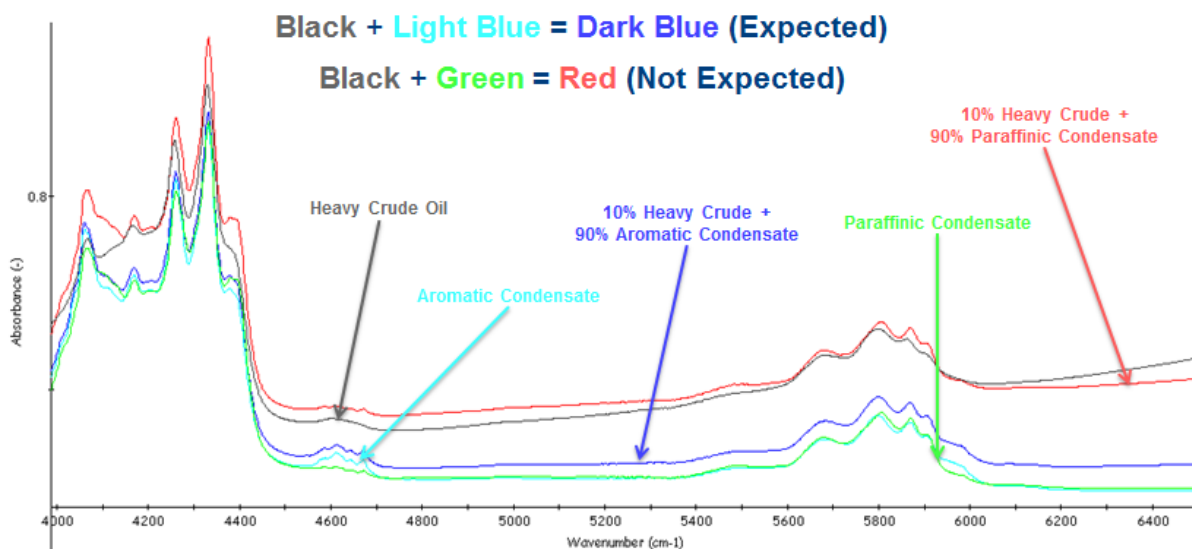


Figure 2-9: Different Crude Oil Spectra Baselines

Light scattering by flocculation of particles is exhibited as a distinct change in the spectral baseline as a consequence of light scattering. Figure 2-9 shows spectra generated as part of the Eng.D project. The basic postulate of spectral blending dictates that for two similar substances the spectra blend linearly, in the figure it can be seen that this is the case for the heavy crude and aromatic condensate, but not true for the heavy crude and paraffinic condensate. This is due to light scattering caused by particle precipitation as a consequence of blending the crude oils.

2.8 Applications of Infrared Spectroscopy in the Hydrocarbon Processing Industry

Both mid and near infrared are versatile spectroscopy methods used throughout the whole of industry for a multitude of purposes. In the oil and gas sector (both upstream and downstream) much evaluation work has been carried out on both methods. Much of the early work on spectroscopy in the field of hydrocarbon processing has been on refined fuels, particularly gasoline. A range of techniques and combinations thereof have been explored to improve the prediction of gasoline properties, with Octane Number being of particular interest.

However, very little has been written on the subject of the application of NIR to crude oils and this is due to the belief that standalone NIR applications are of limited scope because they cannot identify individual molecules (Hsu and Robinson, 2006).

Other work demonstrates that this is not strictly true and the Eng.D project has proven that with the application of good chemometrics, extensive crude oil data can be predicted from NIR spectra. For example Hidajat & Chong (2000) built PLS models to predict distillation data and density of 110 crude oil samples. In their work, they report that the correlations were very good and the predictions had reproducibility limits equivalent to those stated by American Society for Testing and Materials, a benchmark for global laboratories and the standard against which the models in the Eng.D project were compared.

An evaluation by (Chung *et al.* 1999) on kerosene found that in a comparative study of MIR and NIR modelling with PLS that although both techniques showed good correlation with the reference method, NIR provided better calibration performance over MIR. NIR was also found to have a greater signal to noise ratio than MIR. This meant that although more qualitative information could be gained from the MIR spectra (due to the specific, sharp and highly absorbing peaks); the NIR gave more spectral variation and quantitative information necessary for PLS modelling.

NIR and MIR was compared by (Felicio *et al.* 2005) for the prediction of Research Octane Number (RON) for gasoline and flash point for gas oil. Models of NIR and MIR spectra were built individually and a combined model was also created using single PLS, multiblock PLS (MB-PLS) and Serial PLS (S-PLS). The single PLS models were found to be the preferable method as they achieved accurate results and in a reasonable time. The overall best predictive results however were achieved using S-PLS which consistently achieved better results than both single PLS and MB-PLS on both MIR and NIR and proved to be a robust model. MB-PLS was found to give results that were an average between the single PLS and S-PLS. This was offset however by the fact that S-PLS is a time consuming and computationally expensive algorithm for which only marginal predictive gains were achieved.

When comparing the three PLS methods, MIR gave a smaller Root Mean Squared Error of Prediction (RMSEP) for benzene (6.41 for MIR versus 12.80 for NIR) when predicting gasoline properties, however, NIR was much better when predicting flash point for gas oil (2.98 for NIR versus 3.38 for MIR). NIR was also superior when predicting RON number in gasoline (0.52 for NIR versus 1.83 for MIR).

A comparison of three techniques (NIR, MIR and Raman spectroscopy) was carried out by Qiao & Kempen (2004) for characterising amino acids in animal feeds. This investigation found

that although NIR is the quicker and easier system for scanning and characterising the samples that MIR actually yielded better results, this is because for this particular application it achieves better quality spectral responses. However, the paper does state quite firmly that the MIR system requires a much more stringent and complicated sample handling; also, the samples must be finely ground, as the system used was not ideal for solids. In this investigation Raman spectroscopy was found to be an unsuitable method due to its susceptibility from noise, to the extent that Qiao & Kempen (2004) abandoned building a calibration model for Raman spectroscopy. This investigation while applicable to the thesis in its comparison of spectral methodologies also demonstrates the strengths of using NIR for predictive purposes by demonstrating the wide applications of spectroscopy and modelling in other industries.

Later work on NIR and MIR spectroscopy has been compared by (Gaydou, Kister and Dupuy, 2011) for detecting adulteration of diesel and biodiesel blends in vegetal oil using Hierarchical PLS (H-PLS) and S-PLS regression analysis. H-PLS is a methodology that forms a PLS variable matrix with PCA scores and performing the regression on several concatenated PCA score matrices. The analysis suggested that NIR gave better predictions than MIR giving consideration to the pre-treatment and selected variables in the analysis. The study also concluded that the H-PLS gave slightly better predictive performance than S-PLS.

Balabin & Safieva (2008) analysed three different classification methods for gasoline and gasoline fractions, linear discriminant analysis (LDA), soft independent modelling of class analogy (SIMCA) and multilayer perceptron (MLP). Classification work of this type is important in terms of both quality control and also in cases of gasoline adulteration and contamination (Balabin and Safieva, 2008). The most effective method found in this study was MLP with an average classification error of 12% in comparison to an average error of 20% for LDA. It is important to note that in this study no pre-processing was carried out on the spectra to attempt to improve the model discrimination, it was also only a small dataset and thus it is possible there was not sufficient data variability for modelling.

In a paper by (Balabin, Safieva and Lomakina, 2007) 6 different regression techniques are applied to NIR spectra for predicting properties of gasoline. These are multiple linear regression (MLR), principal component regression (PCR), linear PLS, polynomial partial least squares regression (Poly-PLS), spline partial least squares regression (Spline-PLS) and artificial neural networks (ANN)(Balabin, Safieva and Lomakina, 2007). The three PLS techniques used investigate both linear and non-linear PLS. The regular PLS algorithm is a linear method of

data analysis. However, by changing one step in the algorithm, it can be transformed to a non-linear analysis technique. In poly-PLS the function is altered to polynomial and in spline-PLS a spline (or piecewise polynomial function) is added (Balabin, Safieva and Lomakina, 2007).

The investigation found that the non-linear methods were the most effective predictive model, suggesting that the properties of gasoline are non-linear. In terms of predictive capability and minimising the error of prediction the order of the PLS models was found to be Poly-PLS>Spline-PLS>Linear PLS (Balabin, Safieva and Lomakina, 2007). For this particular investigation, the ANN model performed consistently the best in predicting all six of the gasoline components; this could be because of both its flexibility and non-linear nature.

NIR spectroscopy was used by Kardamakis & Pasadakis (2010) combining Linear Predictive Coding (LPC) and MLR as an integrated estimation technique. Using these methods, a model to predict RON numbers of gasoline was built with an RMSEP of 0.3. The model was applied to a large dataset of 384 samples showing this was a robust characterisation technique; also, no pre-treatment of the experimental raw data was used to build the model that was based on the Linear Predictive Coefficients.

NIR spectroscopy was used to build predictive models of gasoline by (Balabin, Safieva and Lomakina, 2012). In this study nine different multivariate methods were used to build gasoline models and their effectiveness compared. The nine methods investigated were LDA, quadratic discriminant analysis (QDA), regularized discriminant analysis (RDA), SIMCA, partial least squares discriminant analysis (PLS – DA), K-nearest neighbour (KNN), support vector machines (SVM), probabilistic neural network (PNN), and artificial neural network multilayer perceptron (ANN-MLP)'. The study found that when compared with other characterisation methods such as GC and NMR that NIR spectroscopy was comparable in results. The NIR spectral region chosen for this investigation was 8,000cm⁻¹ to 14,000 cm⁻¹.

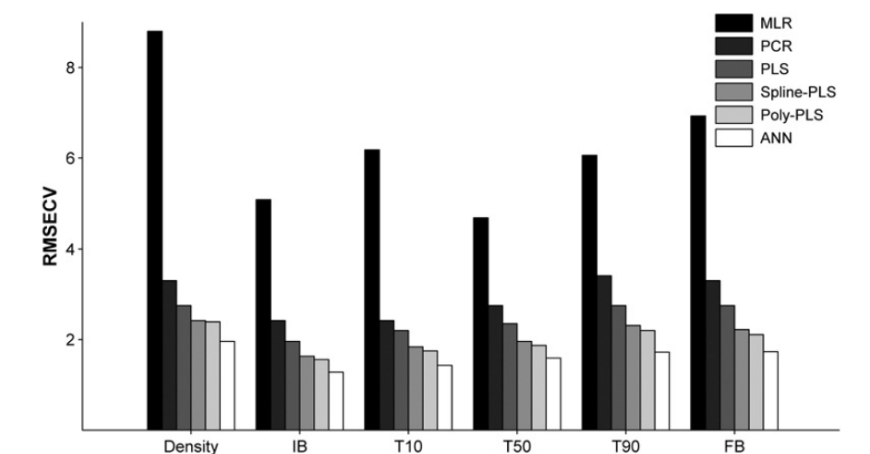


Figure 2-10: Showing the comparison of errors for several models used to predict the composition of gasoline taken from Balabin *et al.* (2007)

In another paper by (Balabin, Safieva and Lomakina, 2008) NIR was once again investigated as a tool for modelling gasoline composition. This time the paper focused on two types of ANN, MLP and Wavelet Neural Network (WNN). The findings showed that WNN was more effective at predicting from the spectra than the MLP.

It can thus be seen that there are wide applications of Near Infrared in the process industry, this is due to the fact that there is a strong response to hydrocarbons within NIR spectra which allow a range of properties to be modelled. It is also quick which means that it can be moved from the laboratory to online, a major benefit within high throughput process industries.

It should be noted however that to date, although there has been much work undertaken on modelling gasoline and fuels using NIR, very little work has been undertaken in the area of crude oils, this is because crude oils are a much more complex system to deal with, with a much larger range of property values and more complex molecular makeups.

2.9 Gas Chromatography

Gas Chromatography is a chromatographic method for separating the volatile components of various mixtures in which the mobile phase is a gas. In its application to crude oil characterisation GC mimics a fractional distillation column but has the equivalent of up to 1,000,000 theoretical plates, meaning that its separation is very efficient (Speight, 2001). Being especially good at characterising gaseous material means that GC out performs conventional laboratory distillation when it comes to measuring the weight percentage of lower boiling point

components. However, at the other end of the spectrum, the large heavy and high boiling point constituents have a very high residence time and thus are not detected as easily by the GC.

GC is now the “preferred technique for the analysis of hydrocarbon gases, and gas chromatographic in-line monitors are experiencing increasing application in refinery plant control” (Speight, 2001). The system works by having a gas (usually nitrogen, helium or argon) that flows continuously through a column (usually made of glass, copper or stainless steel) which is 3 – 6mm in diameter and 1 – 2m long and packed with a solid with a large surface area (commonly diatomaceous earth or crushed firebrick) impregnated with a non-volatile liquid (Speight, 2001). The sample (1 - 5 μ L) is then injected into the column by syringe through a sample port, the liquid is vaporised into the carrier gas and carried into the column. The sample is then transported through the column and the separation occurs by partitioning of the gas and liquid phases, meaning that even a small difference between components can cause a large separation (Speight, 2001). On exiting the column, the sample passes a detector registering a peak on a graph, and the time between injection and the detection is measured giving what is known as the retention time. Shown in Figure 2-11 is a representation of the GC equipment.

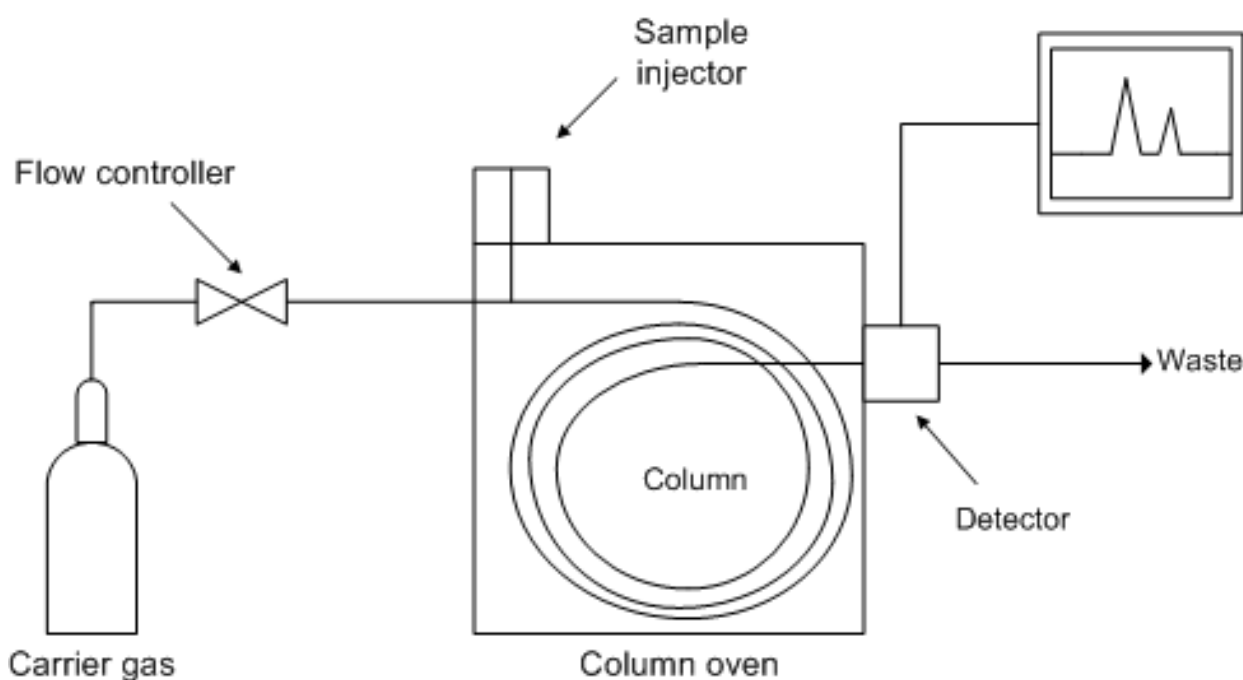


Figure 2-11: A representation of the GC equipment taken from Sheffield Hallam (2010)

Development work on the characterisation of crude oil by GC has been carried out for many years. Burg *et al.* (1997) used gas chromatography to characterise 47 crude oils. They achieve this by measuring the polarity parameter and coefficients of the Linear Solvation Energy Relation (LSER). These parameters inputted into a descriptive equation provided better crude

oil characterisation than by just using standard chromatographic polarity (Burg, Selves and Colin, 1997). The study found that characterisation of 47 crude oils using this method gave good agreement with the chemical composition measured by other methods.

However, the main drawback of the GC method versus NIR is the time taken to undertake the analysis. A typical GC run can take 30 minutes and with data interpretation, to generate a boiling point distillation for a crude oil takes in the region of 1 hour, whereas an NIR spectrum takes 30 seconds and linked to a chemometric model, property generation takes only a few minutes.

2.9.1 *Nuclear Magnetic Resonance*

Nuclear Magnetic Resonance (NMR) spectroscopy is a relative new technique under investigation for the characterisation of crude oils. NMR directly measures aromatic and aliphatic carbon as well as hydrogen distributions. The most common types of NMR spectroscopy in use utilise the Proton (^1H) and carbon-13 (^{13}C) nuclei, however, for specialist petroleum analyses, nitrogen (^{15}N and ^{14}N) and sulphur (^{33}S) have also been used (Speight, 2001). To perform an NMR analysis only a small amount of sample (<10mg) is needed, dissolved in a solvent such as deuterium-chloroform. It is placed in a glass tube approximately 5mm in diameter, which is then placed in a homogenous magnetic field surrounded by one (or more) coils. If the hydrogen nuclei are imagined to be small magnets these interact with a weak radio frequency emitted by the coils, at the correct frequency the nuclei resonate and the spin resonance is detected by a receiver coil (Speight, 2001). The sample position relative to the standard of tetramethylsilane (TMS) is then reported as a chemical shift (δ) which can then be characterised using reference tables.

Work on the characterisation of crude by Flumignan *et al.* (2012) looked at the use of ^1H NMR profiles in predicting a whole manner of physiochemical properties of crudes, such as density, distillation curve, octane numbers etc. To model the spectra standard PLS modelling was used. The investigation found that NMR-PLS modelling gave good results when compared to ASTM standard reproducibility's. Excellent accuracy and precision were also reported. Also the ^{13}C NMR spectra was used in conjunction with Principal Components Analysis (PCA), PLS and PCR to discriminate olive oils and attempt to detect any adulteration in a study by Shaw *et al.*, (1997). The study found that of 66 samples predicted, 65 predicted correctly and the models achieved consistent predictions of over 90% of the samples.

2.10 Organic Deposition

A significant portion of the Eng.D investigation was in the field of crude oil stability and Organic Deposition (OD) in the hydrocarbon supply chain. From production wells to refined products OD (particularly from wax and asphaltenes) causes serious processing problems. As part of this work a close relationship has been established with several refineries across the world, including North America, Europe and Asia. The work has also resulted in patented approaches for the quantification and mitigation of instability in blended hydrocarbon streams.

These approaches have already been applied to numerous applications in the hydrocarbon processing sector including: evaluation of the impact of new well streams offshore, crude oil blending in refineries, heavy fuel oil blending in refineries and marine fuel blending on ships. Many future projects have also been identified and are being actively pursued.

However, process NMR applications are very costly to install (at least 10 times the cost of online NIR) and are very difficult to keep clean, particularly if the refinery is processing very heavy crude oils.

2.11 Background to the problem

The petroleum refining industry aims to optimize its oil production and hence increase its crude oil supply chain by blending more crude oils and increase the use of heavier crude oils to minimise the costs of the blend to the crude distillation unit (CDU). One of the principle issues experienced by many refineries is the precipitation of organic material such as asphaltene and crystalline organics. These problems can be instantaneous, as the crudes are being blended, or the problems can develop over time.

When crude oil is produced it typically contains solids, liquid and gases. The mixture may become more or less stable for a variety of reasons including pressure, temperature, and blending. Less stable crude may precipitate organic solids including asphaltene. Methods have been developed for assessing both solubility and insolubility of asphaltenes in crude oils, primarily using Toluene and n-Heptane (Wiehe and Kennedy, 1999, 1999).

2.12 Refining Economics

The biggest cost to a refinery on a global basis is the cost of crude, and although this has recently fallen refineries continue to source lower cost oils for blending to maximise margins. These opportunity oils have affected market and refinery economics globally; this problem particularly affects European refineries (Figure 2-12, Figure 2-13 and Figure 2-14) due to their aging designs and stringent EU environmental legislation.

Figure 2-12 also shows that the majority of European refineries are in the first quartile when compared to Former Soviet Union (FSU) and African refineries. However, when other factors such as domestic tariffs or crude oil availability are taken into account this is not necessarily a true benchmark of a refineries ability to be profitable. This reinforces the need for refiners to have a thorough understanding of neat crude composition as well as the interactions between crudes during crude blending as it is only through a full understanding of this can process be optimised and margins maximised, thus maintaining a competitive edge. Recognition of this need is a driver for improvement of existing technology and innovation of new technology.

Figure 2-13 shows European refineries identified as most at risk, many have already have already been forced to close with many smaller refineries making less than \$1.00 per barrel net cash margin (NCM), indeed Coryton refinery identified as being at risk in this graph has since closed.

2.12.1 *Net Cash Margin*

NCM is a method of expressing a refineries economics and is defined as:

$$\text{NCM} = \text{Refinery Gross Margin (RGM)} - \text{Operating Costs}$$

Where:

Refinery gross margin = the sum of barrels of each product multiplied by the price of each product (PetroleumOnline, 2012)

Operating Costs = Costs to operate refinery, excluding income taxes, depreciation and financial charges (PetroleumOnline, 2012)

According to Wood-Mackenzie (2012) the benchmark figure for refinery performance is an NCM of \$1 per barrel. Figure 2-14 shows European refiners and their respective NCM. It can

be seen that refiners achieving <\$1/bbl. have been identified as being most at risk. It is also interesting to note that since this work the company Petroplus, identified on this plot as being at high risk of closure has indeed gone bankrupt.

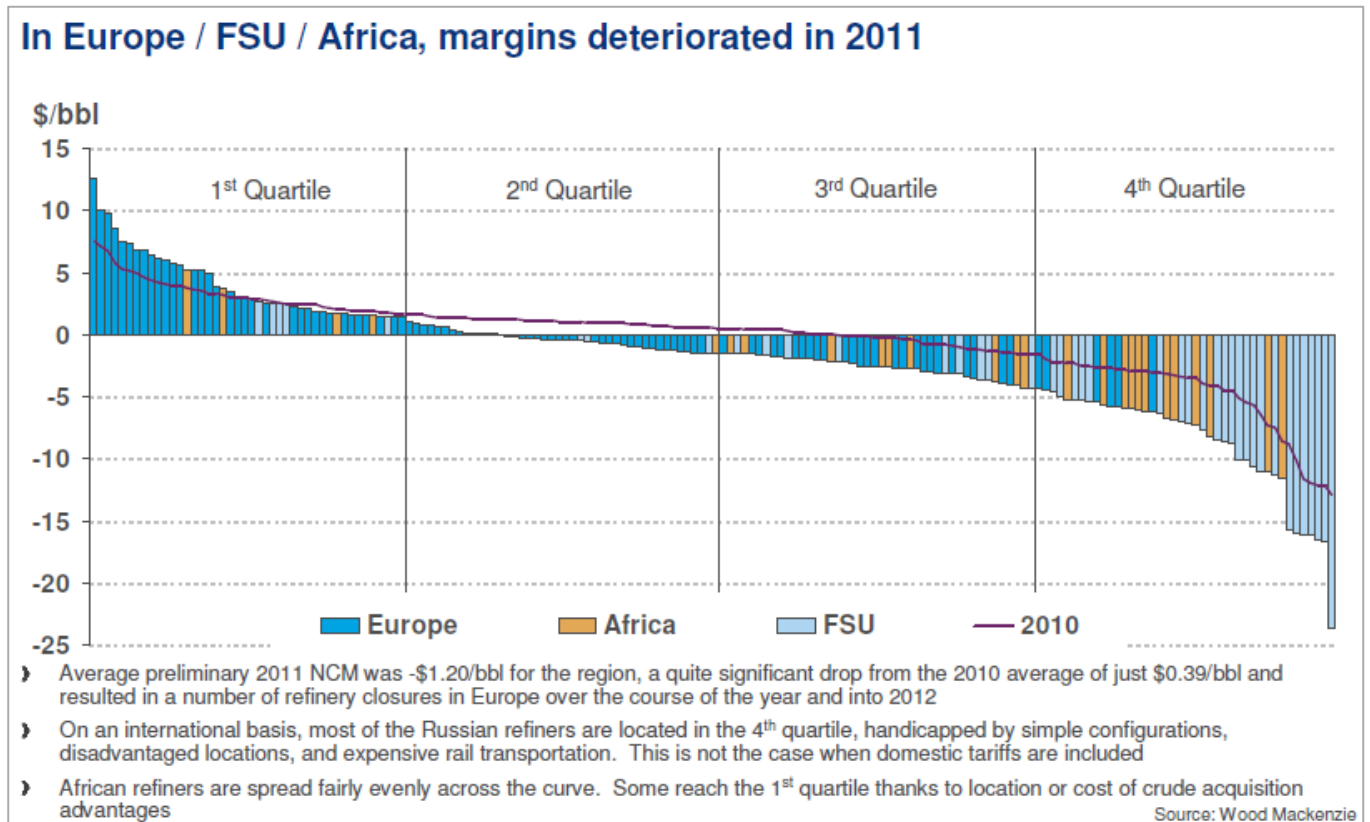


Figure 2-12: A plot comparing margins of refineries in Europe, FSU and Africa taken from Wood-Mackenzie (2012a)

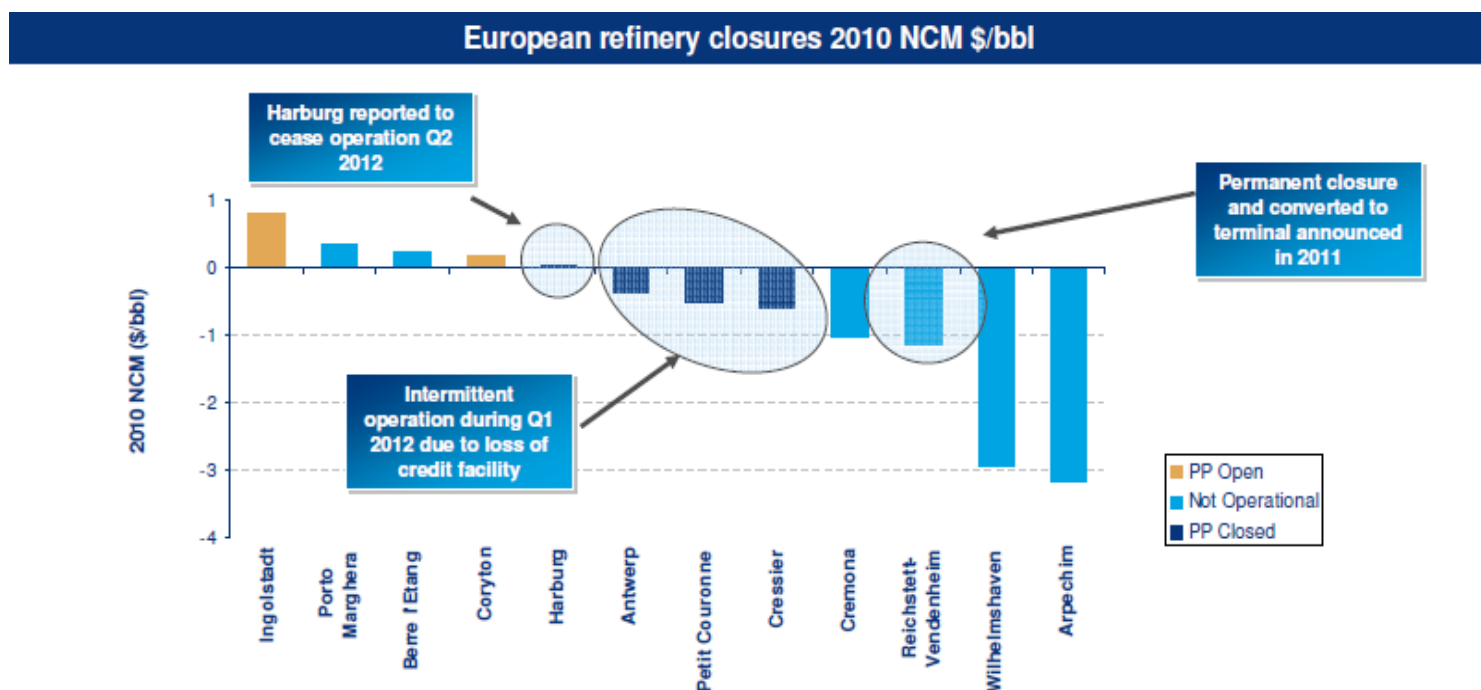


Figure 2-13: Showing NCM in \$/bbl. for a selection of major European refineries taken from Wood-Mackenzie (2012a)

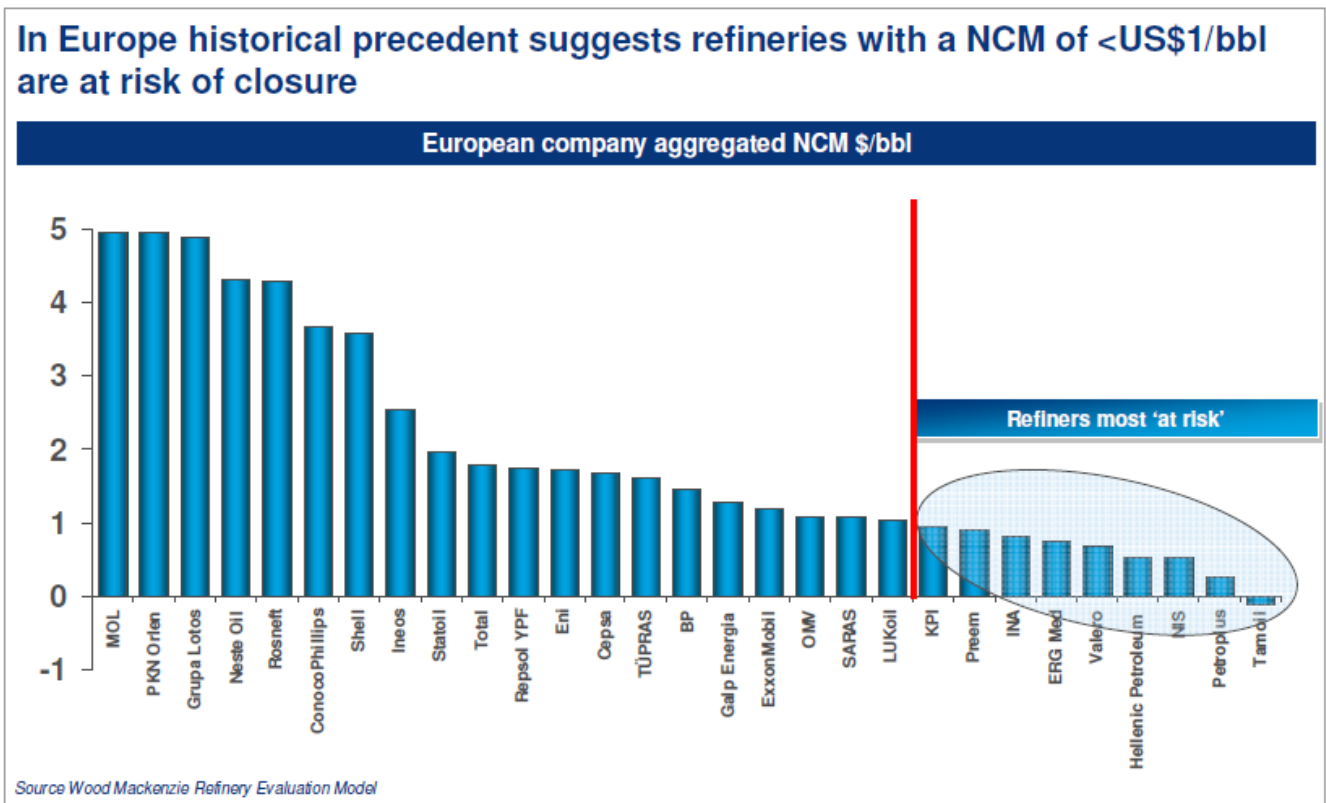


Figure 2-14: Showing NCM in \$/bbl. of major European Refiners taken from Wood-Mackenzie (2012a)

2.12.2 Margin Improvement Strategy?

To improve margins refineries are having to process lower cost heavier crude and blend with lighter crude to achieve optimum crude composition and lower the overall cost of crude purchases. This however brings its own problems. Although the crudes are cheaper they also contain higher amounts of asphaltene and wax, constituents that cause problems when processing a crude oil.

2.13 Asphaltenes

Asphaltenes are a solubility class of the crude oil and composed of many different molecular configurations, generally accepted to be the heaviest and most polar fraction of crude oil, soluble in toluene and precipitating in light alkanes such as pentane, hexane and heptane (Aske, 2002a). Figure 2-15 shows the effect of a range of solvents on the asphaltene solubility of Souedie crude oil, these have been ranked in order of solubility parameter and the crude oil is positioned according to its flocculation parameter (δ_f).

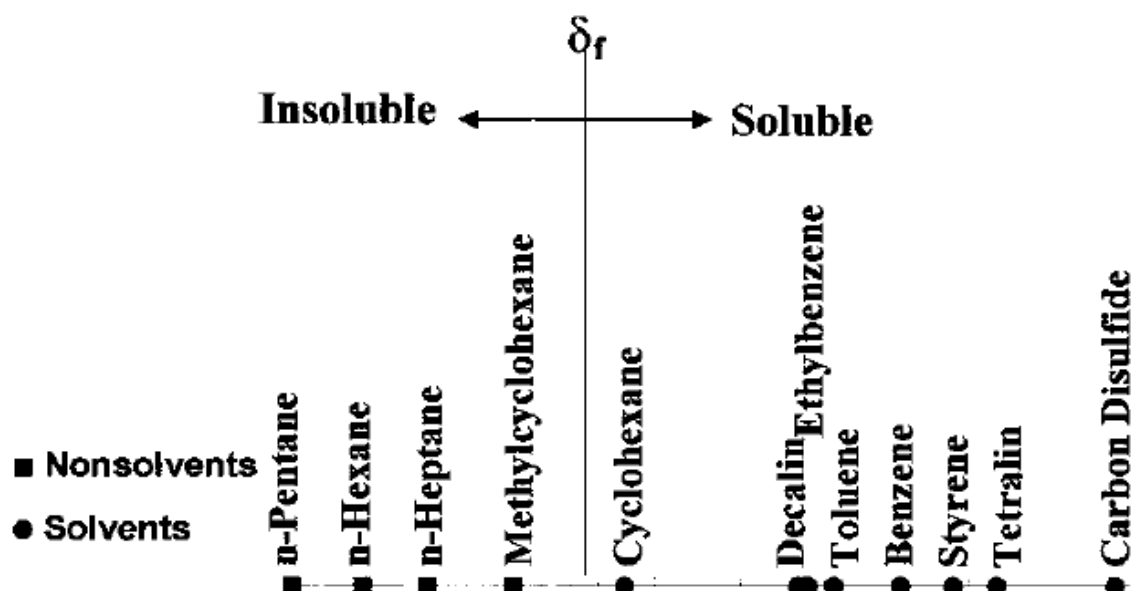


Figure 2-15: Solvents and precipitants for asphaltenes taken from Wiehe and Kennedy (2000b)

Figure 2-16 shows a hypothetical asphaltene molecule, as it can be seen it is a very large molecule, the molecular weight of asphaltene is believed to be in the range of 500 – 2000 g/mole (Aske, 2002a). Asphaltene molecules also contain a high number of heteroatoms and organometallics, they also have the lowest carbon:hydrogen ratio of any component of crude oil. This makes them a good candidate for coking and production of other products such as carbon black.

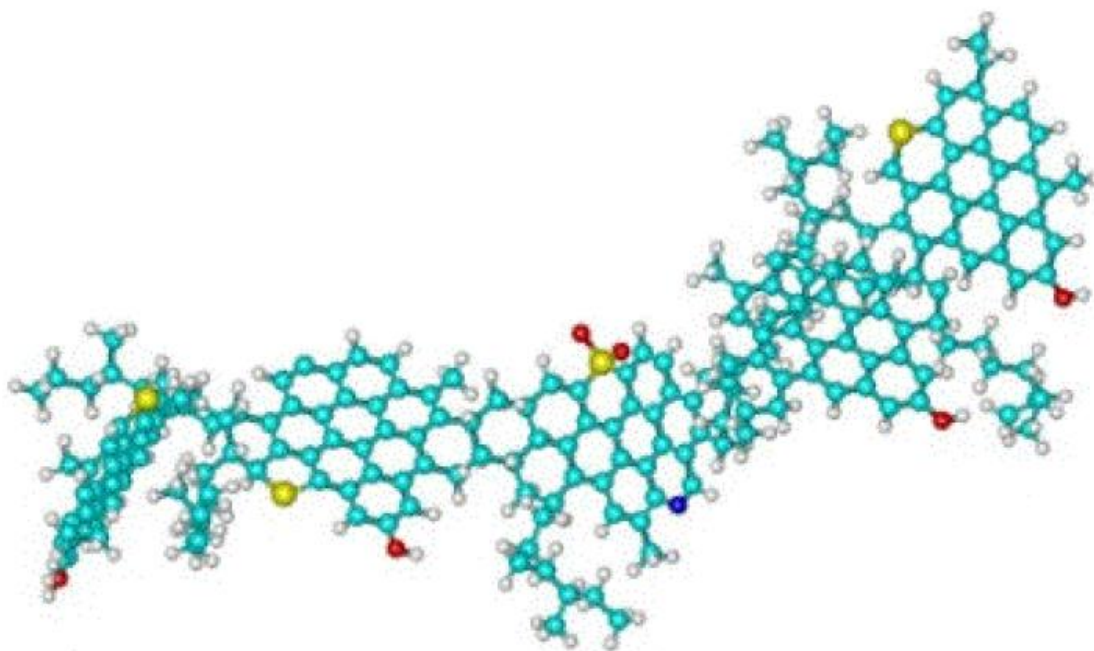


Figure 2-16: A hypothetical asphaltene molecule taken from Aurdal *et al.*, (1998)

2.14 Oil compatibility model and SARA relationship

Crude oil is a complex mixture, composed of a multitude of different components. For ease of classification crude is commonly described in terms of four constituent components, Saturates, Aromatics, Resins and Asphaltenes (SARA). The saturate fraction consists of nonpolar material including normal (or straight chain), branched, and cyclic (also known as naphthenes) saturated hydrocarbons. The aromatic constituents contain one or more delocalised ring structures, and are also much more polarizable. Both resins and asphaltenes have polar substituents, however the distinction between the two is that asphaltenes are insoluble in an excess of heptane (or pentane) whereas resins are miscible with heptane (or pentane) (Fan, Wang and Buckley, 2002).

This exists as a balance in crude oils, which maintains a stable colloidal system. Figure 2-17 shows a physical model postulated by Wiehe & Kennedy, which describes how the SARA components exist in a crude oil to maintain a stable system. According to Wiehe & Kennedy (2000) the largest, most aromatic molecules, the asphaltenes (A) are actually sub microscopic solids dispersed in the oil by the resins (R), the next largest, most aromatic group of molecules. This asphaltene-resin dispersion is dissolved into petroleum by small ring aromatics (a) that are solvents but opposed by saturates (s) that are nonsolvents. Thus, asphaltenes are held in petroleum in a delicate balance, and this balance can be easily upset by adding saturates or by removing resins or aromatics.

The problem with this system is that it is a fine balance, which can also be easily disrupted, this issue is observed in real life when crudes are blended. Wiehe & Kennedy have therefore developed a predictive model capable of assessing crude stability in terms of its behaviour in heptane/toluene systems. This means that using data obtained from laboratory assessments of neat crude oils in heptane and toluene their compatibility for blending can be predicted.

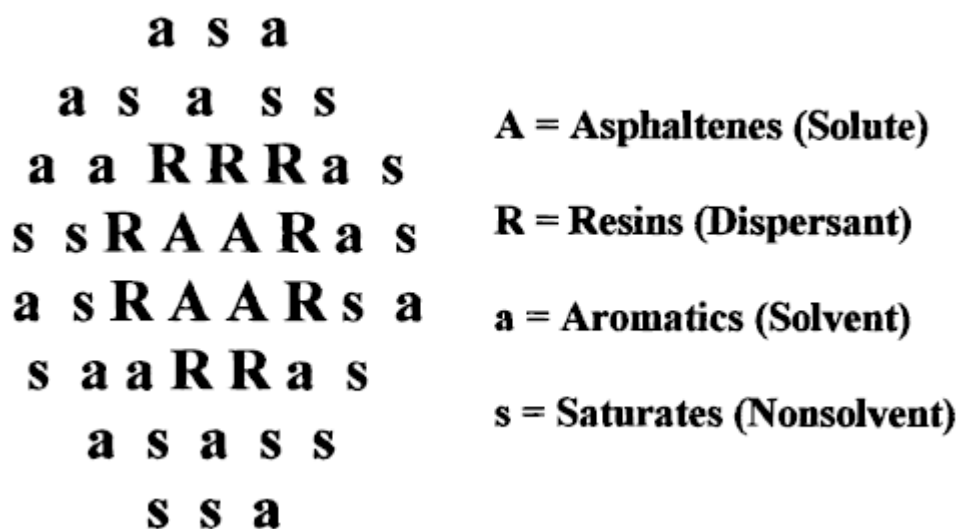


Figure 2-17: Physical model of a petroleum system, showing the SARA balance taken from Wiehe and Kennedy (2000b)

In another paper by Wiehe & Kennedy this model was applied to a real refinery process (Wiehe and Kennedy, 2000a). This application examined a fixed bed hydrotreater, a refinery process for removing impurities such as sulphur, nitrogen, oxygen and metals (Jechura, 2016), blocked by precipitation of asphaltenes, a problem caused by the incompatibility of oils in the feed to the hydrotreater. According to Wiehe & Kennedy insoluble asphaltenes coked a heat exchanger upstream of the hydrotreater; this blockage then flaked off the heat exchanger and plugged the catalyst bed. By applying the oil compatibility model to this system, the feed stream to the hydrotreater was kept within the stability limits for the feed components, thus avoiding future plugging of the catalyst bed.

2.15 Investigating asphaltene precipitation and behaviour

Many studies have been carried out with the intention of studying asphaltene precipitation and behaviour. Marks (2005) investigated the effects of the precipitation of asphaltenes using CO₂. In the study marks monitored the viscosity of fluid using NMR relaxation times as a method of monitoring the process of asphaltene precipitation. To conduct this study CO₂ was injected into crude samples over varying times and under varying conditions. The bubbling of CO₂ through the sample caused a shift in the NMR spectra typically associated with asphaltene precipitation. This was further backed up by a solid precipitate left in the bottom of the container when the liquid was decanted off. This research is in an important area due to the usage of CO₂ in the hydrocarbon industry as an EOR mechanism as discussed in section 2.3.1.

Gawrys & Kilpatrick (2004) made a study of techniques for observing aggregation of asphaltene particles, primarily Pulse-Field Gradient Spin Echo Nuclear Magnetic Resonance (PFG-SE NMR), Small Angle Neutron Scattering (SANS), NIR and Vapour Pressure Osmometry (VPO). In the analysis they observed that NIR is a quick, simple and non-invasive method of studying flocculation and can be used to observe aggregation with changes in temperature, pressure, solvents and additives. However, they note that NIR is not a particle sizing method and although it can see the onset of aggregation it cannot be used to quantify particle size. This is in stark contrast to work by Gossen *et al.* (1993) and Pasikatan *et al.* (2003) where NIR was used for such a purpose, albeit not for determination of asphaltene aggregate size.

Morphology work was carried out using PFG-SE NMR is a “non-invasive, relatively fast instrumental technique to probe molecular self-diffusion coefficients using magnetic field gradients of varying strength to effect large signal attenuation” (Gawrys and Kilpatrick, 2004). Using this technique, it was determined that asphaltene aggregates are not spherical in shape but rather disc like.

The technique also proved that the addition of n-alkane to a model asphaltene solution induces asphaltene flocculation. VPO is a method that monitors change in vapour pressure when a small amount of solute is added to a pure solvent.

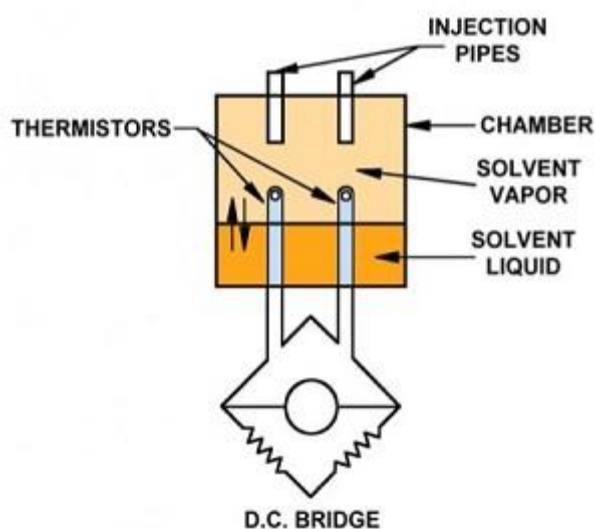


Figure 2-18: Showing a typical Vapour Pressure Osmometer setup taken from UCI (2016)

Figure 2-18 shows the typical apparatus setup which consists of a solvent reservoir with two wicks providing a saturated solvent atmosphere around two thermistors. Within this apparatus a solvent is condensed from the atmosphere into a solution containing the asphaltene placed at

one thermistor. This then releases heat and raises the thermistor temperature until the vapour pressure of the solution matches vapour pressure of the pure solvent. During this process small voltage changes are induced at the thermistor and these in turn can be related to the number-averaged molar (Gawrys and Kilpatrick, 2004) mass of the asphaltene.

Using this method Gawrys & Kilpatrick (2004) calculated molar masses of asphaltenes in different crude oils and observed them to differ depending on the solvent polarity and experiment temperature. Most importantly however the molar mass of asphaltene aggregates was found to be highly dependent on the concentration of asphaltenes in the solution. Figure 2-19 shows how the molar mass of asphaltene aggregates increases sharply with asphaltene concentration in solution before plateauing out, this plot also shows the effects of temperature on molar mass of asphaltene aggregates.

Finally SANS is a technique used for determine sizes and morphologies of agglomerates formed from colloidal solutions, SANS uses elastic neutron scattering at small angles to determine these attributes. To employ SANS deuterated solvents must be used however this is expensive. SANS analysis suggests that asphaltenes form highly porous aggregates and that asphaltene aggregate size increases with the resin content in the presence of insoluble asphaltenes.

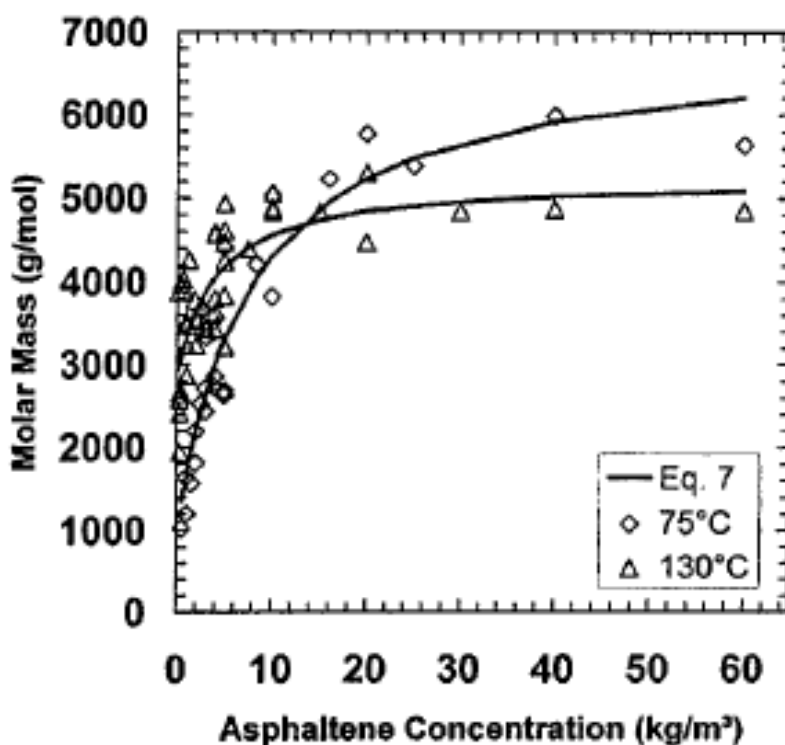


Figure 2-19: VPO determined molar masses in Athabasca bitumen taken from Gawrys and Kilpatrick (2004)

VPO and SANS was also used by Spiecker, Gawrys & Kilpatrick (2003). In this work asphaltenes were fractionated from four different crude oils using heptane and toluene, the fractions were then analysed using VPO and SANS. Studies conducted using these techniques indicated that the fractions generated from the crude oils that were less soluble formed asphaltene aggregates much larger than those sub-fractions which were more soluble. This described a general trend, which saw aggregate size increasing as a function of decreasing aromaticity of the solvent. It was also observed that the individual aggregate sizes increased to a maximum at the solubility limit and after that began to decrease. This was due to flocculation of individual asphaltene aggregates.

In another paper Spiecker *et al.* (2003) also employed SARA fractionation of crude oils combined with SANS analysis to analyse the effect of petroleum resins on asphaltene stability in crudes. It was found that addition of resins to the crude oil reduced the aggregate size of asphaltenes by interrupting the chemical bonding of asphaltene molecules. Increasing concentration of resins also reduced the interfacial tension of the asphaltenes, reducing the ability of asphaltenes to stabilise water in oil emulsions. It was also observed that reducing the amount of resin in crude rendered the higher molecular weight asphaltenes insoluble in solutions of heptane/toluene. Thus proving the importance, asserted by Wiehe & Kennedy (2000b) of resins for stabilising asphaltenes in crude oils.

Work by Tharnivasan (2012) centred around the whole area of asphaltene precipitation from crude oil blends and emulsions. The thesis main focus was to develop a model to describe the phase behaviour of these systems and to be able to predict the onset and amount of precipitation from oils and oil blends being subjected to depressurisation. The research and development work drew conclusions for three main areas: blends, live oils and the effects of water on asphaltene precipitation.

For blends, Tharnivasan (2012) developed a model which would predict unstable blends; however, the model did not work as well with high concentrations of diluents such as toluene. This is to be expected due to the definition of asphaltenes as the most polar toluene soluble fraction of crude oil, asphaltene precipitation becomes more difficult to force even with large amounts of saturates in the presence of large amounts of toluene.

In live oils, a methodology was developed which characterised live crude oils for solubility parameters of asphaltenes. Ultimately, a model was configured to predict precipitation onset

pressures for live oil, applied to depressurisation of crude oil in offshore applications. This model however was not very robust and was found to be very sensitive to certain variables, limiting its predictive performance, furthermore, the predictive performance of this model was only tested on a single light oil.

Tharnivasan (2012) also discovered that emulsified water had no discernible effect on the solubility of asphaltenes in solvents or in a crude oil above the onset of precipitation. It has to be noted however that the water used to conduct the tests was deionised water and this is not a true test because water used in offshore applications is usually brine and thus ion rich, indeed the thesis states that “the presence of ions may possibly interact with asphaltene molecules to alter the precipitation behaviour”.

Investigations into asphaltene solubility using Infrared (IR) techniques were carried out by Aske *et al.* (2001). Eighteen different crude oils and condensates were investigated, applying Near Infrared (NIR) and High Performance Liquid Chromatography (HPLC) to aid crude characterisation. The HPLC method was used to split the oils and condensates into their corresponding Saturates, Aromatics, Resins and Asphaltenes fractions. A diagram outlining this separation can be seen in Figure 2-20 below. It can be seen that the HPLC utilises different solvents to elute the four SARA fractions of the crude oil.

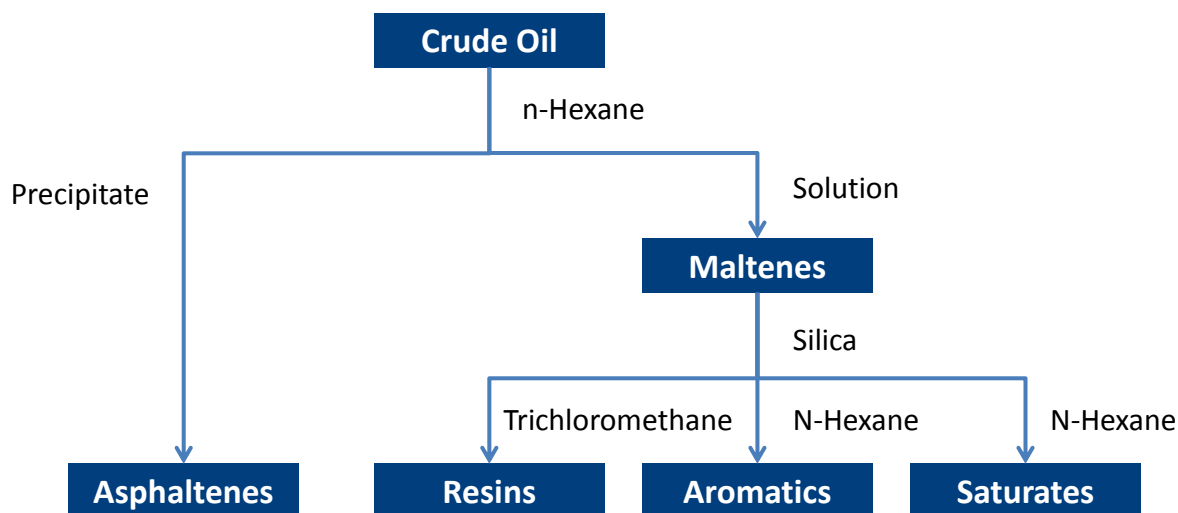


Figure 2-20: SARA Fractions Methodology taken from Lundanes and Greibrokk (1994)

Multivariate Analysis techniques such as Principal Components Analysis (PCA) and Partial Least Squares (PLS) the predictive capability of the spectra were assessed. In this paper Aske *et al.* (2001) discover that the spectra (particularly NIR) give good predictive models for the

SARA properties, with errors of prediction comparable in magnitude to the uncertainties of the HPLC method.

The SARA components of crude oils can also be separated using Open Column Chromatography (OPC). This method involves using a silica packed column and eluting the column with the solvents heptane, toluene and toluene/methanol. In a paper by Islas-Flores *et al.* (2005) OPC was compared with HPLC as a technique for separating crude oils into SARA fractions. It was determined however that HPLC gives a much sharper separation of the fractions, particular between the resin and nonpolar aromatic fractions. In OPC the fraction eluted in toluene has to be considered as part of the resin fraction however because the toluene and toluene/methanol eluting solvents fail to separate the aromatic fraction from the low polarity resins.

Aske *et al.* (2002) also investigated the aggregation of asphaltene by pressure depletion methods on live crudes. This particular paper explores offshore application problems where asphaltene molecules precipitate when the pressure is reduced during extraction of the oil. As with other work (Wiehe and Kennedy, 2000b; Spiecker, Gawrys and Kilpatrick, 2003; Tharnivasan, 2012) model systems of asphaltenes in toluene with n-alkane solutions were also studied to model ideal behaviour. The system was monitored during depressurisation by NIR and PCA. It was observed that a significant shift occurred in the principal component scores at the onset of asphaltene aggregation and this can be seen in Figure 2-21.

The experiments showed that the behaviour of the model system was very similar to that of real crude oils however, “while the asphaltene aggregation in the crude oil is more or less completely reversible with re-pressurization, indications of only a partial re-dissolution are seen in the model systems” (Aske *et al.*, 2002). It was found that to re-equilibrate the asphaltenes after precipitation a pressure of 300 bar and a time period of 72 hours was required, this not only demonstrates the stability of asphaltenes once precipitated but also highlights the difficulties faced with dealing with asphaltene deposition issues after precipitation. This study also shows that a combination of NIR and PCA is an effective system for detecting asphaltene aggregation. The setup of this system is such that it could also be easily taken online if necessary, indeed as part of the Eng.D research several online systems were evaluated and studied.

SARA fractionation was also carried out by Cho *et al.* (2012) and then the fractions were analysed using Fourier transform ion cyclotron resonance mass spectrometry (FT-ICR MS)

equipped with atmospheric pressure photoionisation (APPI). The analysis performed produced expected results, with each fraction containing compounds with expected behaviour and appearance, i.e. “the saturates fraction was composed of less aromatic molecules with long or multiple alkyl chains”(Cho *et al.*, 2012).

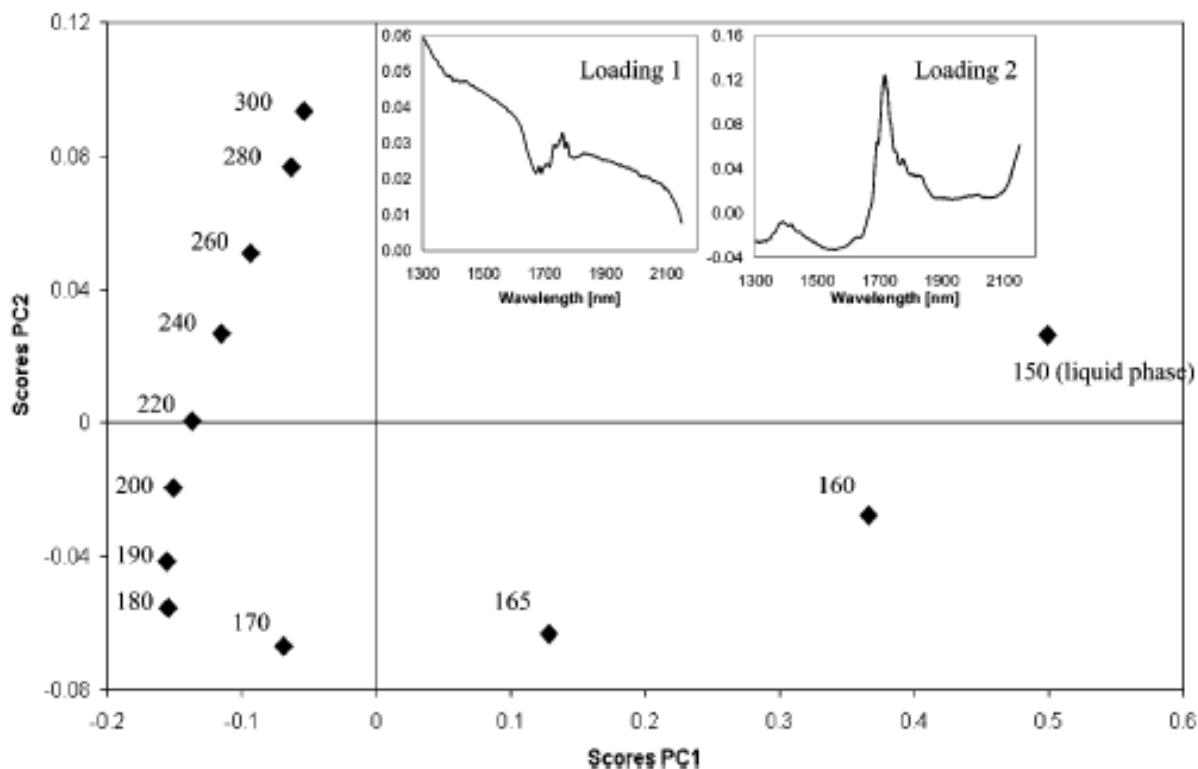


Figure 2-21: A Plot Showing the Shift in Principal Component Scores of a Crude Oil Sample during Depressurisation taken from Aske (2002b)

Oh *et al.* (2004) investigated asphaltene precipitation using n-heptane from four different solvents; tetrahydrofuran (THF), toluene, trichloroethylene (TCE) and pyridine. The onset of asphaltene aggregation was monitored using NIR and observing the optical density at 1600nm every thirty seconds. The onset of aggregation was determined as the point at which the optical density was at its minimum, i.e. when asphaltene aggregation occurs an increase in optical density is observed despite diluting with heptane. It was also observed that the solubility parameters of the asphaltenes increased linearly with increasing solvent solubility parameter. It was also found that the best asphaltene solvent of these four was pyridine.

Buckley *et al.* (1998) conducted a study to try and predict the onset of asphaltene precipitation by using refractive index (RI) to characterise neat oils and mixtures of crude oils with precipitants and solvents. It was found that the onset of asphaltene precipitation occurs at a characteristic RI for each oil/precipitant combination.

Work on RI as a method of characterising stability of asphaltenes in solution was also carried out by Dinadayalene *et al.* (2012). They describe a novel method whereby a correlation is first drawn between SARA fractions and density of the crude. A relationship is then made between density and RI to infer a link between RI and SARA fractions. This relationship is then used to investigate stability of asphaltene in crudes. The rules drawn are (Dinadayalene, Farag and Fujita, 2012):

- (i) Crude oil with an $RI > 0.060$ are more likely to have stable asphaltenes
- (ii) Crude oil with $0.045 < RI < 0.060$ are in the border region
- (iii) Crude oil with $RI < 0.045$ are more likely to have unstable asphaltenes

When compared with previous work this gives a good approximation model for predicting asphaltene precipitation.

Buenrostro-Gonzalez *et al.* (2004) study asphaltene precipitation from two Mexican crudes oils and measure it with a combination of high pressure isothermal expansion and atmospheric titration with n-alkanes. A theoretical study for these systems was performed “using the statistical association fluid theory for potentials of variable range (SAFT-VR) equation of state (EOS) in the framework of the McMillan–Mayer theory” (Buenrostro-Gonzalez *et al.*, 2004). Using this it was found that a good prediction of asphaltene precipitation could be found over a wide range of temperatures and pressures.

2.16 Techniques for Dealing with Aggregation

Due to the problems caused by asphaltenes during processing there has also been a lot of work carried out investigating possible methods for dealing with asphaltene precipitation. (Hashmi and Firoozabadi, 2012) investigated controlling asphaltene aggregation by using electrostatic repulsion generated by adding aromatic chemicals to the oil. Increasing electrostatic repulsion between asphaltene molecules inhibits the growth of aggregates and stops asphaltene precipitation.

Earlier work by Khvostichenko & Andersen (2010) also looked at methods of stabilising asphaltenes in crude oil by addition of three different stabilisers: toluene, petroleum resins and a synthetic additive p-nonylphenol. All three components led to dissolution of asphaltenes in heptane. The main effect observed with addition of these components was the charge on the asphaltene particles. Depending on the method of mixture preparation, addition of toluene could cause the asphaltene to be positively, negatively or neutrally charged. Addition of petroleum resins neutralised the charge on asphaltene particles and p-nonylphenol did not affect the charge

of the asphaltene particles. The most interesting conclusion from this work is that asphaltene deposition could be reduced or even stopped if the asphaltene particle charge is neutralised. The other solution would be to charge the asphaltenes and use electro deposition to remove them from the oil completely.

Acevedo *et al.* (2008) studied solutions of 3% asphaltene in resins using Freeze Fracture and Transmission Electron Microscopy (FF-TEM). This method fractures a solid sample to create a surface, which is then sprayed with platinum and observed under the Transmission Electron Microscope (TEM). The study found that with increasing the temperature the samples were prepared at, smaller asphaltene aggregates were observed. Falling from 5 microns to 3.5 microns and finally settling at approximately 2.5microns for sample preparation temperatures between 100°C and 250°C.

The re-dissolution of asphaltene back into crude oil was investigated by Ashoori *et al.* (2006) on a heavy Iranian crude oil. Asphaltenes were precipitated from the crude oil and then re-dissolution was facilitated with a range of temperatures and solvents. The study found that under the correct conditions asphaltene precipitation can be completely reversed.

2.17 Oil in Water Emulsions

As well as the inherent problems caused by asphaltene deposition from crude oils throughout the entire hydrocarbon supply chain, asphaltenes also cause other problems as a consequence of other undesirable properties. One such property is the asphaltenes ability to stabilise water in oil emulsions. This causes problems in crude processing when the crude is being de-watered, an effect that has been observed in offshore applications and in refineries.

Work by McLean & Kilpatrick (1997) examined the effects of asphaltene aggregation on the stability of water in oil emulsions. They found that model emulsions were most stable when a concentration of 30-40% toluene was present and interestingly the effect was greatest at low resin:asphaltene ratios, a finding contradicted in the work of Spiecker, *et al.* (2003) where it is noted the inverse, that increasing resin:asphaltene ratios in crude oil reduced the efficacy of asphaltenes for stabilising water in oil emulsions. It was also determined that the primary factors governing asphaltene stability are: “the aromaticity of the crude medium (as controlled by the heptane/toluene ratio), the concentration of asphaltenes, and the availability of solvating resins in the oil”(McLean and Kilpatrick, 1997). This is backed up by the postulate in the paper by Wiehe & Kennedy (2000b). Finally, the experiments conducted suggested that the asphaltenes

had the greatest power for stabilising water in oil emulsions if the asphaltenes were at the point of precipitation.

This problem has also been investigated by Graham *et al.* (2008) who fractionated crudes into SARA fractions and then further separated the asphaltene fraction into two fractions called binding resins (BR) and residual asphaltenes (RA). To assess the power of the asphaltene to stabilise a water in oil emulsion they used the concept of $R = BR/RA$. It was noted that this ratio correlates with the tightness of water in oil emulsions and increasing R means a less stable emulsion is formed. In the oils studied only the oil with $R > 1$ did not form a stable water in oil emulsion and as R decreased the stability of the emulsion increased. This is in line with what would be expected from the work of asphaltenes Spiecker *et al.* (2003) due to the fact that increasing R means increasing the ratio of resins to asphaltenes.

In other work Poteau *et al.* (2005) are investigating this phenomenon from a completely different perspective, the objective of the work is to create stable oil in water emulsions to help facilitate the transportation of heavy, viscous oils. They find as with Khvostichenko & Andersen (2010) that the key feature to the emulsion stability is the charge on asphaltenes and thus investigate the effects of pH on the stability of these emulsions. It is found that both high and low pH charge the asphaltene functional groups and enhance their surface activity. Both high and low pH environments allow the asphaltenes to prevent the coalescence of water droplets and thus help form stable emulsions.

2.18 Modelling

Converting the spectral data into predicted values for the substance of interest can be carried out using a variety of different methodologies, which will be explored, in this section.

2.18.1 *Pre-processing*

Spectral pre-processing is a large part of the whole work undertaken on modelling. It can in fact account for as much as 90% of the total work of modelling. Most of this work is simply looking at the data for the purposes of detecting and removing any questionable points, which do not reflect the true system behaviour. Treatment of missing data is also a large part of the pre-treatment, sensors can go down or not log a measurement for a number of reasons. In these instances the missing data can either be cut totally, or, if the user has confidence in the method

the missing data points can be filled with a variety of such as n order interpolation, average infilling or local average infilling.

Spectrally, techniques such as standardising the data by mean centre or taking standard normal variance (SNV) can scale the data and improve model performance (Cui *et al.*, 2012). Spectral scatter can also be corrected to an extent to improve the signal to noise ratio by using multiplicative scatter correction (MSC).

Spectral variation can also be increased by taking derivatives of the spectra. Typically a higher order than 2nd order is not used because of the amount of noise it can create. Treating spectra using this plethora of techniques has improved several studies. (Cui *et al.*, 2012) found that treating NIR spectra with 2nd order derivatives greatly improved the discrimination of a PLS model for predicting cotton genotypes. The study also found that when 2nd order derivatives were coupled with SNV that the model discrimination was further improved with a classification accuracy of 100% for seeds and 97.6% for leaves.

In the paper by (Balabin, Safieva and Lomakina, 2007) different pre-processing methods are investigated and applied to the appropriate properties in each of the models. The methods used are normalisation, magnitude normalisation, linearisation (taking the logarithm), differentiation, double differentiation, auto scaling, and range scaling in different intervals (Balabin, Safieva and Lomakina, 2007). The most frequently used technique was differentiation giving most improved signal to noise ratio of the spectra.

2.18.2 *Principal Component Analysis*

Principal Component Analysis (PCA) is a technique used to examine the variability in large datasets. Going beyond simple two-dimensional correlation, PCA works in many dimensions, having as many dimensions as variables in the dataset. Each principal component is a linear combination of the coefficients of n number of variables in the dataset. The first principal component explains the line of greatest variability in the data; the second principal component explains the second greatest line of variability in the dataset, orthogonal to the first principal component and so on.

By way of example, the below figure shows a group of triangles illustrating data points and these have been distributed in an oval shape. A vertical line has been drawn with the points projected on to illustrate a random line of variability in the dataset.

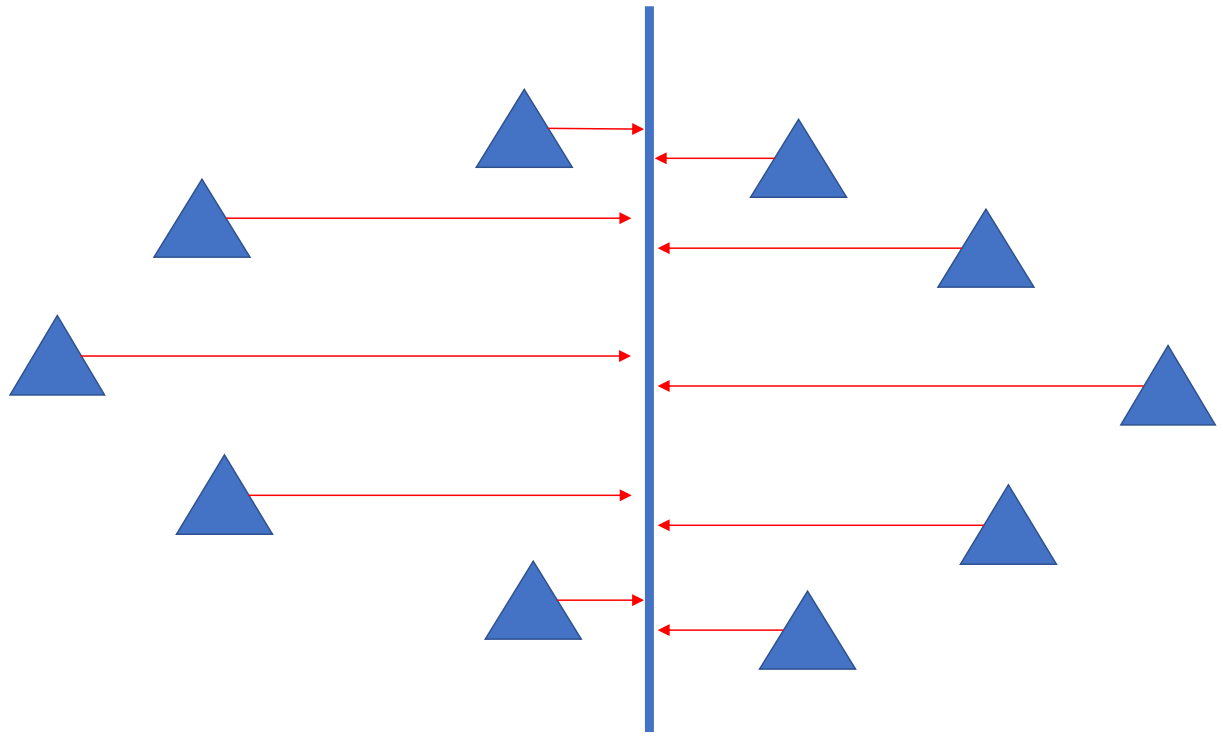


Figure 2-22: PCA Example 1

It can be seen that the data in this region is not spread out and hence the variance will be low. The objective of principal components analysis is to find the principal components that explain a dataset. In the second example below, the line has been drawn horizontally through the same dataset.

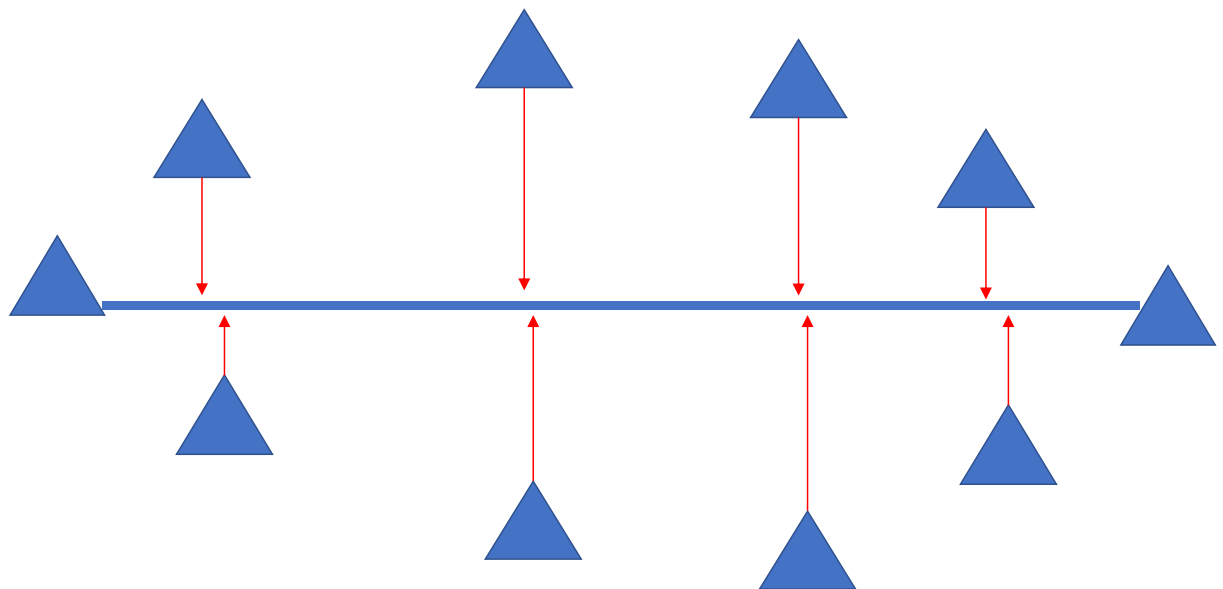


Figure 2-23: First Principal Component

In the second example, it can be seen that the data is more spread out and has a much larger variance, indeed, it would not be possible to move the line to any other position and increase the variance captured in the dataset, hence, this is the principal component of this dataset.

The lines drawn between the samples and the line of best fit are at right angles to it and this is known as the orthogonal projection of the data. The next line of best fit will then be drawn at a right angle to the first line of best fit. The orthogonal projections will once again be made as shown in the figure below.

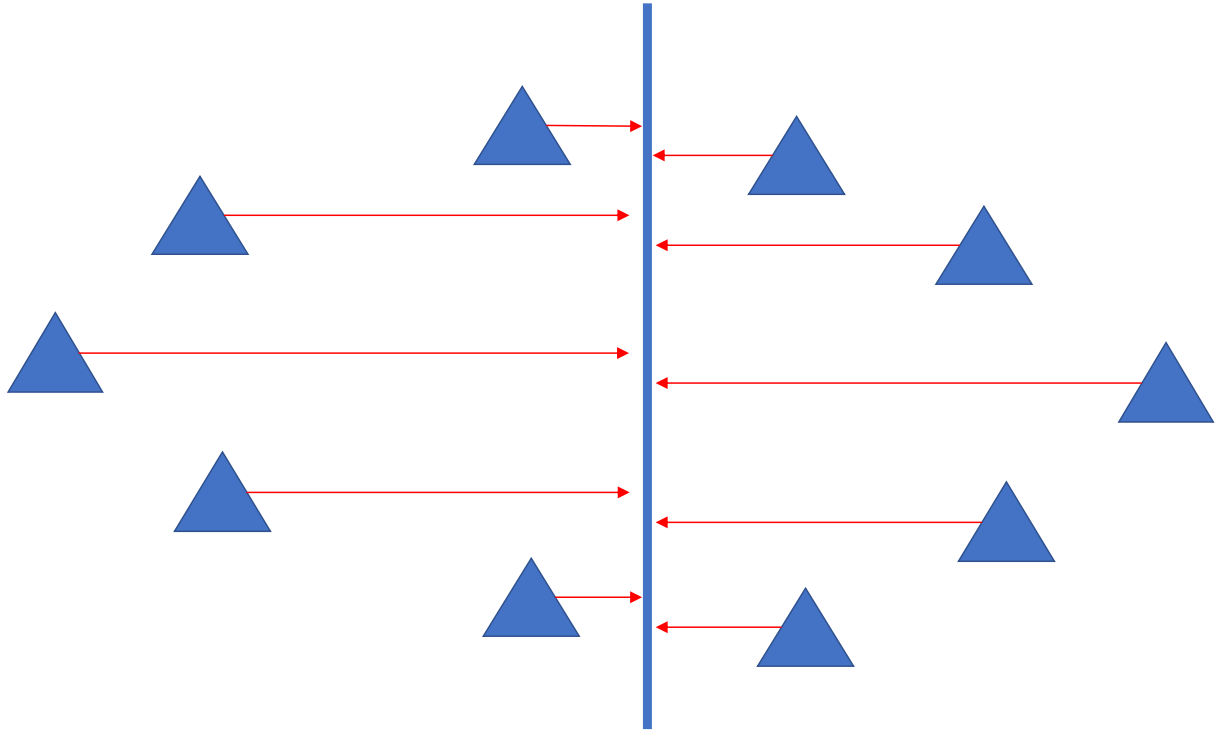


Figure 2-24: Second Principal Component

This is the second principal component and it is this orthogonality that allows underlying trends and relationship to be easier visualised.

By way of example the full Non-Iterative Least Squares (NILES) algorithm for PCA is shown in Appendix C of this document, however, the result of the PCA procedure is then a decomposition of the full data matrix, X , into principal components of score and loading vectors:

$$X_{n \times m} = t_1 p_1^T + t_2 p_2^T + t_i p_i^T + \cdots t_k p_k^T + E_{n \times m} \quad (2-10)$$

Where: t_i = the score vector, p_i = the loading vector and E is the residual matrix.

To contextualise this into a real-life example, Another excellent example of the application of principal components analysis is on the following example using data from DEFRA on diets in the United Kingdom.

Table 1: Food Consumption in the UK (g/person/week) taken from Richardson (2009)

	England	Wales	Scotland	N Ireland
Cheese	105	103	103	66
Carcass meat	245	227	242	267
Other meat	685	803	750	586
Fish	147	160	122	93
Fats and oils	193	235	184	209
Sugars	156	175	147	139
Fresh potatoes	720	874	566	1033
Fresh veg	253	265	171	143
Other veg	488	570	418	355
Processed potatoes	198	203	220	187
Processed veg	360	365	337	334
Fresh fruit	1102	1137	957	674
Cereals	1472	1582	1462	1494
Beverages	57	73	53	47
Soft drinks	1374	1256	1572	1506
Alcoholic drink	375	475	458	135
Confectionery	54	64	62	41

As it can be seen this data is complex, the columns (countries) are the samples and the rows (foodstuffs) are variables. By looking at this dataset it is not immediately obvious if there are any underlying trends, however, by the application of principal component analysis the dataset can be interrogated as a whole.

The first principal component finds the line of maximum variability in the dataset and is actually the equivalent of the least squares line of best fit through the data. Using the principal component orthogonal projection a new set of axes can be drawn to interrogate the data. figure shows the projection of the data onto the first principal component.

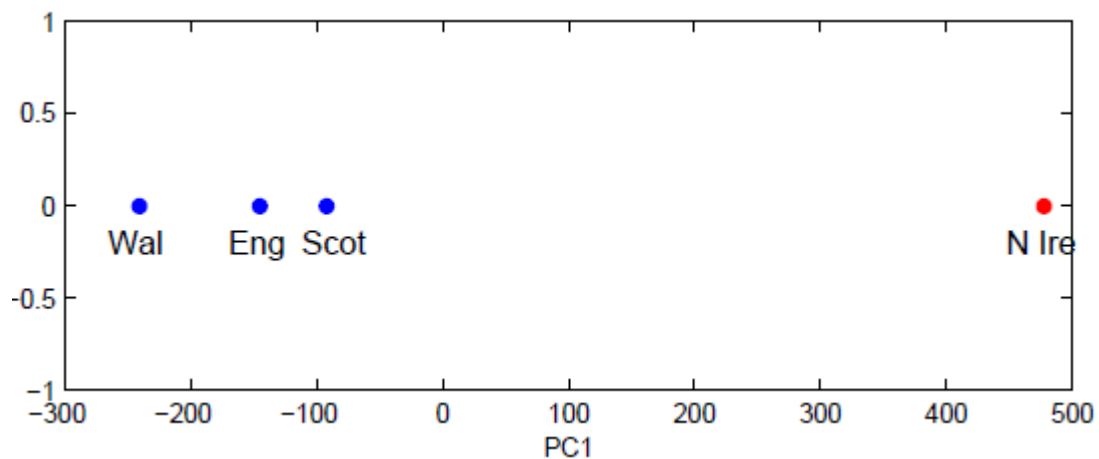


Figure 2-25: Projection to Principal Component 1 taken from Richardson (2009)

This diagram is known as a score plot and it is already obvious that data clustering is being achieved, it seems there is something in the data that differentiates Northern Ireland from the remainder of the dataset.

By then obtaining the second principal component it allows a two axis, or bivariate plot to be produced which should further discriminate between the clusters. This is shown in the below figure.

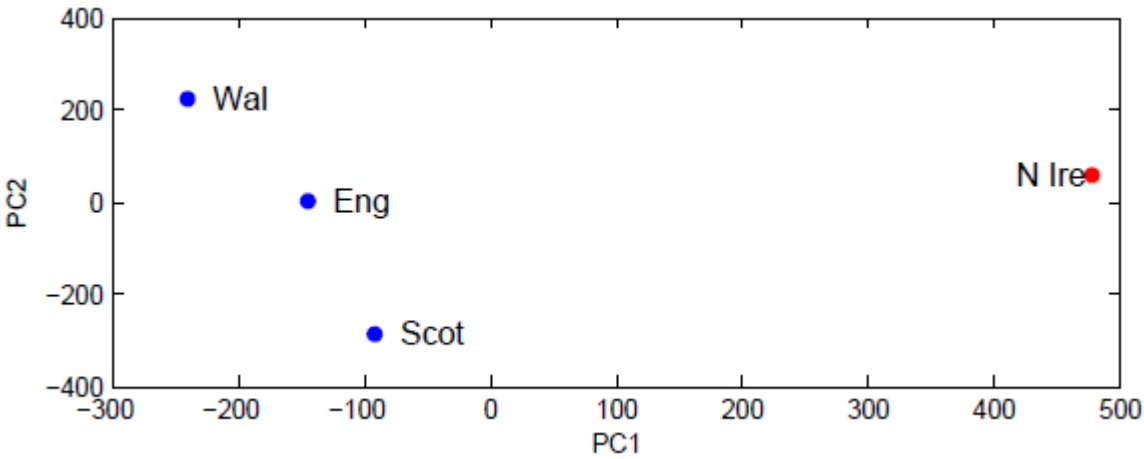


Figure 2-26: Bivariate Scores plot (PC1 v PC2) taken from Richardson (2009)

It is now obvious that Northern Ireland is indeed an outlier, to interrogate which variables caused this, the analysis can now proceed to the relevant loadings. As scores are related to samples, loadings are thus related to the variables and bivariate loadings plots, using the same two principal components as Figure 2-26 are a very useful way to understand what is affecting the clustering. Figure 2-27 below shows the bivariate loadings plot of PC1 v PC2 for the dataset.

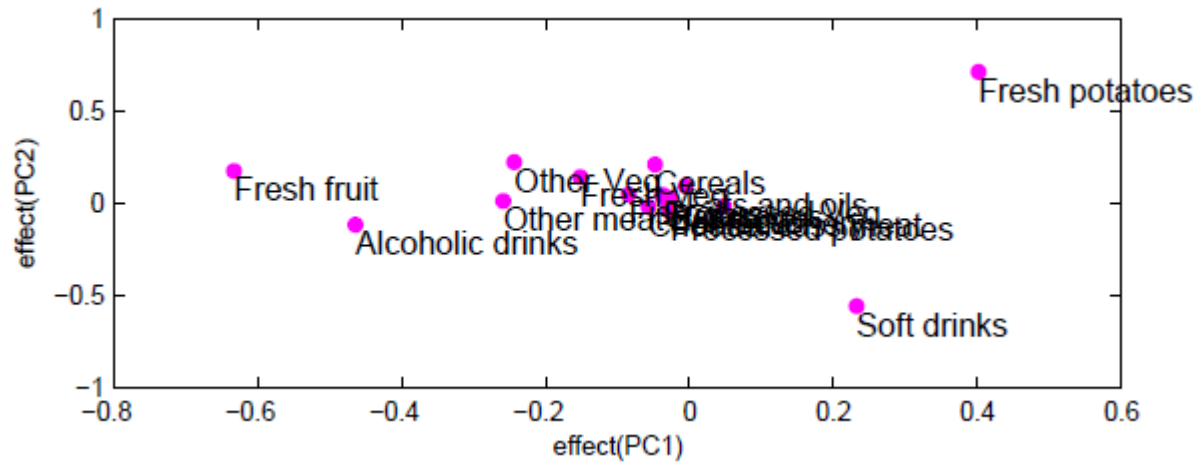


Figure 2-27: Bivariate loadings plot (PC1 v PC2) taken from Richardson (2009)

It is obvious from the plot there is a cluster of samples in the middle, however, 3 variables are particularly interesting, Fresh fruit, Alcoholic drinks and Fresh potatoes. It can be seen that these Fresh fruit and Alcoholic drinks are in the area of England, Scotland and Wales and Potatoes are in the Northern Ireland region. When looking at the data it can indeed be seen that Northern Ireland consumes more potatoes and less fresh fruit and alcoholic drinks than England, Scotland and Wales and this is what causes the differentiation.

To further demonstrate that the scores vector obtained is a very powerful tool in PCA. Figure 2-28 shows the application of PCA to a refinery and the bivariate scores plot of PC2 v PC3.

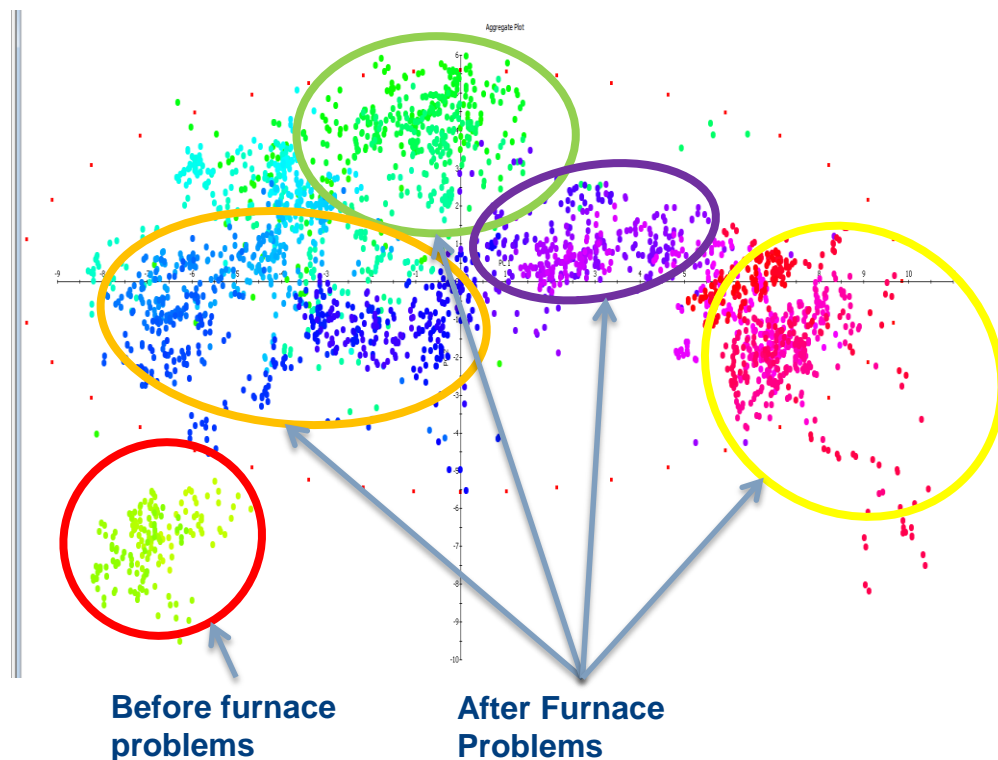


Figure 2-28: Bivariate Scores Applied to a Refinery Dataset

The two main regions are before and after issues with a furnace and drilling down into the dataset further then allowed these operating regions to be related to production of diesel fraction.

2.18.3 *Partial Least Squares*

Partial least squares (Projection to Latent Structures or PLS) is a powerful regression tool and is in essence an extension of PCA. However, whereas in PCA decomposition the scores and loadings are the vectors that best describe the variance of the X matrix, in PLS decomposition the scores and loadings are the vectors that have the highest covariance with the response vector Y. After decomposition a regression between score vectors and the response is then performed”(Aske, 2002a).

In practice, this means that a regression can be formed on a full block of X values rather than just one as with ordinary least squares. If once again the UK diet example is taken this means that by taking the diet of an unknown individual, a PLS model could be built on the dataset which would allow the user to predict the country of origin of the individual.

The full algorithm for the Non-Iterative Partial Least Squares Approach used later in the thesis is shown in Appendix C of the document.

Many examples of the industrial applications of PLS are documented in the literature. In a study on detecting vegetal oil adulteration in diesel and biodiesel by Gaydou, Kister and Dupuy (2011) using PLS predictive models found that NIR gave better results than MIR. (Gaydou, Kister and Dupuy, 2011) also discusses the use of multiblock PLS to combine the two methods to form a predictive model based on a combination of analyses. Three methods of multiblock PLS are investigated in the paper.

The first method is called the concatenated method and works by combining the matrices of both NIR and MIR data into a signal matrix, the PLS method is then applied to this matrix, it is important to ensure that if this method is applied both matrices of data are correctly scaled to achieve sensible results.

The second method discussed considers each data matrix independently, by application of PCA to the data scores are obtained for each block of data. The scores are then collected and combined to form a super matrix (Gaydou, Kister and Dupuy, 2011). This method is called Hierarchical-PLS (H-PLS) and is also described by Bastien, Vinzi and Tenenhaus (2005).

The third method used by Gaydou, Kister and Dupuy (2011) is known as Serial Partial least squares (S-PLS) and was proposed by (Berglund and Wold, 1999). This method uses PLS on each data matrix to obtain scores. As with H-PLS the scores are then combined into a single super matrix upon which PLS is once again applied. Out of the three methods the one that yielded the best results was H-PLS with a prediction error of 2.03%. These findings raise the intriguing possibility of improving model discrimination by using combined analytical methods.

In a study by (Balabin, Safieva and Lomakina, 2012) PLS was used as to predict gasoline data using NIR spectra. The method was found to be only moderately effective for predicting gasoline composition. K nearest neighbour modelling was found to be the simplest of the algorithm assessed and also more effective. This is a well-known phenomenon and is due to the simplicity and lack of variability in gasoline datasets.

2.18.4 *Nearest Neighbour*

Nearest neighbour (or K Nearest Neighbours or KNN) is a non-parametric classification method whereby a distance (Euclidean distance) is assigned between all points in a dataset. The distance between each point is expressed as the root of square differences between the coordinates of the objects being examined and is described by the following formula:

$$d = \sqrt{\sum_{i=1}^n (x_i - y_i)^2} \quad (2-11)$$

The neighbours of the sample under scrutiny are then ordered by distance and a parameter (K) is then given to optimise the numbers of neighbours selected to describe the sample. Variations on this method have been also been applied, for example a weighted KNN is a similar algorithm which tries to introduce bias to the model by assigning weights to the samples nearest neighbours to alter the effects that nearest neighbour samples have on the final predicted result.

(Balabin, Safieva and Lomakina, 2012) investigated the use of (amongst other algorithms) KNN modelling for predicting gasoline composition. The study showed that it was actually one of the most effective methods for classification all three of the datasets investigated. This is shown by the model errors shown in Figure 2-29. It can be seen that in all three models the

KNN model had one of the lowest classification errors, it can be seen that both SVM and MLP also do very well. This also validates the usage of nearest neighbour in Chapter 3.

R.M. Balabin et al. / Analytica Chimica Acta 671 (2010) 27–35

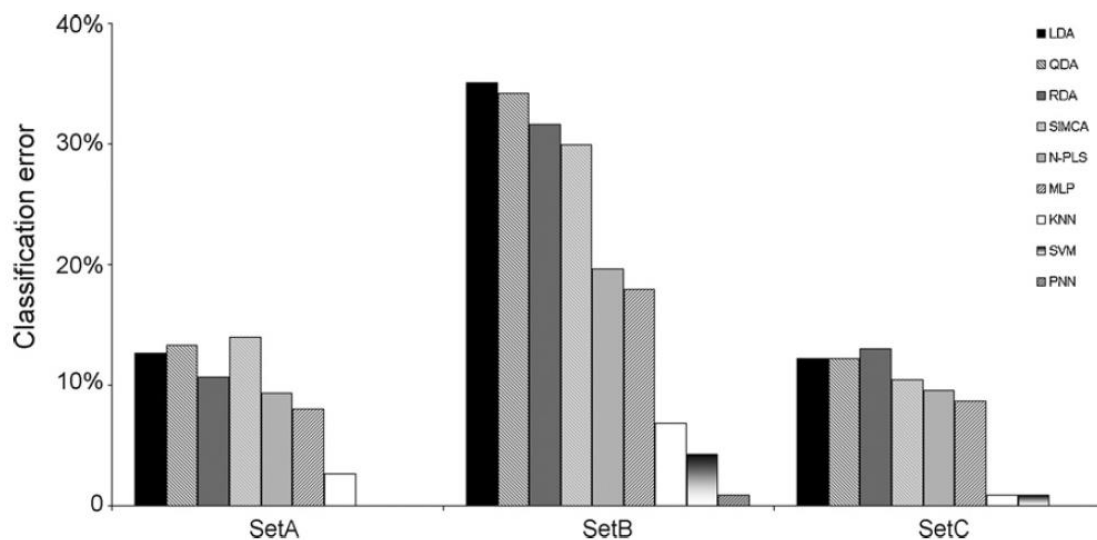


Figure 2-29: Showing modelling errors for different methods used to build a gasoline model taken from Balabin *et al.* (2012)

Chapter 3:

Refinery Crude Oil Quality Monitoring

Chapter 3. Refinery Crude Oil Quality Monitoring

Chapter 3 describes a novel technology application within a major Asian refinery. As described in the literature review, the application of NIR in the hydrocarbon processing sector is well understood and widely applied for predicting the properties of refined streams, particularly gasoline and diesel.

However, the application of NIR for modelling crude properties is an area that has not been explored due to the difficulty of modelling a stream with the complex chemistry of crude oil. This difficulty is further compounded by the variability of crude feedstocks bought and processed by refineries meaning that a successful model would need to cover a high range of crude types with a variable range of properties.

Currently refineries monitor the quality of each crude delivery with a measurement of API gravity and Sulphur and compare this to the expected quality of the delivery. This is quick and simple and given the results match the quality expectation the crude will be processed. However, API gravity and sulphur measurements are not always indicative of crude quality and indeed for the same API gravity and sulphur measurements, the distillation behaviour of a crude oil and the fractions it yields can be very different.

The opportunity therefore is to develop a technique, which can provide a refiner with as much information about the crude oils being delivered and processed as possible, whilst still being quick and simple to deploy. The benchmark for the model was to tune the predicted parameters to be within the laboratory reproducibility limits, as defined by ASTM. This gives the customer confidence that the results generated by the model can be treated as if they were generated by conventional laboratory analysis and are performing to the same standards.

This project meets objectives 1 and 2 of the thesis and addresses this opportunity by taking Intertek's proprietary chemometric modelling package (PT5Technology) and database of global crude oils (circa. 1200 global oils) which has been built over a ten year period to develop a successful model for a major Asian refiner.

This introduction to PT5 provides a brief description of the technology with its hardware, benefits and the underlying principles of PT5Technology and PT5Crude with the Intertek Global Crudes Database.

3.1 Introduction

PT5 measurement technology is used across the entire crude oil supply chain, including crude oil production, pipelines, refining and biofuel blending activities. The combined topological modelling and near infrared analysis combination supports quality control and control systems, enhances production yields and more, helping customers run their business more efficiently and profitably.

PT5 software is combined with on-line near infrared (NIR) analysis to provide rapid product analysis, exploiting real time property measurement for improved control and optimisation of the hydrocarbon supply chain. When Intertek's PT5 software is combined with on-line NIR Analysis, accurate and real-time data is available for online composition measurement and quality assurance on platforms and pipelines, fiscal allocation and hydrocarbon accounting for shared pipeline system, well-stream allocations, multiphase meter validation, hydrocarbon reconciliation and more. The technology can be used in conjunction with several spectroscopic techniques which include MIR, NMR and GC but the predominant analysis technique modelled is NIR.

3.2 Methodology

The measurement of physical properties in a laboratory requires properly calibrated equipment and skilled personnel using a well prepared sample. The collection of a representative sample is critical to good laboratory analysis, used for plant operation. In addition, the design of the sample point and sampling method must ensure that the sample is not contaminated, does not lose components, and is representative.

NIR predictions become attractive compared to conventional laboratory analytical methods particularly because of speed, for example the conventional laboratory analytical method is particularly time consuming. Measurement of TBP (True Boiling Point) of crude oil requires two separate distillations to give the full distillation curve. Firstly an ASTM D2892 distillation takes the crude from its Initial Boiling Point (IBP) to the method cross over temperature typically 350°C, this is known as the atmospheric distillation and simulates the fractionation of crude in a typical refinery atmospheric crude distillation unit (CDU).

The second method, ASTM D5236, is charged with the 350°C+ atmospheric residue from the first method and the distilled under vacuum to approximately 550°C equivalent. This is known as a vacuum distillation and the remaining crude portion of 550°C+ is the vacuum residue, this simulates a typical refinery vacuum distillation unit.

The measurement can form part of an on-line or at-line measurement which is updated every few minutes. These measurements can be used as the input to a control loop and / or input to a process optimiser. Typical spectrometers are shown in Figure 1.



Figure 3-1 - Typical Spectrometers (courtesy of ABB 2017)

To take measurements a transmission cell is used. This enables the NIR beam to be used to check for deposits on cell windows and to measure path length to ensure that the instrument is working as designed. The technology is used within Intertek to deliver a valued service to many key customers. A picture of the laboratory in Aberdeen is shown in Figure 3-2.

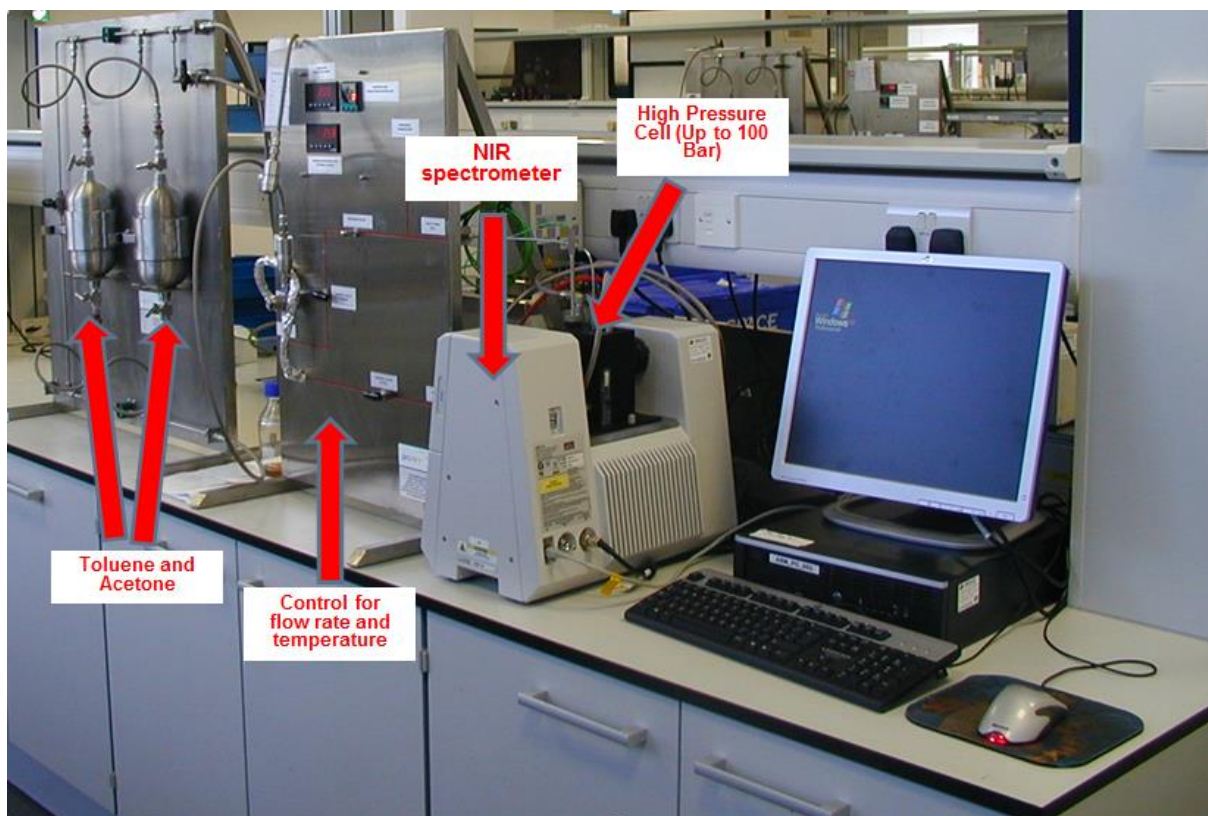


Figure 3-2 - Laboratory Crude Oil Sample Handling and Spectrometer

In the case of crude oil analysis, live crude oil and on-line systems can operate at pressures of up to 100 Bar. For refinery blending operations the sample can be handled at atmospheric pressure.

3.2.1 *NIR Spectra in PT5*

Typical industrial application using NIR utilises spectra with wavenumbers between 4000 and 4800 cm^{-1} which is the combination band between MIR and the first overtone (as described in section 2.7). In MIR each chemical compound has a specific finger print and in mixtures the individual amounts of the compounds can be deduced.

In the NIR spectra there are no peaks for individual compounds and the absorption spectra overlap for different compounds (Figure 3-3). When measuring refinery streams or crude oil the problem is further complicated by the very large number of chemical compounds present in the analyte.

When combined with the inherent signal to noise ratio of the instrument there is no practical way of reading the spectra. The shape of the spectra does however give a qualitative view of the composition as shown in Figure 3-3.

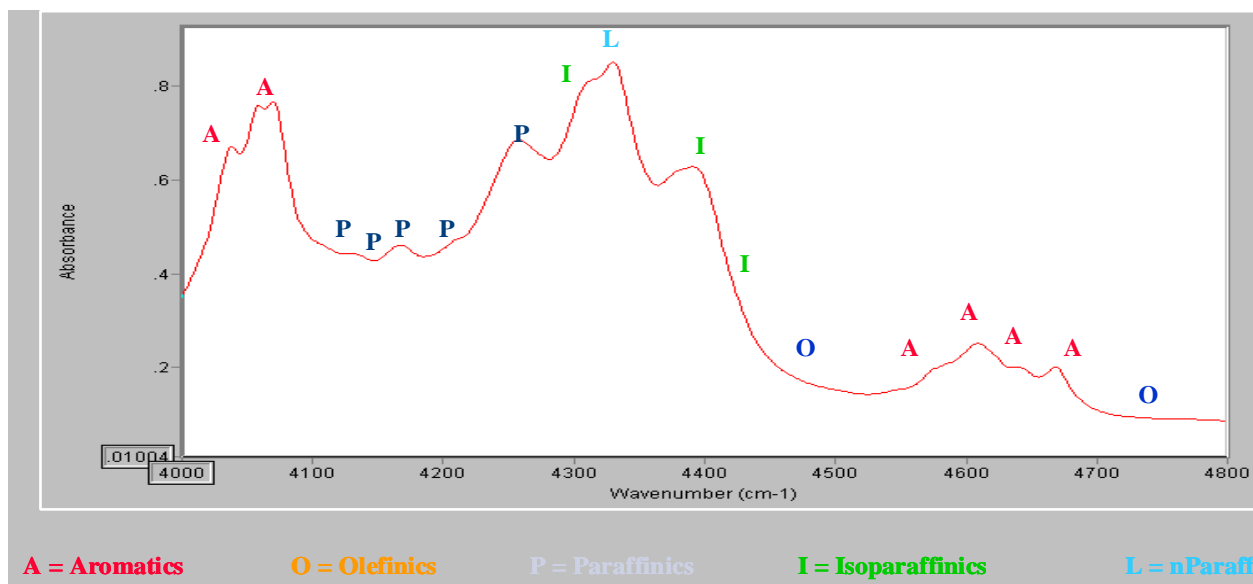


Figure 3-3 - Hydrocarbon absorption in Near Infra-Red radiation

Whilst there is no peak for properties e.g. TBP, API, Pour Point, RON or Sulphur the information is in the spectrum as a finger print. Figure 3-4 shows that for any measured spectra there is a set of properties measured in the laboratory.

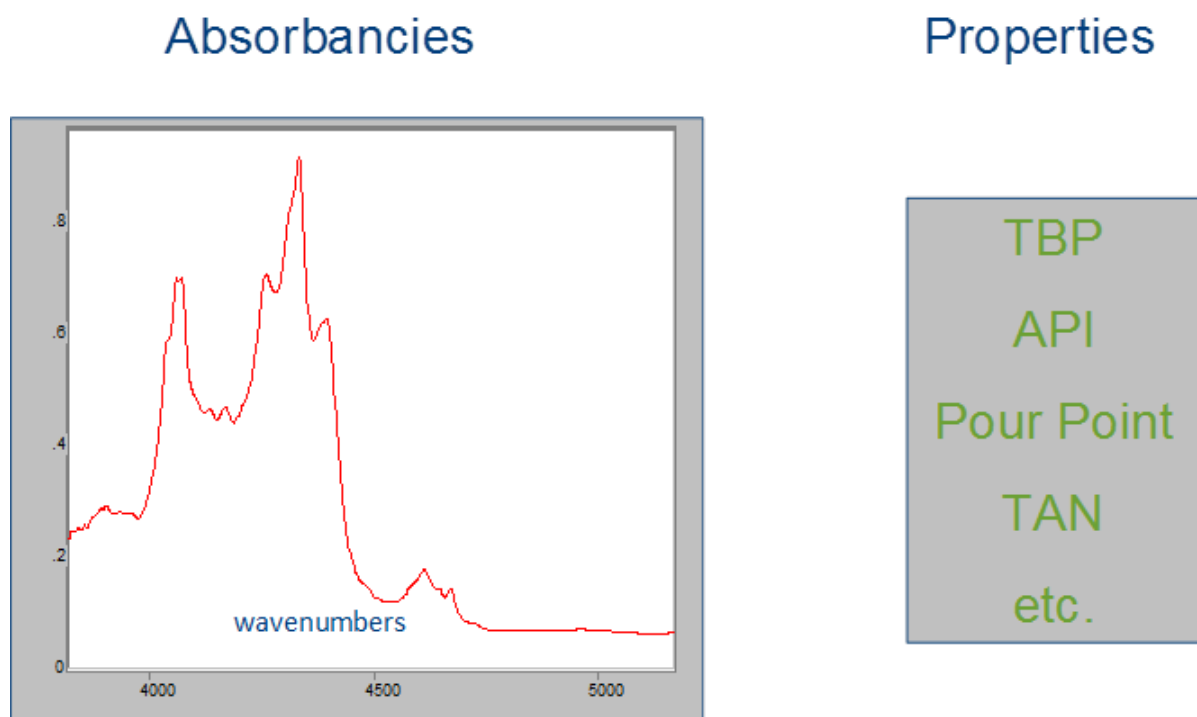


Figure 3-4 - Link Spectrum to Properties

3.2.2 PT5Technology - Chemometric Modelling Process

The link between the spectra and properties measured by laboratory analysis is a chemometric model as shown in Figure 3-5. The chemometric model is an empirical correlation built using known laboratory samples that have spectra and laboratory analysis.

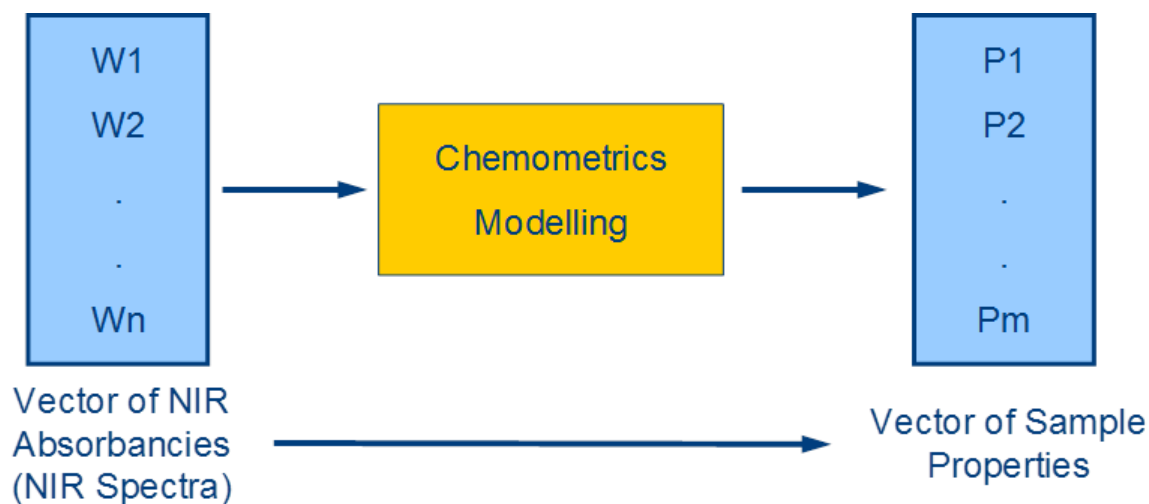


Figure 3-5 - NIR as Information Vector

PT5Technology works on the basic understanding that the same sample has the same spectra and the same properties. A hypothetical example of this is shown in Figure 3-6, in this case the unknown sample (spectrum B) has been matched to the database sample (spectrum A) and hence the predicted properties would be those of spectrum A as the two are identical.

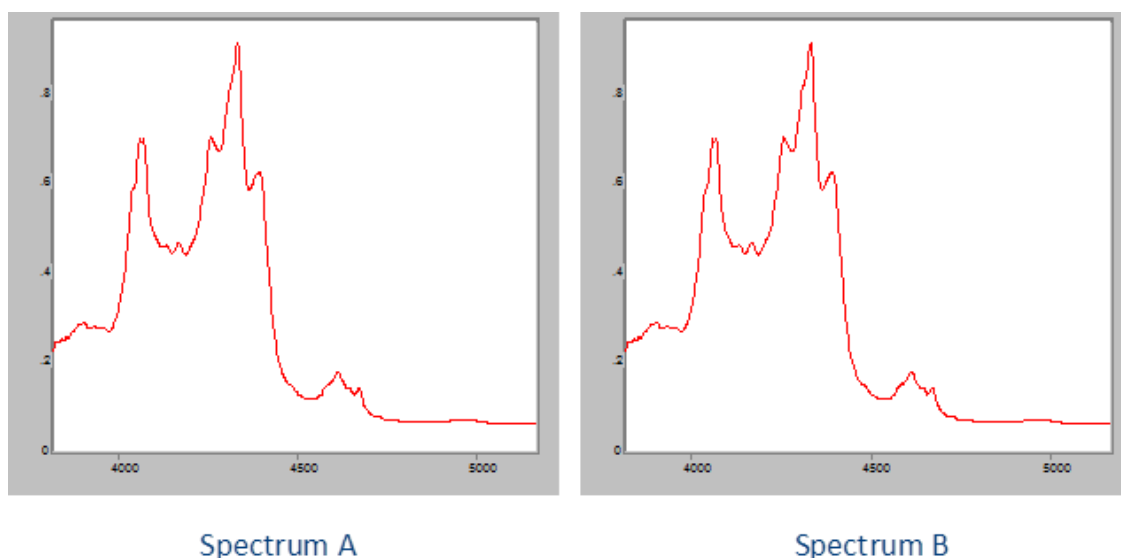


Figure 3-6 - Same Sample have Same Spectrum

Figure 3-7 demonstrates this in practice. The spectrum and properties of sample A are known and reside within the database. When the spectrum of sample B is collected the properties of that sample will be predicted using A as this is the closest match.

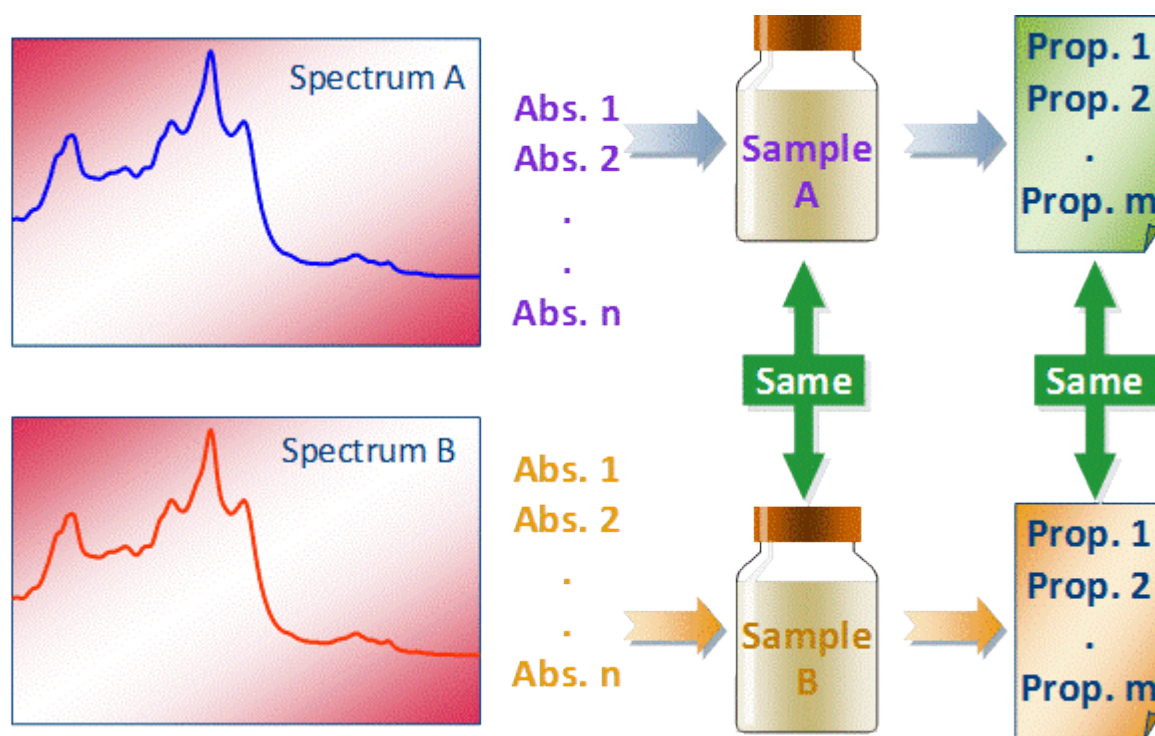


Figure 3-7 - Same Spectra Same Properties

3.3 PT5Technology Aggregate Plots

The only way to give a quantitative measurement is to have a model to interpret the spectra. PT5Technology uses a completely non-linear modelling paradigm based on nearest neighbours.

Spectra contain the finger print of the chemical compounds of the sample. These finger prints fall into families which can be evaluated as a function of the absorbance at different wavenumbers – these functions are called aggregates and the general form is shown in Equation (3-1)

$$\text{Aggregate} = f(W_{\lambda 1}, W_{\lambda 2} \dots W_{\lambda n}) \quad (3-1)$$

To give an example of the generation of an aggregate parameter, the case of a simple spectra will be considered. Figure 3-8 shows a simple sample spectra cover 4000 to 4016 wavenumber region of the NIR spectra, it can be seen that each wavenumber has a corresponding absorbance on the y axis.

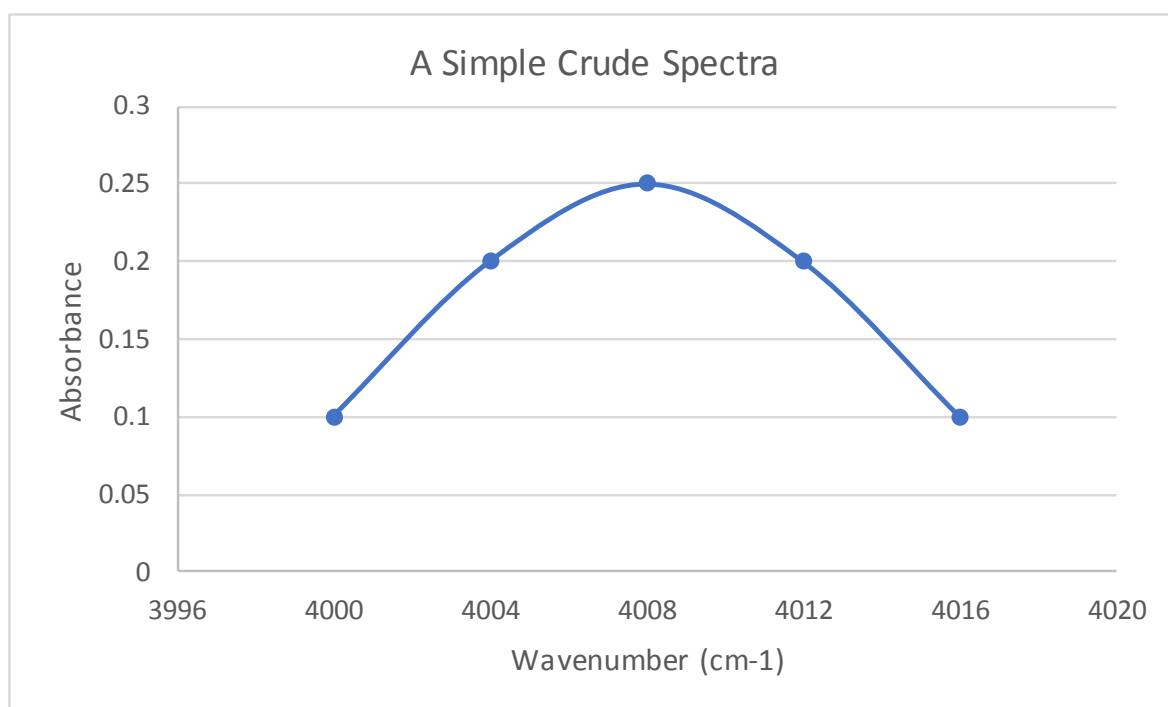


Figure 3-8: Simple sample spectra

If parameter 1 is related to the absorbance at 4000 wavenumbers and this is called EA1 (Example Aggregate 1) then the aggregate expression, according to equation 3-1 would be as follows:

$$EA1 = Abs(4000) \quad (3-2)$$

$$EA1 = 0.1$$

Layers of complexity can then be added. For example, if a second aggregate (EA2) for parameter two is then taken as being related to the absorbance at 4008 multiplied by the absorbance at 4016 the following aggregate expression would be created:

$$EA2 = Abs(4008) \times Abs(4016) \quad (3-3)$$

$$EA2 = 0.25 \times 0.1 = 0.025$$

By plotting the values of two aggregates the spectra can be seen in their families on a spectral plane. For the above example this would lead to the following 1 sample aggregate:

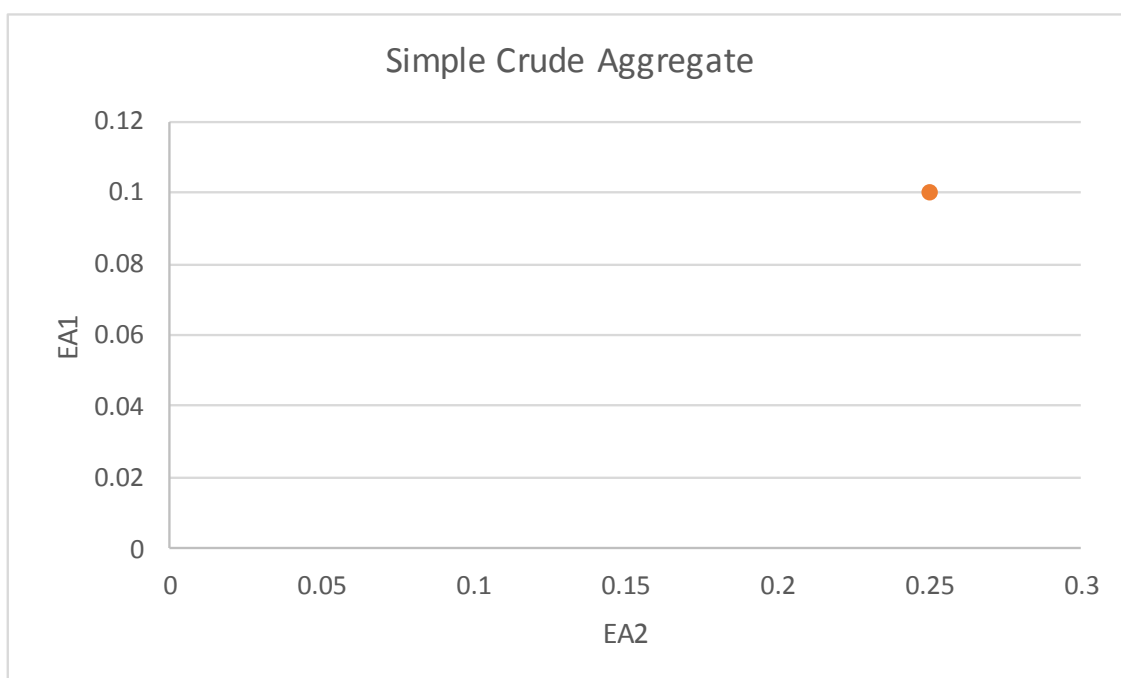


Figure 3-9: Simple Aggregate

With multiple sample spectra, aggregate plots are constructed as shown in Figure 3-10. These areas for each family can be enclosed by a box which defines the limit of the different families. This box is positioned by both operator experience, sample characteristics (such as a crude oil family) and use of a nearest neighbour clustering algorithm. The aggregates used in this example are proprietary expressions designed to take features from the spectra related to chemical signatures of the samples. In this case KARO and KCY have been used. KARO is related to areas of the spectra which describe sample aromaticity and KCY is related to areas of the sample related to cyclicity.

The colour of the sample is determined by the z axis bar (on the right of the plot) and represents the magnitude of the selected property value – in Figure 3-10 this is Total Acid Number (TAN) which is a measurement of the acid content of a crude oil and the value is directly from the titration of a crude oil with potassium hydroxide and expressed in milligrams of potassium hydroxide (mg/KOH) require to neutralise the oil. It is a useful parameter for refiners because a higher TAN value means more KOH required to neutralise the oils and thus the crude is more likely to be corrosive.

The coloured Z axis is thus a useful visualisation (and its use will be described in the case study) and it can be seen that crude oil families tend to share very similar property values and spectra.

The aggregate planes and associated boxes can be used to identify the family of an unknown sample and also track the spectral changes of samples over time. The boxes can be drawn either by hand, utilising user experience or by utilising the nearest neighbour clustering algorithm.

This is the simplest qualitative prediction of sample family and a very powerful tool. In practice this means that using only a NIR spectra the customer can identify if the crude oil batch is the same as historically or if it has deviated in some way.

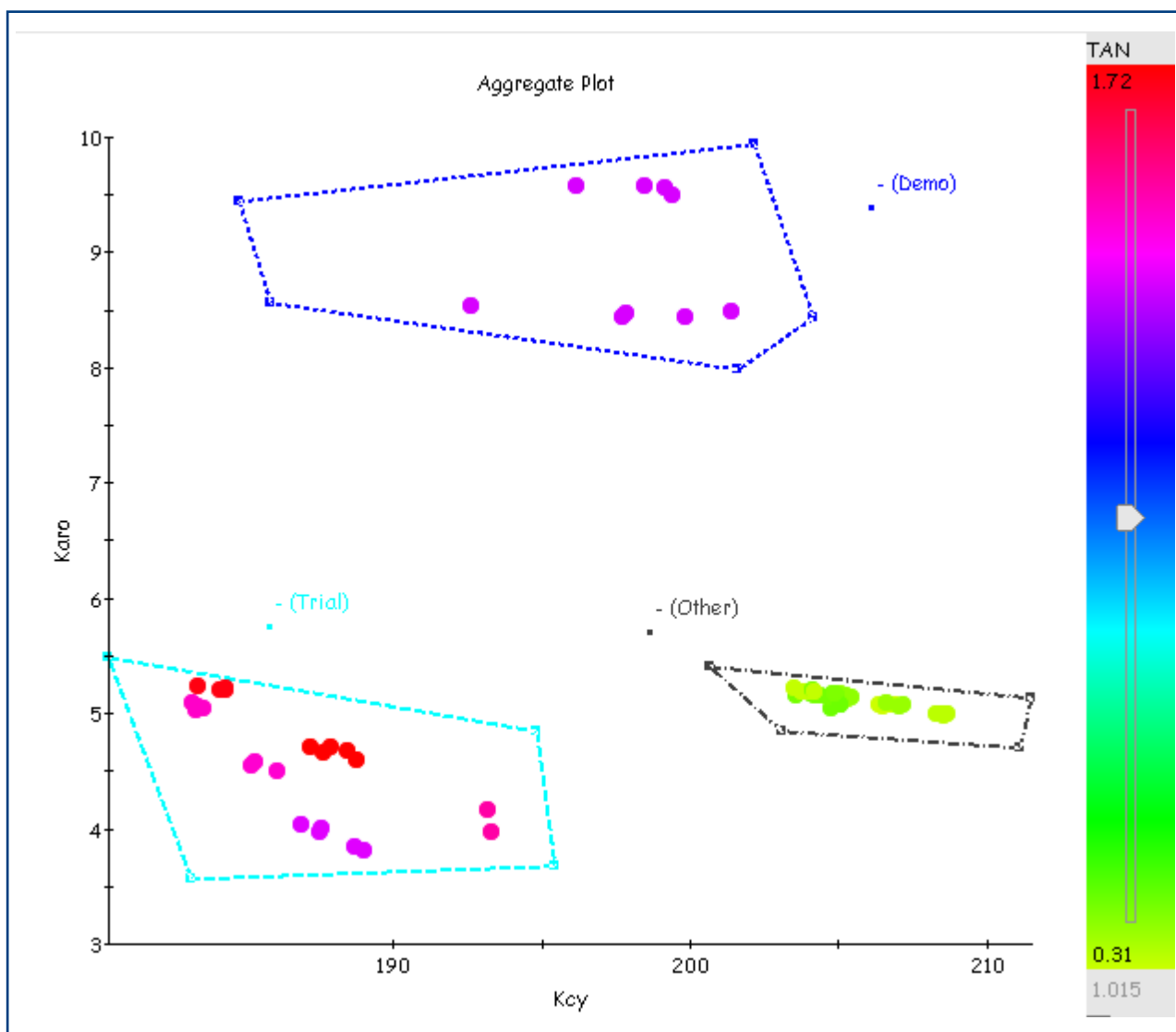


Figure 3-10 – Spectral Plane with Boxes of sample families

3.3.1 Finding properties for spectra

PT5 uses historical samples to find neighbours and make a prediction. These historical samples are held in a database. The spectral database shown in Table 3-1 is constructed by collecting process samples and for each sample performing NIR scans to get the spectra and conventional laboratory analysis to get the properties. In normal plant operation the conventional laboratory

analysis will be performed, therefore the only additional work is performing the NIR scan which is a simple task.

Table 3-1: Database Structure

Sample	Spectra	Properties				
Sample 1	Spectra 1	Prop 1	Prop 2	.	.	Prop m
Sample 2	Spectra 2
Sample 3	Spectra 3
Sample 4	Spectra 4
Sample 5	Spectra 5
Sample 6	Spectra 6
Sample n	Spectra n

Given a new spectrum with unknown properties PT5 will search the database for similar spectra. The spectra are ranked by calculating a nearest neighbour distance and the properties of the unknown sample are predicted as those of the closest spectrum in the database (Figure 3-11).

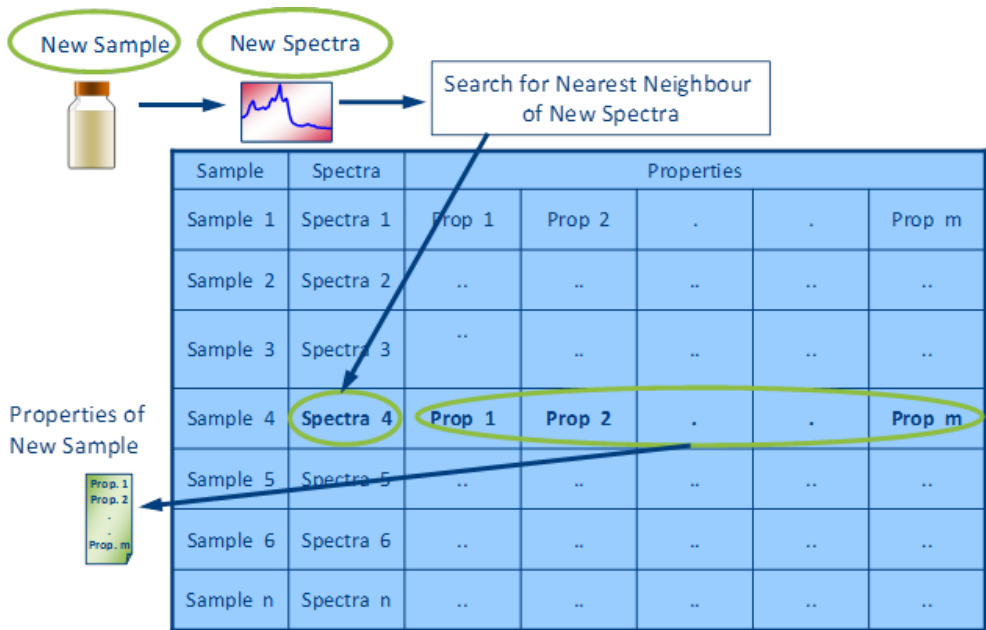


Figure 3-11 - PT5Technology Prediction - Database Search

The simple database search only works in practice when there are many samples and the chemical components do not vary significantly. In practice the closest sample is too far away and / or the closest sample has measurement errors itself and it is prudent for the prediction to use more than one sample.

To predict sample properties, the PT5 prediction engine identifies a set of close neighbours from the database. The neighbours to be used in the prediction are selected using nearest neighbour clustering. The distance the software will use to search for neighbours it believes are spectrally similar to the unknown sample is termed RSphere.

This is shown as the blue circle in Figure 3-12 and is defined by selecting a Euclidean distance with sufficient magnitude to select a training set with enough variability to make an acceptable prediction, without including samples with properties which are dramatically different from that of the unknown sample. In this particular example, the software has picked four samples from the database ($N1 \rightarrow N4$) as spectral matches for the unknown sample (green circle) based on the size of the RSphere, conversely it has excluded four samples ($M1 \rightarrow M4$) as too far away to be useful in making a prediction.

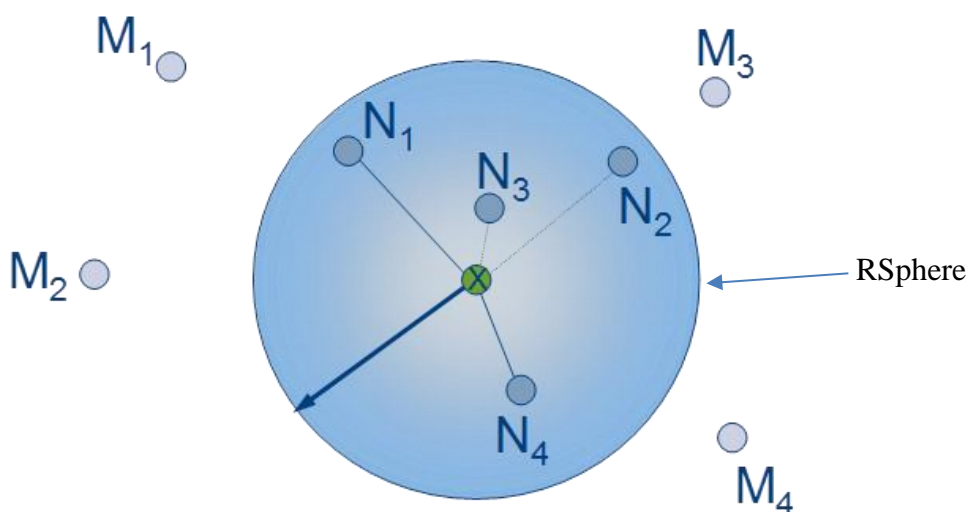


Figure 3-12 - Topological Modelling Using Nearest Neighbours

The model then takes the property values of the selected neighbours and the predicted properties are then calculated. This calculation is based on proportional blending of the properties of each of the known samples from the database. For illustration, in this example $N1 \rightarrow N4$ have been selected as neighbours for the unknown sample and, for a given property, the model will take the property values of these samples and proportionally blend them as shown by equation (3-4):

$$\text{Property (x)} = f(N_1 \times w_1 + N_2 \times w_2 + N_3 \times w_3 + N_4 \times w_4) \quad (3-4)$$

Where:

N_x = Property value of sample N

w_x = proportional weighting assigned to that sample

For illustration if it is assumed that the samples $N_1 \rightarrow N_4$ have individual property (x) values $1 \rightarrow 4$ respectively, if these are proportionally blended at a weighting of 25% each then the property (x) for the unknown sample would be calculated thus:

$$\text{Property (x)} = f(1 \times 0.25 + 2 \times 0.25 + 3 \times 0.25 + 4 \times 0.25) = 2.5$$

To improve the robustness of the prediction PT5Technology also automatically generates samples using spectral blending in ‘real time’ so as to create more near neighbours, for this example the N samples would be blended to create the Y samples, shown in Figure 3-13.

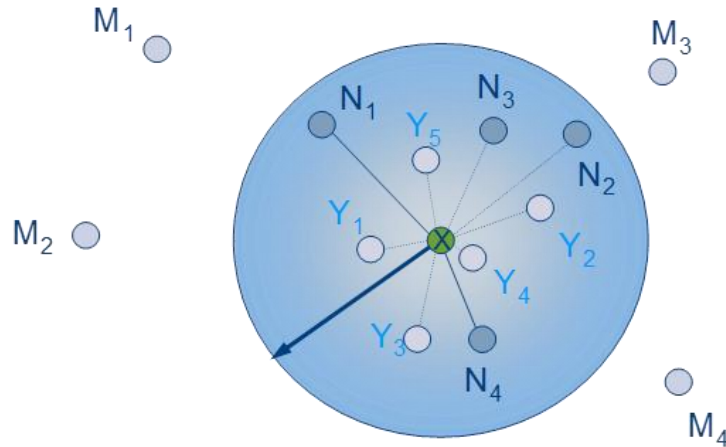


Figure 3-13 - Topological Modelling Using Artificial Nearest Neighbours

The unknown sample properties would then be calculated using the Y samples, as well as the N samples, using the principles described for equation (3-4) and shown in equation (3-5)

$$\begin{aligned} \text{Property (x)} = f(N_1 \times w_1 + N_2 \times w_2 + N_3 \times w_3 + N_4 \times w_4 + Y_1 \times w_5 + Y_2 \times w_6 \\ + Y_3 \times w_7 + Y_4 \times w_8) \end{aligned} \quad (3-5)$$

Where:

N_x = Property value of sample N

Y_x = Property value of sample Y

w_x = proportional weighting assigned to that sample

The properties (P) for the artificial samples are calculated using mixing rules, the simplest rules are linear and examples are shown in Equations (3-6) and (3-7) for the concentration (c) of each component in the blend and the absorbance at a specific wavenumber (W).

$$W_{\lambda}^{Mixture} = c_1 W_{\lambda}^{(1)} + c_2 W_{\lambda}^{(2)} \quad (3-6)$$

$$P^{Mixture} = c_1 P^{(1)} + c_2 P^{(2)} \quad (3-7)$$

By reducing the distance over which the properties are predicted allows the neighbours to more closely match the unknown spectrum whilst still having sufficient close neighbours as shown in Figure 3-14. With a smaller RSphere the prediction is typically more accurate but as there are less neighbours this configuration can introduce instability. A larger RSphere will predict more spectra but may include samples that are of an increasingly different property.

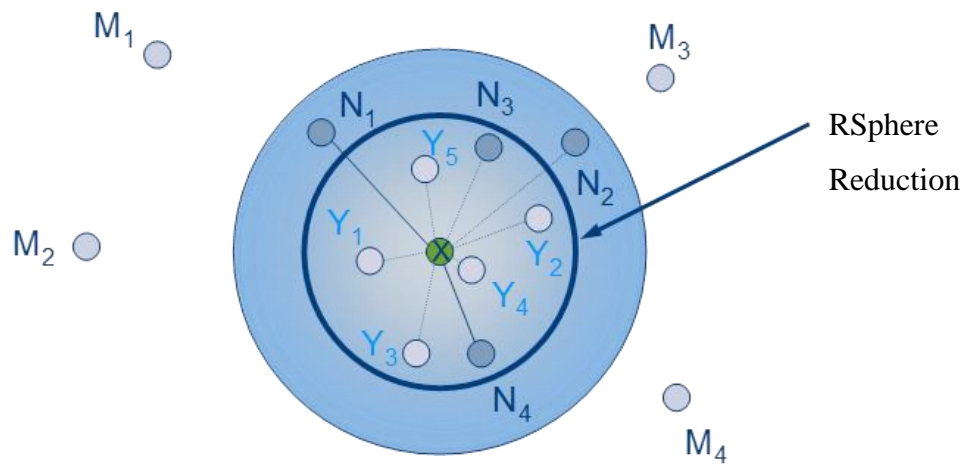


Figure 3-14 - Effect of R-Sphere

The variation of property with distance away from an unknown spectra (marked “?” in Figure 3-15) will exhibit the underlying variation from the variance in experimental error from the conventional laboratory analysis. This will typically be limited to the Reproducibility of the method, R.

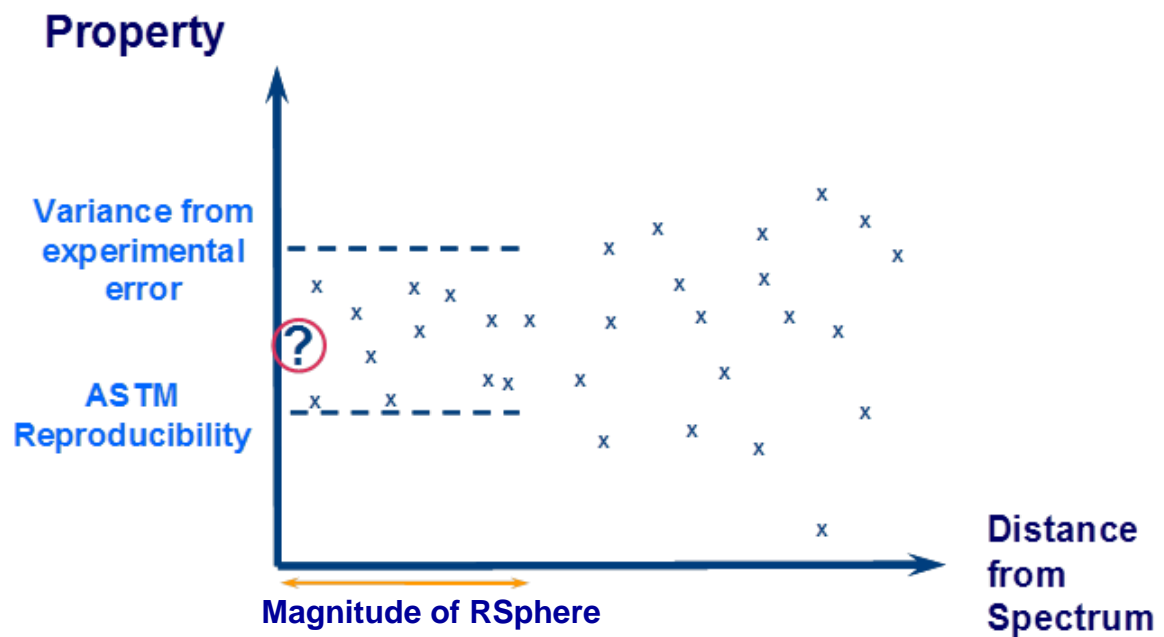


Figure 3-15 - Change of property with distance

If PT5 cannot find neighbours within the RSphere then the unknown spectrum will not be predicted.

3.3.2 *Sparse Data*

For some samples the spectrum will be near the unknown sample but the properties will not be present for those spectra. When data is analysed from the plant some property analysis will be more frequent on critical values. This is ideal for model building as more critical values typically have more analysis. PT5Technology modelling workbench makes predictions with missing values (often referred to as sparse data) as shown in Table 3-2.

Table 3-2: Database Management

Sample	Spectra	Properties				
Sample 1	Spectra 1	Prop 1	Prop 2	.	.	Prop m
Sample 2	Spectra 2	..	x
Sample 3	Spectra 3
Sample 4	Spectra 4	x	..
Sample 5	Spectra 5	x
Sample 6	Spectra 6	x	x	..
Sample n	Spectra n

The PT5 database is able to hold outliers without interfering with the prediction of “normal” spectra. When samples with spectra outside the operating box of the model are reviewed they can be left in the model. As new data becomes available when the operating point of the plant changes these data become valuable and they will be used for predictions. It is imperative to never throw away the sample data as this can potentially be used at a later date.

3.4 Treatment of outliers

Rather than being lost in a numerical correlation PT5Technology shows exactly which historical samples are being used to make the prediction and therefore simplifies tuning and model review as the issues are closely related to the industrial process and the associated information of batch, date, type etc. Areas of the model can be investigated to understand how many samples are present and the best approach to collect new samples as shown in Figure 3-16.

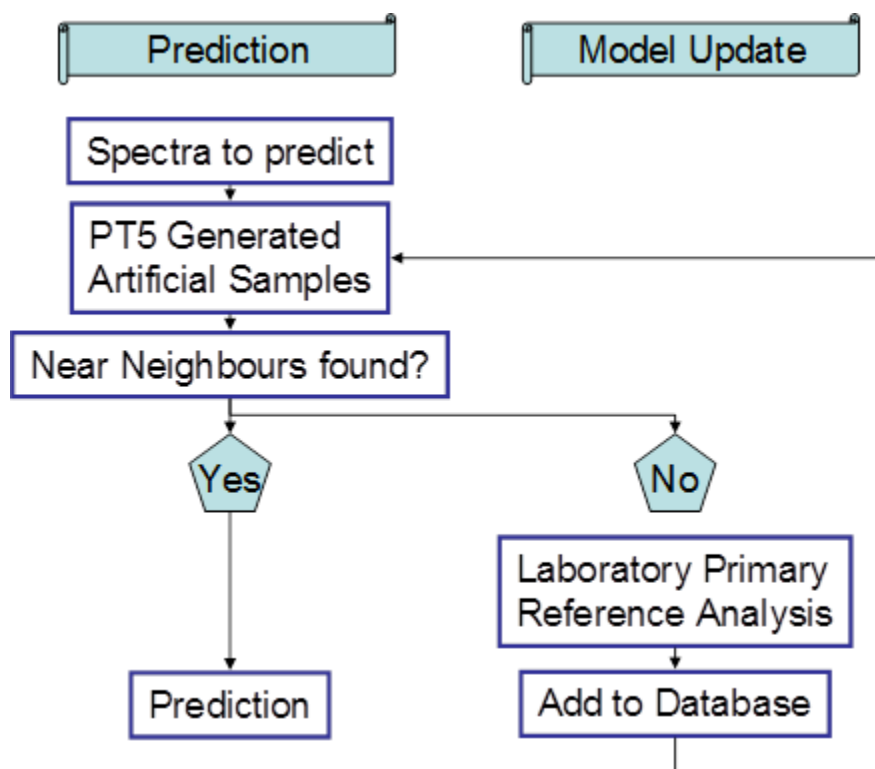


Figure 3-16 - Prediction and Model Update

3.5 Case Study 1 – PT5Technology in an Asian Refinery

In case study 1 PT5Technology is applied in a large Asian refinery for both online and offline crude quality monitoring. The application included setting up the model to predict the properties of crude deliveries and allow the customer to benchmark this against expected crude quality. An online spectrometer was then used to predict the composition of the blend to the CDU ultimately allowing for continuous process improvement.

The novelty of this case study lies in the fact that no NIR chemometric solution had ever before been implemented for such a large refinery with such a high variability in terms of crudes in the blend to the CDU.

As already discussed, PT5Technology can predict the properties of a crude oil sample purely from a NIR spectrum. This case study was prepared to demonstrate the use of the technology in an Asian refinery, carried out as part of the Eng.D research. This case study also highlights the advantages that PT5Technology can give refiners. It achieves this by analysing the variation of a given crude type in this case with the sanitised name “XX”. The case study focuses on four samples of XX delivered to a refinery in chronological order over a period of 8 months.

A summary table of the crudes being scrutinised in this case study are shown in Table 3-3. The important values in this case study are API Gravity (density of the crude oil) and wt% Sulphur, as these are the common measurements that refiners make of the crude. As mentioned API Gravity is related to the density to crude oil and is expressed relative to the specific gravity of water (SG) at 15°C and given by the following formula:

$$API\ Gravity = \frac{141.5}{SG} - 131.5 \quad (3-8)$$

API is a measure of the heaviness of crude oil by relating the density of crude oil to water. This means the higher the API the lighter the crude. Coupled with API measurements, Sulphur analysis also gives important information about crudes. Although not as indicative as API, Sulphur content can also be used to get a feel for the heaviness of crude (in fact the sulphur measurement is used in the crude scheduling) with the trend being that the lower the sulphur content the lighter the crude.

API and Sulphur measurements are quick, easy and readily available methods of characterising crude oils. These values are widely used to confirm the value of the crude and are measured at both the load port (where the crude is loaded onto the tanker) and refinery jetty (where the crude is unloaded).

The 565°C+ property represents the amount of residue in the crude, i.e. the percentage which will boil off over 565°C. Table 3-3 thus shows the API, Sulphur and 565°C+ values for the 4 samples.

Table 3-3: Four samples of type XX with their API, Sulphur and the cut 565°C+ from TBP

	SampleID	API	Sulphur	565°C+
	Sample_01 – 05/09/11	32.8	0.9	7.6
	Sample_02 – 06/11/11	33.8	0.8	6.0
	Sample_03 – 19/01/12	37.9	0.3	11.6
	Sample_04 – 23/02/12	33.0	0.8	6.2

As discussed earlier it is normal for refineries to carry out measurements of API, sulphur and water on all imported crude cargos.

However a full distillation is never carried out on every crude delivery and as can be seen from the value of 565°C+ in Table 3-3 this can vary between batches for the same crude. Refiners use assay data to update Linear Programme and optimisation software, obviously if the real crude composition is deviated from expectations then the refinery does not operate optimally.

API gravity and Sulphur analysis therefore does not provide sufficient information to properly evaluate the value of each crude cargo. In Table 3-3 Samples_01, _02, and _04 form a group with similar properties, Sample_03 is different. The API gravity of Sample_03 would suggest a lower residue and more valuable crude, however, the 565°C+ cut is double the other members of this group which indeed means the opposite, this crude has twice as much residue and is therefore likely to be less valuable. If this pattern was repeated then 25% of the crude cargos being processed would have twice as much residue as expected, impacting margins.

3.5.1 *Utilising the Aggregate Plot*

NIR scans were taken of each of the four crude oils as shown in Figure 3-17 below.

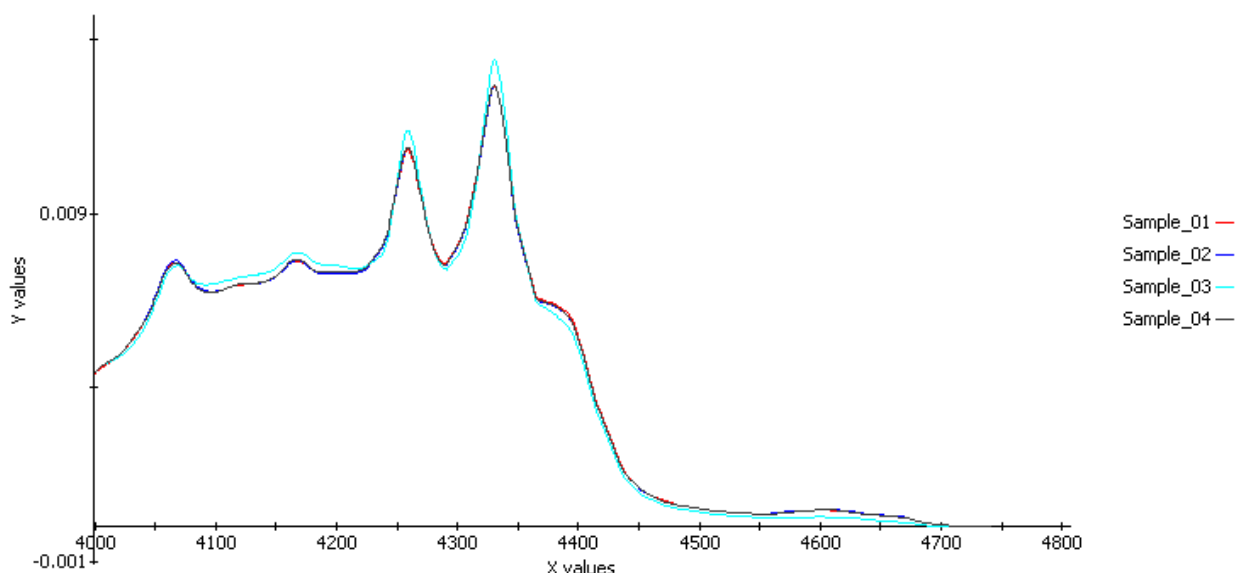


Figure 3-17: Case Study Crude Spectra

It can be seen that the spectra of Sample_03 shown in light blue is considerably different to the clustered samples of Sample_01, Sample_02 and Sample_04. However, the reason for this needs to be assessed utilising chemometric approaches in PT5 Technology.

The first tool used to deconvolute the data are PT5Technology aggregates, which show the spectral variation within a crude type. Figure 3-18 shows an aggregate plot of a group of crudes from the same geographical location within the PT5Crude global crudes database. The trend in the aggregate plot is that API Gravity is lower in the lower right of the box and increases as the crudes get lighter to the upper left of the box. This can be seen also in the 565°C+ property aggregate where the heavier crudes with the higher 565°C+ are in the lower right of the box and lighter crudes with less 565°C+ are in the upper right of the box.

The points are colour coded and the higher the value of the property the darker the colour, i.e. high API gravity are the red points in the upper right of the box (Figure 3-18a) and high 565°C+ are the red points in the lower right of the box (Figure 3-18b). Conversely, as the property value gets lower the colour tends towards green as can once again be seen in the aggregates of Figure 3-18a and Figure 3-18b. The axes used in these figures are the Intertek proprietary aggregate expression ag1 and ag3, these use the principles described in section 3.3 and are related to the API gravity and the 565°C+ residue content respectively.

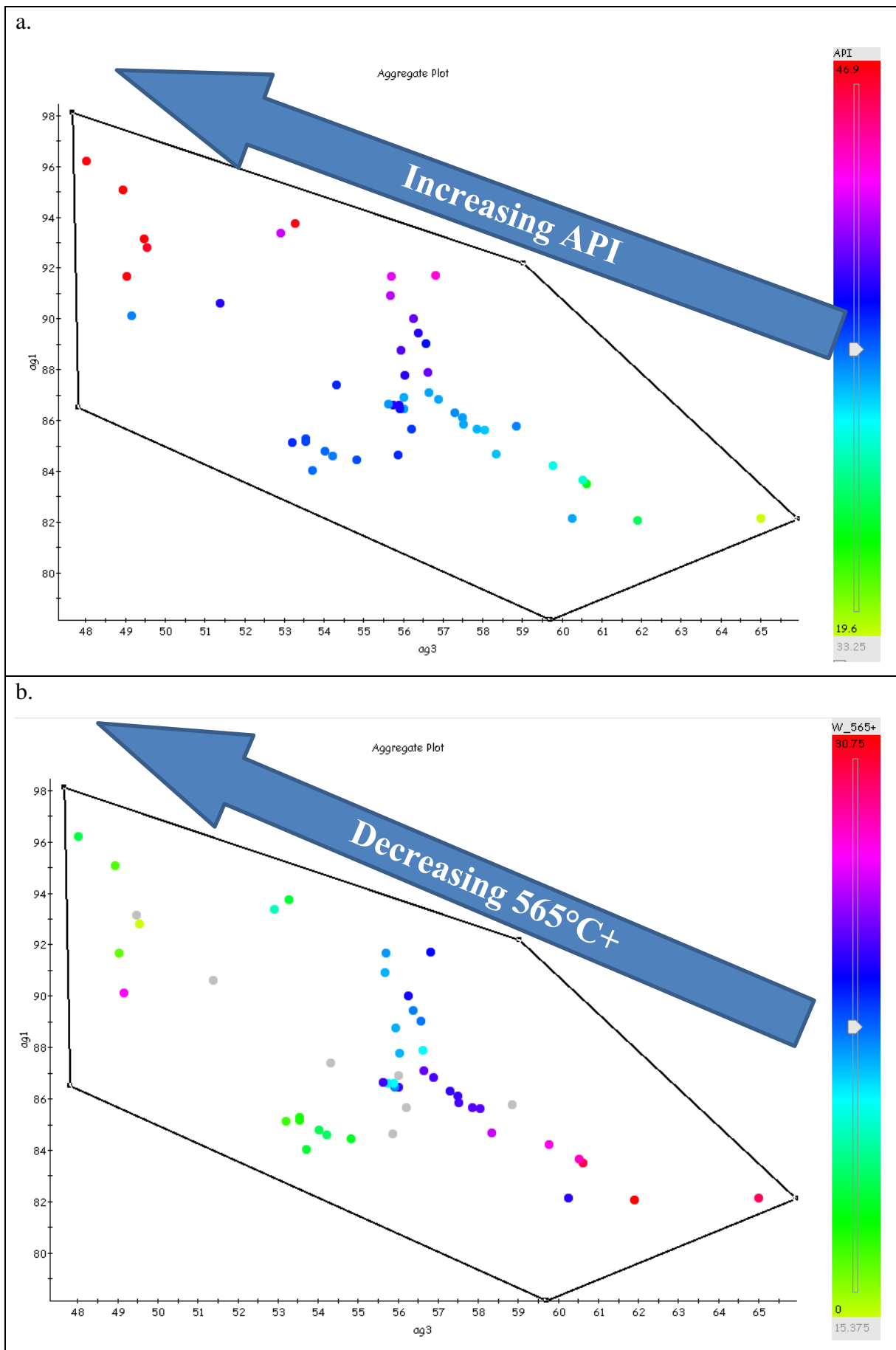


Figure 3-18: PT5 Aggregate Plots of all Example Crudes showing API gravity aggregate (a) and 565°C+ aggregate (b)

The aggregate plot is shown below in Figure 3-19 is of example crudes is shown next to a plot of physical properties of API gravity and 565°C+.

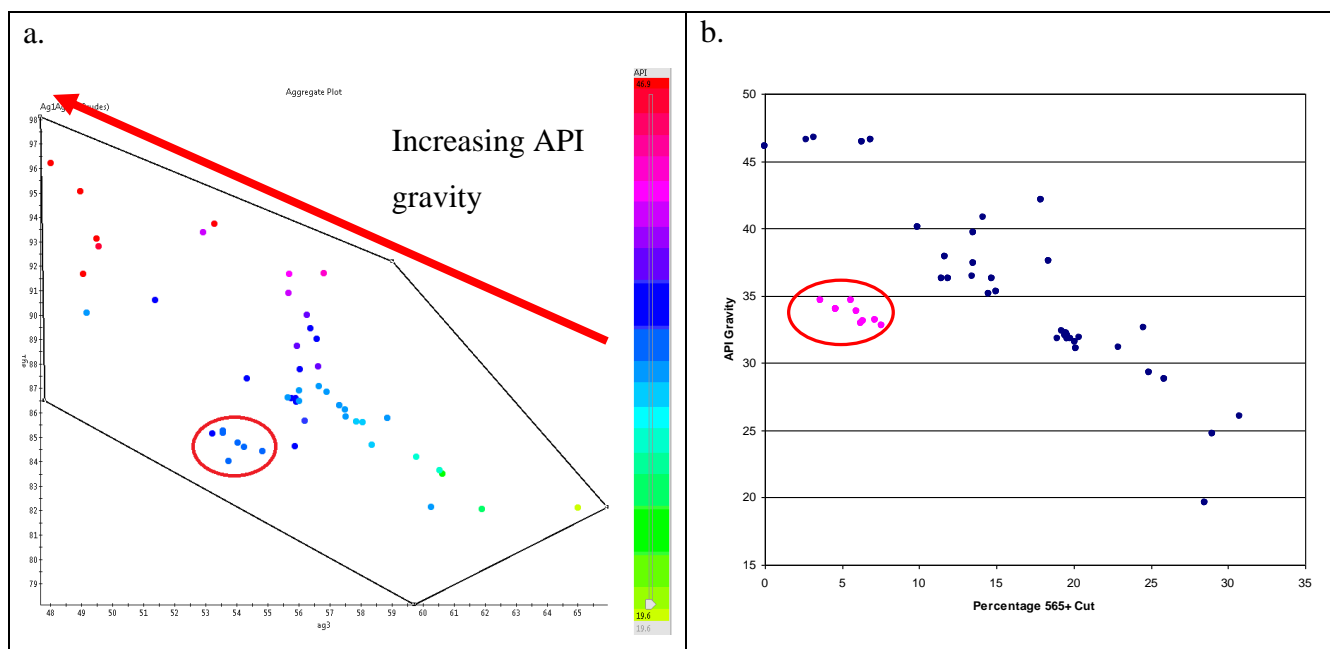


Figure 3-19: Showing PT5 Aggregate plot (a) and a physical properties correlation (b)

Figure 3-19 shows that the spectral aggregates from PT5 (Figure 3-19a) mirror the clustering of crude properties from the properties correlation (Figure 3-19b). The correlation shown in Figure 3-19b is between the variables of API gravity and 565°C+ and clearly shows the relationship that with decreasing API gravity comes increasing 565°C+.

This particular correlation demonstrates that for very similar API gravity you can have significant change in the TBP, in this case an API gravity of value of 35 is associated with a TBP 565°C+ cut range of between 3% and 15%. Thus demonstrating that is not prudent to rely on this as a key marker for crude quality, it also shows how the aggregate plot can be used to relate spectral space to measured laboratory values.

3.6 Crude Type XX Analysis

The PT5Crude aggregate plot in Figure 3-20 shows how Sample_03 is identified by the spectra as being different from the other three samples. The crude is shown as the red point. It is important to note that the red colour of this dot is assigned to it by the PT5 aggregate legend and is derived from its properties; it is not a flag colour to indicate the crude is different.

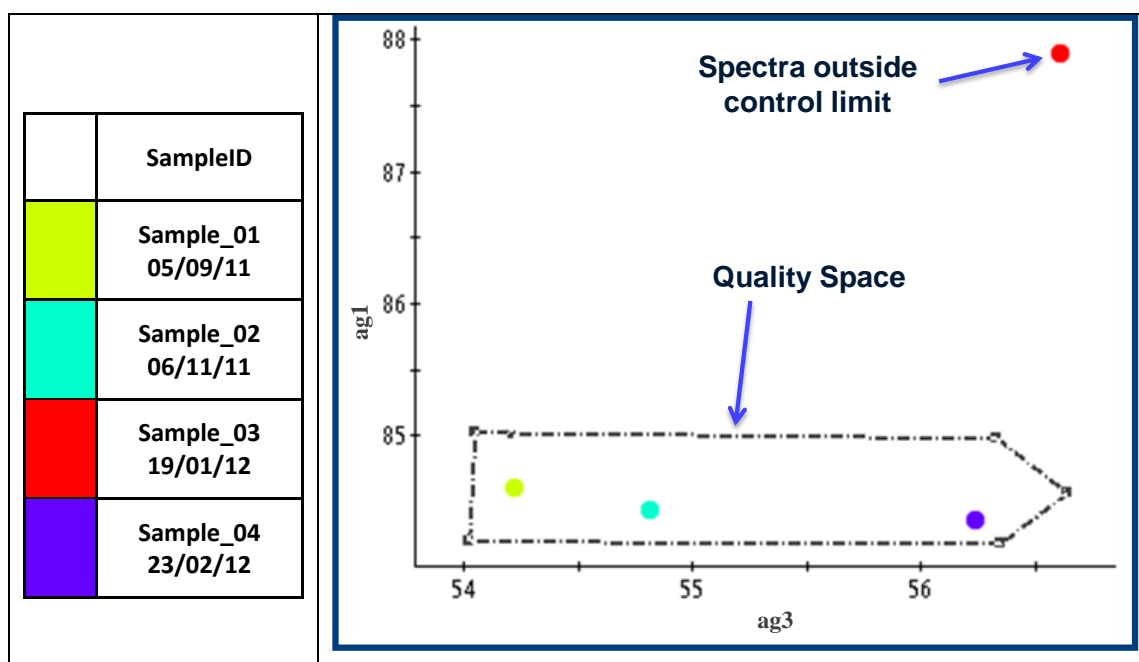


Figure 3-20: PT5Crude Aggregate Plot of Crude Type XX showing cluster and difference

The API gravity of this crude from Table 3-3 is 37.9 and thus indicates that it is the lightest of the four crudes in question. However, although it is slightly higher up on the y axis than the rest of the crude family it is no further to the left of the x axis. This flags this crude up as different because as has been demonstrated by Figure 3-19, lighter crude tend to move to the upper left corner of the aggregate plot. Looking at the Sulphur content it can be seen it is 0.3 which is the lowest Sulphur content of the four, once again suggesting this would be the lightest and most valuable of these four crudes. This is due to the fact that higher API gravity and lower sulphur suggests a larger quantity of higher value fractions and less sulphur would indicate less downstream desulphurisation requirements.

Due to this obvious outlier further investigation of this crude was carried out. Shown in Figure 3-21 is the laboratory TBP curve of the four crudes. It can be clearly seen that Sample_03 is different to the other three samples and that the TBP curves of the other three samples are very similar.

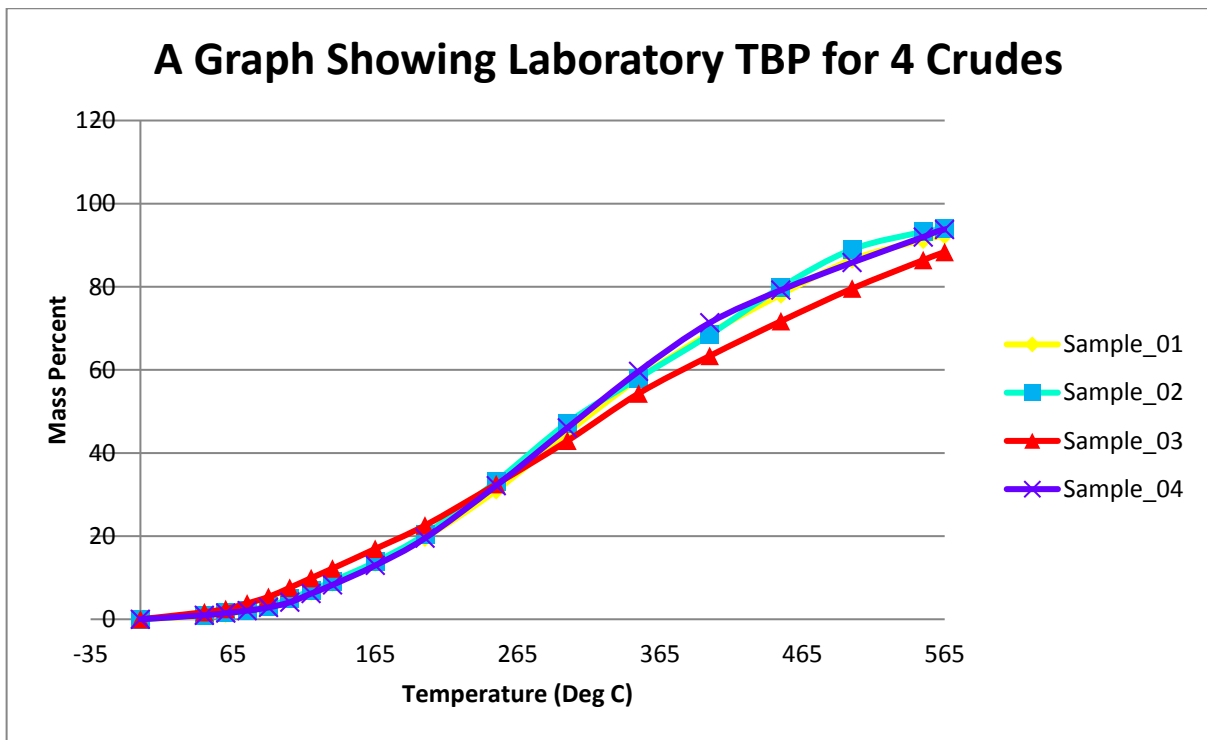


Figure 3-21: TBP Curves for all four crude samples

To further highlight this difference an average was taken for the TBP curves of Samples_01, _02 and _04 and plotted against the TBP curve of Sample_03, this plot is shown on the left of Figure 3-22. On the right of figure five is a plot showing the difference between the average TBP curve of Samples_01, _02 and _04 and the TBP curve for Sample_03. These two plots clearly show the difference between these two crudes in terms of composition.

Looking at both plots in Figure 3-22 it can be seen how below 250°C, the sample_03 crude has higher yield, this is what gives the higher API gravity value than the other three crudes, a fact that would not be possible to see without the TBP prediction from PT5Technology, or a time consuming crude assay. It can also be clearly seen from the differences that above 250°C the crude has less mass up to the 565°C+ region, showing clearly how this crude has more residue. From these plots it thus starts to become clear how, although this crude has significantly more residue compared to the historical samples of the same family, it also has a higher API gravity.

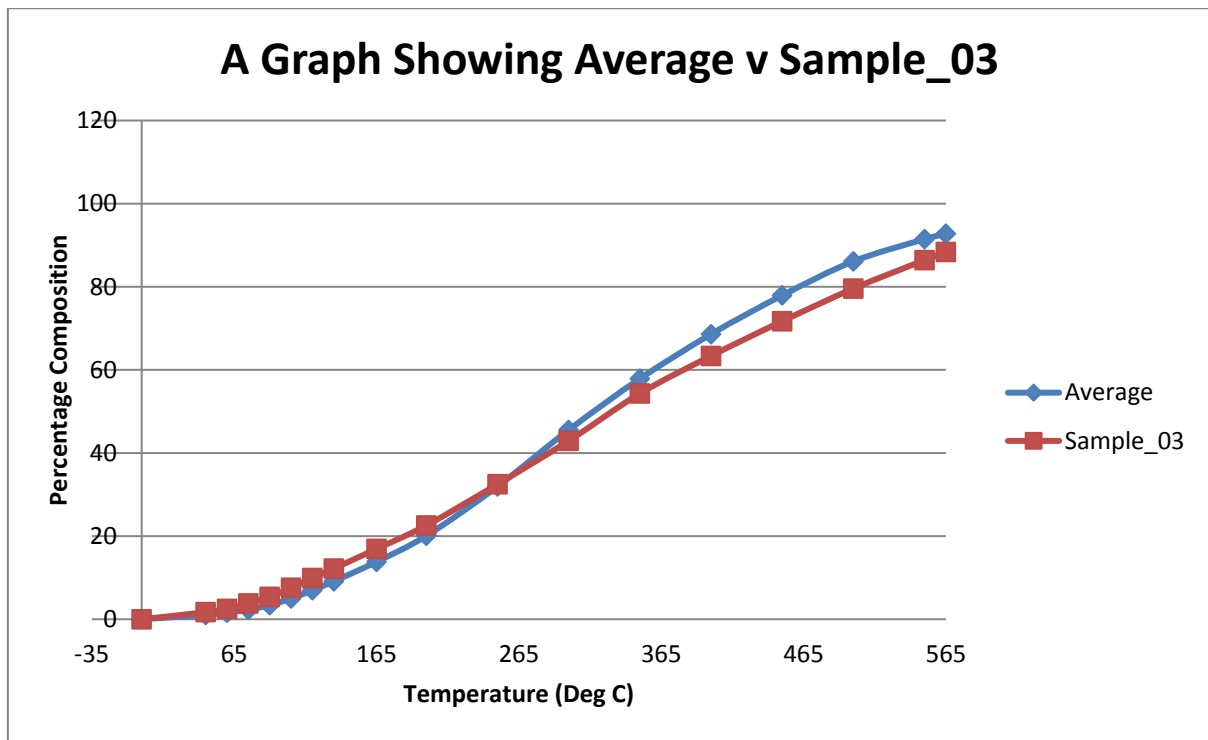


Figure 3-22: Showing Average TBP v Sample_03

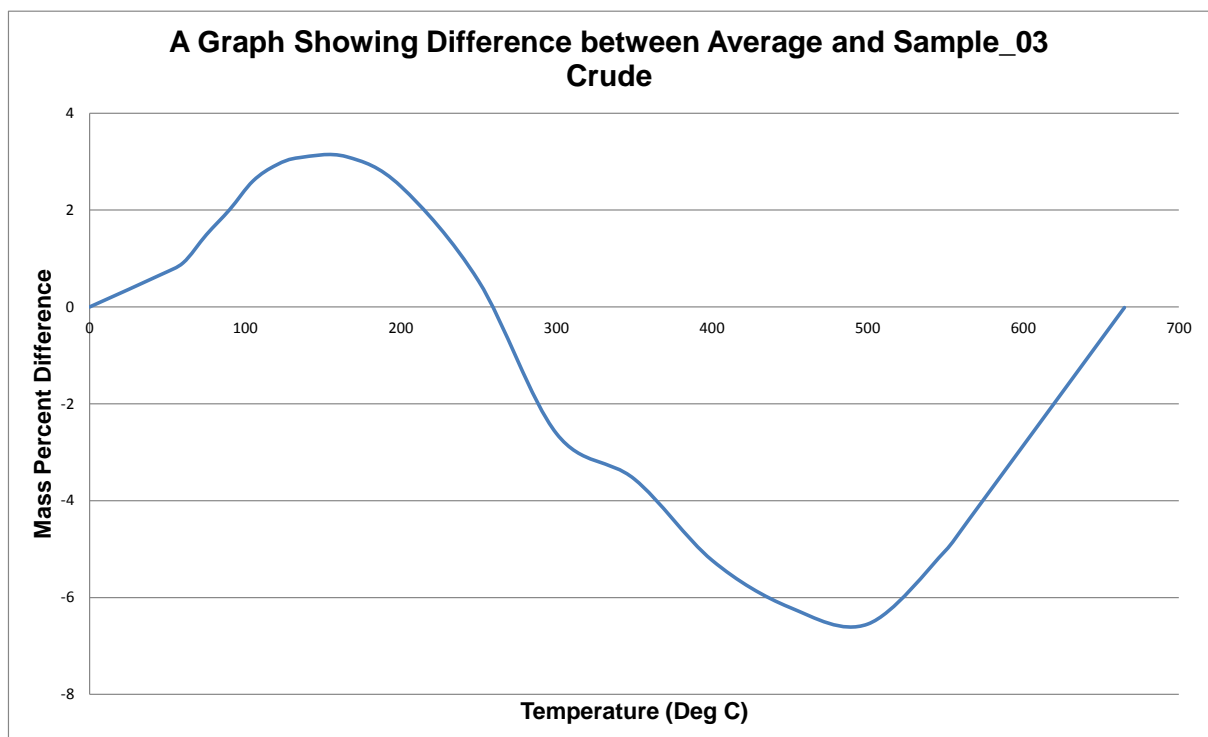


Figure 3-23: the difference between the average and Sample_03

As stated before PT5Technology can predict the properties of a crude sample purely from a NIR spectrum. In Figure 3-24 the NIR predictions are plotted, as with the laboratory analysis from Figure 3-21 it can be seen that once again the chart shows that Sample_03 has the highest amount of light ends and also significantly higher 565°C+ cut (an additional 5%). This

demonstrates that both methodologies are picking up the compositional difference in this sample from the rest of its family, however, it should be noted that the laboratory analysis takes a number of days to produce whereas the prediction can be generated within a few minutes.

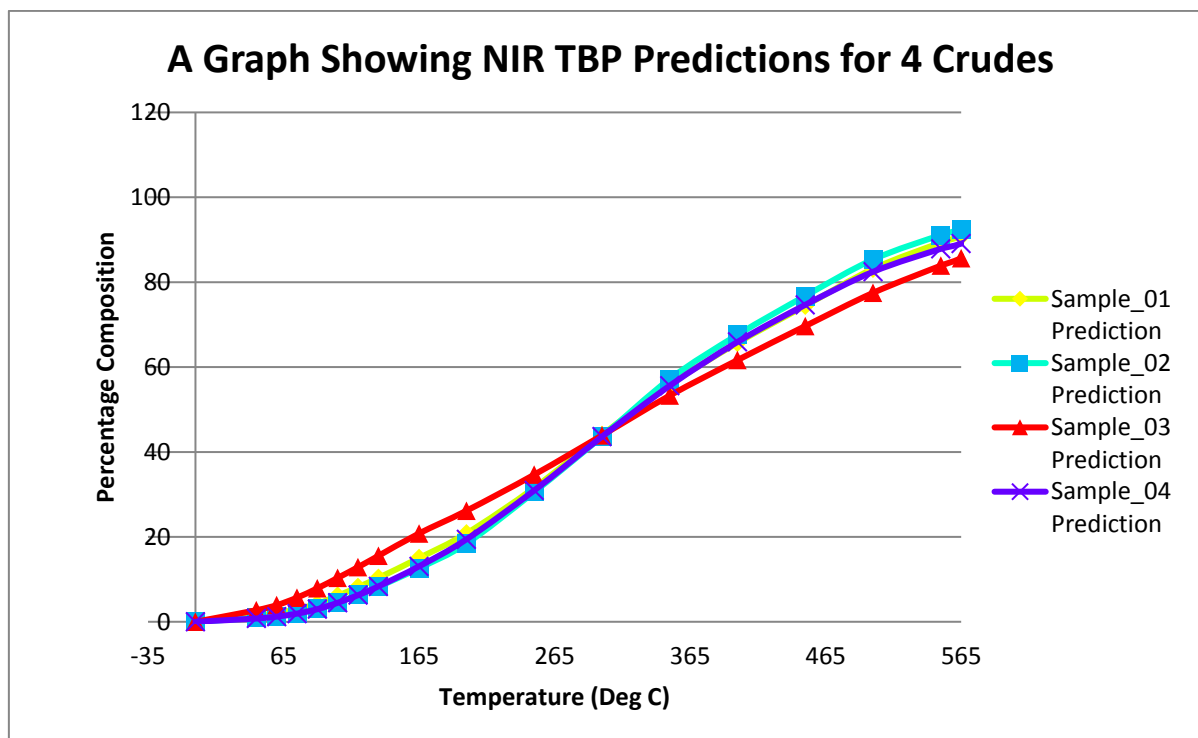


Figure 3-24: TBP curves from PT5 prediction

The distillation curves show clearly that Sample_03 is heavier than the other 3 samples, having more 565°C+ residues. Looking at the predicted values it can be seen they follow the same trend as the actual values. It is also important to note that the outlying crude has been predicted to be different to the other crudes in the same family, this is important because it shows the capability of PT5Technology.

Table 3-4 below shows the Standard error of prediction (SEP) for each of the properties modelled for a database of 60 samples from the same geographical area as the case study crudes. The SEP value is calculated by adding the absolute of the average to two times the standard deviation of the differences between the predicted and laboratory methods. An SEP <100% indicates the model performance is good enough to be released for use.

Table 3-4: Property Prediction Statistics

Property	SEP
API	74%
Sulphur	29%
565C+	91%

This prediction has been made based purely on the NIR spectra and thus the technology ignores the other crudes of the same family for sample_03 because spectrally they are further away. The technology thus uses other spectra that are close to sample_03 and predicts the spectra.

Show in Table 3-5 is the aggregate distance matrix; this is constructed by taking the spectral distance of each sample relative to each other sample. If a crude is within a spectral (Euclidean) distance of 4.5 (based on historical confidence) of another crude then those two crudes are spectrally very similar, any crude within a spectral distance of 10 is used in a prediction. It can be seen looking at the values that Sample_01 and Sample_02 are spectrally identical to each other and Sample_04 is very similar to both Sample_01 and Sample_02. Sample_03 however is spectrally a distance of more than 30 away from the other samples, showing how different this crude is from the other crudes. It is also important to note that because of this distance this crude will not be used in the prediction of the other three samples and the other three samples are not used in the prediction of Sample_03. Looking at the distances however it can be seen that Samples_01, _02 and _04 are within a distance of 10 and thus are all similar enough to be considered the same spectral family.

Table 3-5: Aggregate Distance Matrix

	Sample_01	Sample_02	Sample_03	Sample_04
Sample_01	0.0	3.6	33.3	7.5
Sample_02	3.6	0.0	30.8	5.9
Sample_03	33.3	30.8	0.0	27.6
Sample_04	7.5	5.9	27.6	0.0

Table 3-6 shows the difference between the laboratory analysis and the prediction by PT5Crude Technology. The values were achieved by taking the difference between the laboratory value and predicted value. If the difference between the values lies within the ASTM reproducibility for a particular cut then there is a high confidence in the prediction and laboratory method.

In the table (overleaf) the differences are normalised against the ASTM reproducibility for the laboratory method and expressed as a percentage of the method reproducibility (R). Thus, $\leq 100\%$ is within R and $>100\%$ is outside R. Method reproducibility is an important metric to understand the applicability of the prediction. This is because the model results are treated in industry as if they were laboratory generated values and, the reproducibility is the maximum limit, as stipulated by ASTM that any two laboratories are allowed to differ by.

It is generated by conducting round robin testing between laboratories all over the globe with the same capability and in this case, is expressed in mass percent.

It can be seen that not all fractions predict within ASTM reproducibility, and two example values have been highlighted. These values are in the region of the distillation curve known as the ‘crossover region’ and this is where the residue from the atmospheric ASTM D2892 distillation is taken and moved over to the high vacuum ASTM D5236 distillation. As a consequence, modelling in this region can be difficult as the laboratory primary reference data can have a high inherent reproducibility.

However, despite some deviations, utilising the predictions instead of historical assay data to update the LP results in a much closer match to the measured crude oil composition and thus more optimal refinery operation.

Table 3-6: Difference between prediction and laboratory analysis expressed as a percentage of method reproducibility R

Cut	ASTM R (wt%)	Sample_01	Sample_02	Sample_03	Sample_04
W_IBP-45	1.3	33%	26%	69%	1%
W_45-60	1.3	6%	9%	32%	1%
W_60-75	1.3	1%	9%	34%	4%
W_75-90	1.3	24%	10%	46%	12%
W_90-105	1.3	21%	35%	25%	12%
W_105-120	1.3	14%	12%	28%	7%
W_120-135	1.3	4%	11%	30%	1%
W_135-165	1.3	2%	3%	45%	2%
W_165-200	1.3	12%	32%	12%	8%
W_200-250	1.4	78%	24%	100%	38%
W_250-300	1.4	33%	24%	109%	39%
W_300-350	1.4	4%	263%	151%	84%
W_350-400	2.7	16%	53%	35%	23%
W_400-450	2.5	9%	99%	23%	29%
W_450-500	2	12%	87%	2%	29%
W_500-550	2	29%	29%	12%	19%
W_550-565	2	5%	24%	3%	12%
W_565°C+	2.9	11%	60%	144%	51%

3.7 Net Back Calculations

Net back calculations using Haverly HCOMET software showed that with a simple refinery setup (Table 3-7) this crude would indeed be more valuable purely because of its lower sulphur; however with a complex refinery setup (Table 3-8) this crude was indeed less valuable.

Table 3-7: Simple Refinery Netbacks

Simple Refinery				Sample 1	Sample 2	Sample 3	Sample 4
Feedstocks Consumed (Vol%)							
	Natural Gas for Fuel	@3.00 \$/MBtu	Vol%	1.94	1.89	1.79	2.03
Product Make (Vol%)							
Fractions	LPG	@542.41 \$/MT	Vol%	0.12	0.12	0.12	
	Naphtha	@932.15 \$/MT	Vol%	14.62	14.89	19.18	17.87
	Mogas Prem 95	@986.20 \$/MT	Vol%	3.53	3.53	3.46	
	Jet-A1	@1,009.60 \$/MT	Vol%	13.66	15.76	12.28	15.59
	Diesel @10ppmS	@958.45 \$/MT	Vol%	12.87	14.75	23.99	12.67
	Heating Oil 0.1% S	@930.80 \$/MT	Vol%	17.02	12.76		17.68
	Fuel Oil 1% S	@636.08 \$/MT	Vol%			41.41	
	Fuel Oil 3.5% S	@591.60 \$/MT	Vol%	38.51	38.54		36.84
Products Sum			Vol%	100.33	100.35	100.44	100.65
Crude Est Value			US\$/B	111.95	112	112.21	112.94

Table 3-8: Complex Refinery Netbacks

Complex Refinery				Sample 1	Sample 2	Sample 3	Sample 4
Feedstocks Consumed (Vol%)							
	Natural Gas for Fuel	@3.00 \$/MBtu	Vol%	5.67	5.66	5.33	6.69
Product Make (Vol%)							
Fractions	LPG	@542.41 \$/MT	Vol%	1.04	1.07	1.03	3.21
	Naphtha	@932.15 \$/MT	Vol%	20.82	22.26	24.05	36.88
	Mogas Prem 95	@986.20 \$/MT	Vol%	18.62	18.2	18.88	
	Jet-A1	@1,009.60 \$/MT	Vol%	14.69	20.81	23.97	16.64
	Diesel @10ppmS	@958.45 \$/MT	Vol%	40.61	34.13	27.03	41.99
	Heating Oil 0.1% S	@930.80 \$/MT	Vol%	0.63	0.81		
	Fuel Oil 1% S	@636.08 \$/MT	Vol%	1.56	2.92	7.29	3.21
	Fuel Oil 3.5% S	@591.60 \$/MT	Vol%	5.3	3.43	1.16	3
Products Sum			Vol%	111.16	111.47	110.6	112.69
Crude Est Ref Value			US\$/B	122.44	122.89	121.55	122.31

3.8 Conclusion

The object of this project was to develop a technique, which can provide a refiner with as much information about the crude oils being delivered and processed as possible, whilst still being quick and simple to deploy.

Although process NIR has been used for many years for refined fuels blend optimisation, this project was novel because it was the first application of process NIR to monitor refinery crude oil quality.

The case presented was intended to demonstrate not only that the technology implementation was successful, but also that there is a clear need for this. The business benefit was thus contextualised by looking at the information a refinery would get from the conventional analysis schedule (API and sulphur measurements) and then the extra benefits from being able to quickly analyse crude oil TBP.

The case study clearly shows that whole crude property measurements are not a conclusive method of characterising a crude type to give a refinery the real value of a crude import. In this case the crude Sample_03 had a higher API gravity suggesting a lighter crude oil; however, looking at the aggregate plot shows that it has changed in quality, the PT5Crude prediction then calculated, purely from an NIR spectra, that whilst the light ends are greater, the 565°C+ fraction is higher compared to the rest of its crude type.

The predictive performance was then validated by comparing it against laboratory measured analysis values and ultimately the benefits to the customer were then shown by undertaking netback calculations on the crude oil quality.

Chapter 4:

Blended Hydrocarbon Stability

Chapter 4. Blended Hydrocarbon Stability

Crude oil blending to maximise margins is carried out by the majority of refineries across the globe (single source crude oil refineries are very rare) and has been for many years. The increasing numbers of different crude oils available in today's marketplace gives refineries more chances to source low cost, unconventional crude oils to blend and process, thus giving the opportunity to maximise margins hence the terminology 'opportunity crudes.'

Unconventional crude oils can fall into many categories such as highly paraffinic (waxy), highly acidic (giving rise to corrosion issues) and highly asphaltenic (causing instability issues). As such the chemistry and composition of some of these oils can be very different to those processed historically and as a consequence unexpected issues can arise from blending these opportunity oils.

One issue is the deposition of wax and asphaltene. This can cause problems as serious as causing refinery shutdowns from blocked pipes and process units. The science of asphaltene deposition in isolation is reasonably well understood and can be explained using models such as SARA (discussed in section 2.14), however, how this relates to blending multiple crude oils is not as well understood and much research is being carried out around the world to try and address this issue.

As part of the Eng.D research an innovative approach has been developed to address the issue of deposition of undesirable material that can arise from blending crude oils such as wax and asphaltene. This was undertaken as a consequence of identified weaknesses in existing test methodologies (such as ASTM D7060, ASTM D7112 and ASTM D7157). These weaknesses are significant in that although refineries are blending multiple crude oils, these methodologies assess the crude oils in isolation and instead use pure solvents such as heptane and toluene to assess stability.

Furthermore, the stability is assessed as the titrants are added and does not give consideration to the effects of time on blend stability. As crude is a colloidal system and asphaltene deposition is as a consequence of the colloidal balance being disturbed, time is a major factor when considering crude blend stability. In addition, due to the nature of the assessments they are only considering asphaltenic deposition and not other components such as wax.

Finally the assessment is only on the crude oil sampled at that time and gives no consideration to the quality deviations that can happen in the same crude oil family.

The methodology developed and patented as part of the Eng.D project addresses all the above issues, it assesses stability of the oils being blended in the refinery without addition of components not in the blend (i.e. heptane and toluene). Because of the way the assessments are carried out any time period of interest to the customer can be assessed, indeed in Case Study 2: Assessment of Heavy Fuel Oil Blending in a Refinery the customer was very interested in the effects of time as once the blend was made up it was then stored.

The analysis is carried out using a combination of near infrared (NIR) spectra, microscopy chemometric models and mathematical modelling algorithms meaning it is not specific to the deposition of asphaltene but also wax precipitation, making the methodology very flexible. Using NIR also means that the crude quality monitoring approach can be applied to monitor deviations in quality of crude oil, as significant quality changes can mean the interactions in the blend, and therefore the stability behaviour, can change.

Finally, the methodology can be applied to any hydrocarbon stream as demonstrated in the two applications discussed below where one focuses on a heavy fuel oil blending project and the other one on blends of marine fuels.

4.1 Introduction

To address challenges of instability of crude oil blends in a refinery, the Eng.D project carried out innovative research in this area, resulting in a patented approach which has been used in many different applications and continues to be rolled out across the globe.

The assessment of wax and asphaltene precipitation, known as Organic Deposition (OD), is based on blending hydrocarbon streams from the process. Therefore, the assessment is representative of actual operating parameters and the experimental measurements reveal the interaction between crudes during and after blending.

To allow refiners flexibility in the application of this technique, and also to ensure a robust and representative model, a variety of different ratios in the crude blend are assessed to generate instability and stability limits, this is called a blend recipe evaluation report. The blend recipe evaluation report is kept up to date using NIR spectra from neat crude quality tracking (using PT5Technology).

The samples are assessed for organic deposition by a both NIR spectroscopy and microscopy to ensure that stability is both observed and validated. To assess the response over time multiple samples are stored, NIR scanned and validated by microscopy and mathematical calculations.

The output from the Intertek OD Programme is a series of reports which are described in detail later, however, the main purpose is to provide assessment of combinations of stable and unstable crude oils which can allow the refinery to optimise the process with respect to stability as well as normal operating constraints.

4.2 Methodology

To develop the methodology it was first decided that the spectral behaviour of crude oils when blended should be assessed, particularly how linear blending can be expressed, what happens to the spectra at the point of deposition and after, and also, if this is quantifiable, repeatable and can be validated.

This is why microscopy was undertaken on all blends made up as it is a very visual representation of asphaltene deposition. The drawback of microscopy is that it is a more

laborious process than Near Infrared and also, crucially cannot be take online in a process environment.

The analytical technique selected as the primary reference method was NIR spectroscopy. This was for several reasons. Firstly, the equipment was readily available and widely used within Intertek already, and as the business groups core business is supporting online and offline laboratory NIR solutions to the refining marketplace, additional benefits that could be derived from existing hardware was a very lucrative business proposition, especially given that crude oil stability services is a rapidly growing marketplace.

To visualise deposition, the principals of light scattering by small particles was anticipated to be an observable phenomenon within the NIR spectra. TO be effective this effect has to be greater than the effect on the spectra as a consequence of the dilution of crude oil A in crude oil B.

As discussed previously a spectrometer measures the difference between detected light, with and without the sample. This difference is caused by the following three phenomena (ASTM, 2013):

- Obstacles – When radiation strikes a bluff body, it is scattered back to the source and within solid bodies without retransmission. This baseline shift is not a function of wavenumber. The amount of baseline shift is proportional to the area of the sample obscured by opaque particles.
- Reflection and Refraction - Some radiation is scattered due to the particle size where the light fails to reach the detector as its direction has been changed. The amount of light refracted is a function of wavenumber, particle size, and particle density.
- Absorption – Accelerated electric charges may transform some of the energy into another type of energy, i.e. radiation is absorbed and retransmitted where the retransmitted energy spectrum does not contain energy where the chemical bonds have absorbed the energy.

By monitoring absorption, the chemical composition of the neat crudes and blends can be characterised using PT5Technology, thus giving OD constraints.

To understand linearity of spectral blending, two crudes were first blended which were know, from process experience, to form a stable blend at all ratios. This can be seen in the below figure where crude A was titrated into crude B at 10% increments to form binary blends.

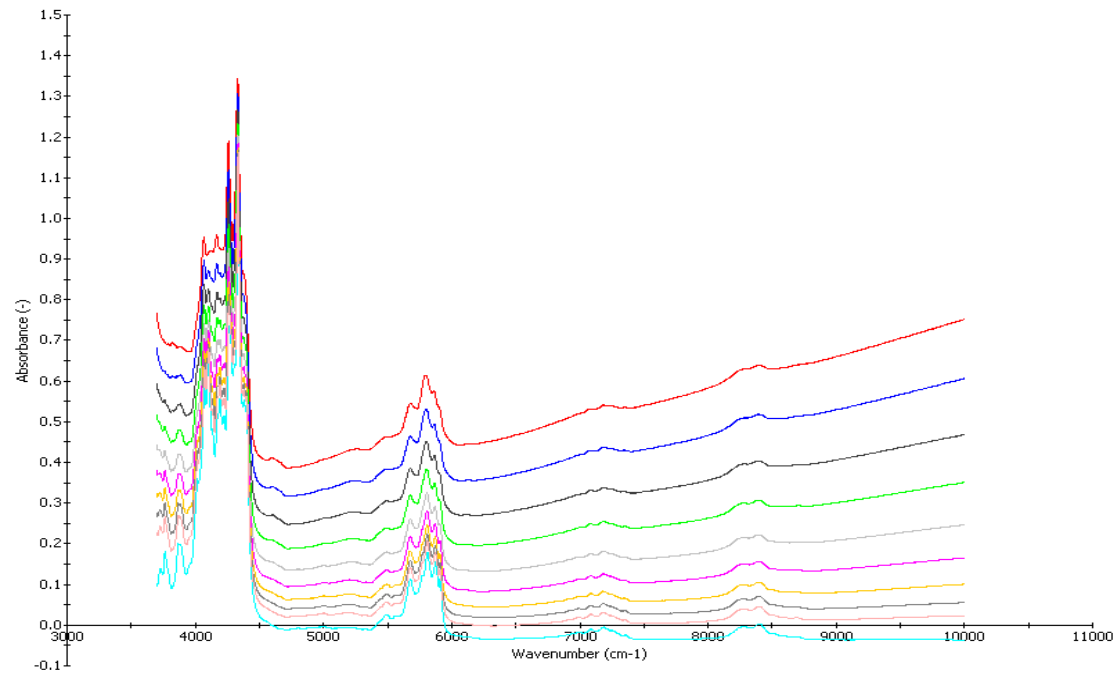


Figure 4-1: Binary Crude Blend Exhibiting linear behaviour

As expected this blend is linear, i.e. as the blend transitions from crude A to crude B the spectra move proportionally and as expected. This becomes more apparent when the percentage of crude A in the blend is plotted against Deposition Aggregate 2 (DA2 = absorbance at wavenumber 8,000)

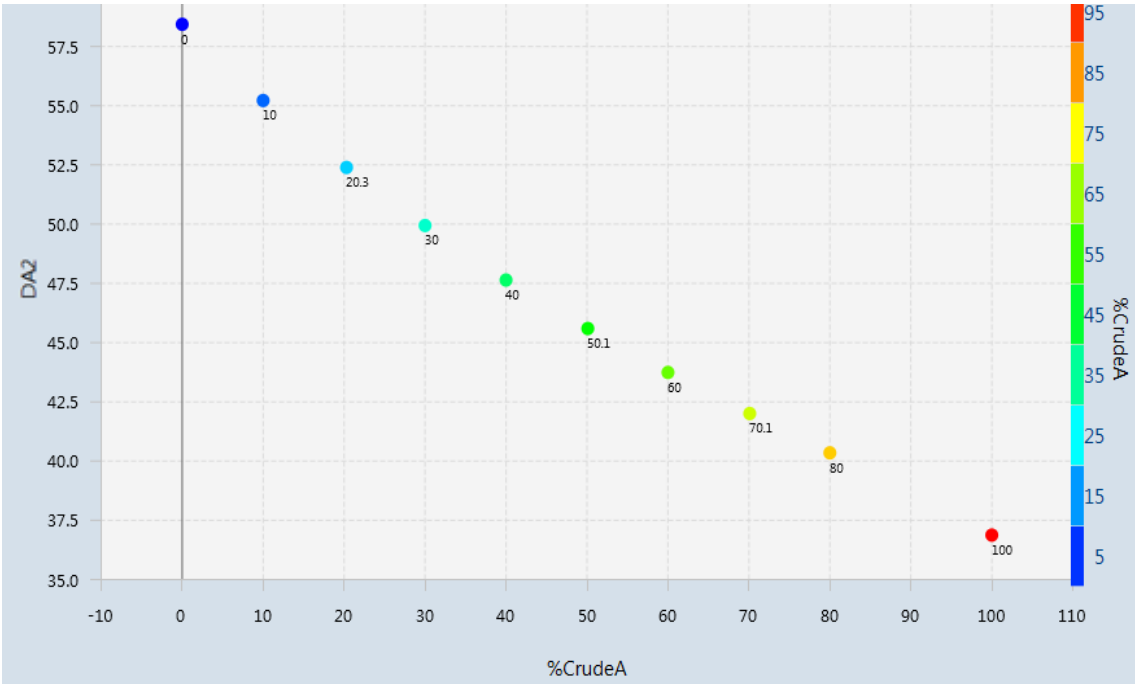


Figure 4-2: Linear Blend Aggregate

It can be seen that the blend plots as a straight line indicating linearity, this is then validated by the microscopy shown below. It can be seen that the crude oil is a flat colour with no precipitated asphaltenes evident.

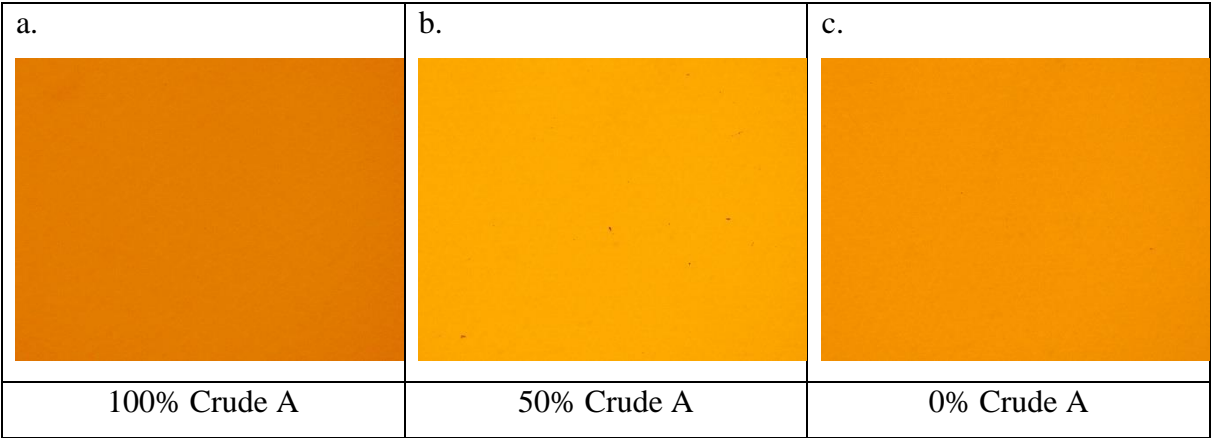


Figure 4-3: Transmitted Light Microscopy 100% Crude A (a), 50% Crude A (b), 0% Crude A (c)

Next a different crude A was selected and titrated into the same B, a blend which was known to cause processing problems, the spectra for this is shown in Figure 4-4 below.

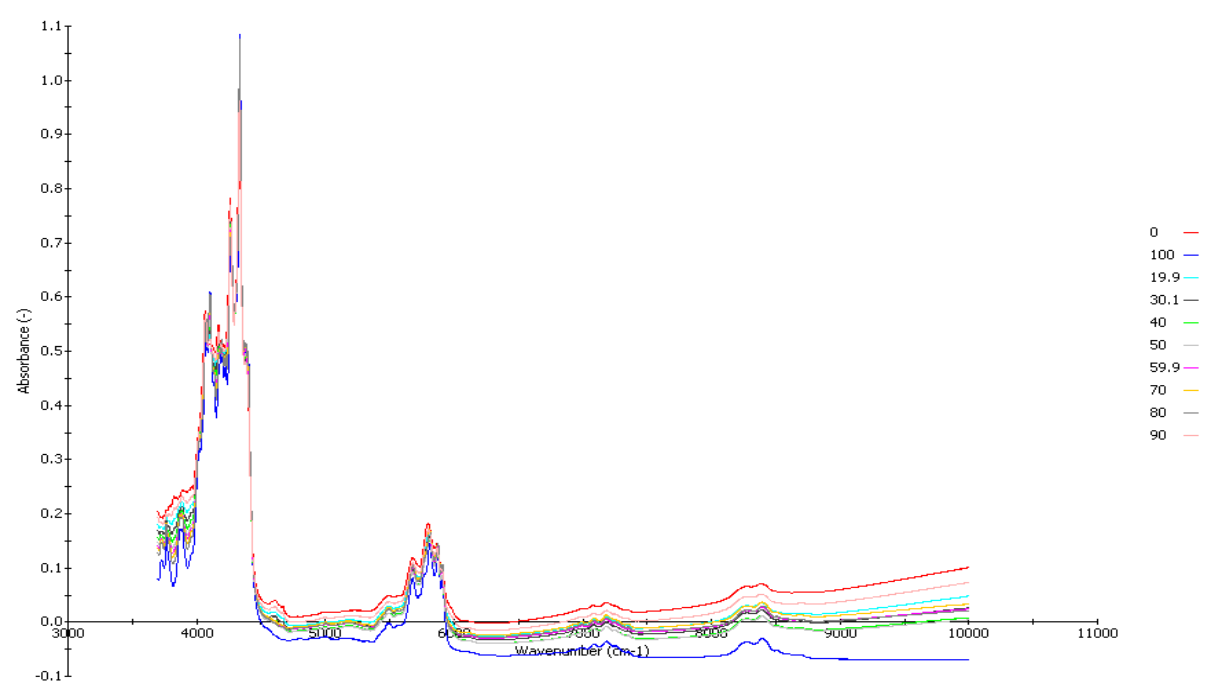


Figure 4-4: Binary Crude Blend Exhibiting Non-Linear Behaviour

As can be seen, the spectra of Crude A is very different in this case, also it is apparent that the blending is not linear, i.e. with increasing B the transition from A to B is not smooth as with the previous example. Taking an expanded view of the spectral absorbances at the 8,000-wavenumber region, upon which DA2 is based this differentiation can be seen.

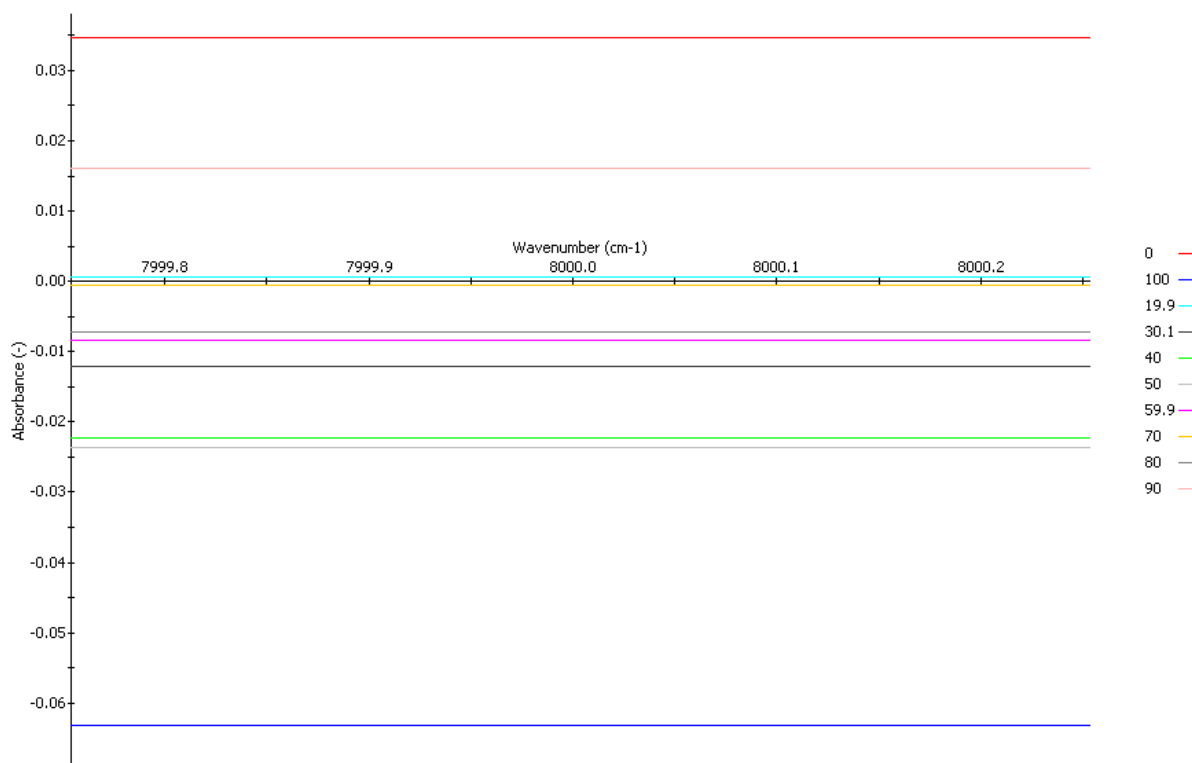


Figure 4-5: 8,000 Region of NIR Spectra Showing Non-Linearity

Looking at the absorbance at 8,000 shows that up to 40% A in B the blending is linear, however, from the 50% A in B binary blend, this linearity ends and the spectral behaviour changes, the absorbance rather than continuing to decrease actually starts to increase, despite the fact that the proportion of A in the blend is continuing to decrease. This is once again better visualised if the proportion of A in the blend is plotted against the DA2 axis.

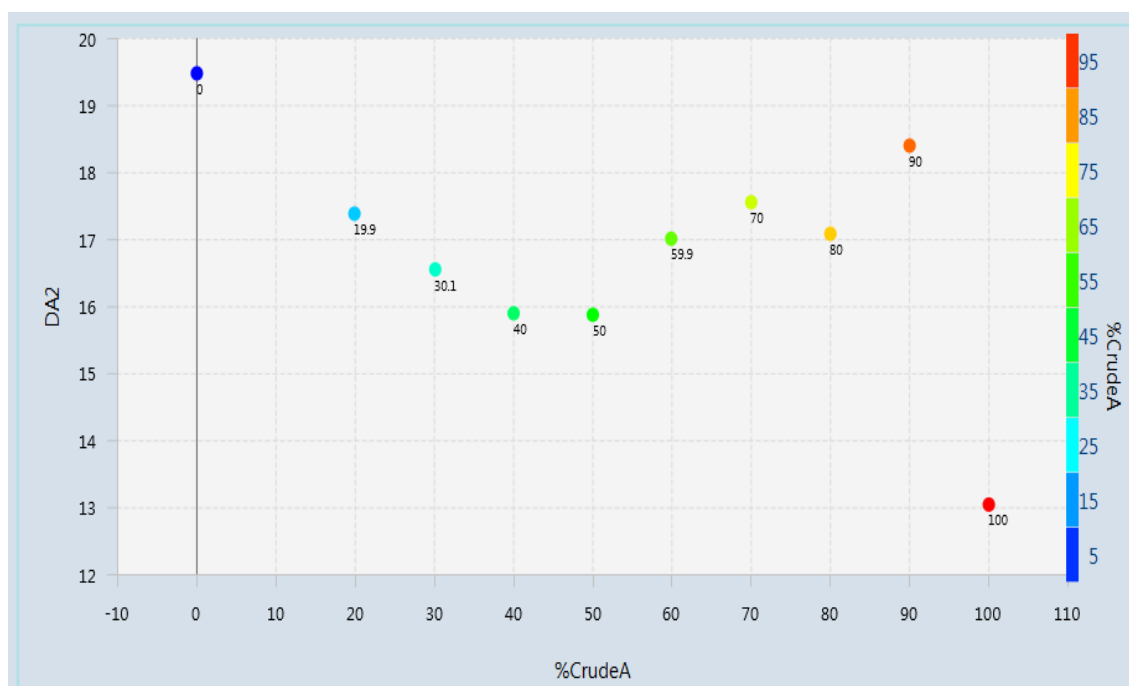


Figure 4-6: Linear Blend Aggregate

It is now very obvious that the behaviour of this crude oil blend is not linear and that an effect is occurring at the 50% A in B point. The behaviour observed is a marked increase in spectral absorbance that is consistent. This means that although the crude is being diluted it is actually absorbing more light. And this effect is stronger than the effect of the dilution of crude A with B.

If the microscopy of this is now examined it can be seen that this blend precipitates particulate material at the 50% mark and it is this deposition that is contributing to the increased spectral absorbance.

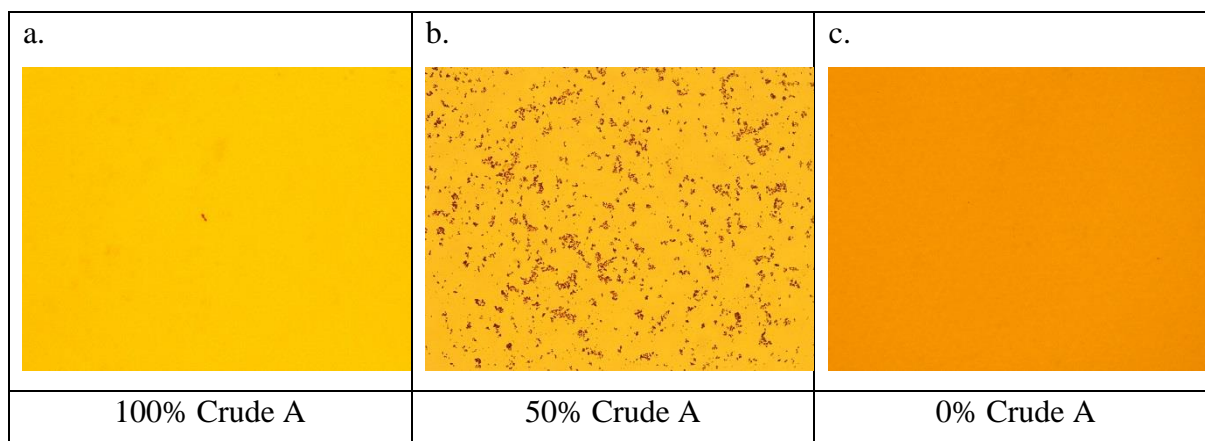


Figure 4-7: Transmitted Light Microscopy 100% Crude A (a), 50% Crude A (b), 0% Crude A (c)

4.2.1 *Observing Organic Deposition by Spectral Inflection*

Through laboratory crude oil titrations, the applicability of NIR to observing this problem has been proved. OD is observed by a NIR spectral inflection point. As discussed in section 3.3.1 spectra blend linearly and as a crude is titrated the spectra moves towards the titrant as shown in Figure 4-1.

However, at the onset of OD an inflection point is observed where even though the amount of titrant is still being increased the spectral trajectory deviates from the expected behaviour, this occurs at the inflection point and is also shown in Figure 4-8.

Figure 4-8 shows the spectral behaviour at the point of OD. Due to scattering of light by particle flocculation the absorbance increases throughout the whole spectrum (3880cm^{-1} to $10,000\text{cm}^{-1}$). Chemical changes due to OD are also observed in the 3800cm^{-1} to 6000cm^{-1} region. Figure 4-8 also shows microscopy pictures validating that the change in spectral behaviour.

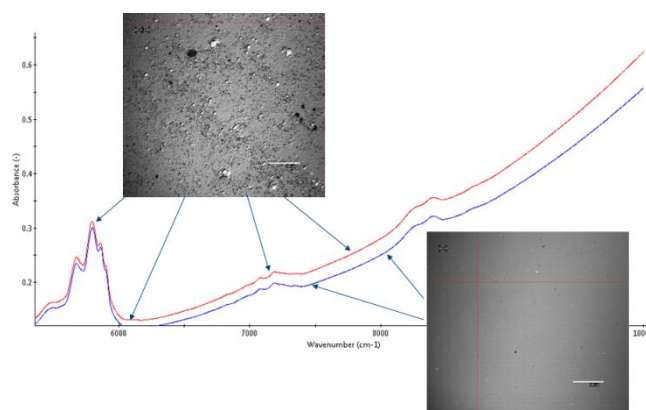


Figure 4-8: Showing inflection point

4.2.2 Neat Crude Tracking

NIR spectra allow finger printing of the neat crudes and provide an assessment of changes in neat crude composition. This assessment is made using PT5Technology, near neighbour analysis, spectral distance analysis and PT5 Aggregates.

Changes in composition of neat crude can affect the OD behaviour in the blend. Should the change be significant, the crude may be subject to re-sampling and/or further laboratory investigation.

Figure 4-9 below shows a PT5Technology spectral aggregate to demonstrate the application of crude quality monitoring in a refinery. This is another case of one delivery from the same crude family (in this case a group of African crude oils) that appears spectrally and analytically different, as discussed in Case Study 1 – PT5Technology in an Asian Refinery.

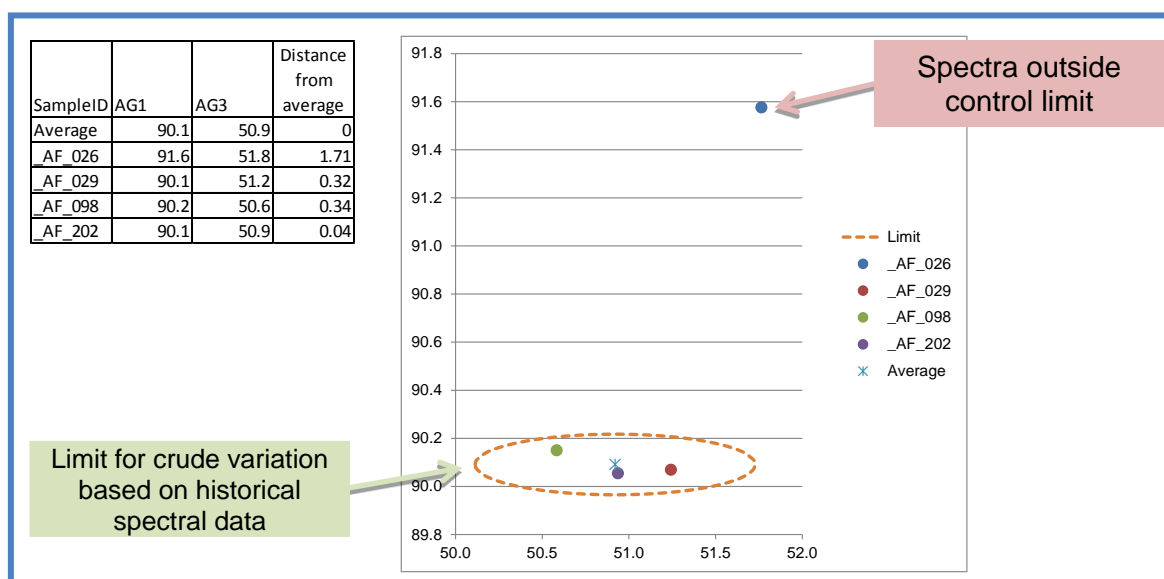


Figure 4-9 - Crude Tracking on PT5 Aggregate

4.2.2.1 *Neat Crude Property Evaluation*

PT5Technology and the Intertek NIR Global Database can be used to predict physical properties of crude. To predict the properties conventional laboratory analysis is required to tune a model. Once the model has been tuned the predictions can be made for every neat crude delivery.

4.2.2.2 *Blend Validation*

NIR spectra are compared to neat crude spectra, spectra from crude blend titrations, pseudo component spectra (i.e. crude blend before addition of titrant crude), titrant crude spectra and optionally actual spectra from the refinery blend.

As a further assessment, the spectra of the neat crudes allow theoretical blended spectra and properties to be calculated using mixing rules within the chemometric model. These calculated samples are compared to spectra obtained from actual blend experiments and refinery operation. The difference between theoretical blends and actual blends is used to assess organic deposition.

The stability of blends is also displayed on the PT5 Aggregate plot. In Figure 4-10 below the areas of instability (red) and stability (yellow) are identified from blend titration. Using these areas, drawn up based on experimental data, spectra of actual blends can be assessed for stability and instability without any additional laboratory analysis.

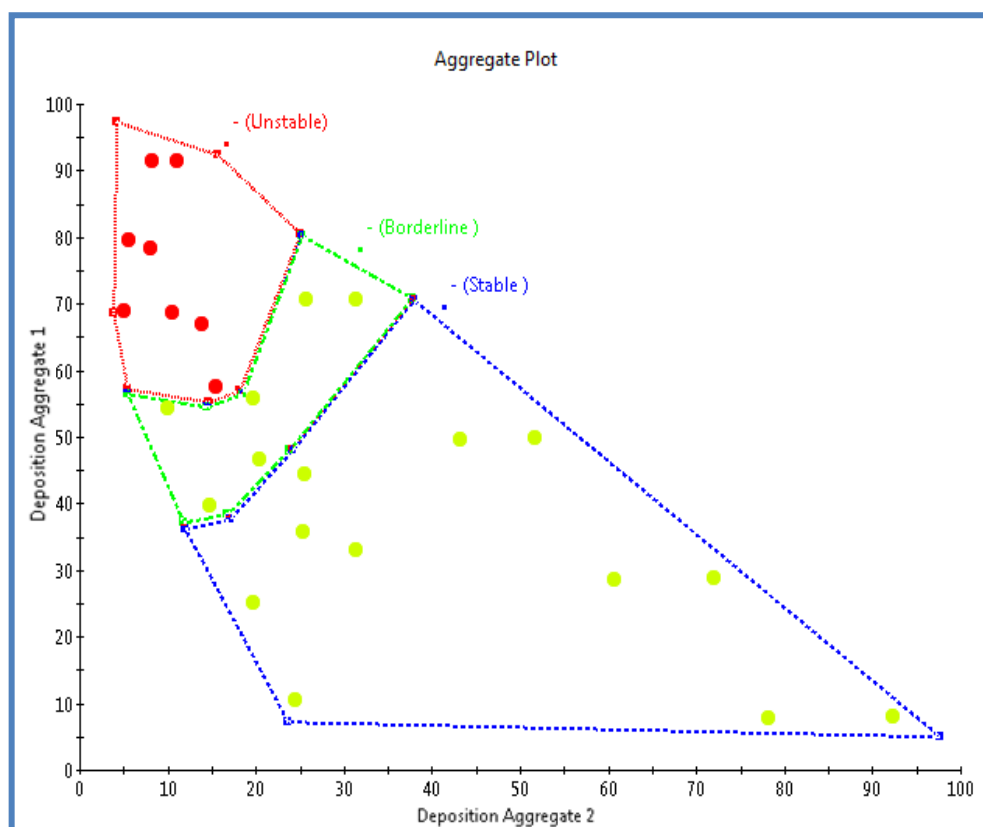


Figure 4-10 - Aggregate plot of instability observed from blend titrations

4.2.3 Neat Crude Stability and Instability Assessments

The current ASTM methodologies (such as ASTM D7060, ASTM D7112 and ASTM D7157) for assessing neat crude stability involve characterisation of each neat crude against paraffinic and aromatic standards (e.g. n-Heptane and Toluene) and follow a procedure as follows.

Firstly, the amount of asphaltene in the neat crude is measured using a paraffinic standard by ASTM D6560 – Standard Test Method for Determination of Asphaltenes (Heptane Insoluble's) in Crude Petroleum and Petroleum Products.

Three vials of neat crude are then combined with different percentage volumes of the standard aromatic. The vials are then titrated with the paraffinic titrant and are continuously assessed using optical density.

The principle is that the optical density will decrease (i.e. the solution becomes more transparent) as the pure paraffinic titrant is added, however, at the point of asphaltene flocculation, the optical density will then increase again. Once flocculation is observed in a vial, the level of paraffinic titrant added is recorded.

By plotting % volume aromatic solvent in the test liquid against 100 x volume of oil divided by the volume of test liquid, for a minimum of three tests, a straight line is drawn as shown in Figure 4-11

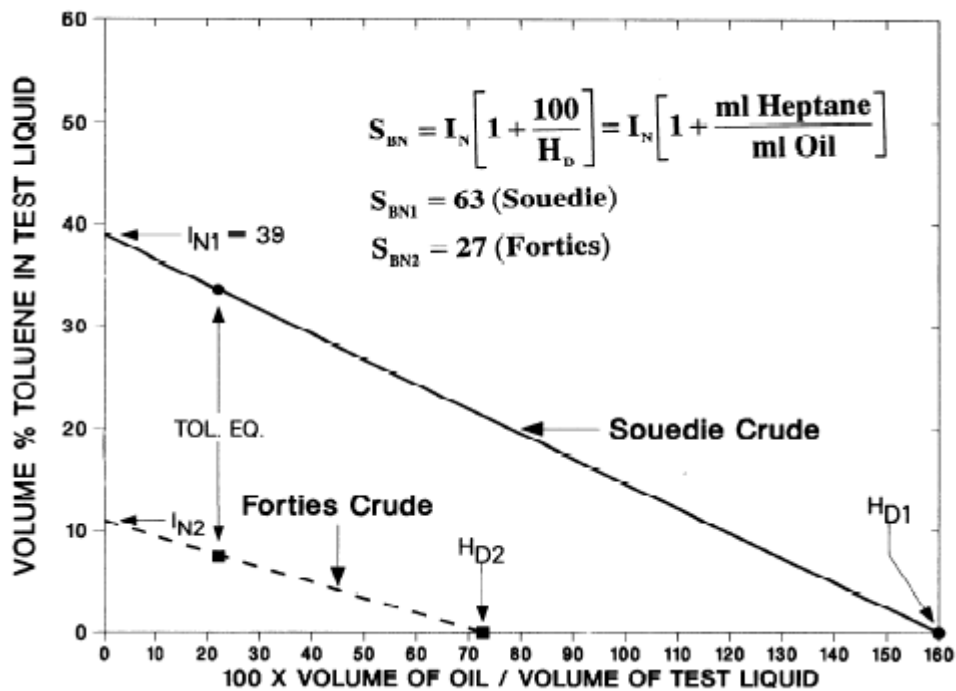


Figure 4-11: Determination of Insolubility Number and Solubility Blending Number for Forties and Souedie Crude Oils
taken from Wiehe, Kennedy and Dickakian (2001)

The Y intercept gives the Insolubility number for the crude oil and thus the Solubility Coefficient (S_c) can be calculated using the following equation:

$$S_c = I_N(1 + 1/H_D) \quad (4-1)$$

Where:

I_N = The instability coefficient of the crude (y-intercept)

H_D = Heptane Dilution limit (x-intercept, the point at which the crude precipitates asphaltenes with no additional toluene)

The above test assumes that deposition will be elicited and observed from the test oil with an excess of heptane. If organic deposition is not initiated in the neat crude being assessed by the standard paraffinic then a previously assessed neat crude is blended with the neat crude being assessed to form a binary (two crude) blend. The binary (two crude) blend is assessed using the same method as neat crude. The change in Stability and Instability of the binary blend compared to the previously assessed neat crude is attributed to the neat crude being assessed.

The S_C and I_N are produced for each crude in the blend and then proportionally blending (according to the percentage of each crude in the blend) to determine the overall blend S_C . Blend stability is assessed by ensuring that the blend S_C is no less than 1.4 times the I_N of any neat crude in the blend.

However, this methodology does not account for the interactions between crudes when blended, the batch to batch variations in crude quality as well as any time dependent stability effects,

4.2.4 *Generating Blend Stability / Instability Coefficients by Experimentation*

To address the weaknesses of the neat crude assessment methodologies, the Eng.D project focussed on developing a new methodology which could provide a true to life assessment of the stability of crude oil blends in a refinery.

This first starts by assessing all the neat crudes in a recipe cluster (see section 4.4.1) and establishing the practical minimum and maximum percentage volume (based on refinery design constraints) These percentage volume ranges are used to design a series of blend experiments which cover the range of refinery blending.

For each blend experiment a titrant is chosen, from the blend (usually the most paraffinic) that will make the blend go from stable to unstable. The remaining neat crudes are then blended into a pseudo component to be used with the titrant crude. In the example below (Table 4-1) a set of five refinery crude oil have been blended in various ratios to form a designed experiment.

Table 4-1: Example Blend Experiment

Blend	Crude_01	Crude_02	Crude_03	Crude_04	Crude_05
110	74.4%	4.7%	4.7%	16.3%	0.0%
111	52.1%	3.3%	3.3%	11.4%	30.0%
112	44.7%	2.8%	2.8%	9.8%	40.0%
113	37.2%	2.3%	2.3%	8.1%	50.0%
114	29.8%	1.9%	1.9%	6.5%	60.0%
115	22.3%	1.4%	1.4%	4.9%	70.0%

The experimental methodology is then as follows. The pseudo component is blended for the experiment (i.e. blend 110). Vials of the pseudo component are combined with different percentage volumes of the titrant crude (in this case Crude_05). The vials are scanned and an algorithm in the chemometric model monitors the NIR-spectra and identifies when flocculation has occurred by looking for an inflection point (section 4.2.1) and validating whenever possible using microscopy.

The initial screening series of vials uses large increments of titrant (e.g. 10%). To fine tune the assessment of the point of instability, after screening with large increments, smaller increments are used (e.g. 1%). The vials are scanned following mixing and after one or more retention times (e.g. 0 hrs. +24 hrs). As time increases, the crude blends can become more instable resulting in increased precipitation. Duplicate vials are available for microscopy and laboratory analysis which can be selectively triggered based on the information obtained from the assessment from the NIR spectra.

The onset of OD for each blend is then input into the Matrix Blending Algorithm to calculate the coefficients for each crude in the blend.

4.3 Blending and regression fitting

Having obtained the experimental data from the blend titration it is useful to fit a regression to enable stability of any crude ratio in a blend recipe to be calculated. The confidence in the regression can also be calculated to ensure that sufficient, repeatable measurements have been made in the blend titrations.

4.3.1 *N-1 Factor Blend*

Using N-1 factors gives one more set of results to estimate the error purely from experimentation and also eliminates the collinearity within the equation, as the proportions of each crude in the blend will add to 1 (Deming and Morgan, 1993).

When all the experimental blends have been completed the relative stability of the neat crudes in the blend can be calculated. Over the range of the experimental blends a linear approximation is practical.

At the point of flocculation, the coefficient of instability for the blend is equal to the coefficient of stability for each component in the blend, multiplied by its percentage volume. Thus the following assertion can be made:

$$IC = SC_0V_0 + SC_1V_1 + SC_2V_2 + \cdots + SC_nV_n \quad (4-2)$$

Where

- IC - Instability Coefficient
- SC_n - Stability Coefficient for component n
- V_n - Percentage Volume of Component n

In addition, the sum of the volumes of the components must equal to 1:

$$1 = V_0 + V_1 + V_2 + \dots + V_n \quad (4-3)$$

Therefore

$$V_n = 1 - V_0 - V_1 - \dots - V_{n-1} \quad (4-4)$$

Substituting into (4-2) gives:

$$V_0 = \frac{IC - SC_n}{(SC_0 - SC_n)} + \frac{(SC_n - SC_1)}{(SC_0 - SC_n)} V_1 + \dots + \frac{(SC_n - SC_{n-1})}{(SC_0 - SC_n)} V_{n-1} \quad (4-5)$$

Which is also of the multiple linear regression form:

$$Y = \beta_0 + \beta_1 X_1 + \beta_2 X_2 + \dots + \beta_{n-1} X_{n-1}$$

Where:

$$\beta_0 = \frac{IC - SC_n}{(SC_0 - SC_n)}$$

$$\beta_{n-1} = \frac{SC_n - SC_{n-1}}{(SC_0 - SC_n)}$$

Thus solving for the stability coefficient of the nth component (SC_n):

$$SC_n = \frac{IC - \beta_0 SC_0}{(1 - \beta_0)} \quad (4-6)$$

And solving for the n-1 component (SC_{n-1}):

$$SC_{n-1} = SC_n - \beta_{n-1}(SC_0 - SC_n) \quad (4-7)$$

As this type of assessment is a designed experiment conducted on a relatively small number of samples covering a narrow operating region, a matrix solution to the least squares fit is appropriate. This generates the coefficients for this range of neat crude blends for refinery organic deposition.

$$\mathbf{B}^{\wedge} = (\mathbf{X}'\mathbf{X})^{-1}\mathbf{X}'\mathbf{Y} \quad (4-8)$$

Where

\hat{B}	- Regression coefficients $\beta_0 \dots \beta_n$
Y	- Vector of percentage of Titrant Crude in each blend
X	- Matrix of percentages of each crude in the pseudo component blends

Once the coefficients have been calculated for each crude oil equation (4-2) instructs us that at the point of instability the volumetrically blended coefficients of each crude in the blend will give a number equal to the instability coefficient. If this overall SC is higher than IC it means that the blend is stable and vice versa.

4.3.2 Comparison of Methodologies

The SC and IC from the developed methodology were then compared to the I_N and S_N from the established ASTM methodology on the same crude blends. It was envisaged that two scenarios are possible.

1. All of the SC and S_N are similar and within experimental repeatability. This means there is little interaction between the crudes when blended and the coefficients can be used for any of the crudes in the recipe. In this case the ASTM methodology would be quicker and simpler to implement as it requires less crude blending and analysis.
2. Some of the SC and S_N are not similar and different by more than experimental repeatability. This means that interactions between crudes are observed when blending and the ASTM methodology would not work in this case.

In Table 4-2 below two different blends are shown (where L denotes a low percentage of a crude in the blend and M a medium percentage of the crude in the blend) and were tested using both methodologies. It was established that Crude001 had a destabilising effect on Crude003 and thus Blend A was more stable than Blend B. In this case more testing would be involved to provide stability coefficients for specific combinations and ratios of crude.

Table 4-2: Stability testing for variation in crude ratios

Blends	Crude001	Crude002	Crude003	Crude004	Crude005	Crude006	Crude007	Crude008
A	L	M	M	M	M	L	L	L
B	M	L	M	M	M	L	L	L

Assessing the blended crudes thus allows SC to more accurately match the refinery operating conditions. Providing more accurate constraints will improve the optimisation of the financial and operating outcomes of the blend under specific conditions.

4.4 Condensate Testing of Crude Blends

The recipes processed by refineries are planned to stay away from instability. In practice, the plan will use previously generated coefficients to assess blend stability. However, when the crude qualities change and / or a new crude is introduced then the stability of the new blend needs to be assessed in the laboratory.

Ideally a titration is required for each crude in the blend, so the number of titrations equals the number of crudes. However, this is a significant amount of testing and a simpler way is desirable.

Thus, a single titration with a reference crude determines if the new recipe with the new crude is more or less stable than expected. The single test provides enough information to inform processing decisions. The reference crude is a yard stick to measure the relative stability of recipes.

Whilst the reference crude is not in the refinery recipe, the crude recipe tested exactly matches the chemistry of the refinery. Close to instability the amount of reference crude added is small and therefore the assessment of instability is close to refinery conditions.

Table 4-3 shows an example titration dataset for a blend of 4 crudes which have been titrated with reference crude to determine the point of instability. Each row shows the percentages of each crude in the blend, plus the reference crude.

It can be seen that depending on the ratio of the four crudes in the blend, differing amounts of reference crude are required to force the precipitation of asphaltenes from the blend. TO understand the impact of crude 4 on the blend stability it can be seen that blends 06 – 09 do not contain any crude 04.

Table 4-3: Laboratory Results, condensate Matrix

Blend	Intertek Reference Crude	Crude01	Crude02	Crude03	Crude04
01	35%	26%	29%	7%	3%
02	25%	15%	45%	8%	8%
03	30%	21%	28%	16%	5%
04	30%	25%	25%	13%	8%
05	30%	7%	56%	5%	2%
06	40%	6%	27%	27%	0%
07	40%	12%	24%	24%	0%
08	45%	17%	19%	19%	0%
09	50%	25%	13%	13%	0%

The pattern of the data dictates the number of possible solutions that can be calculated for blend stability coefficients. The calculated stability coefficients are relative to SC0 and IC and this testing has the following consequences:

1. The stability coefficients are relative to a selected component SC0 which is the yard stick crude and remains a reference point.
2. Changes in individual crude stability coefficients reflect the different behaviour of the individual crude in those blends.
3. Maintaining a constant value of the blend instability coefficient shows all changes in blend chemistry in the individual crude blend stability coefficients.
4. Solving for individual stability coefficients using different titration sets determines how an individual crude coefficient changes in different mixtures.
5. Testing in the laboratory with an unstable reference crude enables instability to be observed quickly even though a particular blend is stable.
6. The blend assessed relates directly to the refinery operation. Even for a new operating region only this single test is required to assess current operation.

4.4.1 *Blend Feasibility Report*

The crude blend constraints from the refinery plan, production units and crude slate limit the actual blending options available to a refinery planner. The crude blends fall into recipe clusters, which are defined based on the optimum blend recipe based on current refinery demand (i.e. maximise gasoil fraction). These recipe clusters are exercised by the Intertek Matrix Blending Algorithm shown in Figure 4-12.

	Crudes in study								Group01			Groupnn			Typical Blend Properties							TBP																								
Blends	Crude001	Crude002	Crude003	Crude004	Crude005	Crude006	Crude007	Crude008	Crude...	Crude0nn	Crude101	Crude102	Crude103	Crude104	Crude1...	Crude1nn	Cruden...	Cruden...	Cruden...	Cruden...	Crudemnn	API	Sulfur	TAN	Asphaltenes	P	N	A	Pour Point																	
1nn01	P	L	L	P	P	P	L															39.8	0.3	0.5	0.3	45	35	20	-20	6	13	22	30	39	48	57	60	75	81	84						
1nn02	L	L	L	P	P	P																40.2	0.3	0.5	0.3	50	32	18	-25	5	10	19	26	35	44	54	57	73	79	83						
1nn03	P	L	L	P	P	P	L															41.3	0.2	0.5	0.3	52	45	3	-29	8	15	26	34	43	53	62	65	80	85	88						
1nn04	P	L	L	P	P	P	L															39.9	0.2	0.4	0.3	51	31	18	-18	7	14	24	32	41	50	59	62	78	83	86						
1nn05	L	L	L	P	H	P																40.0	0.2	0.5	0.3	48	24	28	-16	7	14	24	32	41	51	60	63	79	84	87						
1nn06		P															P	P		P	P	P																								
1nn07		P		P		P											P			P	P																									
1nn08						P					P	P	P		P	P	P																													
1nn09						P					P		P		P		P				P																									
1nn10						P						P		P	P	P	P				P																									
1nn11		P	P	P	P	P					P		P	P	P																															
2nn01	P			P		P	P	P																																						
2nn02	P			P		P		P		P																																				
2nn03												P		P	P	P	P		P																											
2nn04											P						P	P	P		P																									
2nn05											P					P	P				P																									

Figure 4-12 - Example Blend Recipe Feasibility Report

This is an example of the blend feasibility report. The report is populated in stages as new neat crude samples become available. The report is updated as blending constraints are updated. Each cell in the table shows the following:

- Neat crudes listed in columns.
- Potential recipes are listed as rows, grouped by CDU blend types (recipe clusters)
- Blend Properties (shown on the right)
- Crudes that can be blended together to meet the blend constraints are expressed in terms of their feasibility for refinery processing as follows:
 - P – possible blend component
 - L – low percentage blend component
 - H – high percentage blend component

Areas shaded in yellow represent an initial study carried out for a refinery as part of the development of this methodology. This section shows five crude oil blends which represented the five blends from the refinery recipe cluster. The study consisted of blending the five crudes in different blend ratios (1nn01 – 1nn05) to create a designed experiment which allowed the generation of coefficients to describe the interactions and stability parameters of each crude within the blend (the mathematics of which is explained in section 4.3.1). The physical properties of each blend can then be seen to the right (API, Sulphur, TAN etc.)

Other areas outlined as coloured squares are then a further set of example blends which the refinery could possible process and in the future would need to be checked and evaluated based on NIR spectra, typical blend properties and constraints if the refinery decided to process those ratios.

4.4.2 Experimental Results from Blend Titration

Through a series of crude titrations, the onset of organic deposition is measured at different recipes of neat crudes. The results are summarised as the titration number (i.e. 111) against the percentage of each crude within the blend.

Figure 4-13 below shows the observed organic deposition and the organic deposition predicted by the Intertek blend stability algorithm. This is measured at both time 0 hours (D0) and time 24 hours (D24) and expressed in terms of observed instability (r) and no observed instability (g)

	Crude_01	Crude_02	Crude_03	Crude_04	Crude_05					
Min	0%	1%	0%	4%	30%					
Max	52%	13%	8%	38%	90%					
Average	21%	5%	3%	13%	58%					
Span	52%	13%	8%	34%	60%					
Blend Titration	Crude_01	Crude_02	Crude_03	Crude_04	Crude_05	D0		D24		Comments from Microscopy
						Spectra / Observation	Intertek Blending Algorithm	Spectra / Observation	Intertek Blending Algorithm	
111	52.1%	3.3%	3.3%	11.4%	30.0%	g	g	r	r	
112	44.7%	2.8%	2.8%	9.8%	40.0%	g	g	r	r	
113	37.2%	2.3%	2.3%	8.1%	50.0%	g	g	g	r	
114	29.8%	1.9%	1.9%	6.5%	60.0%	g	g	g	g	
115	22.3%	1.4%	1.4%	4.9%	70.0%	g	g	g	g	
121	1.7%	8.6%	1.7%	37.9%	50.0%	g	g	r	r	
122	1.4%	6.9%	1.4%	30.3%	60.0%	g	g	r	r	
123	1.0%	5.2%	1.0%	22.8%	70.0%	g	g	r	r	
124	0.7%	3.4%	0.7%	15.2%	80.0%	g	g	g	g	
125	0.3%	1.7%	0.3%	7.6%	90.0%	g	g	g	g	
131	50.9%	1.3%	3.8%	14.0%	30.0%	g	g	r	r	
132	43.6%	1.1%	3.3%	12.0%	40.0%	g	g	r	r	
133	36.4%	0.9%	2.7%	10.0%	50.0%	g	g	r	r	
134	29.1%	0.7%	2.2%	8.0%	60.0%	g	g	g	r	
135	21.8%	0.5%	1.6%	6.0%	70.0%	g	g	g	g	
141	40.0%	13.3%	8.3%	8.3%	30.0%	g	g	r	r	
142	34.3%	11.4%	7.1%	7.1%	40.0%	g	g	r	r	
143	28.6%	9.5%	6.0%	6.0%	50.0%	g	g	r	r	
144	22.9%	7.6%	4.8%	4.8%	60.0%	g	g	r	r	
145	17.1%	5.7%	3.6%	3.6%	70.0%	g	g	g	r	
151	3.7%	11.1%	3.7%	31.5%	50.0%	g	g	r	r	
152	3.0%	8.9%	3.0%	25.2%	60.0%	g	g	r	r	
153	2.2%	6.7%	2.2%	18.9%	70.0%	g	g	r	r	
154	1.5%	4.4%	1.5%	12.6%	80.0%	g	g	g	g	
155	0.7%	2.2%	0.7%	6.3%	90.0%	g	g	g	g	

Figure 4-13 - Example Experimental Results from Matrix Blend Algorithm

The top summary table shows the range of percentages of the neat crudes in the blends including Minimum, Maximum Average and Span.

The Intertek Blending Algorithm Stability prediction is generated using Blending Stability Coefficients (BSC) and Blending Instability Coefficient (BIC), the calculation of which is described in section 4.3.1. These coefficients calculated to quantify the effect of neat crude interaction at time 0 hrs. and +24 hrs.

4.4.3 Blend Evaluation Report

The experimental results and calculations from the Blend Recipe Evaluation are used to generate a set of blend reports for target Crude Distillation Unit (CDU) recipes. Figure 4-14 shown below gives an example of the blend stability calculator and contains three main elements: New Blend Recipe, Calculated Blend Stability and Blend Stability Coefficients from the Matrix Blending Algorithm.

Client: Example

Blend Recipe Number: nnnn

Date: 01-Aug-13

1. New Blend Recipe

	Crude_01	Crude_02	Crude_03	Crude_..	Crude_nn	Total
% Volume	0.0%	6.0%	8.0%	12.0%	74.0%	100.0%

2. Calculated Blend Stability

	Assessment	BSC	BIC
BSC-D0	Stable	60	45
BSC-D24	Unstable	56	60

3. Blend Stability Coefficients from matrix blending algorithm

	Crude_01	Crude_02	Crude_03	Crude_..	Crude_nn	BIC
BSC-D0	57	35	55	43	65	45
BSC-D24	45	33	58	42	60	60

Figure 4-14 - Example Blend Evaluation Report

4.4.3.1 New Blend Recipe

The blend recipe shows the % volume of the crudes in the blend. The % volume of each crude in this blend can be changed to evaluate changing blend recipes for organic deposition. The degrees of freedom of the volume percentages of the individual crudes are determined by the refinery blend optimiser.

4.4.3.2 Calculated Blend Stability

The ultimate function of the calculator is to give the refinery an assessment of the blend stability for the current recipe and at all time periods of interest. In Figure 4-14 blend recipe stability is shown at 0 h (BSC-D0) and +24 h (BSC-D24).

In this example, the Stability Coefficient (BSC) at 0 hrs (60 for this blend recipe of crudes) is greater than the Instability Coefficient (BIC) (45 for this group of crudes) and thus the blend is stable at 0 hrs. However, the BSC at 24 hrs (45 for this blend recipe of crudes) is less than the BIC (60 for this group of crudes), hence the blend is unstable at 24 hrs.

4.4.3.3 *Calculated Blend Stability Coefficients from the matrix blending algorithm*

This section details the calculated coefficients at time 0 and 24 hours for each of the crudes assessed.

4.5 Case Study 2: Assessment of Heavy Fuel Oil Blending in a Refinery

This work forms the final deliverable to a refinery customer for the characterisation of the stability of heavy fuel oil blends. The customer was an early adopter of the patented methodology and as such this was the first application of the patented approach to a heavy fuel blending process.

The client had experienced significant organic deposition with 1.8% sulphur blended Heavy Fuel Oil. This initial study was aimed at assessing the stability of 1.8% sulphur Heavy Fuel (HFO) when it is produced by blending 3.0% sulphur HFO from the refinery CDU with 1% sulphur HFO bought in from an external supplier. It is also noted that an additional blend component of Heavy Virgin Naphtha (HVN) also from the CDU is sometimes used to control viscosity of the blend.

The assessment used an Intertek proprietary methodology under patent GB2516126 / P130065WO “Method and System for Analysing a Blend of two or more Hydrocarbon Feed Streams”. By blending the actual hydrocarbon streams the interactions that affect stability are observed. The samples received from the client were as follows:

August 2014:

- 1% Sulphur Heavy Fuel Oil (HFO)
- 1.8% Sulphur HFO (Blended at the refinery but not sold to a customer)
- 1.8% Sulphur Used HFO (Sent back by the refinery’s customer due to observed stability issues)
- 3% Sulphur HFO

December 2014:

- 3% Sulphur HFO (not used in study)
- Heavy Virgin Naphtha (HVN)

4.5.1 Methodology

The customer refinery produces 3% HFO from the CDU which is stored in heated tanks at 40-50°C. 1% Sulphur HFO is bought in to blend with the 3% HFO to meet the specification of 1.8% Sulphur HFO. They also produce HVN which can be blended with the 3% HFO to control viscosity. The table below shows the testing matrix carried out.

Table 4-4: Showing the Full set of blend tested

Test	1% HFO	1.8% HFO	1.8% Used HFO	3% HFO	HVN	Reference Crude	Time Periods (hours)
1	100%						
2		100%					
3			100%				
4				100%			
5					100%		
6	100% - 30%					0% - 70%	0, 72
7		100% - 30%				0% - 70%	0, 72
8			100% - 30%			0% - 70%	0, 72
9				100% - 30%		0% - 70%	0, 72
10	100% - 30%				0% - 70%		
11				100% - 30%	0% - 70%		
12	70%			30%			0, 24, 48, 72, 96
13	65%			35%			0, 24, 48, 72, 96
14	60%			40%			0, 24, 48, 72, 96
15	55%			45%			0, 24, 48, 72, 96
16	50%			50%			0, 24, 48, 72, 96
17	60%-57%			40%-38%	0% - 5%		0, 24, 48, 96
18				100%-60%	0% - 40%		0, 24, 48, 96
19	100% - 50%				0% - 50%		0, 72
20		100% - 50%			0% - 50%		0, 72
21			100% - 50%		0% - 50%		0, 72
22				100% - 50%	0% - 50%		0, 72

4.5.2 *NIR Spectroscopy*

The stability of the sample was assessed using an ABB MB3600 NIR spectrometer and high-pressure cell. All scanning was carried out at 60°C. Samples were assessed for both instantaneous stability (i.e. as materials are added) and time dependent (over a period of five days) stability.

4.5.3 *Microscopy*

Microscopy was performed on the samples to validate spectral observations; this was undertaken on both a Nikon 90i laser microscope and a Nikon Eclipse LV100ND.

Microscopy was carried out in the following forms:

- Transmitted light: Shows sample magnified under normal light, asphaltenes show as black particles, wax appears as light coloured, translucent aggregates.
- Cross Polar: Subjects the samples to polarised light, wax crystals appear as bright star like objects on a black background.

4.5.4 *Physical Property Testing*

Alongside NIR and microscopy, physical properties testing were carried out as per the proposal issued to the client, this included testing of Density, Sulphur, Total Acid Number, Wax Content and Asphaltene Content. Additionally, to determine the nature of the crystalline material in the samples Energy Dispersive X-ray Analysis (EDAX) was also carried out on the samples. Table 4-5 below shows the measured physical properties for each sample as supplied to the client.

Table 4-5: HFO Physical Properties

Test	Units	Method	1% HFO	1.8% Used HFO	1.8% HFO	3% HFO
Density	g/cm ³	ASTM D5002	0.9639	0.9713	0.9661	0.9678
Total Acid Number	mgKOH/g	ASTM D664	0.55	1	0.55	0.7
Sulphur	%wt	ASTM D4294	1	1.69	1.71	2.49
Wax Content	%wt	CBA4	3.8	2.6	3.7	1.7
Asphaltene Content	%wt	ASTM D6560	4.6	6.2	6.1	6.9
Sodium	mg/kg	CBA21 (EDAX)	8.8	21.2	7.5	6.7
Calcium			8.7	14.1	6.1	2.5
Barium			1.4	0.9	1	0.4
Magnesium			0.9	1.4	0.7	0.3
Potassium			0.5	3.1	0.3	0.3
Iron			11.6	10.8	7.9	2.3
Silicon			1.3	1.7	1.2	0.5
Phosphorus			0.3	1.5	0.3	0.4
Aluminium			3.4	4.8	2.1	0.4
Zinc			1.4	1.6	0.8	0.3
Sulphur			8.9	16.3	4.6	1
Nickel			54.8	32.4	50.5	38
Vanadium			80.7	129	132	188

4.5.5 Microscopy

Microscopy images taken of the all four HFO samples using the Nikon 90i Eclipse laser microscope. In these images, the wax particles in the crude oil appear as glowing white shapes on the dark background whereas the asphaltenes are much darker particles.

NOTE: The scale bar represents 10 microns.

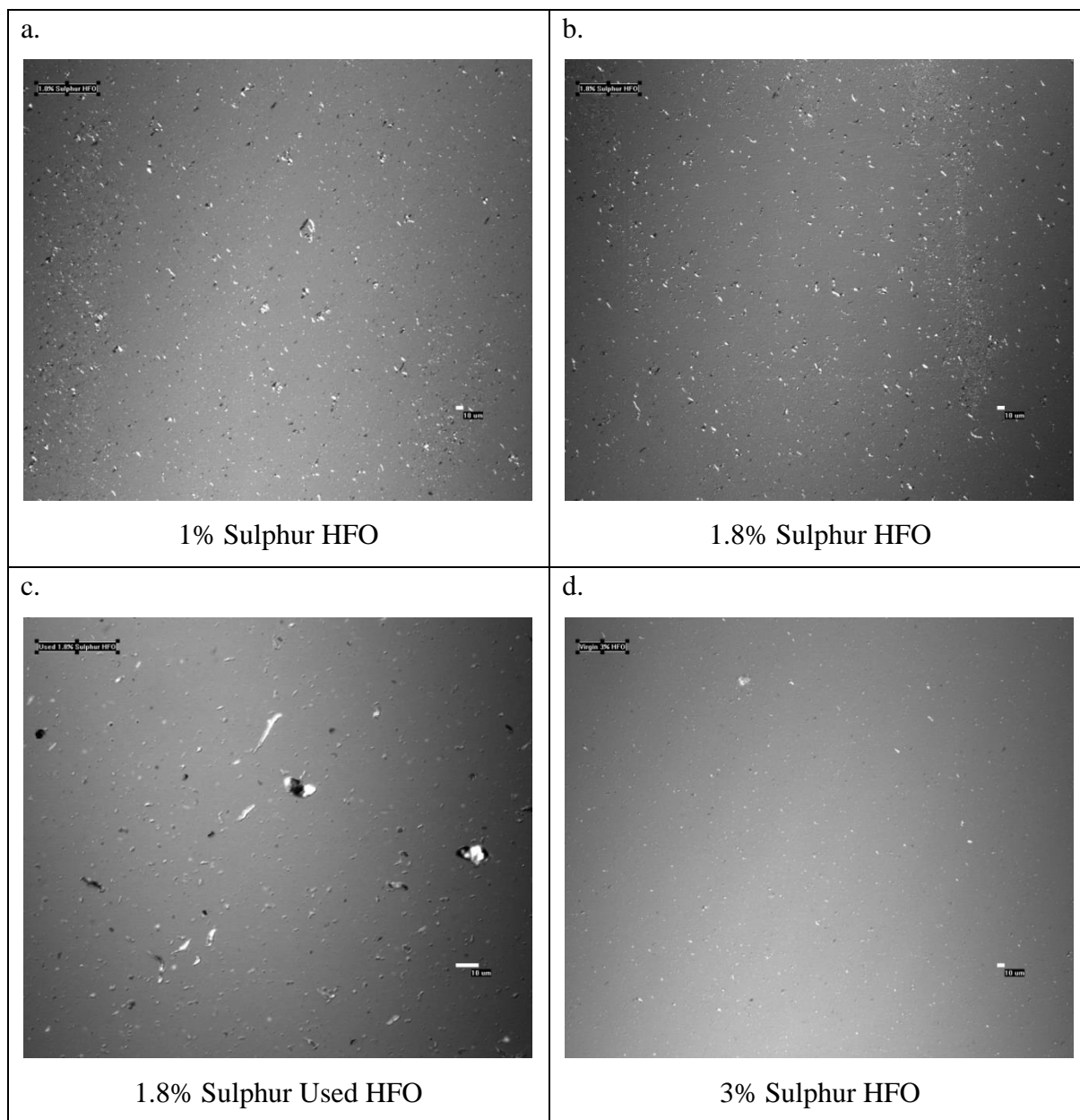


Figure 4-15: HFO Laser Microscopy 1% Sulphur HFO (a), 1.8% Sulphur HFO (b), 1.8% Sulphur Used HFO (c) and 3% Sulphur HFO (d)

It can be seen that the 1% Sulphur HFO is waxier than the 3% sulphur HFO and the 1.8% Sulphur used HFO has much larger waxy agglomerates than the 1.8% HFO.

4.5.5.1 Optical Microscopy – Transmitted Light – Neat HFO

Microscopy images of the 4 HFO samples were also taken using a Nikon Eclipse LV100ND microscope in both transmitted and polarised light. For a full set of microscopy images please see Appendix A for additional microscopy.

NOTE: The scale bar represents 250 microns.

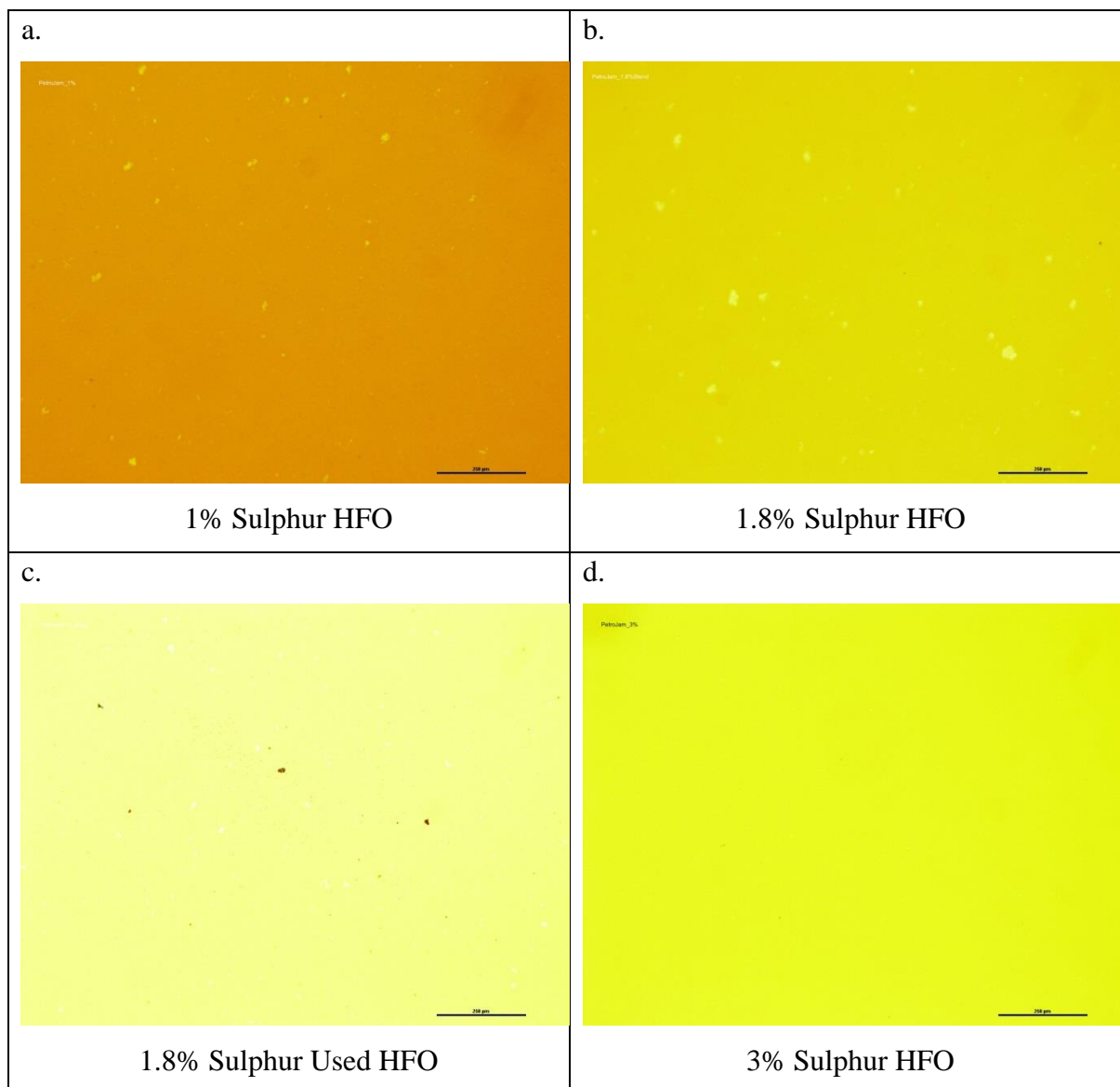


Figure 4-16: HFO Microscopy with Transmitted Light on 1% Sulphur HFO (a), 1.8% Sulphur HFO (b), 1.8% Sulphur Used HFO (c) and 3% Sulphur HFO (d)

1.8% Sulphur Used HFO shows slightly more precipitated asphaltenes (black occlusions) present than in the 1.8% Sulphur HFO sample. However, no obvious bulk asphaltene instability was observed in any of the neat HFO samples.

4.5.5.2 Optical Microscopy – Transmitted Light - HVN Time Lapsed Titrations

HVN diluent was then added to the samples and left for a period of 72 hours to allow for observation of any time dependent blend stability issues. Figure 4-17 below shows a classic bulk asphaltene precipitation phenomenon after 72 hours with HVN diluent.

NOTE: The scale bar represents 10 microns.

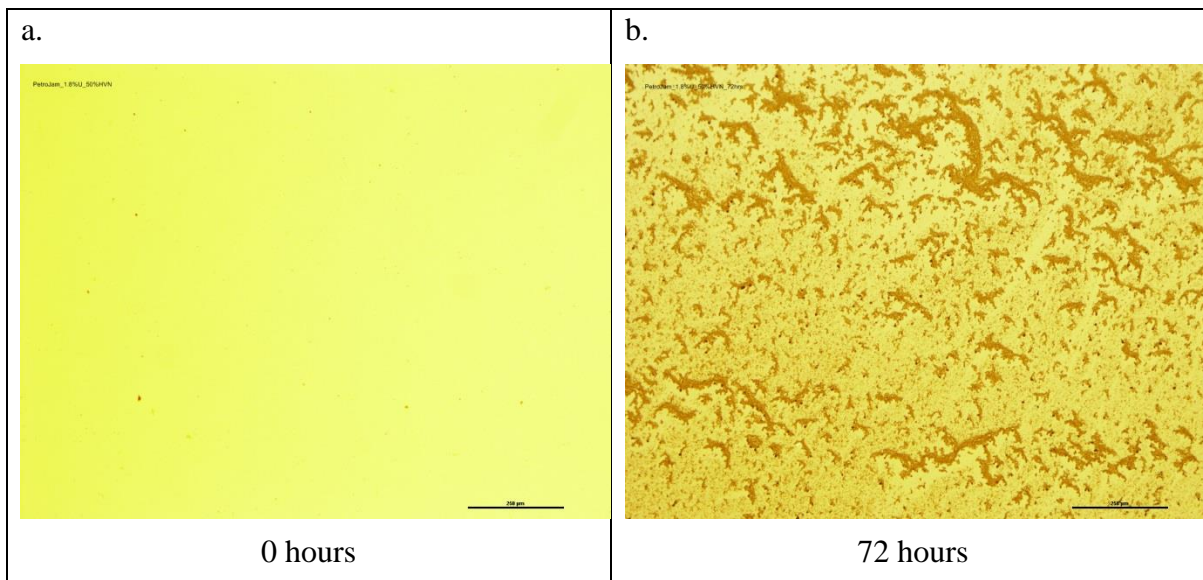


Figure 4-17: 1.8% Used Sulphur HFO with 50% HVN at time 0 hrs (a) and time 72 hours (b)

In Figure 4-17 1.8% used HFO exhibited different behaviour and showed significant precipitation of asphaltene after 72 hours with 50% HVN. No bulk organic deposition was observed in the 1.8% sulphur sample made at the refinery but not marketed. This indicates a difference in the stability of the blend of 1.8% sulphur HFO sent back by the refinery's customer versus that made up at the refinery but not marketed.

No bulk organic deposition observed for the 3% sulphur blend component with HVN even at 50% HVN after 72 hours. This indicates that neither blend component nor the 1.8% blend from the refinery exhibit blend stability problems with HVN. However, the sample sent back to the refinery with observed stability issues did precipitate asphaltenes. This indicates a difference in the blend chemistry and thus its stability.

4.5.5.3 Optical Microscopy – Cross Polar – Neat HFO

Cross polar microscopy uses polarised light to highlight crystalline structures in the crude sample. These can be wax, salt and sand and each has a different visual morphology. Waxes tend to form irregular aggregates, salt and crystals are more regular in shape and tend to be isolated.

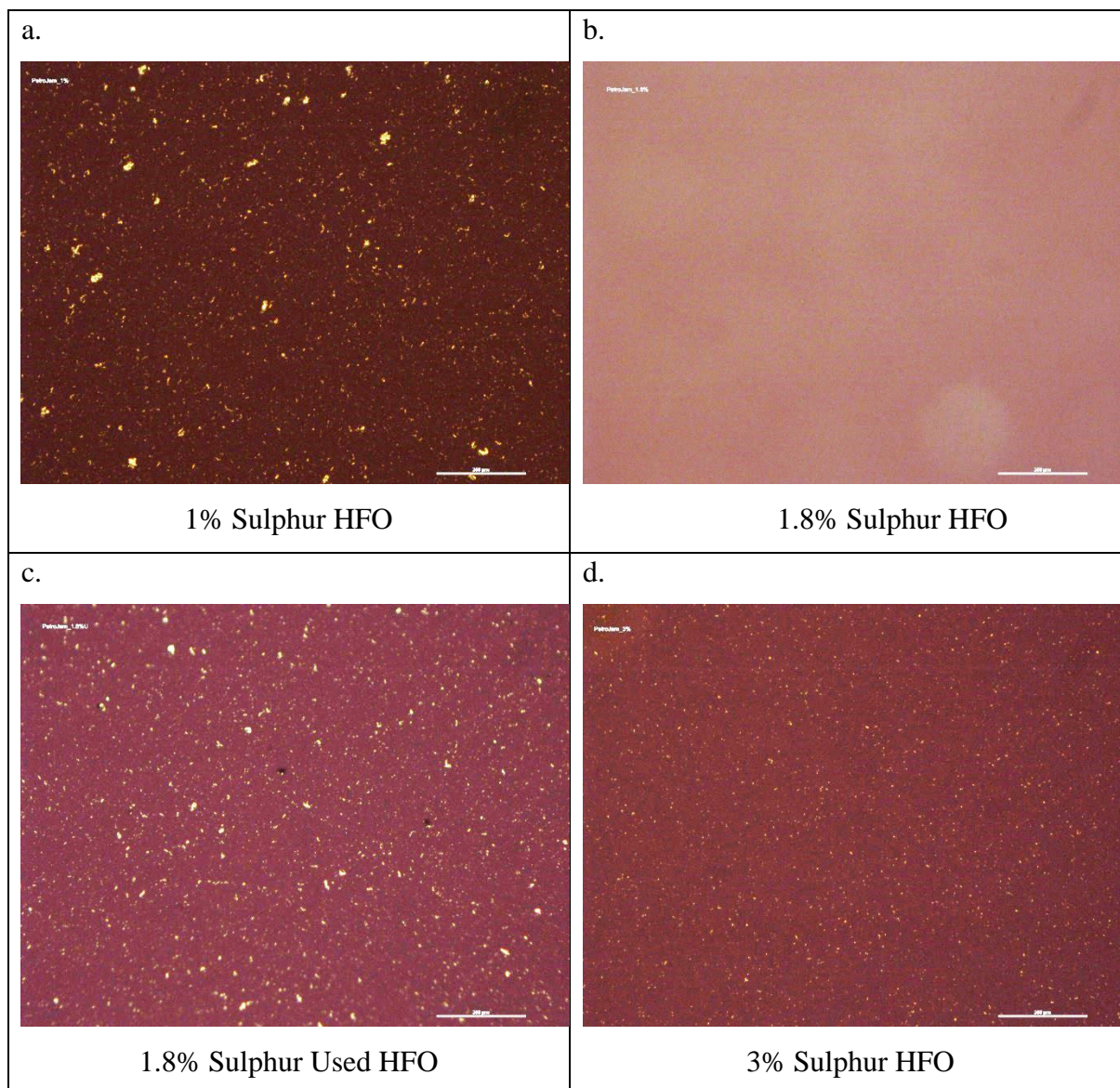


Figure 4-18: Cross Polar Microscopy 1% Sulphur HFO (a), 1.8% Sulphur HFO (b), 1.8% Sulphur Used HFO (c) and 3% Sulphur HFO (d)

Under cross polar microscopy it is obvious that the 1% Sulphur HFO bought in is far more waxy than the 3% Sulphur HFO produced by the refinery. It can also be seen that the 1.8% Sulphur Used HFO contains waxier agglomerates than the 1.8% Sulphur HFO sample.

4.5.6 *Neat HFO Blend Tests*

1% Sulphur HFO and 3% Sulphur HFO were blended to make 1.6%, 1.7%, 1.8%, 1.9% and 2% Sulphur HFO to test the effects of varying the blend ratios without addition of HVN. These blends were scanned at time 0, +24, +48 and +96 hours to check time dependent sample stability.

All the spectra show change in stability with time, Figure 4-19 and Figure 4-20 shows the time dependent stability test for a blended 1.8% Sulphur HFO with no HVN and a 3% Sulphur HFO with 20% HVN diluent respectively. It can be seen that although there is some spectral movement (circa 0.04AU) at the 5000cm⁻¹ region for the 1.8% Sulphur HFO this less is than half the movement from the HFO with diluent (circa 0.1AU).

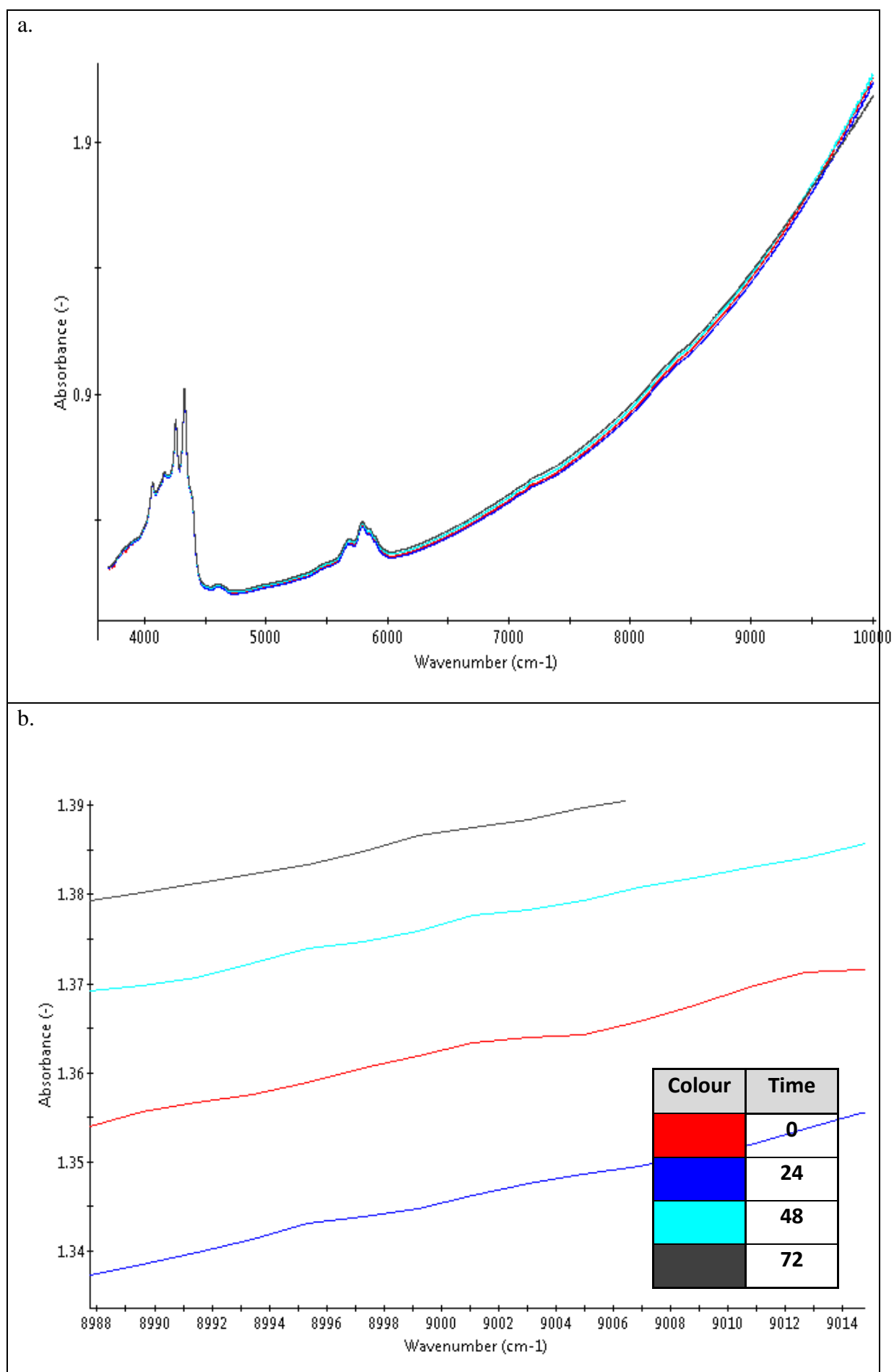


Figure 4-19: Showing full spectra for 1.8% Sulphur Blend (a) and 9000 wavenumber region (b)

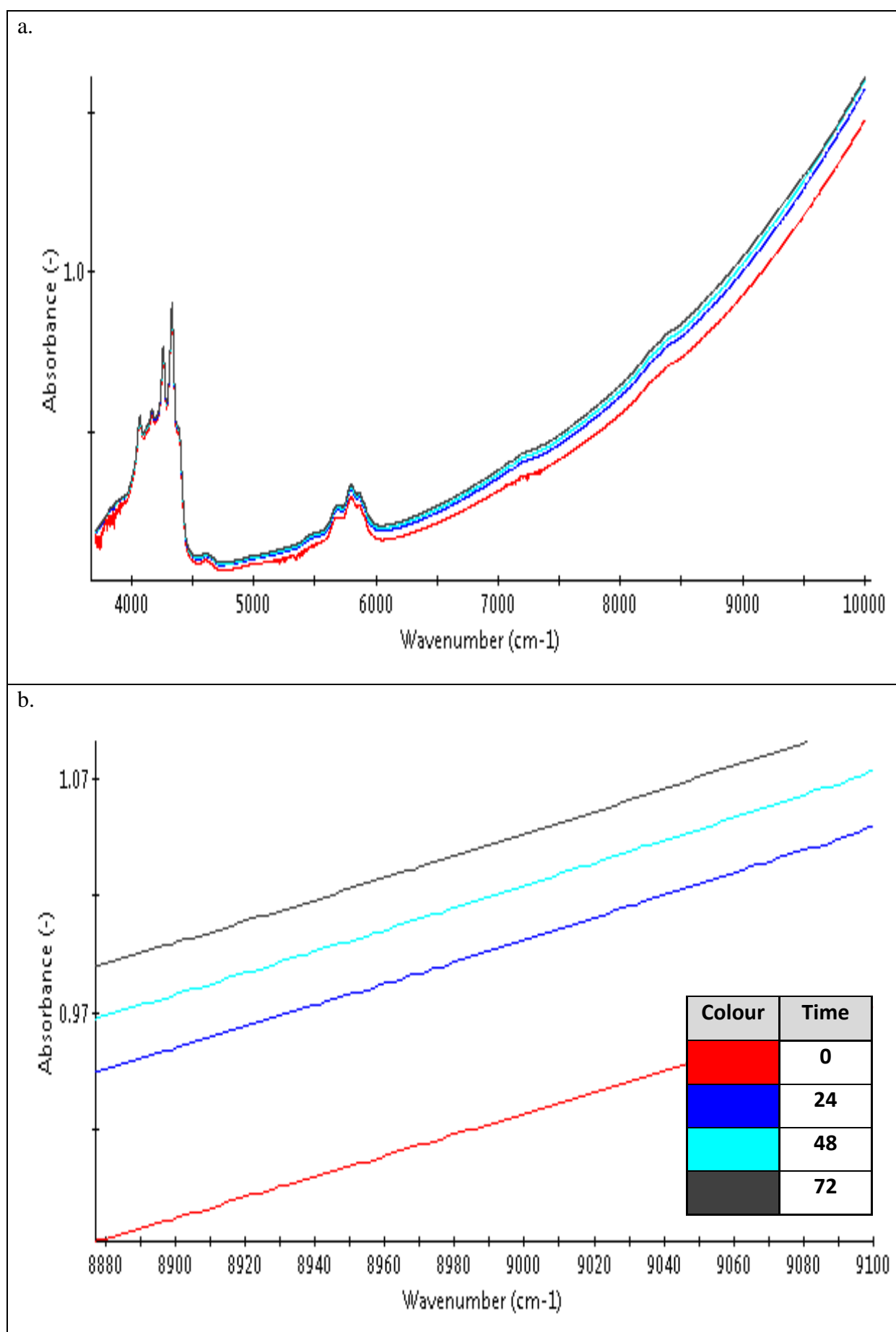


Figure 4-20: Showing full spectra for 20% HVN titration (a) and 9000 wavenumber region (b)

4.5.7 HVN Titrations (Instantaneous) - Observations

No bulk instability was observed with an instantaneous titration of both 1% and 3% Sulphur HFO with HVN.

4.5.8 HVN Titrations (Time Dependent) - Observations

A change in stability was observed with a time dependent titration of 1% increments from 1% - 5% HVN in 1.8% Sulphur HFO over a period of 96 hours. A change in stability was also observed with titration of 10%, 20%, 30% and 40% HVN in 3% Sulphur HFO over a period of 96 hours.

4.5.9 Reference Crude Titrations

The HFOs were also titrated with Intertek proprietary reference crude. This is a blend of consistent set of hydrocarbons used to check the relative stability of neat HFO samples.

Table 4-6: Percentages of Reference Crude (RC) around the point of instability

Sample	Stable (% RC)	Unstable (%RC)
1% Sulphur HFO	40	50
1.8% Sulphur Used HFO	40	50
1.8% Sulphur HFO	40	50
3% Sulphur HFO	50	60

Table 4-6 shows the percentages of reference crude needed to make the sample go unstable. All samples except the 3% Sulphur HFO were stable at 40% reference crude and unstable at 50% reference crude. The 3% Sulphur HFO however was stable at 50% reference crude and unstable at 60% reference crude. This suggests that the 3% Sulphur HFO is more stable than the 1% Sulphur HFO.

In the blend of 1.8% Sulphur HFO the 1% Sulphur HFO has a higher leverage at 60%wt compared to the leverage of 3% Sulphur HFO at 40%wt. Therefore, the stability of the 1.8% Sulphur HFO blend is more dependent on the stability of the 1% Sulphur HFO.

4.5.10 Conclusions

Observations of stability of HFO blends was undertaken using the proprietary stability methodology developed as part of the Eng.D project. Based on the set of samples studied it was

concluded that a change in stability was observed in all blends made from blending 1% Sulphur HFO and 3% Sulphur HFO in the range 1.6% to 2.0% Sulphur.

The change in stability occurred at the time that the HFO was blended. The sample instability worsened over time i.e. from blending (0 hours) to the end of monitoring (96 hours).

It was suspected that the paraffinic HVN diluent would cause instability problems and indeed increasing the amount of HVN in the blend increased the tendency for instability. The 1.8% Sulphur Used HFO sample (returned by the customer's customer) was the only one exhibiting instability when blended with HVN after 72 hours. Instability with HVN was not observed with 1% Sulphur HFO, 1.8% Sulphur HFO or 3% Sulphur HFO.

It can be concluded that 1.8% Sulphur Used HFO and 1% Sulphur HFO are more unstable than 1.8% Sulphur HFO and 3% Sulphur HFO. Coefficients of blend stability for 1.8% Sulphur HFO were not calculated as the sulphur constraint did not cover a region that exhibited both stable blends and gross unstable blends within 96 hours from blending.

Figure 4-21 below shows a line diagram of the physical property measurements from the customer sample.

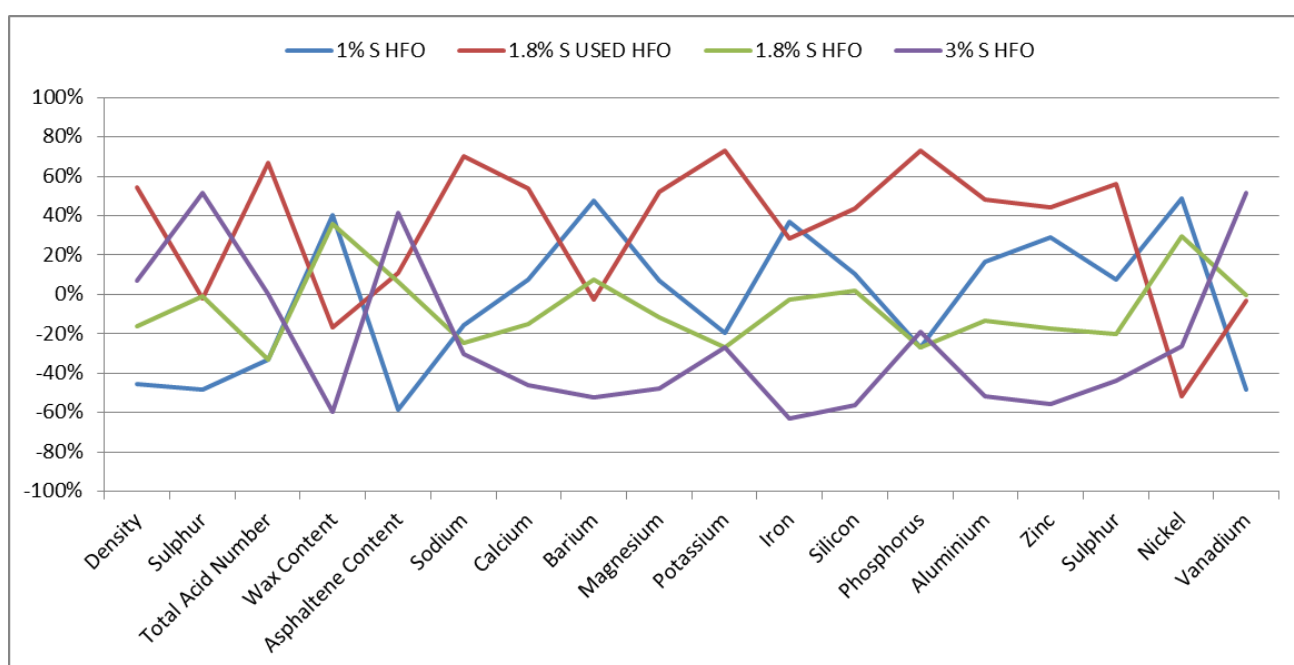


Figure 4-21: Comparison of physical properties to average

It can be seen that the density of 1.8% Sulphur Used HFO is the highest of all customer sample densities. The 1.8% Sulphur HFO will have been made from blending 1% Sulphur HFO and

3% Sulphur HFO in the ratio 60:40 and therefore the density must be between the density of the two blend components. As the density is higher than 3% Sulphur HFO the blend components of the 1.8% Sulphur Used HFO must be different from the samples tested.

After further discussion of the results with the customer it was determined that the 1% sulphur HFO blend component was sourced from different suppliers. The two 1.8% Sulphur HFO samples were made with different 1% Sulphur blend components and it was thus determined that 1% Sulphur blend component from a particular supplier was not compatible with the customer 3% Sulphur HFO.

1% Sulphur HFO is waxier than 3% Sulphur HFO and the EDAX results in conjunction with the physical properties analysis and cross polar microscopy suggest the crystalline material to be predominantly organic in nature.

From the microscopy observations, it was determined that the 1% Sulphur HFO is less stable than 3% Sulphur HFO when blended with reference crude and bulk organic deposition was only observed with 1.8% Sulphur Used HFO with 50% HVN after 72 hours but not with 1% Sulphur HFO, 1.8% Sulphur HFO or 3% Sulphur HFO.

1% Sulphur HFO is less stable than 3% Sulphur HFO when blended with reference crude and blends of 1.6% to 2% Sulphur HFO without HVN exhibit a change in stability with time. However, 3% Sulphur HFO with HVN does exhibit change in stability with time. Blends of 1.8% Sulphur HFO made from 3% and 1% Sulphur HFO and HVN from 0% to 5% do exhibit a change in stability with time.

4.5.11 ***Recommended action:***

- Blend order and mixing is critical to prevent bulk instability when blending with HVN. At the point of mixing there is the potential for a local high concentration of HVN.
- Establish the level and quality of HVN, 1% Sulphur HFO, and 3% Sulphur HFO, storage times and the blend order that have been associated with customer issues.
- Monitor quality of blend components and evaluate blend stability before making up batches of 1.8% Sulphur HFO
- Monitoring the quality of 1.8% Sulphur HFO is critical based on the significant difference between 1.8% Sulphur HFO and 1.8% Sulphur Used HFO.
- Establish the critical processing parameters for the customer i.e. the level of organic deposition that can occur whilst the HFO remains usable.

Case Study 3 – Assessment of Blends of Marine Fuels

This application of the organic deposition programme was directed at solving issues experienced with deposition in the marine fuels industry. This can cause major issues because if asphaltene precipitates whilst fuels are blended on board they can block fuel filters and potentially shut down the engines.

This issue arises because ships have two tanks of fuel on board. One containing a high sulphur (residual) fuel oil and one containing a low sulphur (distillate) marine diesel. It is necessary for ships to transition between fuels when passing through Emission Control Areas (ECAs). Currently the global Sulphur cap is 3.5% however in European waters (Baltic, North Sea and English Channel) this drops to 0.1% (Commission, 2016). This blending within the fuel line can cause stability problems when the paraffinic diesel is mixed with the highly asphaltenic fuel oil.

This study saw intensive collaboration with both marine operatives and refineries producing the fuel. Furthermore, studies have been undertaken with additive manufacturers to assess the levels and efficacy of additives used to help prevent these problems occurring.

4.5.12 *Part 1 – Characterisation and Feasibility Phase*

This details the results of blending marine fuel oils. The assessments focused particularly on the linearity of spectral blending of fuel oils and the stability of blended fuel oils

The work was initiated following a discussion between Intertek and a spectrometer manufacturer regarding the possibility of installing a spectrometer in a ship's fuel line to monitor the progression from Heavy Fuel Oil (HFO) to Marine Diesel Oil (MDO). This monitoring is a value-added service to shippers in ECAs.

A selection of samples of HFO and MDO were selected for testing in the Intertek laboratory. Testing work was carried out in April - June 2015 with various blend recipes assessed using Near Infrared (NIR) spectroscopy and microscopy.

Blends were made up at 10% increments of the following pairs of samples:

- Blend 1: DL231202 – HFO (3.43% Sulphur) / DL231229 – MDO (0.03% Sulphur)
- Blend 2: DL231193 – HFO (3.30% Sulphur) / DL231311 – MDO (0.04% Sulphur)

- Blend 3: DL231210 – HFO (1.96% Sulphur) / DL231232 – MDO (0.10% Sulphur)

4.5.13 Methodology

To undertake the study, the Intertek marine specialist division (Shipcare) supplied samples of High Sulphur Fuel Oil (HSFO) and Ultra Low Sulphur Gas Oil Equivalent), The physical properties for the samples are shown in Table 4-7 below.

Table 4-7: Physical Properties for Samples

Lab Ref	Fuel Type	Density (g/cm ³)	Viscosity (Centipoise)	Water (%m/m)	Micro Carbon Residue (%m/m)	Sulphur (%m/m)
DL231202	HSFO	.987.5	285.4	0.15	10.9	3.43
DL231193	HSFO	990.6	302.3	0.15	15.4	3.30
DL231210	HSFO	988.7	303.3	0.15	13.7	1.96
DL231232	ULSGOE	887.7	5.4	0.05	0.04	0.10
DL231311	ULSGOE	839.9	2.9	0.05	0.01	0.04
DL231229	ULSGOE	832.1	2.7	0.05	0.06	0.03

4.5.13.1 NIR Spectroscopy

The assessment was carried out with an ABB MB3600 NIR spectrometer and high-pressure cell, scanning at 60°C with manual injection using a syringe. Samples were assessed for both instantaneous stability (i.e. as materials are added) and time dependent (over a period of five days) stability.

Organic deposition occurs when the spectra detect wax and asphaltene agglomerates, thus linear blending is no longer applicable. This is termed the “inflection” point as seen in **Error! Reference source not found.** PT5Technology aggregate plot.

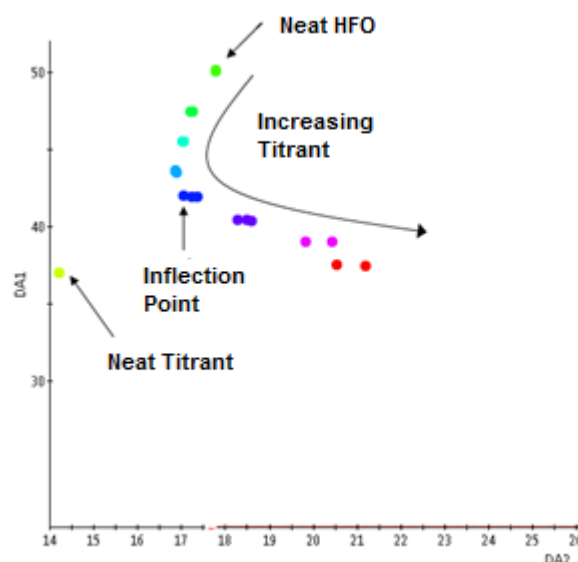


Figure 4-22: Showing the an inflection point

4.5.13.2 Microscopy

Microscopy was performed on the samples to validate spectral observations; this was undertaken on both a Nikon 90i laser microscope and a Nikon Eclipse LV100ND.

Microscopy was carried out in the following forms:

- Transmitted light: Shows sample magnified under normal light, asphaltenes show as black particles, wax appears as light coloured, translucent aggregates.
- Cross Polar: Subjects the samples to polarised light, wax crystals appear as bright star like objects on a black background.

4.5.14 Results

Blends were made up at 10% increments of the following pairs of samples:

- Blend 1: DL231202 – HFO (3.43% Sulphur) / DL231229 – MDO (0.03% Sulphur)
- Blend 2: DL231193 – HFO (3.30% Sulphur) / DL231311 – MDO (0.04% Sulphur)
- Blend 3: DL231210 – HFO (1.96% Sulphur) / DL231232 – MDO (0.10% Sulphur)

4.5.14.1 Sulphur Assessments

Figure 4-23 shows a PT5 aggregate plot of the sample spectra. It can be seen from these plots that as the percentage of MDO is increased from neat HFO (yellow) to neat MDO (red) that the spectra blend linearly (i.e. form a straight line).

The aggregate values (LIN1 and LIN2) are proprietary to Intertek, and were constructed as described earlier in the thesis. The intention of these aggregates was to select sections of the spectra which linearised the aggregate plot and were not affected by the non linearities caused by the deposition of particulate material.

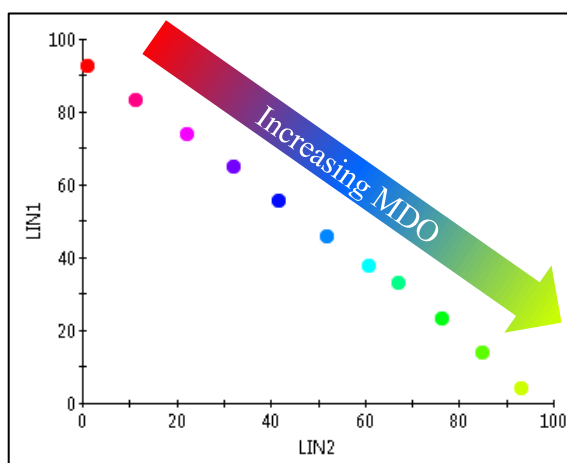


Figure 4-23: Linear Spectral Blending

Figure 4-24 shows that linear blending is interrupted on organic deposition aggregates at the point of 60% MDO in HFO, however, it is possible to construct linear aggregates to accommodate this effect shown in Figure 4-23. This is critical to implementing this customer application as the instrument was intended to monitor percentage Sulphur in the blend online and thus cannot be affected by any particulate precipitation.

4.5.14.2 Instability

Using spectroscopy and organic deposition aggregates the point of inflection due to instability can be seen at 60% MDO in HFO for both blends 1 and 2 (Figure 4-24 a and b)

Characteristic behaviour of the point of instability is the deviation of the spectra from a straight line. If no deposition occurs the spectra blend linearly and straight line is observed between the two pure components.

The aggregate values on this axis are once again constructed from spectra using principles discussed earlier. KARO selects wavenumbers of the spectra related to the aromaticity of the hydrocarbon material, an important factor given that increasing aromaticity would indicate a tendency for the blend to solubilise any precipitated asphaltene.

Deposition Aggregate 10 (DA10) is a further development of the organic deposition aggregates discussed in section 4.2 and takes wavenumbers within the spectra which relate to the deposition of particulate material, specifically in blends of marine fuels.

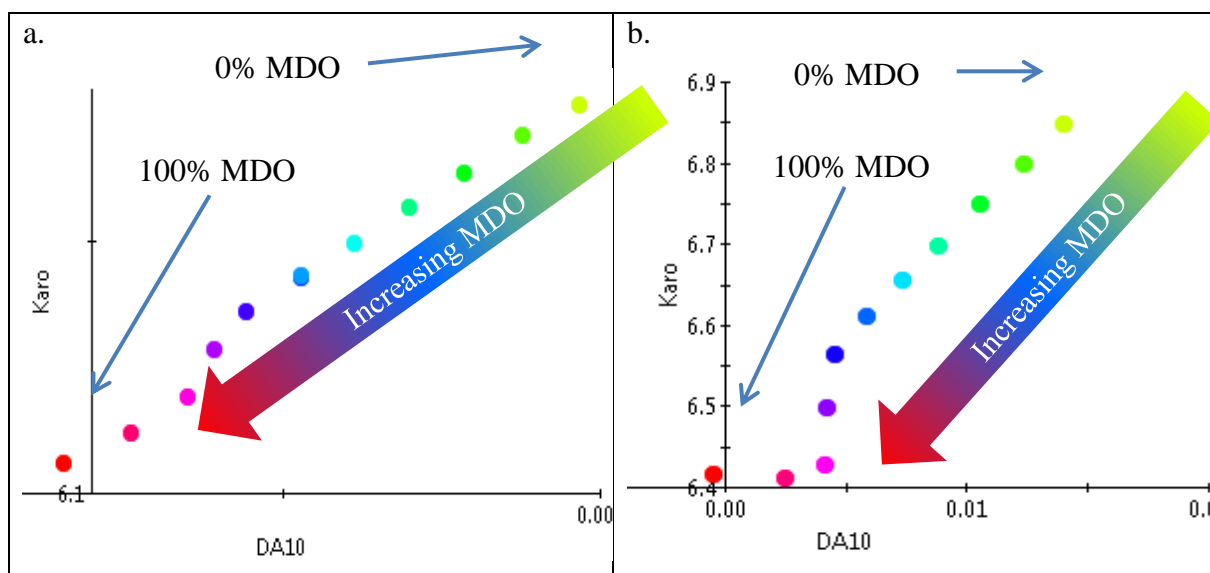


Figure 4-24: Blend 1 (a) and Blend 2 (b) aggregate plots

4.5.15 *Microscopy*

Microscopy images of the samples were taken using a Nikon Eclipse LV100ND microscope with transmitted illumination. The images are used to validate the organic deposition results from spectroscopy. Both blends show that organic deposition occurs in a blend with greater than 50% MDO in HFO.

Blend 1 was made up of DL231202 – HFO (3.43% Sulphur) and DL231229 – MDO (0.03% Sulphur)

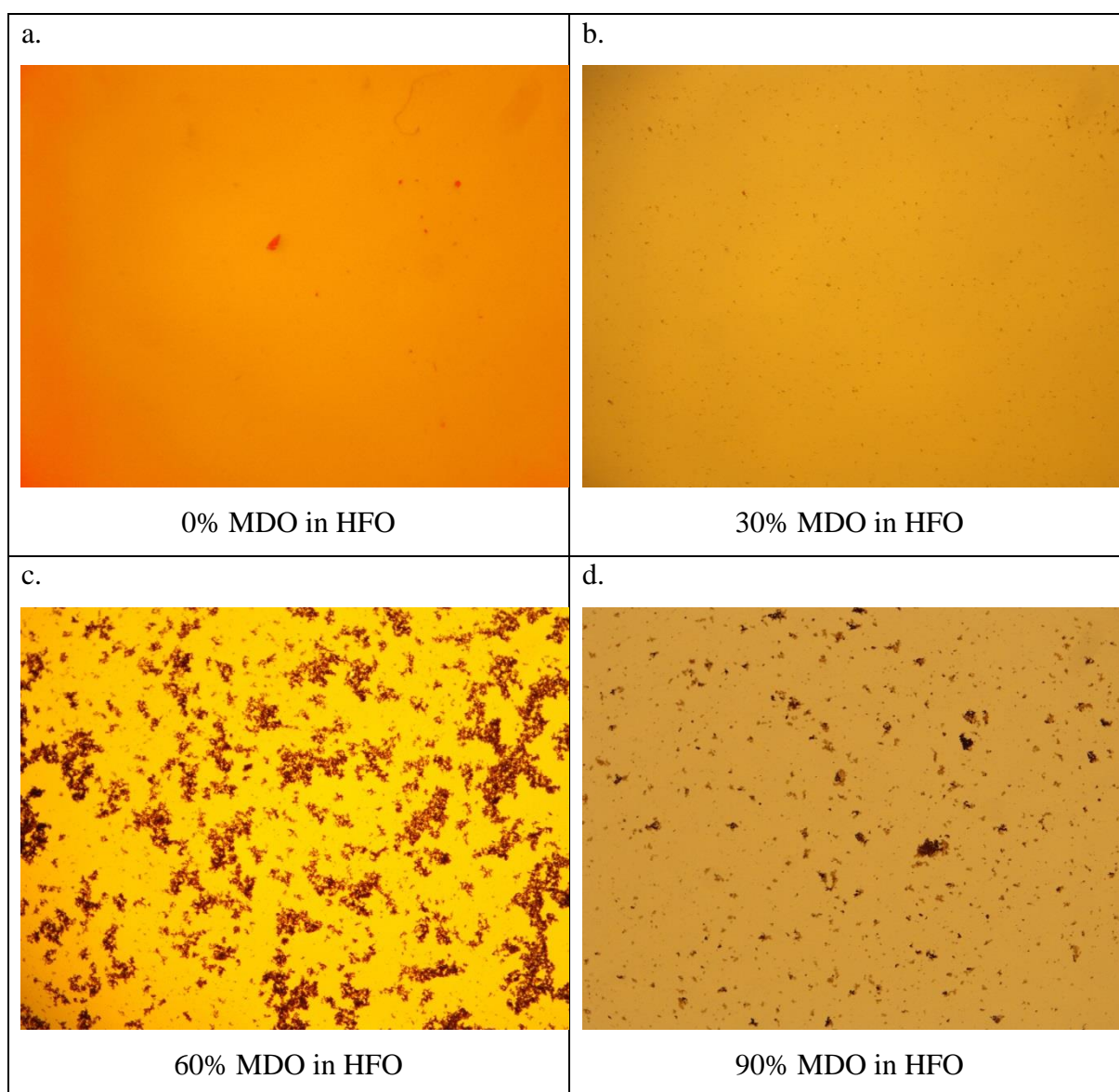


Figure 4-25: Blend 1- MDO in HFO at 0% (a), 30% (b), 60% (c) and 90% (d)

Figure 4-25 shows how the blend precipitates asphaltenes quite severely at 60% MDO in HFO.

Blend 2 was made up of DL231193 – HFO (3.30% Sulphur) and DL231311 – MDO (0.04% Sulphur).

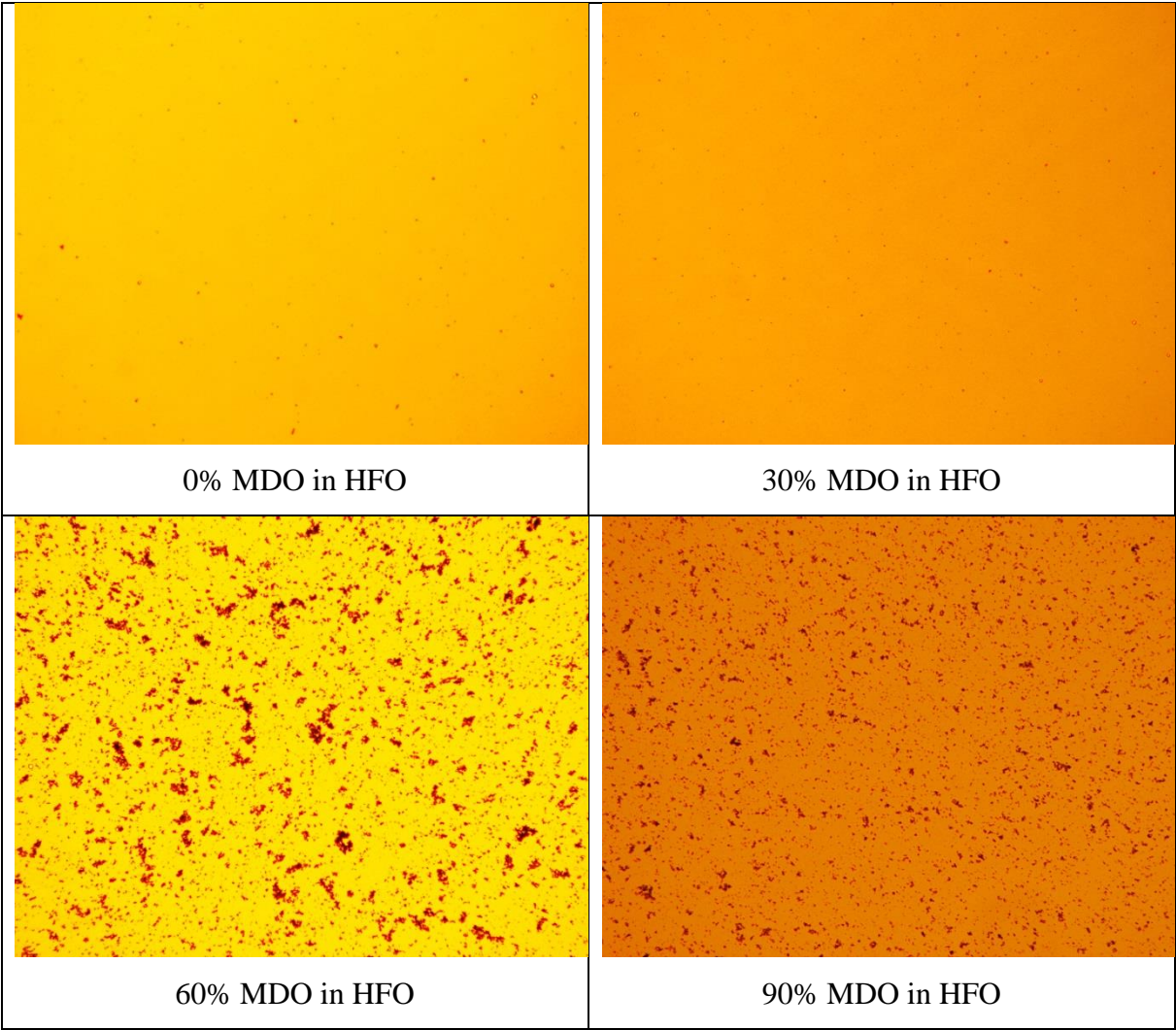


Figure 4-26: Blend 2 - MDO in HFO

From Figure 4-26 it can be seen that Blend 2, although not as severely as Blend 1, still precipitates asphaltenes at 60% MDO in HFO.

4.5.16 *Part 2 – Additive Efficacy Assessments*

Part 2 goes on to show the results of blending marine fuel oils and additives. The assessments focused particularly on the stability of blends of fuel oils containing Marine Diesel Oil (MDO) and Heavy Fuel Oil (HFO) with and without an additive.

The project work was initiated following discussions between Intertek Process Assurance Group and Intertek Shipcare. Part 1 of the study demonstrated that blends of HFO and MDO precipitate asphaltenes both instantaneously and over time.

Following on from further discussions there was significant interest in assessing the effects of investigating a solution to the problem in the form of asphaltene stabilising additives. The ability to quantify the effects of additives on fuel oil blend stability will allow Intertek to offer solutions to customers experiencing these issues.

A selection of samples including HFO and MDO were selected for testing in the laboratory. Testing work was carried out in September - November 2015 with various blend recipes assessed using Near Infrared (NIR) spectroscopy and microscopy. The oils were blended at predetermined ratios (shown below) and tested with and without additive.

Blends were made up at 20% ratios of the following pairs of samples:

- Blend 1 DL242838 – HFO (2.57% Sulphur) / DL243169 – MDO (0.076% Sulphur)
- Blend 2 DL242840 – HFO (2.49% Sulphur) / DL243094 – MDO (0.083% Sulphur)
- Blend 3 DL242837 – HFO (2.41% Sulphur) / DL243017 – MDO (0.083% Sulphur)

4.5.17 *Physical Properties*

The physical properties for the samples provided by Shipcare are shown in Table 4-7 below.

Table 4-8: Physical Properties for Samples

Lab Ref	Grade	Dens	Visc	H2O	MCR	SUL
DL242838	HSFO	988.4	378	0.25	10.6	2.57
DL242840	HSFO	991	405.5	0.15	16.2	2.49
DL242837	HSFO	989.8	344.8	0.2	15.1	2.41
DL243017	ULSGOE	908.7	82.7	0.05	4.6	0.083
DL243094	ULSGOE	908.7	82.2	0.05	5.2	0.083
DL243169	ULSGOE	862.5	21.66	0.05	0.1	0.076

The blends were assessed under the same regime as the feasibility study by using microscopy and NIR spectroscopy.

4.5.18 *Results*

Blends were made up at 20% increments of the following pairs of samples:

- Blend 1 DL242838 – HFO (2.57% Sulphur) / DL243169 – MDO (0.076% Sulphur)
- Blend 2 DL242840 – HFO (2.49% Sulphur) / DL243094 – MDO (0.083% Sulphur)
- Blend 3 DL242837 – HFO (2.41% Sulphur) / DL243017 – MDO (0.083% Sulphur)

Table 4-9 (below) is a summary table showing laboratory observations of the blends analysed.

Table 4-9: Summary table

Blend Number	Date	Fuels in blends	Additive amount (g)	Comments	
				Microscopy	Spectroscopy
1a	02/10/2015	80% of DL242838 and 20% of DL243169	0.02123	No change	No change
1b	02/10/2015	60% of DL242838 and 40% of DL243169	0.00764	No change	No change
1c	02/10/2015	40% of DL242838 and 60% of DL243169	0.00828	No change	No change
1d	02/10/2015	20% of DL242838 and 80% of DL243169	0.01965	No change	No change
2a	03/11/2015	80% of DL242840 and 20% of DL243094	2.2	Additive shows improvement	Spectra confirms additive improves
2b	03/11/2015	60% of DL242840 and 40% of DL243094	2.2	Additive shows improvement	Spectra confirms additive improves
2c	03/11/2015	40% of DL242840 and 60% of DL243094	2.2	Additive shows improvement	Spectra confirms additive improves
2d	03/11/2015	20% of DL242840 and 80% of DL243094	2.2	Additive shows improvement	Spectra confirms additive improves
3a	06/11/2015	80% DL242837 and 20% DL243017	4	No change	No instability
3b	06/11/2015	60% DL242837 and 40% DL243017	4	No change	No instability
3c	06/11/2015	40% DL242837 and 60% DL243017	4	No change	No instability
3d	06/11/2015	20% DL242837 and 80% DL243017	5	No change	No instability

As seen in the table, the additive improved a number of samples including blend 2a, b, c and d. All blends with the exception of blend 3 showed instability at certain blend ratios.

4.5.19 *Blend 1 (DL242838/DL243169)*

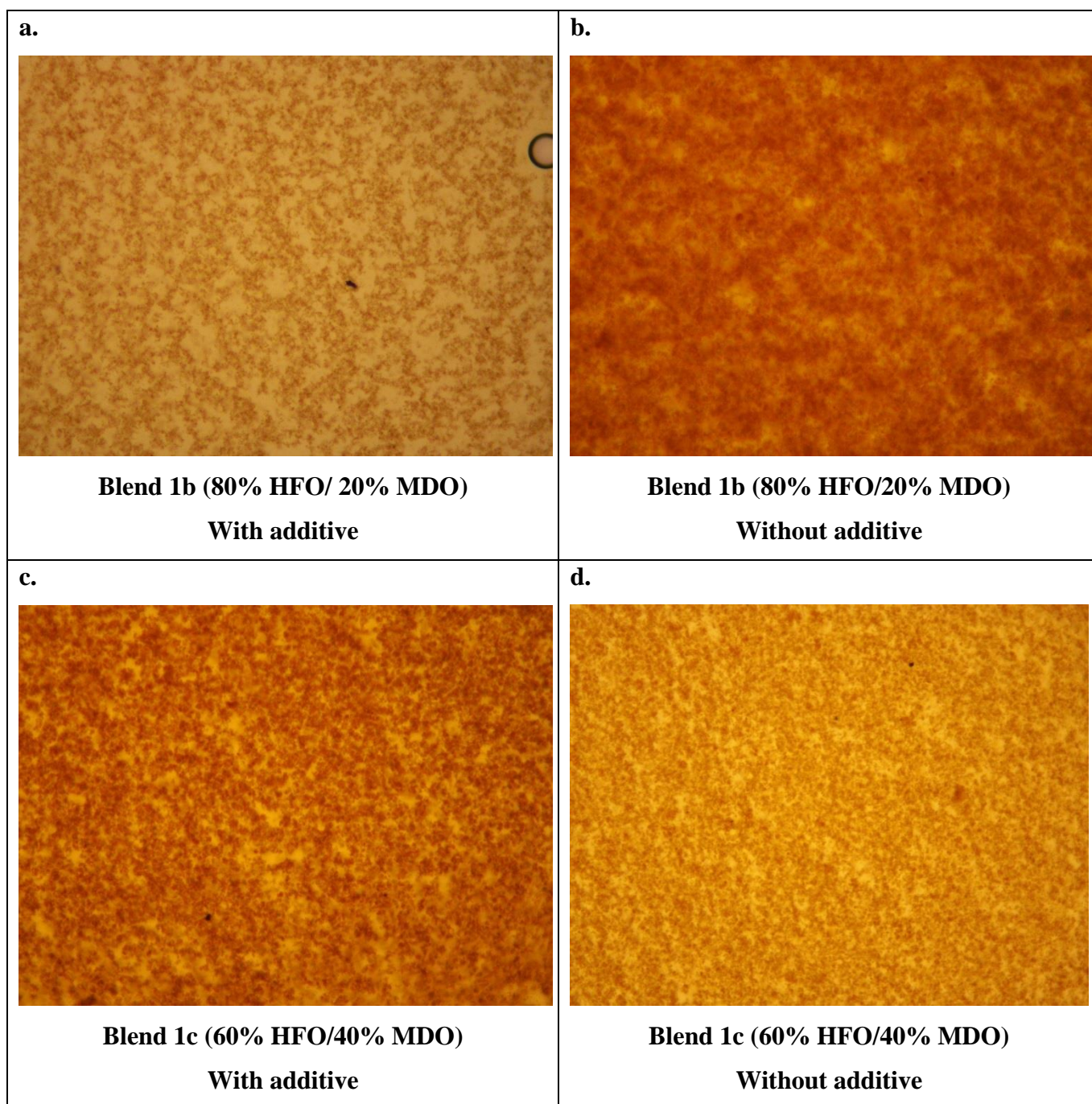


Figure 4-27: Showing blends with additive (a) and (c) and without additive (b) and (d)

In blend 1 the additive did not improve the stability of the blend, the blend was equally as unstable without the additive as it was with the additive.

4.5.20 Blend 2 (DL242840/DL243094)

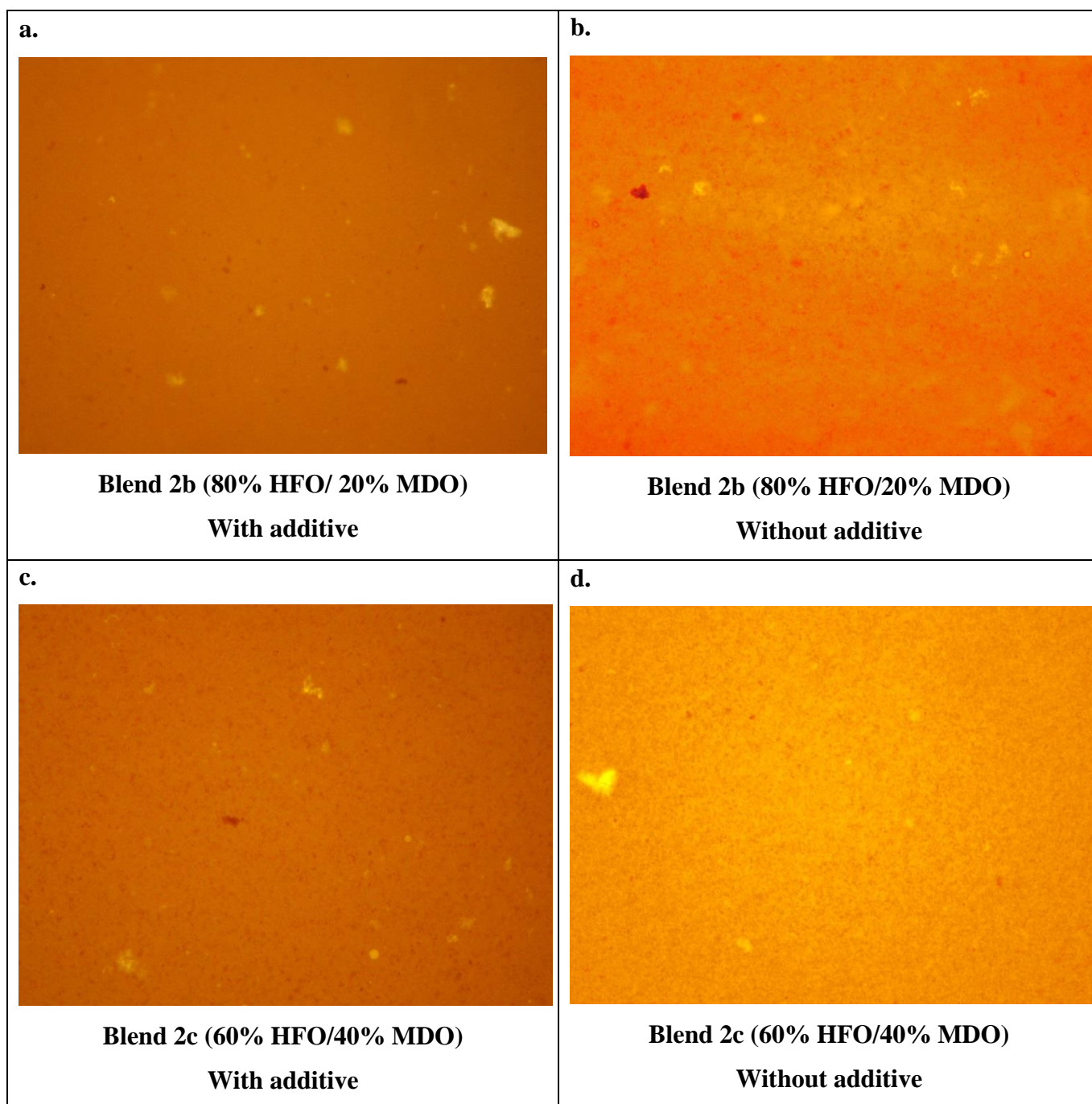


Figure 4-28: Showing blends with additive (a) and (c) and without additive (b) and (d)

In blends 2b and 2c (above) it can be seen that the additive has made a difference to the stability of the blends, if the a photo is considered, it can be seen that there is no particulate deposition, however, looking at the d photo, the black precipitated asphaltene particulates can be seen.

Appendix B contains the results for blends 3b and 3c in which it can be seen that the additive has not made a difference to the stability of the blends, this is because no instability was observed in the blends before addition of additive. The spectroscopy validates these findings.

4.5.21 *Additive*

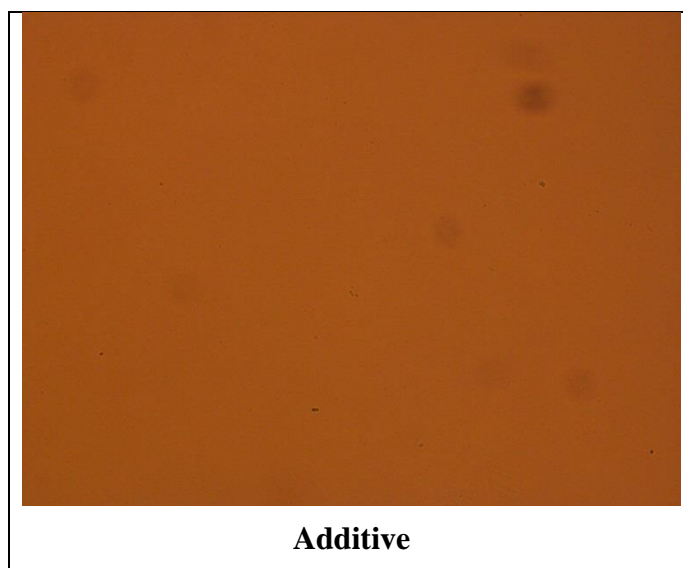


Figure 4-29: Neat Additive

By scanning and taking microscope pictures of the additive, validation of the physical effects of the additive on the crude blend is possible i.e. the additive does not contain (in itself) particulate asphaltene or waxy agglomerates which would affect spectra.

4.5.22 *Conclusions*

From the assessment of marine fuels it is clear that the methodology developed can also deal with instability problems in the marine industry. This has the potential to be developed into a ship fuel monitoring service to profile sulphur levels as the transition occurs from HFO to MDO when passing through SECA's.

It was also proved that the chemometric modelling technique discussed in 0 can be applied to monitor sulphur transition during marine fuels blending. This has the potential to be rolled into an online service which can be placed on board a ship to monitor both Sulphur transition and blend stability.

Furthermore the case study demonstrated the applicability for the technique to assess the efficacy of additives on blends of marine fuels. A capability that can be applied in other areas of the hydrocarbon processing sector.

Intertek can offer this as a service to additive manufacturers to assess efficacy of additives and provide them value added information to take to the marketplace.

Chapter 5:

Troubleshooting Upstream Process Issues with Data Analytics

Chapter 5. Troubleshooting Upstream Process Issues with Data Analytics

As part of the provision of chemometric modelling services to clients of Intertek, it was a logical next step to widen the modelling capability of the PT5 toolbox and provide troubleshooting for client issues based on data other than NIR spectra.

The process industry in general has a multitude of online instrumentation, interfaced to process data historians (such as PI). Contained within these datasets is valuable information and knowledge that, when coupled with domain expertise, can be used to achieve a variety of benefits including: more efficient maintenance scheduling, improved performance, reduced downtime and maximised margins.

However, this valuable information is hidden in the quantity of data and further compounded by dataset issues such as the noise from unrepresentative operation such as process upsets and malfunctioning instrumentation. Hence, to simplify analytics, operators usually focus on time series trending and first order effects.

Much work has been undertaken on the application of multivariate data analytics to process data, particularly for its applications in Process Analytical Technology (PAT) and Quality by Design (QbD). A review of these approaches to bioprocess datasets was undertaken by (Mercier *et al.*, 2014) with the conclusion that data analytics in this industry, although implemented, is still in its infancy and much more development work is required to achieve wider marketplace penetration

Furthermore, applications are also implemented in the pharmaceutical industry, (Rioloa *et al.*, 2017) undertook a review of the applications of data analytics for PAT within the pharmaceutical industry, with a specific focus on Raman spectroscopy.

However, the drivers for development of this technology in food and pharmaceuticals is clear, these are tightly regulated industries producing goods generally for human consumption and thus the margin for error is very slim. Very little has been written on the implementation within the oil and gas industry however, this is due to a traditional mindset and an attitude that the status quo works and thus the balance should not be upset.

During the course of the Eng.D project, an opportunity was identified with an upstream client experiencing problems with two pumps on an offshore installation. Pump failure not only

resulted in maintenance costs to repair the pump but also deferred production costs, i.e. the cost associated with not producing oil. This problem was not new however and pump failures had been plaguing the installation for many years.

The Eng.D project was focussed on working as part of an engineering solutions team to identify the root cause of pump failure and thus develop a novel solution which could be implemented to monitor the issue and mitigate the problem to the greatest extent possible.

The problem was suspected to be caused as a function of the ratio of gas:liquids in the stream to the pump, affected by the well configuration. Therefore, this fits well with the theme throughout the Eng.D programme which has focussed on blended hydrocarbon streams.

5.1 Case Study 4: Offshore Data Analysis

A client has experienced operational issues with regard to two pumps installed on a platform. There has been a significant history of issues including vibration and other mechanical problems. Although remedial work has been carried out performance remains less than optimal. In the last one – two years however one of the major failure points of the pump has been the process seals. Below is a schematic diagram showing the basic process flow:

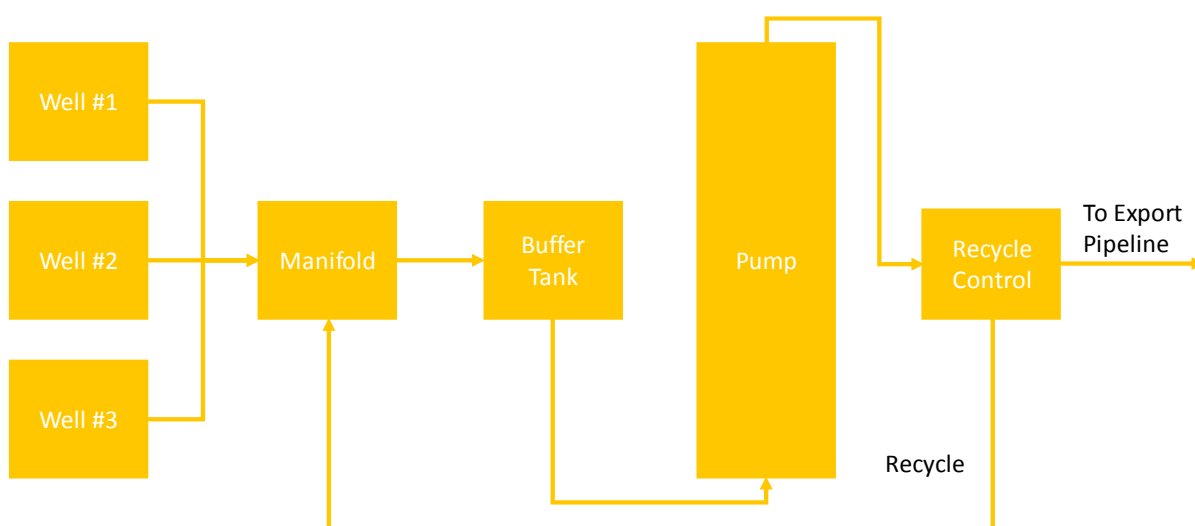


Figure 5-1: Process Flow Diagram

It can be seen that the crude oil flows from several wells into a manifold where it goes to a buffer tank. This is intended to control the consistency of the fluids entering the pump. Fluids go through the pump and onto a recycle control where some flow is diverted back to the

manifold prior to the buffer tank and some is sent to export. This is controlled based on the flow rate of the wells.

Figure 5-2 below shows a basic schematic of the pump. The arrangement is twin screw with two rotating shafts. These are sealed at each end however there is movement, thus the shafts are able to oscillating both horizontally and vertically (z axis displacement).

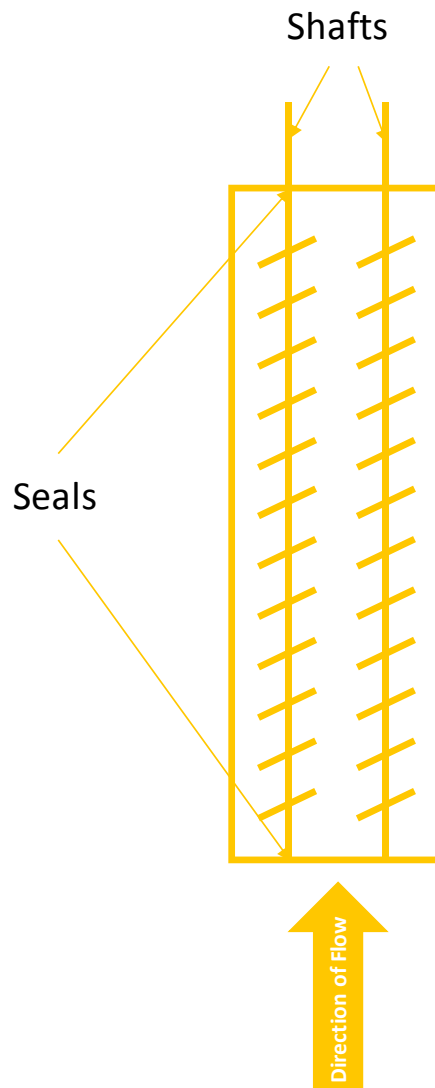


Figure 5-2: Pump Schematic

They have an expected (and historical) life of approximately 18months, however recently the client experienced failure after much shorter operational intervals. It is unknown at this time if this is as a result of a historical project to minimise vibration or if there has been a major change in process conditions, the goal of the data analysis is to understand the process and what factors from the process can indicate or cause the seal failure noted in recent years.

The client supplied Intertek with the following 5 datasets:

Period number	Time period summary	Length	Interval	Usage
1	Smooth operation - no failures	14 days	5 mins	Used as steady state indicator
2	Failed control attempt 1	~1 hour	10 sec	Low variability
3	Failed control attempt 2	~1 hour	1 sec	Low variability
4	Failure Period A	7 days	5 mins	Analysed in depth
5	Failure Period B	7 days	5 mins	Analysed in depth

5.1.1 *Data Pre-Processing*

Prior to carrying out any data analysis a number of pre-processing steps were made to ensure that the data was fit for use, this involved searching the data set for incomplete ranges, text in place of numbers.

In period 4 and 5 there was a regular I/O error which appeared in two separate groups, one group had the error in the first row of data the other in the 15th row., these I/O errors had to be removed prior to data analysis.

5.1.2 *Univariate Analysis – Pump A*

The customer noted that the change in axial displacement was a likely cause of the seal failure, going on to discuss that the magnitude of displacement was not high compared to normal operation. This prompted initial observations of not just the magnitude but also the rate of change of axial displacement across the time period in question and across time period 1 as it was considered a good indication of ‘normal’ operation.

Focusing on period 1, 4 and 5 for the rate of change charts below, the rate of change is simply the current time period minus the next one, as these data points are 5 minutes it was not deemed necessary to smooth this by using a pre-processing algorithm.

As can be seen below, when looking at ZI-37261A (z axis displacement sensor), throughout period 1 (Figure 5-3) and period 4 (Figure 5-4) pump A has a very small rate of change of axial displacement, the blue line is the rate of change and the red is the actual value of the sensor.

The only exception to this small rate of change is noted at the end of period 4 when there is a sudden change in axial displacement caused by pump B shutting down due to seal failure. This change is so large that the shaft actually moves past its calibrated 0 and hence shows as a negative displacement.

This also demonstrates that the two pumps interact with one another to a certain extent and this could be due to a number of factors including the physical proximity of the two units or (more likely) the common discharge.

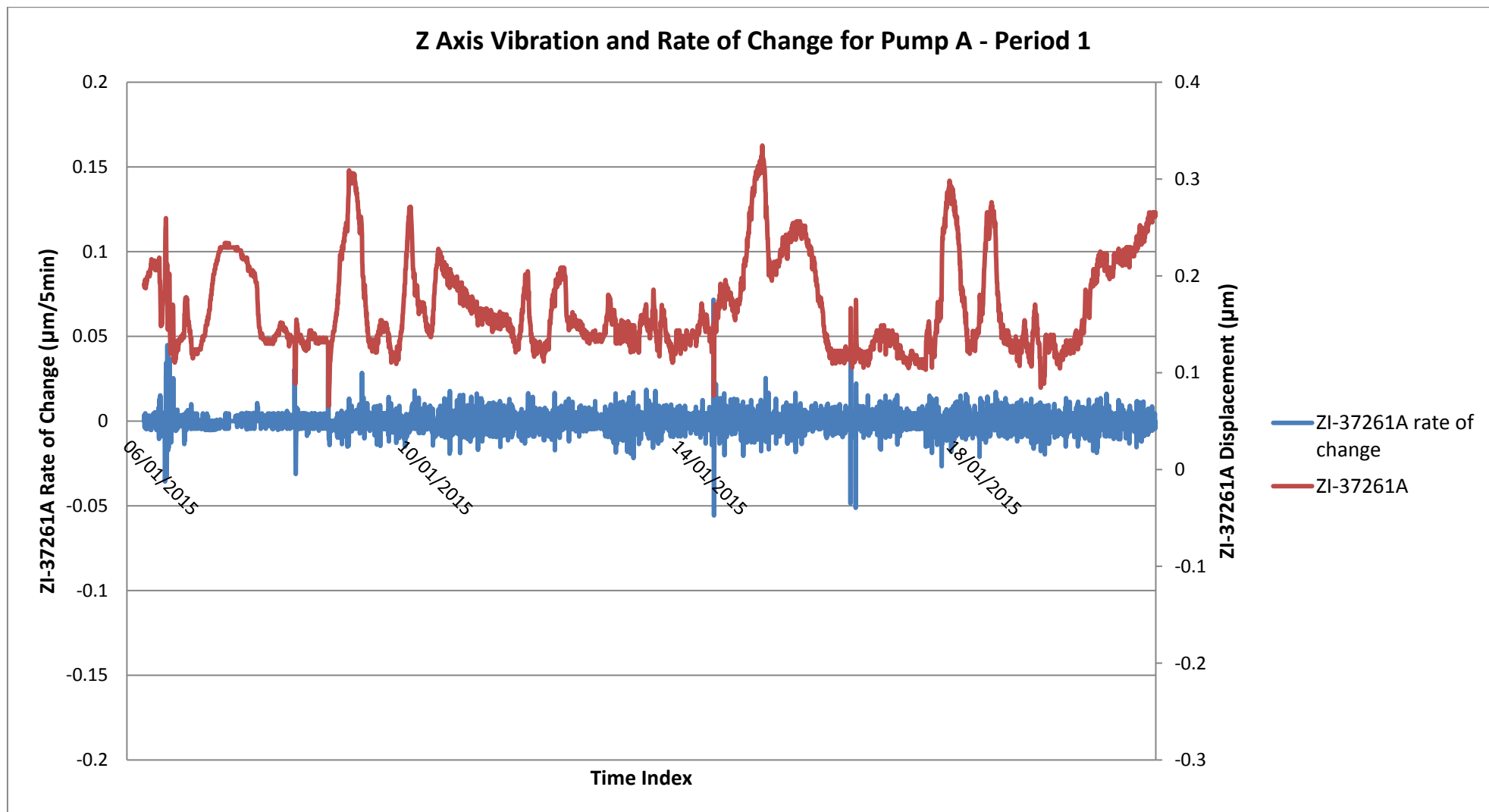


Figure 5-3: Pump A throughout time period 1

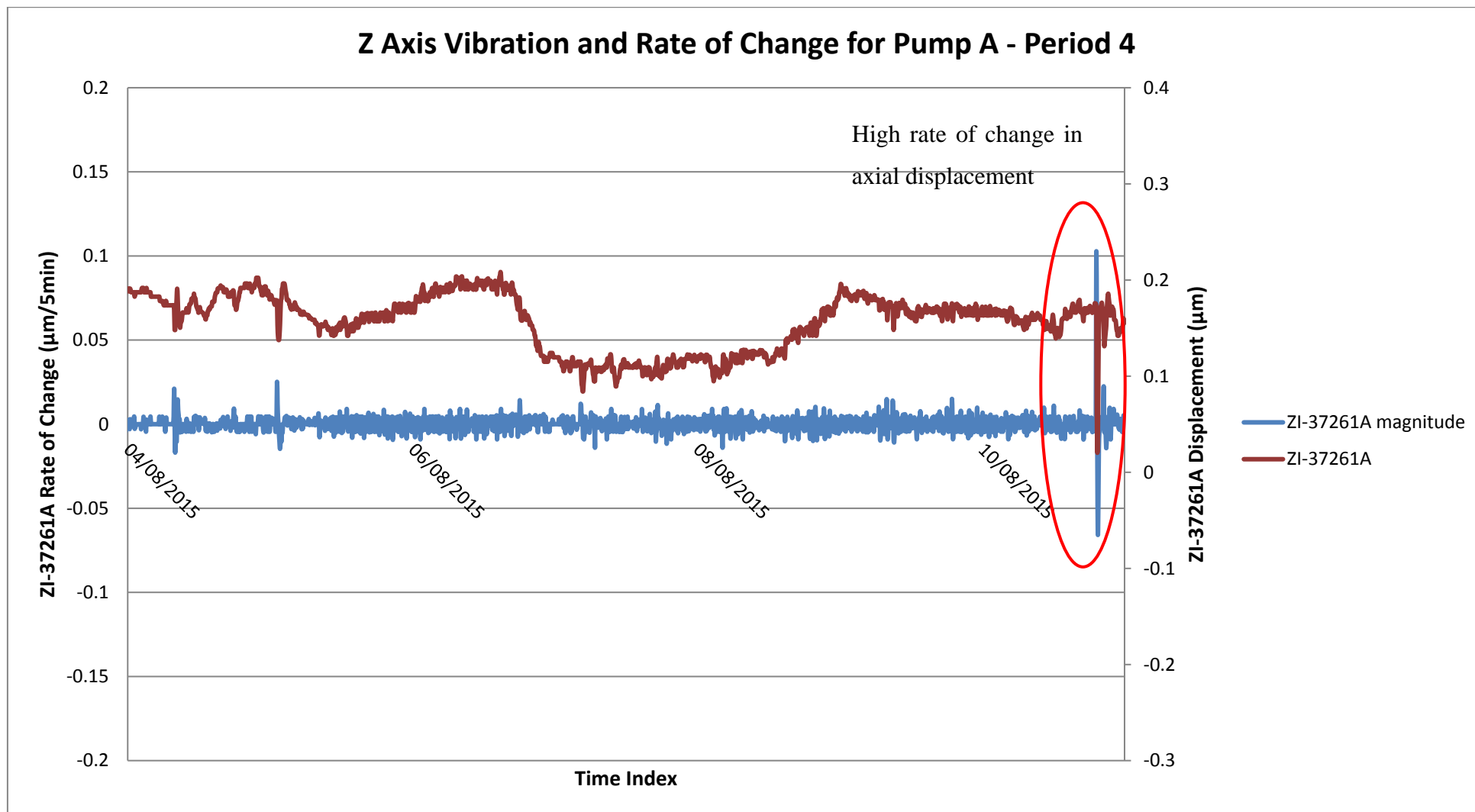


Figure 5-4: Pump A throughout period 4

In Figure 5-5 which examines ZI-37261A (z axis displacement sensor) for pump A in period 5 there only one pump in operation (pump A), however, towards the end of the period pump A is initially shut down and attempts are made to restart B which ultimately are unsuccessful. After this A is brought back online again but subsequently suffers a seal failure and has to be shut down. As only one pump is online throughout time period 5 it may have slightly different characteristics to a time when both pumps are running.

In Figure 5-5 there are three clear periods where there is a sudden change in the axial displacement as shown by high values on the rate of change plot (blue). Event 3 is the point where the pump shuts down due to the failure of the seal.

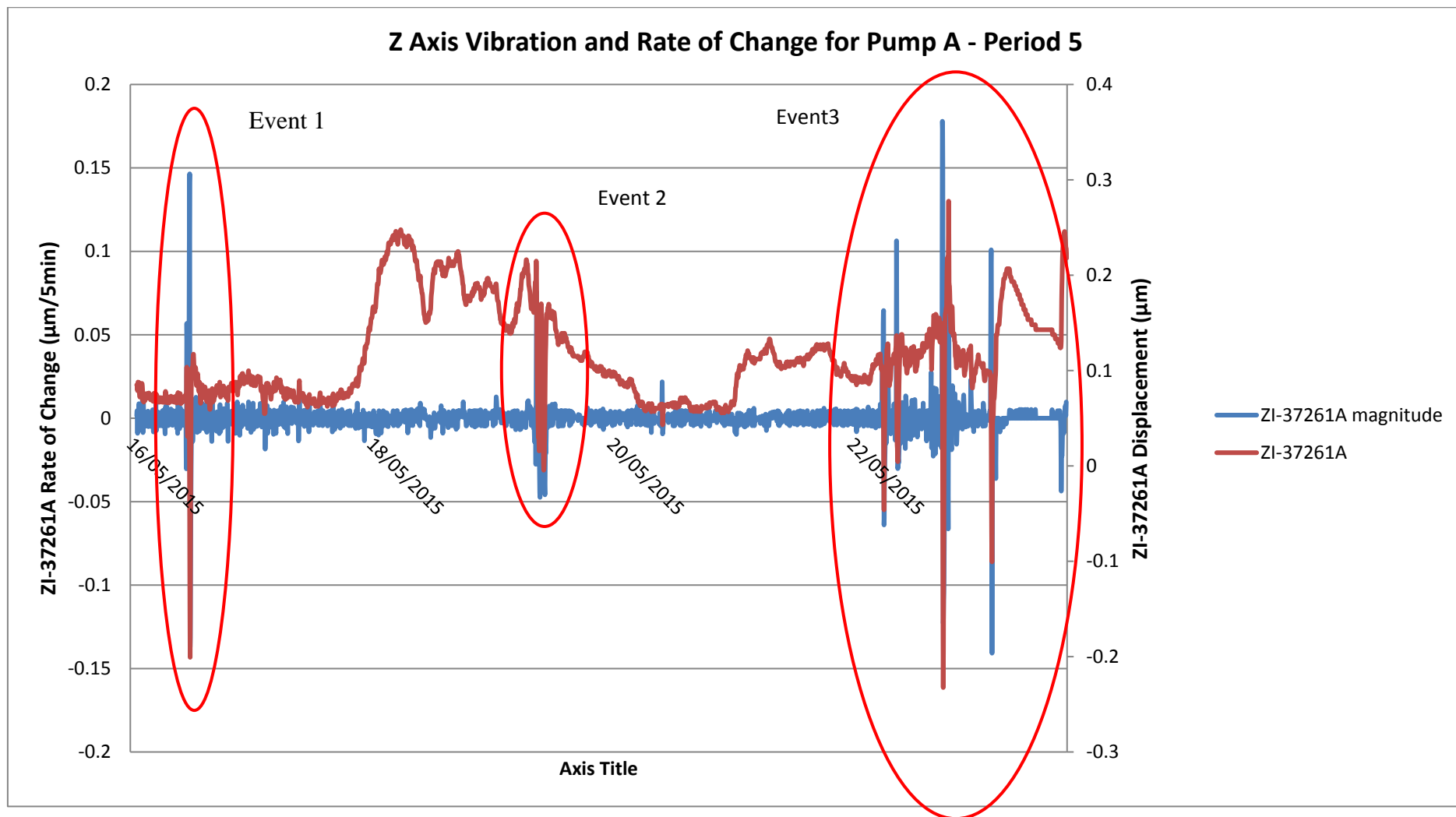


Figure 5-5: Pump A throughout Period 5

Focusing in on the second event there are some large fluctuations noted in the axial displacement of the shaft as shown on Figure 5-5 and Figure 5-6.

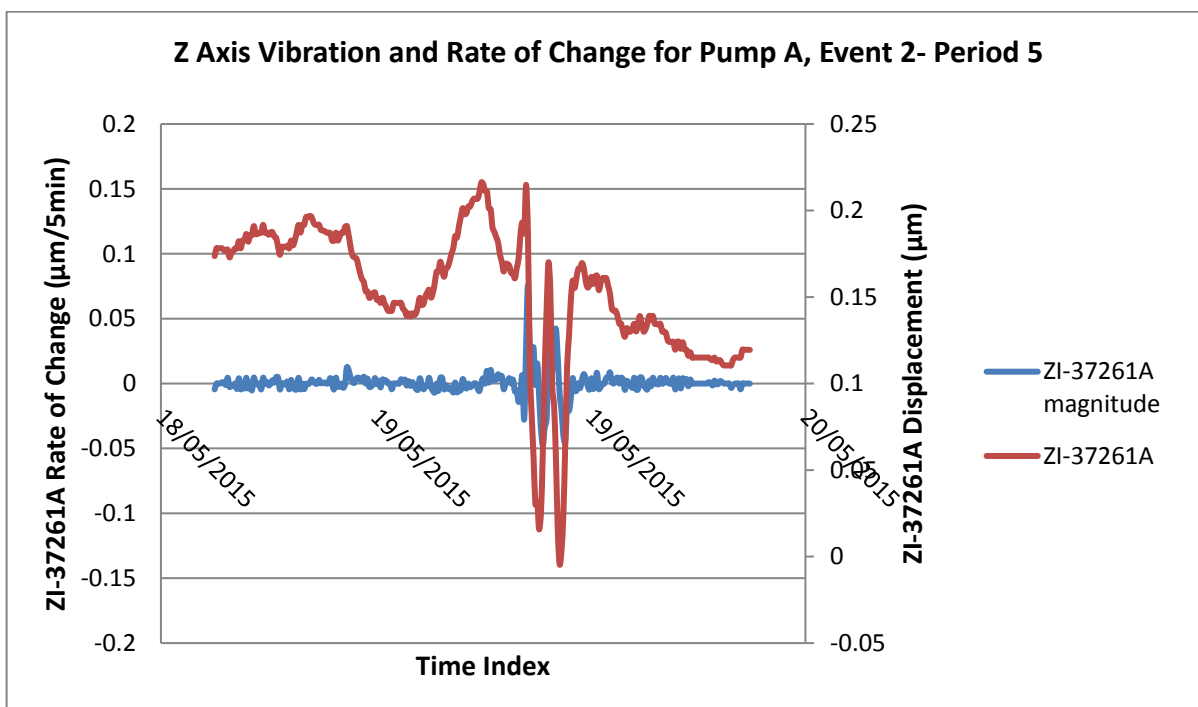


Figure 5-6: Axial Displacement

When this change in axial displacement occurs it is also noted a subsequent disturbance in the level of the buffer tank. As seen in Figure 5-7, there is a sudden drop in level (LI-37202A) at the buffer tank for pump A, as the distance between the tank and pump is short it is a safe assumption that these two events are linked. This drop in level is also an indicator of lean (high gas flow) and thus potentially a slug of gas moving through the system.

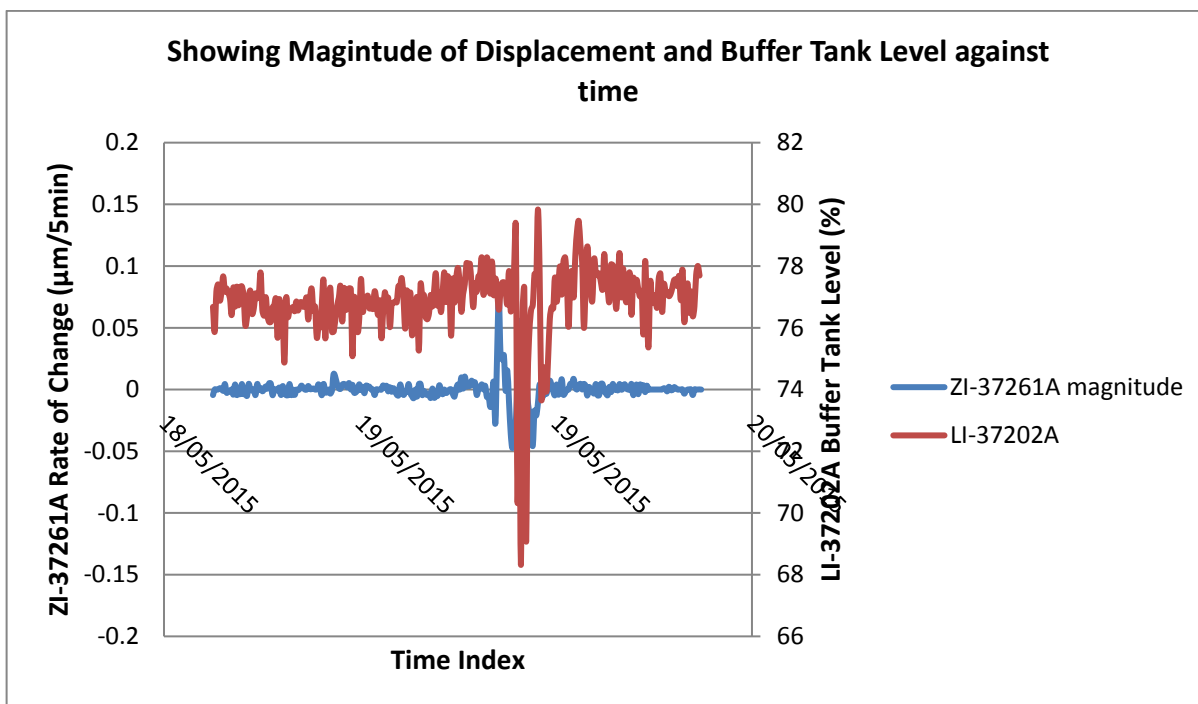


Figure 5-7: Buffer Tank Level

This coincides with the phenomenon of slugging wells, a common offshore phenomenon and one that is well known for causing a range of process issues. Liquid slugs in particular would be seen in the data as a peak in torque and flow rate.

Looking at the flowrate to the pump (FI-37216A) and torque (JI-37219A) throughout the event 2 this behaviour is not seen, rather there is an erratic torque value (red) but ultimately a drop accompanied with a sudden drop in flowrate (blue) over the period of increased axial displacement.

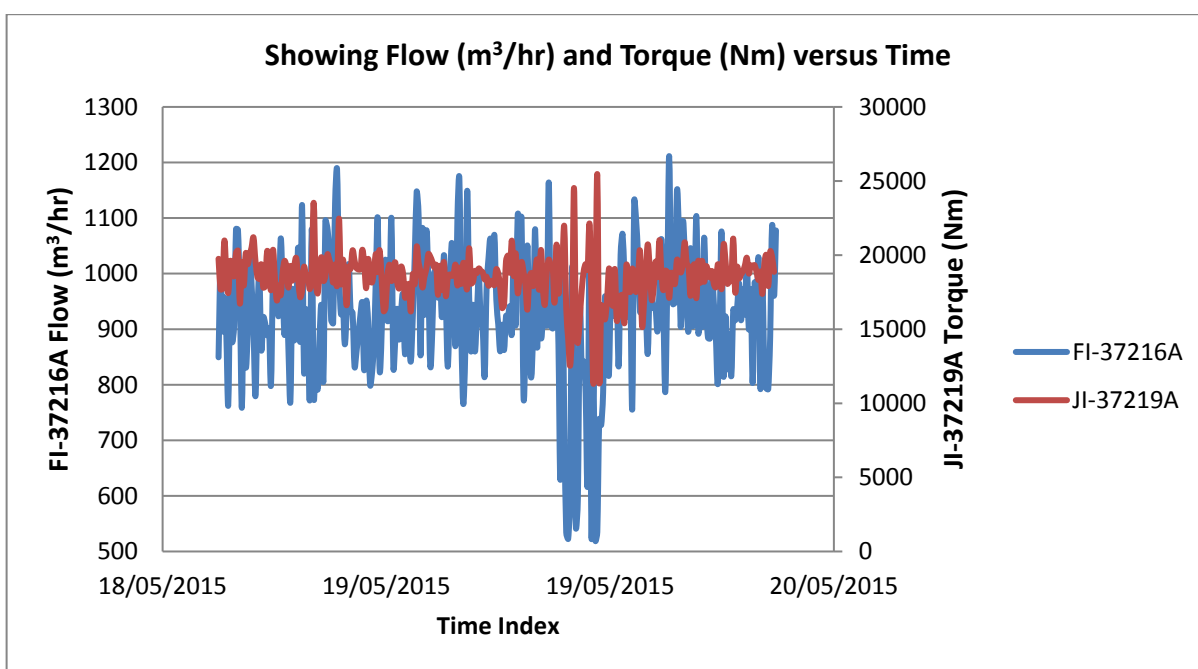


Figure 5-8 Flow Rate and Torque

As this behaviour is opposite to that associated with a liquid slug and the fact that there is a drop in liquid level in the buffer tank (Figure 5-7), It is suspected that this behaviour is actually indicating a period when overall less mass is entering the pump. This shows that during this period of time the liquid content of the incoming fluids was lower than normal.

The gas slug theory is further justified if the inlet temperature to the pump is taken as an indicator of composition of the stream entering it. If it is assumed that the heat extraction capability of the inlet cooler is near to constant (a safe assumption as the cooling utility would not change significantly over a short period of time) then any change is due to process fluctuations.

Therefore, an increase in temperature would show that the incoming energy from the system also increased and this could be caused by one or a combination of the following: a general temperature increase of the fluids, an increase in total flowrate or an increase in the liquid fraction. Conversely if a temperature drop was noted it would indicate a combination of a reduction in specific heat capacity of the fluid (i.e. more gaseous), a drop in temperature for the system or an overall reduction in flowrate.

Figure 5-9 shows the DP vs inlet temperature for pump A in period 5, coloured by events. Event 1 is the large axial displacement change noted at the beginning of the period, event 2 is the event discussed in detail earlier.

As can be seen event 2 begins in the main cluster, then moves to an area of lower temperature and DP, indicating a reduction in flowrate or a reduction in specific heat capacity, showing either a disruption in flow or a change in density and then returning to the cluster which indicates normal operation. Event 1 goes through a very similar process but with much lower temperatures. Event 3 is the actual failure event, again is very similar to the two others, but most closely resembles event 1.

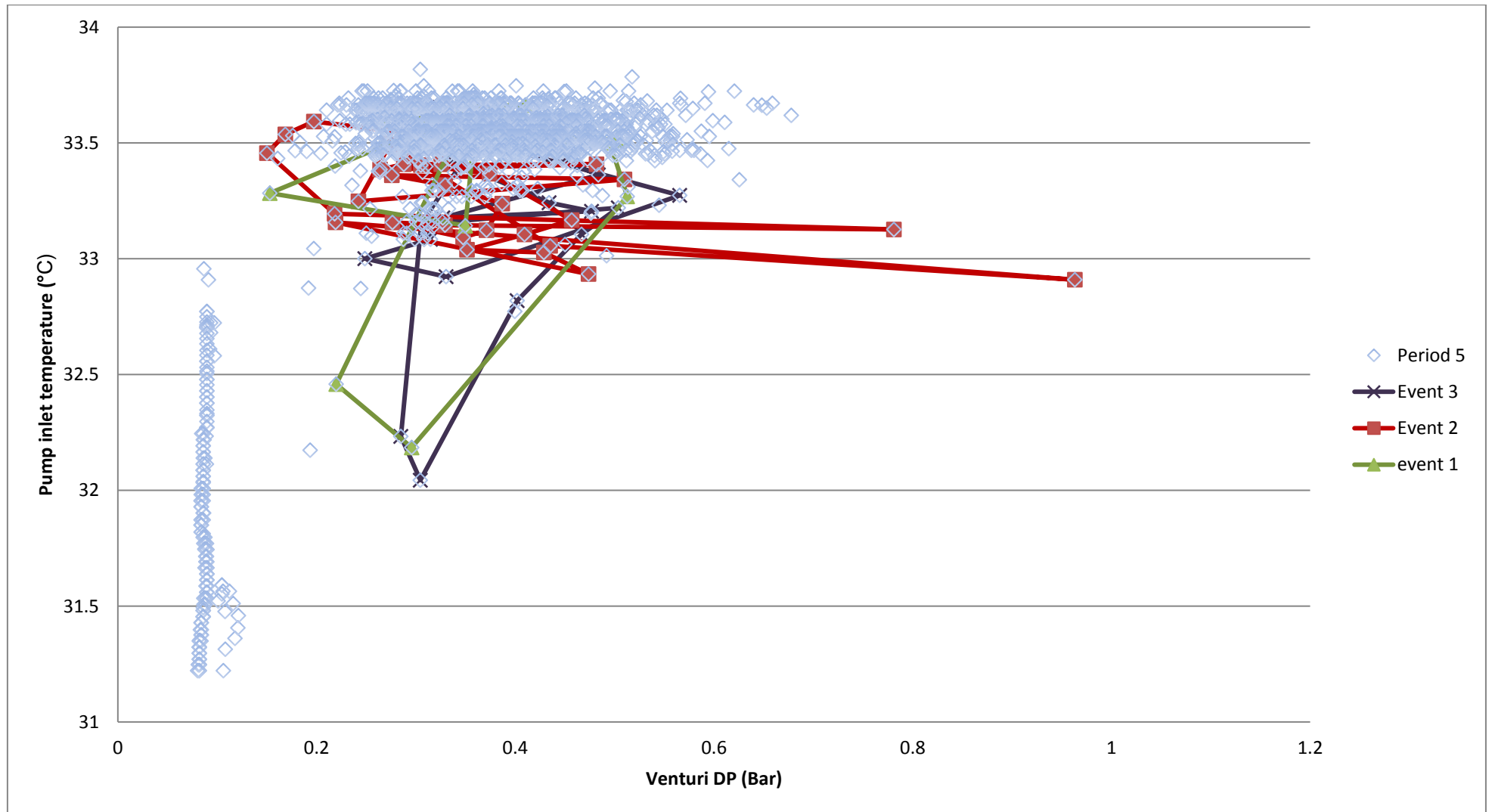


Figure 5-9: Inlet Temperature vs DP

All three of these events were similar as they all had a high rate of change in axial displacement of the pump. In conclusion, the failure event can be categorised by a large change in axial displacement in the pump, the cause of this will require further investigation using multivariate analysis.

5.1.3 *Univariate Analysis – Pump B*

Following on from the investigation of pump A a further investigation was undertaken of the parallel pump B. It was noted in a customer report that seals on pump B also experiences failure. To validate the earlier theory from pump A the customer noted a sudden change in axial displacement prior to the failure, this was thought to be caused by a liquid slug. As with pump A the failure was accompanied by a significant drop in the level of seal oil.

A similar approach was taken with B where rate of change of axial displacement was plotted through time period 1 and 4. In this case period 5 has been omitted as it does not include a long period of operation for analysis of pump B.

As before the change in axial displacement is relatively small throughout the entirety of time period 1 showing the pump is not going through any major disruptions. In time period 4 it is observed that there are two clear events where there was sudden change in axial displacement (Figure 5-11).

Event 1 results in a shutdown of the pump and subsequent restart, there is a large amount of axial displacement during event 2 as it is the event which coincides with the failure of pump B (noted in customer reports). It should be noted that in the analysis of pump A a period of sudden axial displacement was seen to result in seal failure, and this event looks very similar.

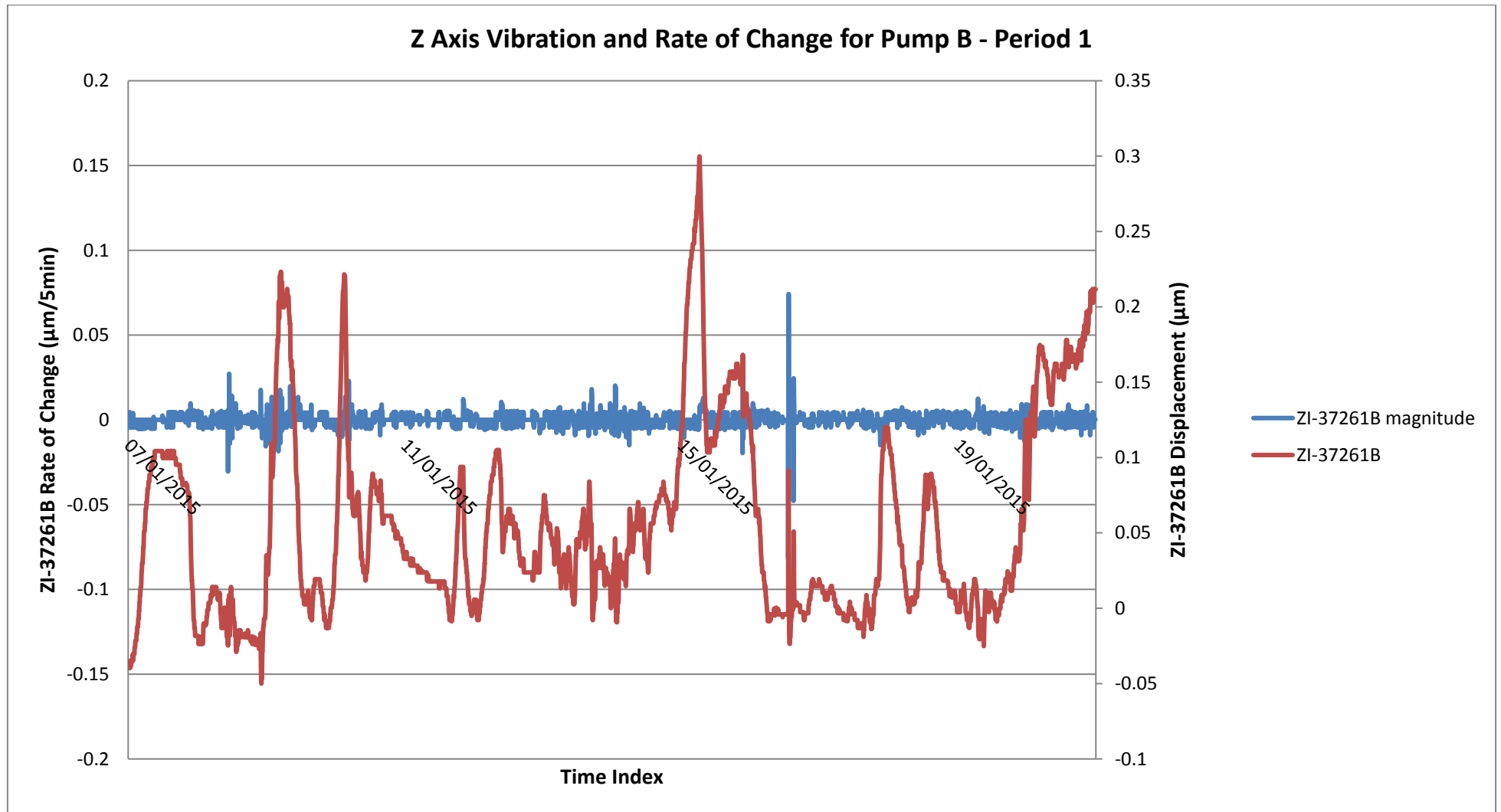


Figure 5-10: Axial Displacement of MPP B through time period 1

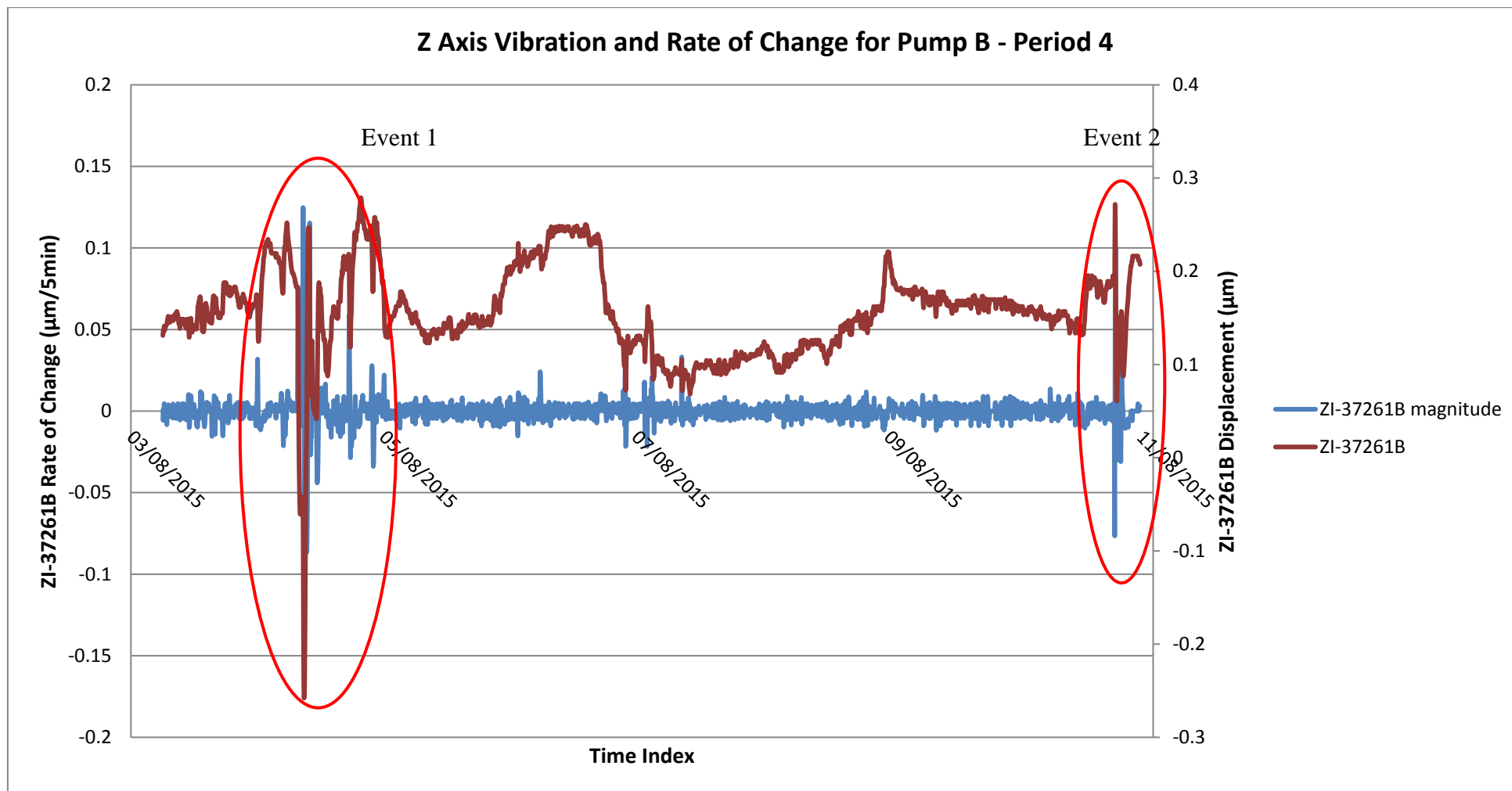


Figure 5-11: Axial displacement of MPPB throughout time period 4

As with pump A period 4 was analysed to try and correlate any commonalities between the high periods of change in axial displacement (noted in event 1 and 2 in period 4).

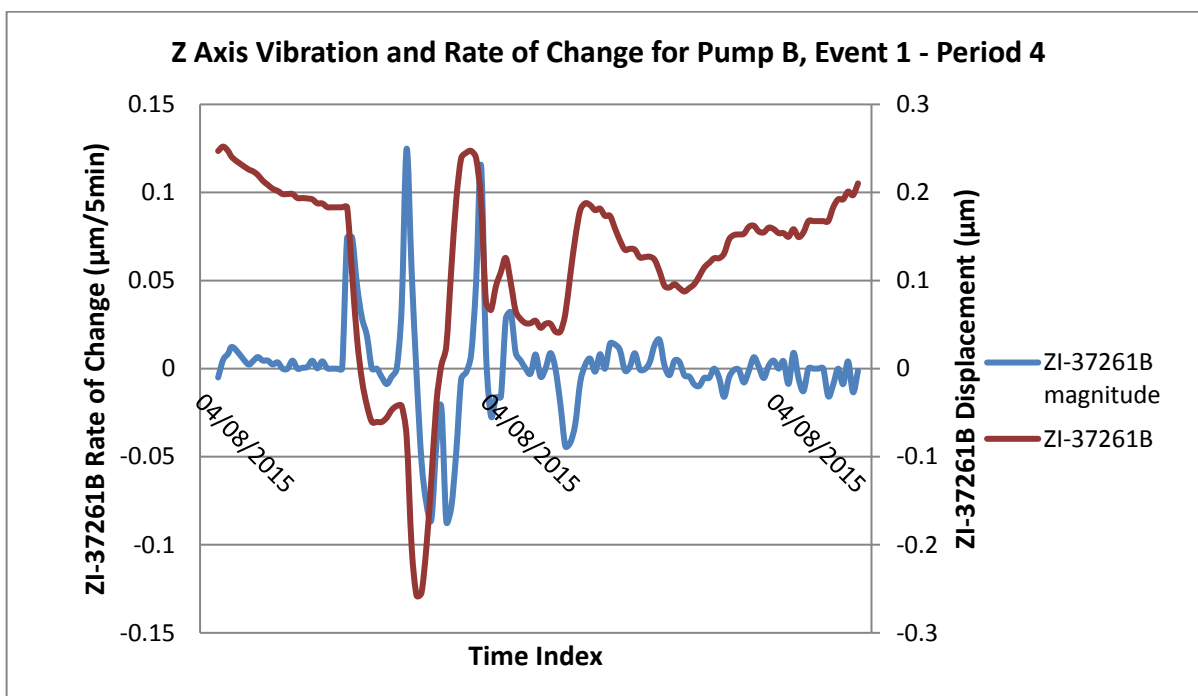


Figure 5-12: Pump B event 1 period 4

The correlation between z axial displacement of B and buffer tank level of B (LI-37202B) was also undertaken (Figure 5-13). It is observed that, once again, at the point where seal failure is noted, there is again a drop in level, indicating lean (high gas) flow.

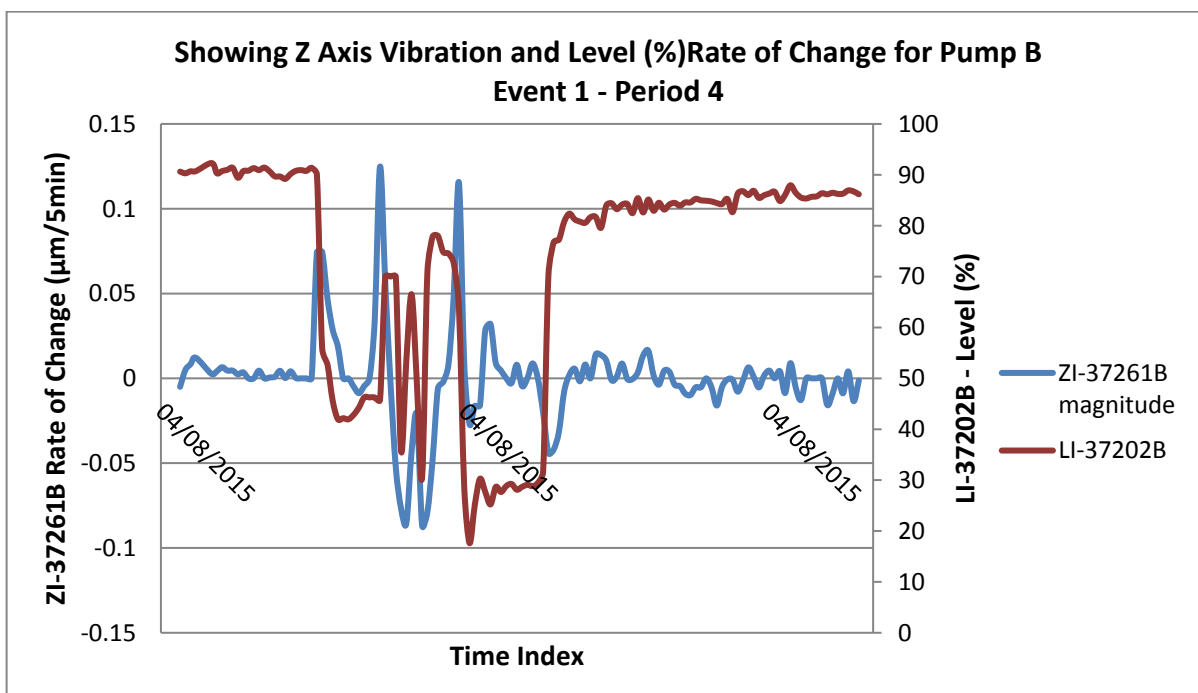


Figure 5-13: Buffer tank level through event 1

The correlation between torque (JI-37219B) and flow rate (FI-37216B) is shown in (Figure 5-14).

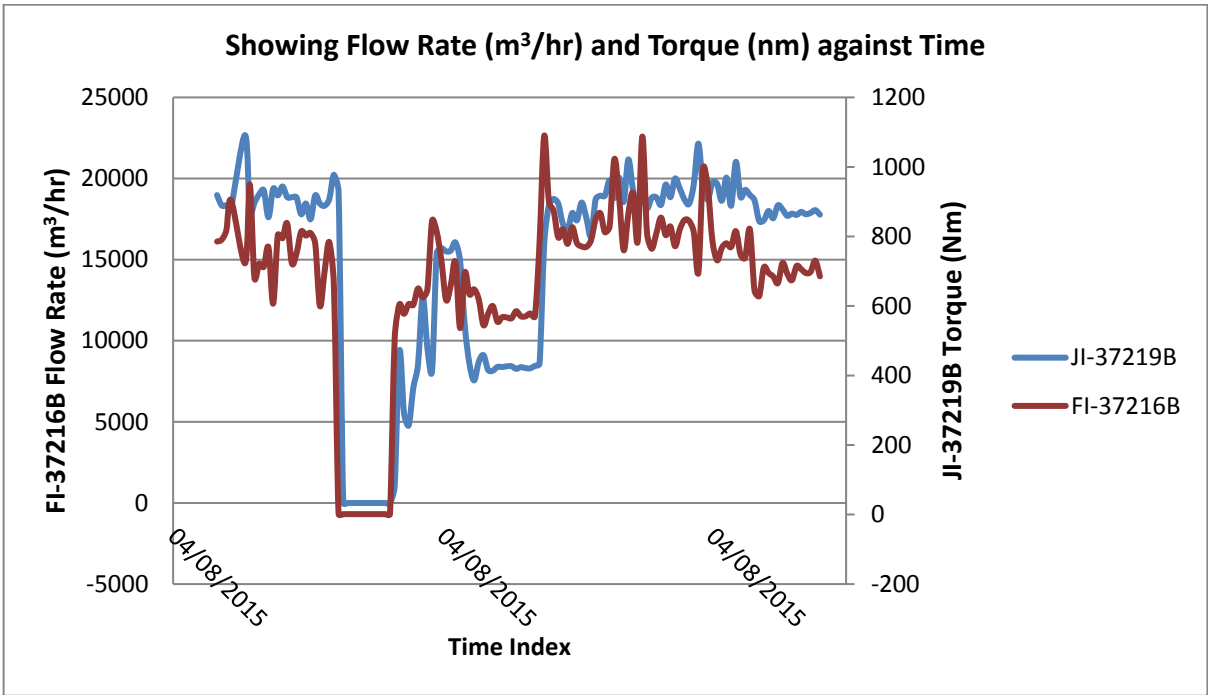


Figure 5-14: Flow and Torque through event 1

As can be seen from Figure 5-14 there is an obvious shutdown in this period where both the flowrate and torque values reach a 'zero' there is then subsequent period which is distinctly noisy where the pump is once again started.

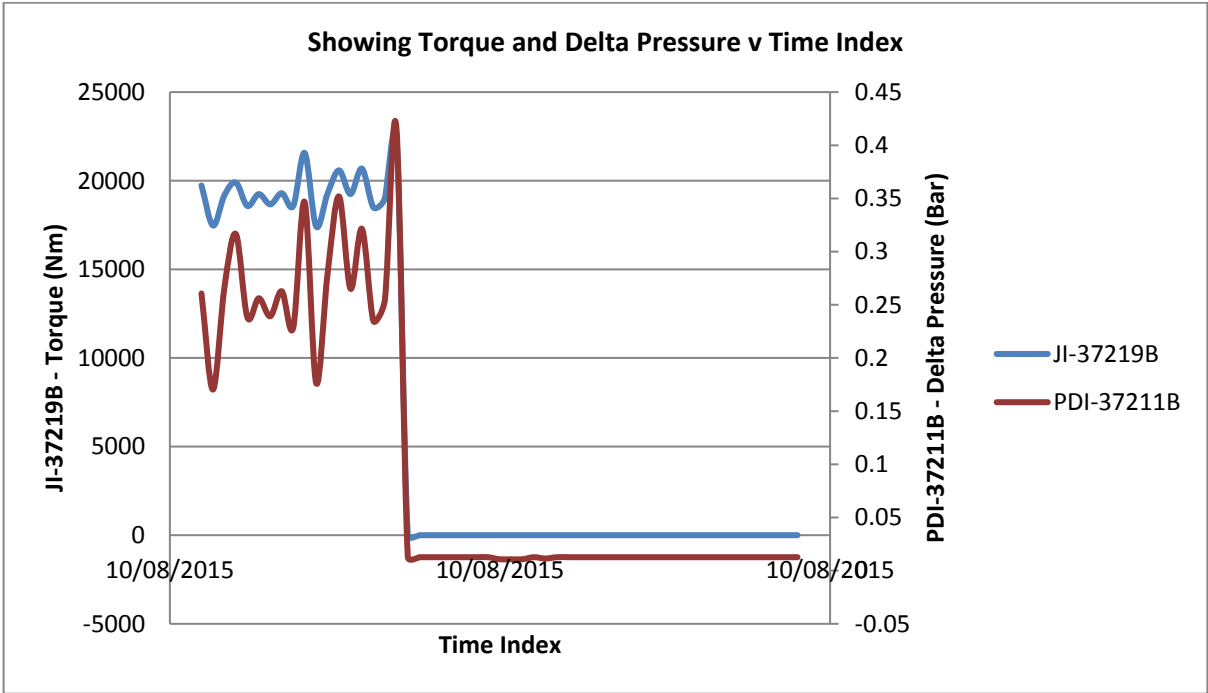


Figure 5-15: Pump B event 2 period 4 Torque and DP over the venturi

Similar results are observed when examining event 2. The other interesting correlation is that torque does follow differential pressure (PDI-3721B) as shown in Figure 5-15 and this linearity is even more apparent if they are plotted on a scatter graph Figure 5-16.

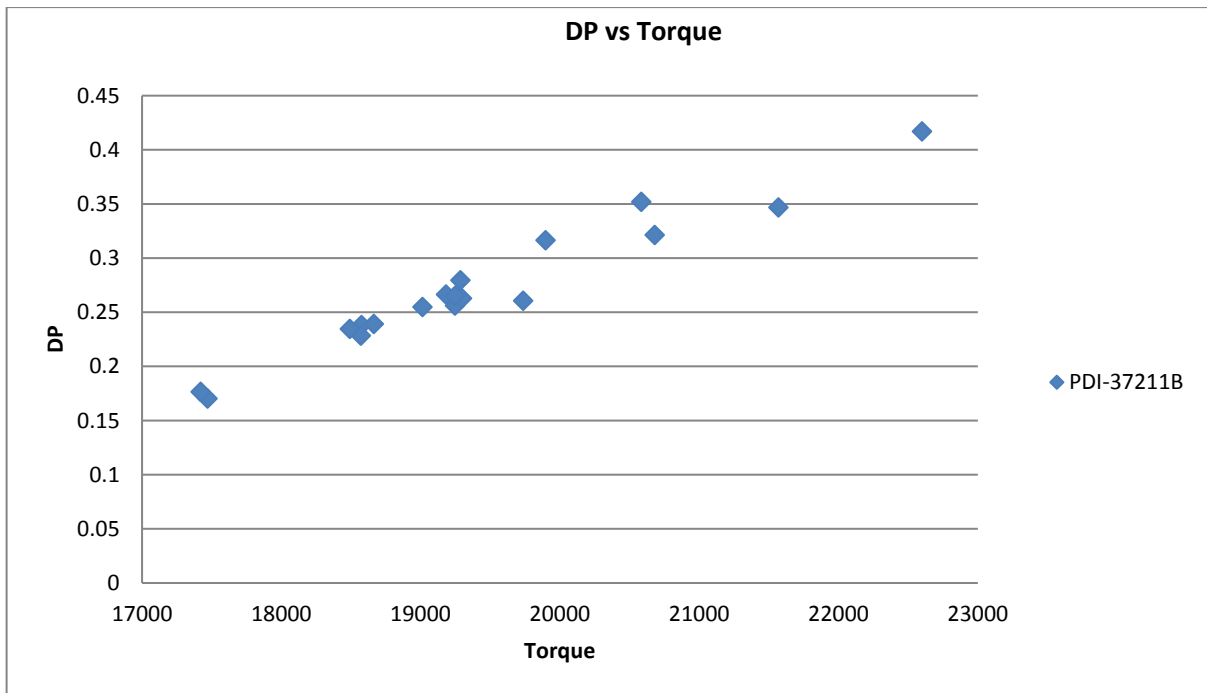


Figure 5-16: Venturi DP vs Torque

At this stage it is not possible to hypothesize on what caused the failure of pump B due to the lack of resolution in the data, to allow further analysis data with higher resolution has been requested. It has also been requested that a member of the Intertek team is given access to the PI server to allow the speedy recovery of data.

5.2 General Observations and Future analysis

Through working with this data set a number of things came to light which could also give an indication of how the pump is operating.

5.2.1 Axial Displacement

Throughout this analysis Axial displacement has been the focus, the hypothesis being that a sudden change in axial displacement is the mode of seal failure, indeed it has been demonstrated during times of seal failure there is a corresponding sudden change in axial displacement.

However building on this it may actually be possible to determine what gas/liquid ratio is flowing through the pump during certain time periods. An off state can clearly be seen when the axial displacement goes to zero, and a normal operating zone can also be seen when axial

displacement is around 0.2mm. At the time of the suspected slug displacement goes above 0.2mm and when it is suspected that fluids are leaner the displacement is lower, with more information it may be possible to categorize the operation into zones.

5.2.2 *Lean fluid periods*

Another area of interest for future analysis would be periods where the fluids are leaner and lower in liquid. According to the customer they are working on a mostly gas service when they had originally designed the pump to work on more of a 60/40 split gas/liquid.

It is believed that a drop in liquid content of the incoming fluids could result in a drop in liquid level in the buffer tank, a reduction in torque and drop in volumetric flowrate, however, all three of these things can also categorize simply low flow, therefore more information will be required, section 5.2.3 discusses other ways of determining density, this would give a much better understanding of low flow versus lean flow.

5.2.3 *Density*

The biggest challenge faced in this analysis has been the lack of information on the density of the fluid. Using other measurements it will be possible to understand mass flow. The inlet temperature to the pump is a very constant figure around about 33°C, there are however a number of occasions however when it goes lower than 33°C.

As discussed earlier if a constant cooling load is assumed these points of low temperature can be categorized as low flow periods, whether that low flow is due to change in density or just a reduction in flow needs to be further analysed with more data, well online or offline information would aid greatly in this.

5.2.4 *Torque and pump power*

Finally, the torque of the pump is one of the best measurements of what is flowing through the pump. For example. if it is flowing a lot of mass it will have to work a lot harder to achieve the same pressure increase, using a combination of sensors with torque again an estimation of what the fluids are made up of can be made.

5.3 Multivariate Data Analysis

In other sections of this report variables were investigated singly and in combination by plotting and manually observing coinciding trends and events. By applying statistical tests relationships can more rapidly be identified between the variables and groups of variables, search for similar events, and quantify the significance of those events.

Human intuition often produces false positives, and comparing observations against a significantly large dataset can inform us if they are true, false, or somewhere in between. Going forward the results of these tests can lead to diagnostics and software solutions based on engineering knowledge.

5.3.1 *Data Cleansing*

In order to perform multivariate analysis the dataset has to be prepared to ensure that the values are both complete and comparable. The following steps were performed before proceeding with the analysis.

- a) The dataset was time aligned.
- b) A joint dataset of all the periods was constructed for use in certain analysis.
- c) All non-numeric and empty values in the data received was converted to nulls
- d) Empty variables were removed
- e) All samples containing a variable with one or more null value were removed.
- f) A scaled dataset was created (referred to as ‘scaled data’).
- g) Variables with constant values were removed.

5.3.2 *Investigation of Variables*

After this the first step in the analysis workflow was to study the sensor variables in isolation, comparing variables with themselves at different times, rather than to other variables or as part of a multivariate group. These steps are undertaken first so that data with outliers or data that doesn’t change can be excluded from later analysis. If this stage revealed that all sensors of one type produced the same results, they could safely be removed from analysis, or combined as an average so as not to provide any significant bias to the dataset.

5.3.3 *Interpolation during Data Export*

Before covering the results themselves it is important to mention a feature of the received dataset that may have significant impact on the analysis. The five periods received were

produced using PI queries with a start time, an end time, and a set length of interval. However OSIsoft PI historian will not necessarily be logging values at exactly that time. Indeed, depending on how the system has been configured it will not be storing data at set intervals at all and instead is logging data only when a change in the sensor above a certain threshold occurs.

Given this the PI historian will interpolate (either directly or via a smoothing function) between the values it does have to produce an estimate for the exact time that has been queried. Therefore it has to be considered that:

- a) Events that happen faster than the interval are lost
- b) Interpolation can produce unrealistic values (i.e. a binary value that can only be 0 or 1 but could be interpolated as 0.6 if the time when it changes isn't aligned with the query interval)
- c) Interpolation can distort the true distribution of the variables values (a distribution may be observed when the variable is in fact only shifting between two values).

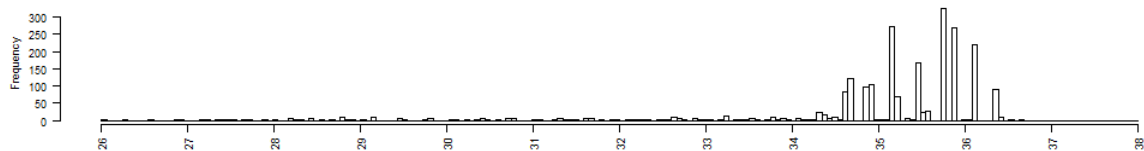


Figure 5-17: Example of Interpolation histogram

In the example above interpolation can be seen in a histogram of the values for a sensor during period 5. The actual sensor reading will be a certain value as seen by the peaks at the fraction of interval values, but there are additional values between these peaks. Where these come from can be shown by focusing on a particular section of the sensor log (Figure 5-18).

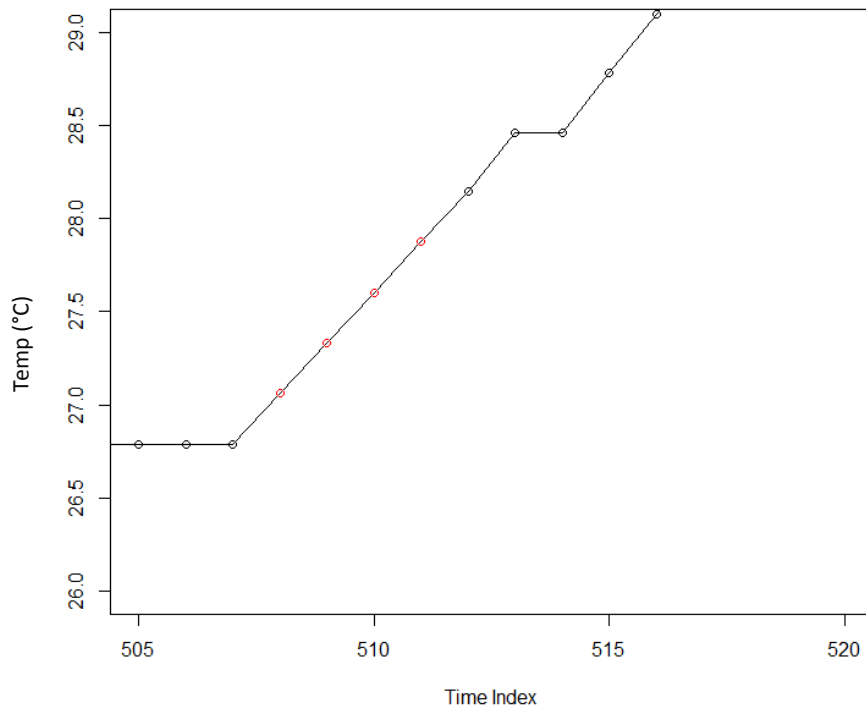


Figure 5-18: Close examination of interpolation

The actual values the historian has recorded internally would be 26.8°C at time index 506 and 28.2°C at time index 511. However it was queried at four intervals between these records and thus interpolated a temperature estimate (red dots). The difference between each of the points in the period is the same which would not be expected of noisy physical phenomena. Although unavoidable this phenomenon must be given consideration when drawing conclusions from the data.

5.3.4 Variable Statistics

Before comparing variables, summary statistics were generated for each sensor's values for both observing anomalies and constructing further statistics. The summary statistics were:

- Mean and standard deviation of the variables
- Kurtosis – this measures the ‘tailedness’ of the distribution, if there more or less values than expected outside the primary normal distribution of the data. Taken with skew this gives a guide to if the data can be treated as a normal distribution.
- Skewedness – is the measure of the asymmetry of the distribution, if it spikes above its normal values or spikes below it. It is related to kurtosis but includes direction as well magnitude. Both skewedness and kurtosis have trouble with trending data, when the mean of the variable changes over time skew will be overestimated if the mean is assumed constant.

From the summary statistics the useful observations are:

- a) The values for sensors of motor RPM and torque on both pumps have zero standard deviation and do not change within the dataset. They are therefore not useful for statistical analysis and have been discarded
- b) Period 3 is only for 1 hour and as a consequence many variables do not change over its time. This suggests period 3 is less useful for statistical analysis.
- c) Periods 1 and 5 had the most skewedness results for pump A, this implies either that in these periods the pump was more unstable or saw a significant shift in operation. Period 4 is similar for pump B. Although the events causing these are known (A shuts down in period 5, B in period 4, and A is turned down in period 1) it is useful to see how high level summary statistics can quickly categorise and compare the data.
- d) Period 4 has the lowest kurtosis, suggesting the values for the sensors are the closest to a normal distribution during this period, with fewer large outliers or data trending.

5.3.5 *Variable Histograms*

Following from summary statistics, particularly after observing the high skew value of some variables, distributions can then be directly visualised. Producing histograms of the frequency of the values for the variables in each period will provide a way to spot interpolation, outlier events, and the overall differences between the periods.

For example in the histogram of a temperature sensor from pump B (Figure 5-19) it can be seen that periods 1 and 4 are broadly comparable with one or more outliers of lower temperature in period 4. It can also be seen that period 5 is substantially different, and periods 2 and 3 are both small samples of the larger distribution seen in period 1 & 4.

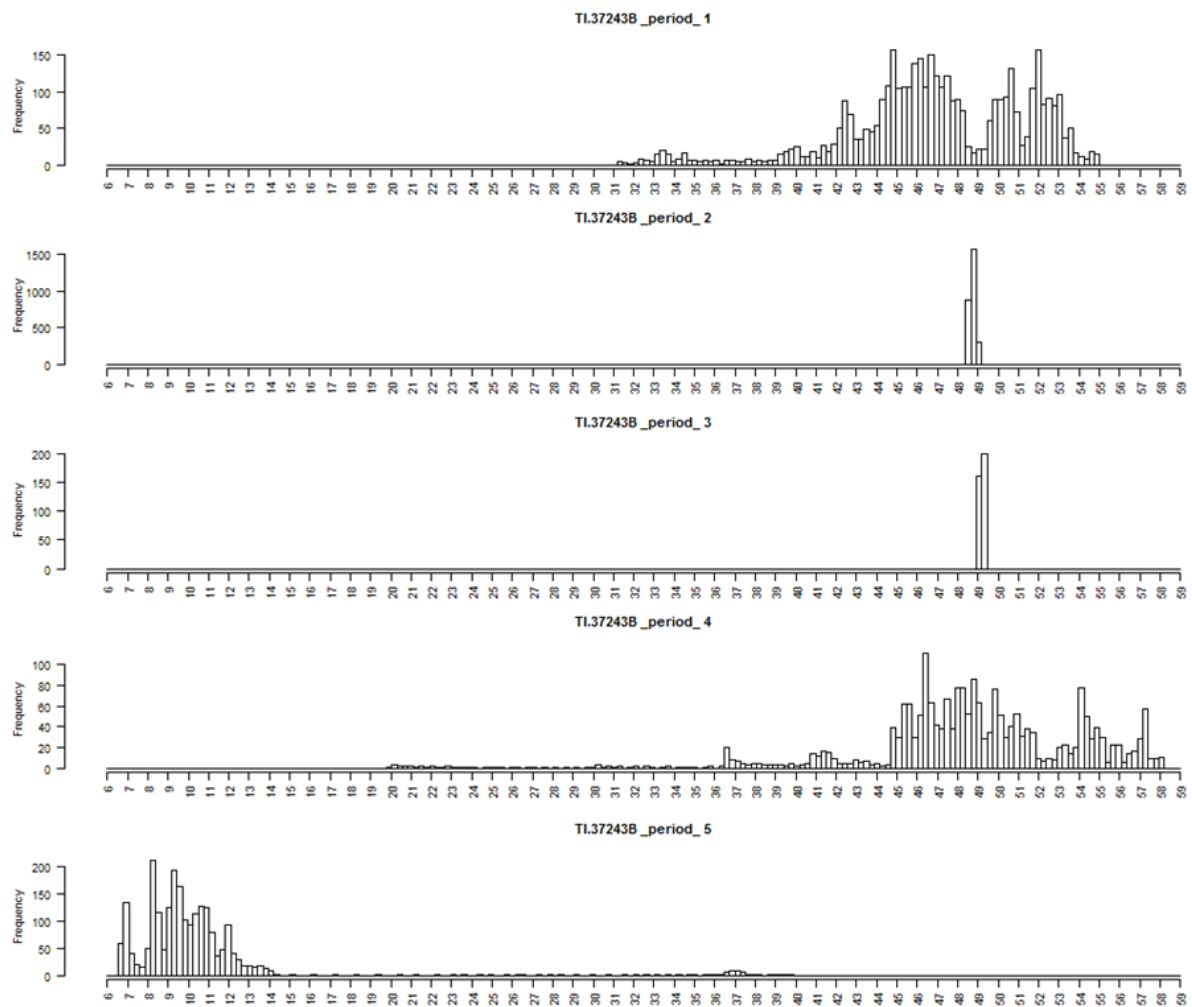


Figure 5-19: Example frequency histogram

A summary of the observations of the distributions is shown in Table 5-1. The majority of the variables appeared to be normally distributed in at least some of the periods provided, or normally distributed with long outlying tails. This implies that the variables are recording a ‘standard’ operation in at least some of these periods, and that divergences from normal operation may be of statistical significance.

Table 5-1: Summary of histogram observations

Observed in Histogram	Normal Distribution	Normal distribution with Long tails	Appearance of Interpolated Data
Number of Occurrences	19	53	12

5.3.6 Variable Autocorrelation

The summary statistics and examination of the histograms indicates there are excursions from the distribution of the variables (the long tailed distributions and the high skew values). It is possible these excursions or other features of the data may be periodic in nature (shift or daily

changes, or shorter time cycles emerging from feedback by control systems). To test for underlying patterns an autocorrelation algorithm was therefore applied to each of the variables.

Autocorrelation is the comparison of a variable with itself at different points in time; the similarity between measurements a set time-lag apart. The null hypothesis of no autocorrelation would see 100% correlation with no time lag that smoothly decreases to the noise threshold, whilst a cycle with a frequency of one day would see a correlation peak at the 1-day interval. In the example in Figure 5-20 it is demonstrated how a shutdown every 24 hours would appear in the autocorrelation graph – as a peak above the significance threshold.

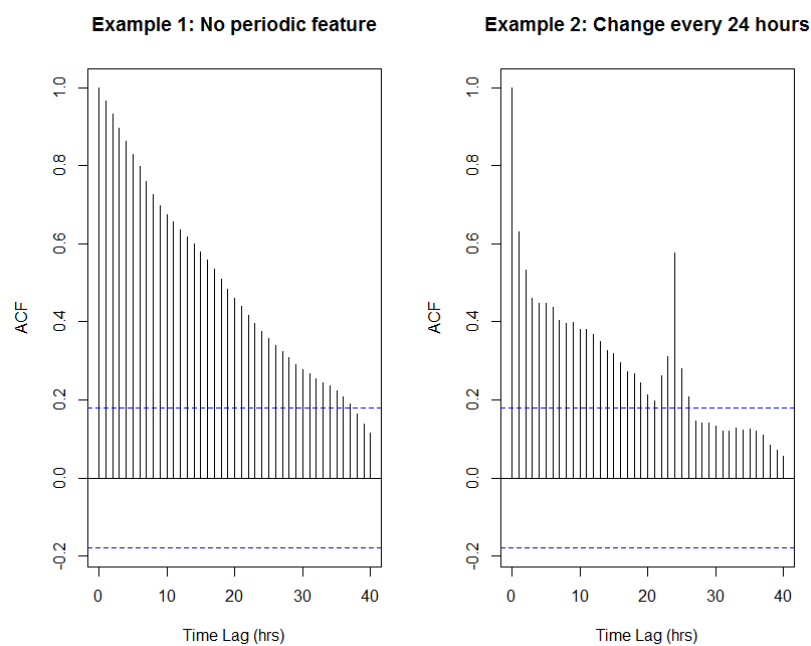


Figure 5-20: Example Autocorrelation plot

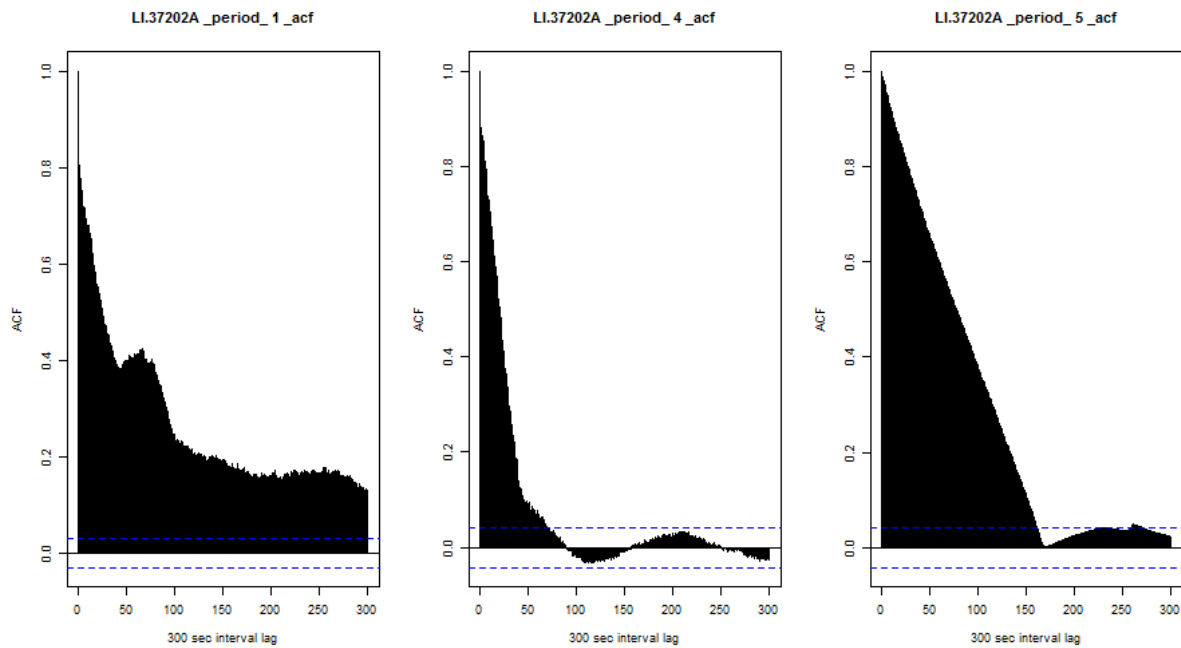


Figure 5-21: Autocorrelation plot for buffer tank percentage in pump A

An autocorrelation graph was produced for each variable. Due to covering only a small amount of time and containing little variation, periods 2 and 3 were excluded from the analysis as they only covered a very short (1 hour) time period. In the example in Figure 5-21 showing a level sensor it can be seen that even though there is not an obvious strong periodicity it can still be seen that periods 4 and 5 feature significant shifts in the value recorded by the sensor as correlation between times falls off rapidly. In comparison period 1 is more stable with a possible slight periodic event early on.

Other features can be observed with autocorrelation: as shown in Figure 5-22. The temperature of the inlet pipe during period 4 has periodicity in the 8 to 16 hour window – with warm days in august the morning and afternoon will be similar temperatures 8 hours apart whilst being dissimilar to noon and night-time temperatures. Axial vibration during period 1 shows a reversion to 0 correlation as time interval increases but changes to negative correlation, indicating this sensor is recording a general in movement over this period.

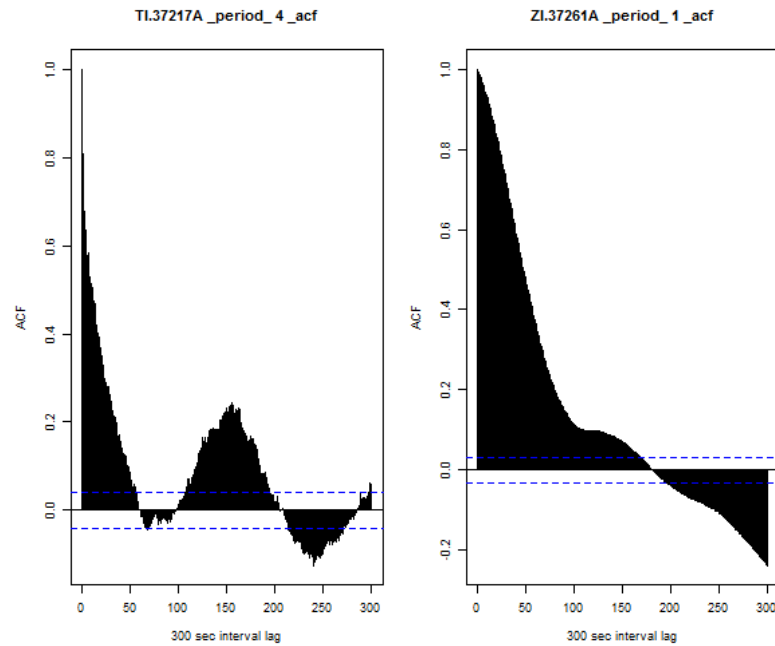


Figure 5-22: Inlet Temperature (left) and axial vibration (right)

It was noted that other sensors also demonstrated some periodic correlation including additional temperature sensors showing periodic variation in line with ambient temperature flow sensors of a pump exhibiting autocorrelation with its partner suggesting interaction when the two pumps are flowing.

5.3.7 *Comparison of Variables*

The second step in the analysis workflow was to compare the sensor variables with each other (a 'pairwise' comparison). With the less statistically interesting variables excluded by the first stage and a greater understanding of the ranges and periods, pairwise comparison bridges the gap between univariate and multivariate analysis. Sets of variables with high correlation and even collinearity will be examined and combined or removed as appropriate prior to the multivariate analysis, it is also of note that the pairwise comparisons can yield important discoveries on their own.

Correlation is variables co-varying and indicates some kind of dependent relationship between the variables. Correlations are useful for grouping variables and developing predictive relationships to work out the unknown values from known.

Since the previous statistical tests revealed each period is substantially different rather than forming a continuum of values, it was therefore decided that correlation tests should be performed on the periods separately and then the results aggregated.

Pearson's correlation was chosen for this as it is more appropriate for datasets containing interval values. Figure 5-23 shows the Pearson's heatmap which correlates each variable in the study against every other variable. Red is assigned a value of 1 denotes a 100% positive correlation (i.e. variables A and B increase directly proportionally). Blue is assigned a value of -1 denotes a 100% negative correlation (i.e. as variable A increases variable B decreases directly proportionally).

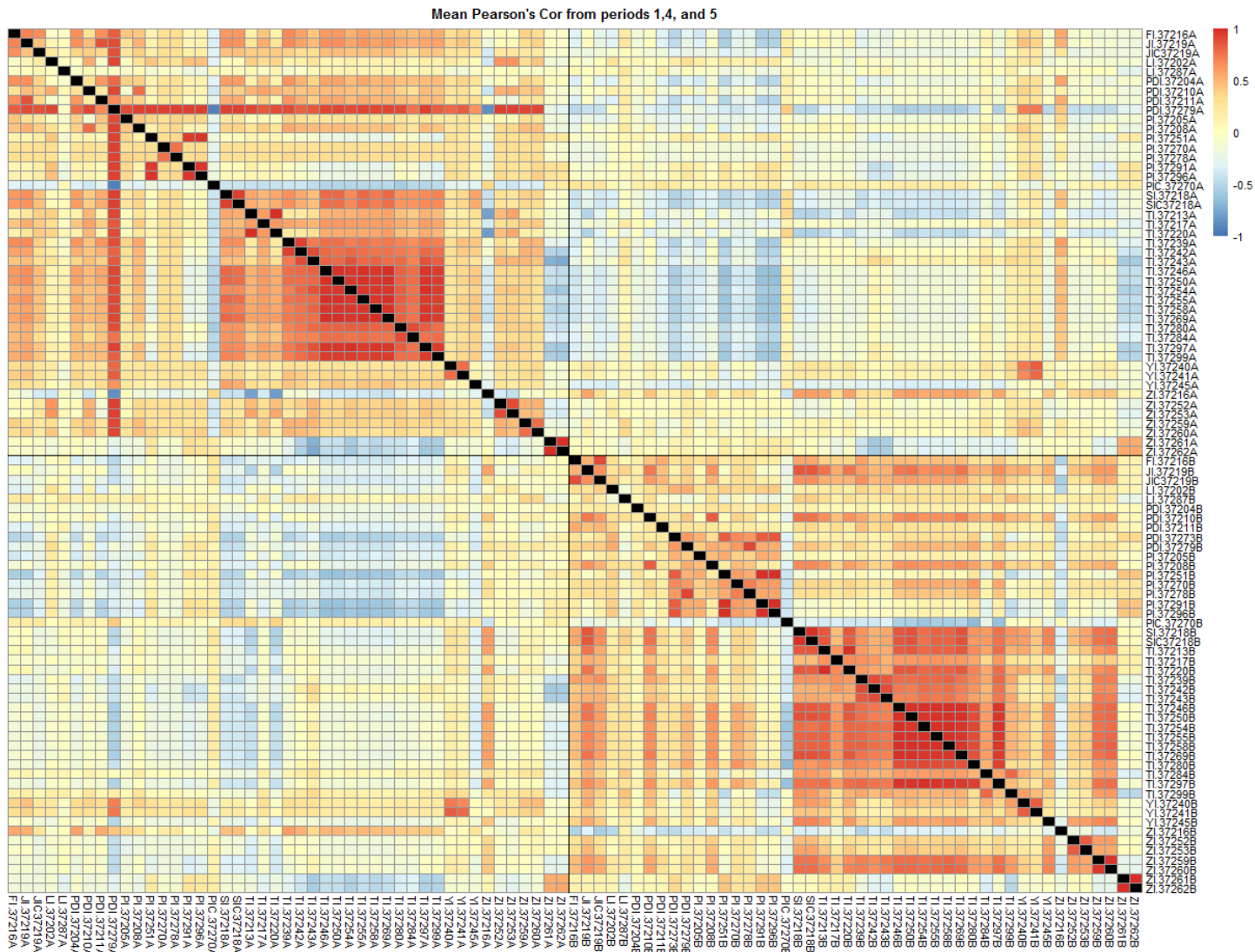


Figure 5-23: heatmap of mean Pearson's correlation coefficient across the longer time periods (1, 4, 5)

From the figure several interesting structures can be observed, with varying degrees of confidence.

- The majority of temperatures sensors form a highly correlated block. Driven and Non-Driven mechanical temperatures, Lube temperatures, Seal oil temperatures, and cooling air temperature – these components are closely connected so heat transfer correlation is to be expected.
- The displacement sensors also form a block, albeit less tightly coupled. These sensors measure displacement of various components on the XYZ axis so their correlation is

understandable. Also, linking this displacement to heat is a sensible assumption as more energy will drive vibration and cause components to expand.

- c) Flow and Torque are correlated with each other and broadly with the temperature sensors.
- d) Several of the pressure sensors are strongly correlated with other pressure sensors in both pumps, for example lube oil pressure with the pressure of the lube oil pump and lube oil seal are all correlated.
- e) The Seal Oil pressure appears to have negative correlation with nearly all the other variables within the same pump. This is an interesting relationship as it seems unclear why the seal oil pressure should vary against all the other values.
- f) The controller for Seal Oil Pressure appears to have strong positive correlation with nearly all the other variables within the same pump, but only in pump A. This behaviour not being as noticeable in both pumps is interesting and indicates the correlation is due to outliers.
- g) When comparing between pumps, the sensors for non driven end have positive correlation. This may be due to vibration within the structure of the platform affecting both pumps at the same time.
- h) When comparing between pumps there is a general negative correlation between the pressures and flows of one pump and the other. This is likely due to two of the periods provided having one pump shut down whilst the other is turned on.

Correlations within the pump and between the pumps were investigated even though they are operated independently there may still be feedback or other interaction between the pumps via the surrounding infrastructure or human operators.

5.3.8 *Partial least squares regression*

The crucial choice in a PLS investigation is what to use as the objective measurement; in other investigations measures such as production volumes, profit, or composition have been used.

In this study the client emphasised stability as one measure (without an overt quantification) and seal wearing on the Non-Driven End of the shaft. If stability was to be measured by frequency of failure events, there aren't a sufficient number of samples to attempt to fit a PLS model. One possible proxy for wear on the seals is when the shaft is closer to the end of the pump – the Z-axis displacement, so a PLS analysis was performed on how the value of Z-axis displacement varied against all the other non-temperature sensors, with results shown in Figure 5-24.

For pump A in the Z-axis displacement the first two components explain 24% of the variance in the axial displacement; this is a weak relationship and suggests high variability in the dataset. The second component features the on/off state of the data, whilst the first component is composed of the other displacement measures, the pump speed (and pump speed controller),

the flow measurement, and the gearbox accelerometer. If it is assumed the other displacements are co-varying with the Z-axis rather than driving it the it can be theorised that the axis is moving as the motor works harder.

For pump B in the Z-axis displacement the first two components explain 52% of the variance in the axial displacement; this is stronger than for pump A and indicates that the variability is more homogenous and thus more was explained. As with A the second component features the on/off state of the data, whilst the first component is composed of the other displacement measures, the pump speed (and pump speed controller), and the gearbox accelerometer. If it is assumed the other displacements are co-varying with the Z-axis rather than driving it can be theorised that the axis is moving as the motor works harder.



Figure 5-24: PLS Loadings for each pump's non-temperature sensors against the pump's Z-axis displacement as an objective function.

5.4 Part 3 – Dimensionality Reduction by Principal Component Analysis

Having considered variables by themselves and in relation to other variables, the analysis can proceed to considering large groups of variables at once in a multivariate analysis. Therefore the key technique in this multivariate analysis is dimensionality reduction via finding principal components for the dataset.

As discussed earlier the current understanding of the dataset supports performing analysis on the Pumps separately and both with and without temperature data. Also due to their greater

variability and similar time intervals the analysis will only use data from the longer periods (1, 4, and 5).

5.4.1 *Pump A PCA*

Figure 5-25, Figure 5-26 and Figure 5-27 summarise the PCA analysis of pump A. From the cumulative variance it can be seen that the first three components explain over 80% of the variance and the subsequent components explain increasingly less, imply the first three are good ‘aggregates’ of sensors and as a consequence the first three were retained and the remaining discarded from analysis,

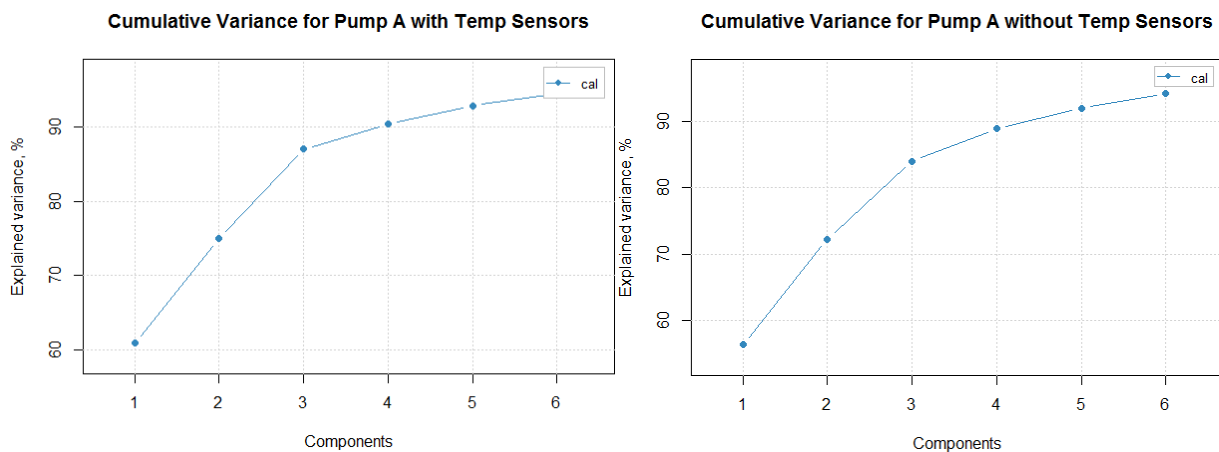


Figure 5-25: Variance explained by the Principal Components fitted to the dataset.

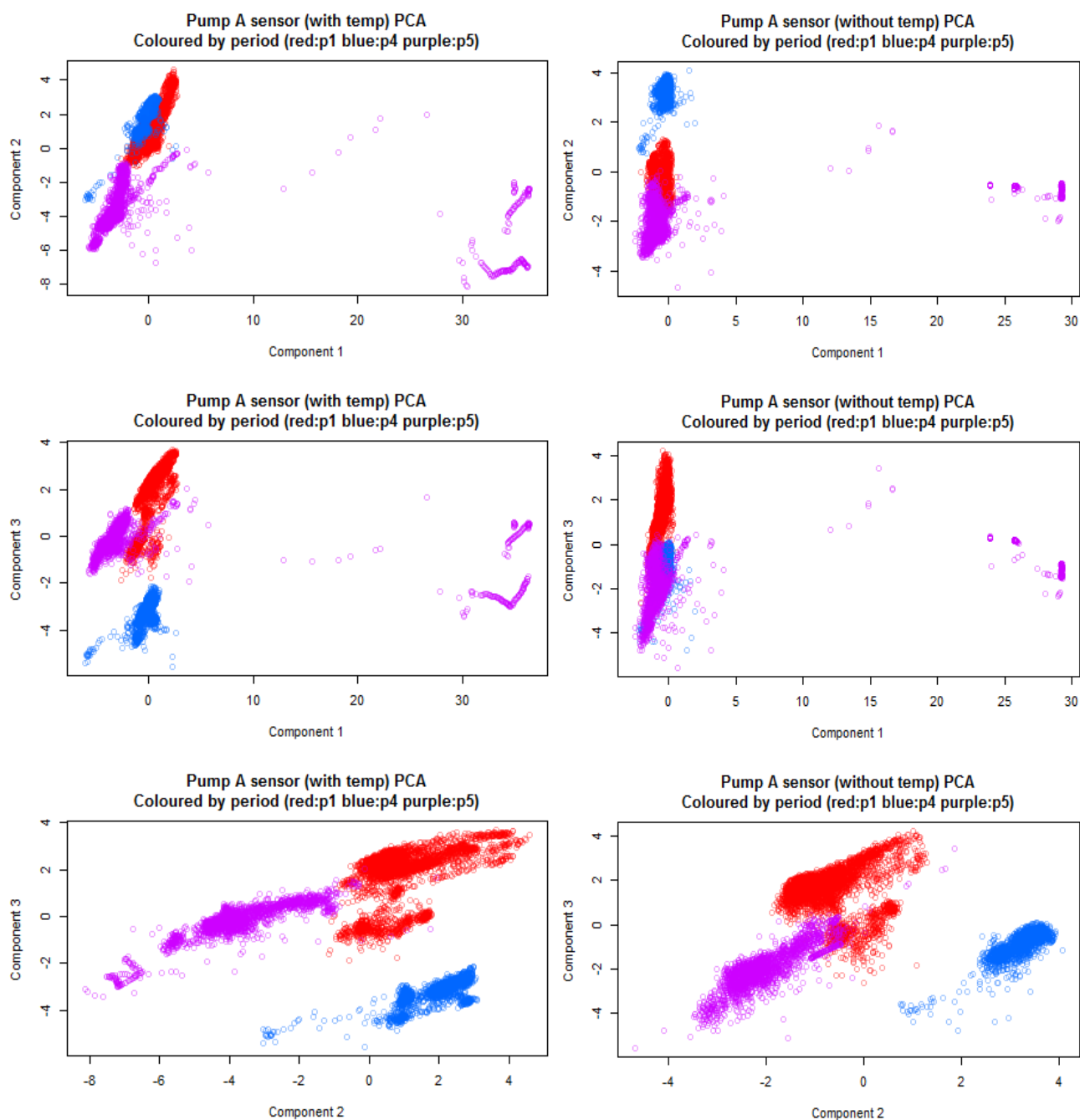


Figure 5-26: Plotting the individual time points by their position each principle component, coloured by the period of origin.

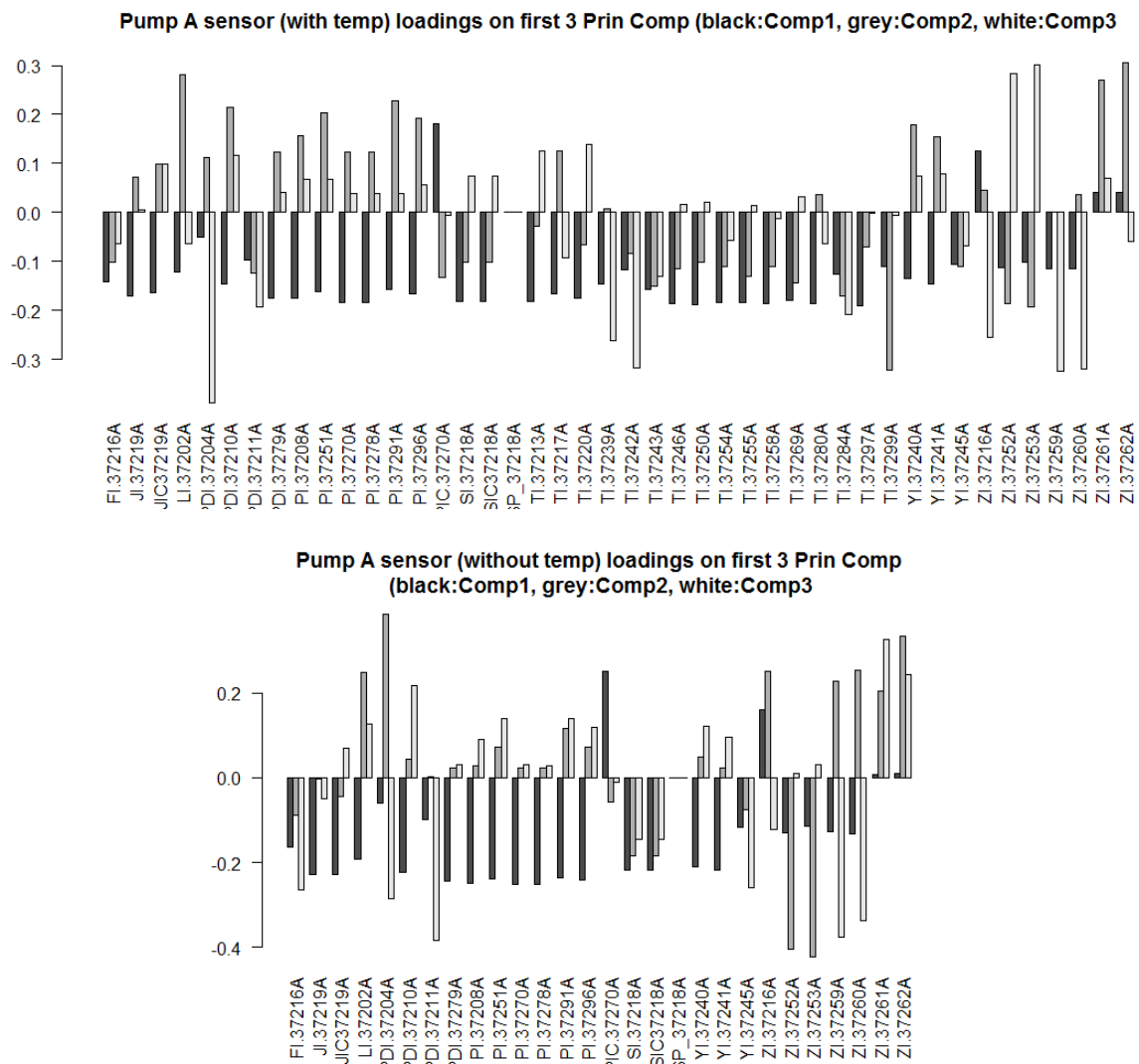


Figure 5-27: Bar plots of how each sensor value contributes to the first 3 principal components in the PCAs with (above) and without (below) temperature sensors.

It is clear to see that the first principal component is driven by the Pump being active or inactive; in normal operations there is not much change in component 1 until the end of period 5 when the pump is shut off and moves across component 1 to its off state. This is confirmed by the loadings – comp1 is driven by the negative of nearly all variables except for Seal Oil pressure and recycle percentage. When recycle and seal oil pressure go up and all other variables go down, comp1 increases.

The second principal component is driven positively by buffer tank pressure/percentage and Non-Driven End axial displacement, and negatively by Driven end displacement. It is an aggregate quality of the displacement and buffer pressures, and perhaps indicates how the shaft is sitting in the Pump. The periods overlap in terms of component 2 (though inclusion of

temperature separates the generally warmer period 4 out), though it is interesting that period 5 is nearest the off state.

The third principal component also emerges from Non-Driven End displacement, but in combination with Venturi Pressure differential and discharge flow rather than the buffer tanks. Although the other components explain more variance, it is possibly component 3 that is most interesting in terms of best operation during normal circumstances. Again the periods overlap in terms of component 3, suggesting a ‘normal’ operational envelope.

In the aggregate plot of component 2 against component 3 it can be seen that the various structures of the periods operation – period 1 begins at higher flow (similar to period 5) before being moved to a lower flow rate making its values move positive in terms of component 3. The period 4 cloud has a clear separation between most of the period and the end (when pump B turns off and more stress is put on pump A), and that ending sees a decrease in component 3. It is possible that component 3 can be taken as a measure of the ‘stress’ the pump is undergoing.

Taking these components, the path of the pumps variables through the component space over the course of the periods was investigated. Period 5 data points projected against components 1 and 3 are shown in Figure 5-28, coloured by time. It can be clearly seen that the Pumps state moves through the ‘normal’ region over time, with numerous excursions at different points over the seven days, before eventually moving away from the normal region of components 1 and 3 when it reaches the shutdown period in the last half a day. This may provide useful diagnostic tools if the excursions from the normal can be tied to particular events, and if further data reveals whether or not that their frequency and structure precedes other shutdowns.

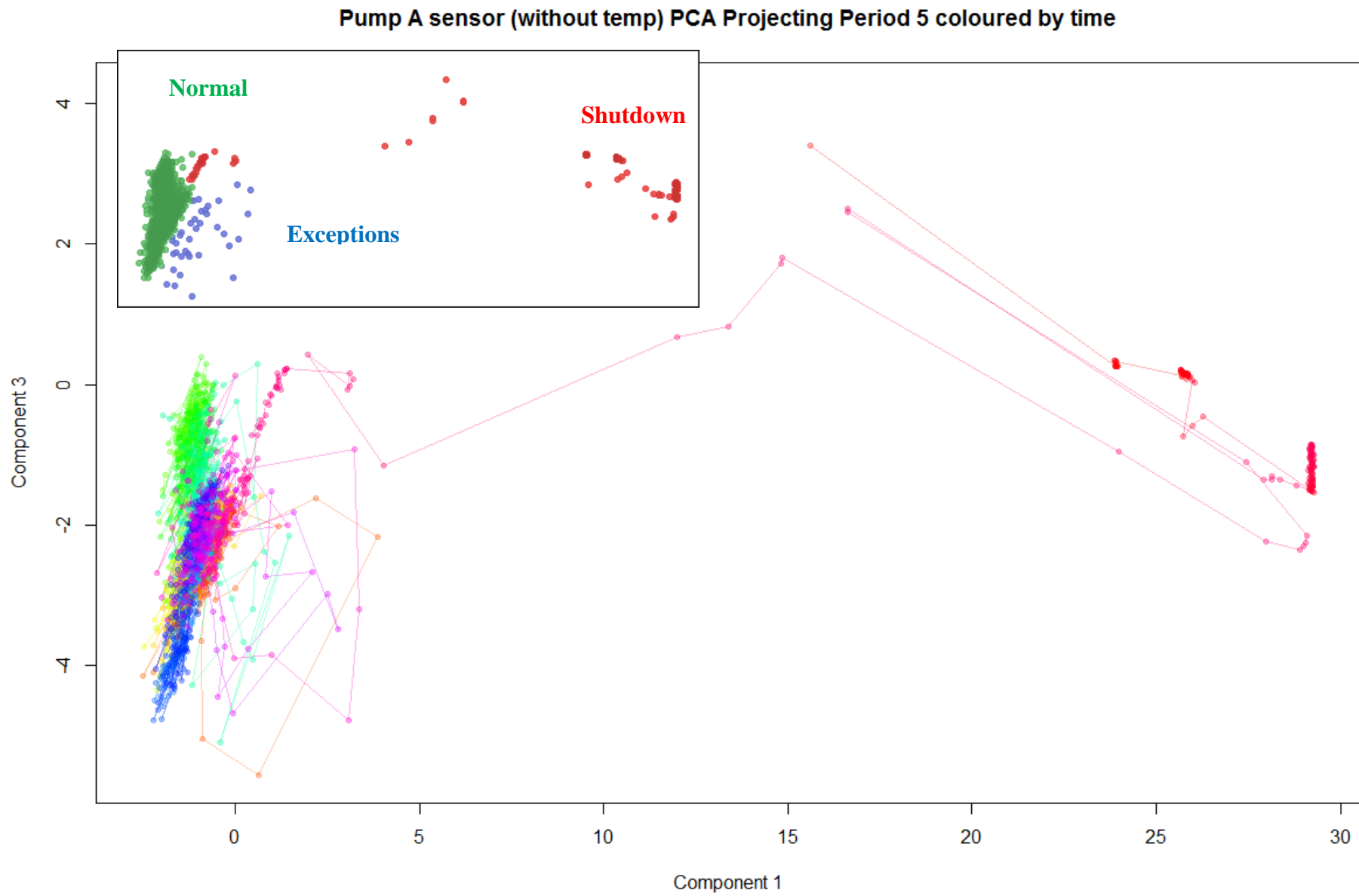


Figure 5-28: Operating Regions PCA

5.4.2 Pump B PCA

Figure 5-29, Figure 5-30 and Figure 5-31 summarise the PCA analysis of pump B. Due to period 5 being very different for Pump B than the other periods a PCA was performed including all periods and another including only periods 1 and 4 to observe the magnitude of effect of period 5. Although (as with pump A) analysis was also performed both with and without the temperature sensors, the plots including temperatures are not shown here because, much like the analysis Pump A, the inclusion of temperature data did not significantly change the loadings of the principal components.

The cumulative variance explained by each successive principal component is shown in Figure 5-29. It can be seen that the with all the data the first three components explain over 80% of the variance (Figure 5-29a), or just under 80% of the variance (Figure 5-29b) when period 5 is removed, and the subsequent components explain increasingly less as a consequence the first three have been retained.

The fact that omitting period 5 decreased the explanatory power of the first component was very interesting, implying that the brief shutdown of the pump at the end of period 4 didn't contain enough data to properly characterise an on/off spectrum.

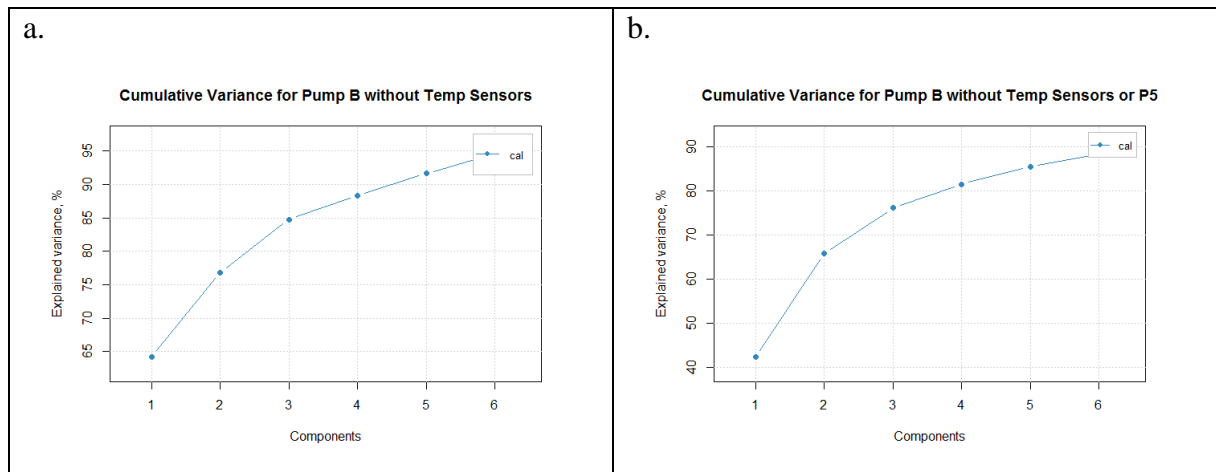


Figure 5-29: Variance explained by the Principal Components fitted to the dataset with temperature sensors (a) and without temperature sensors and period 5 (b)

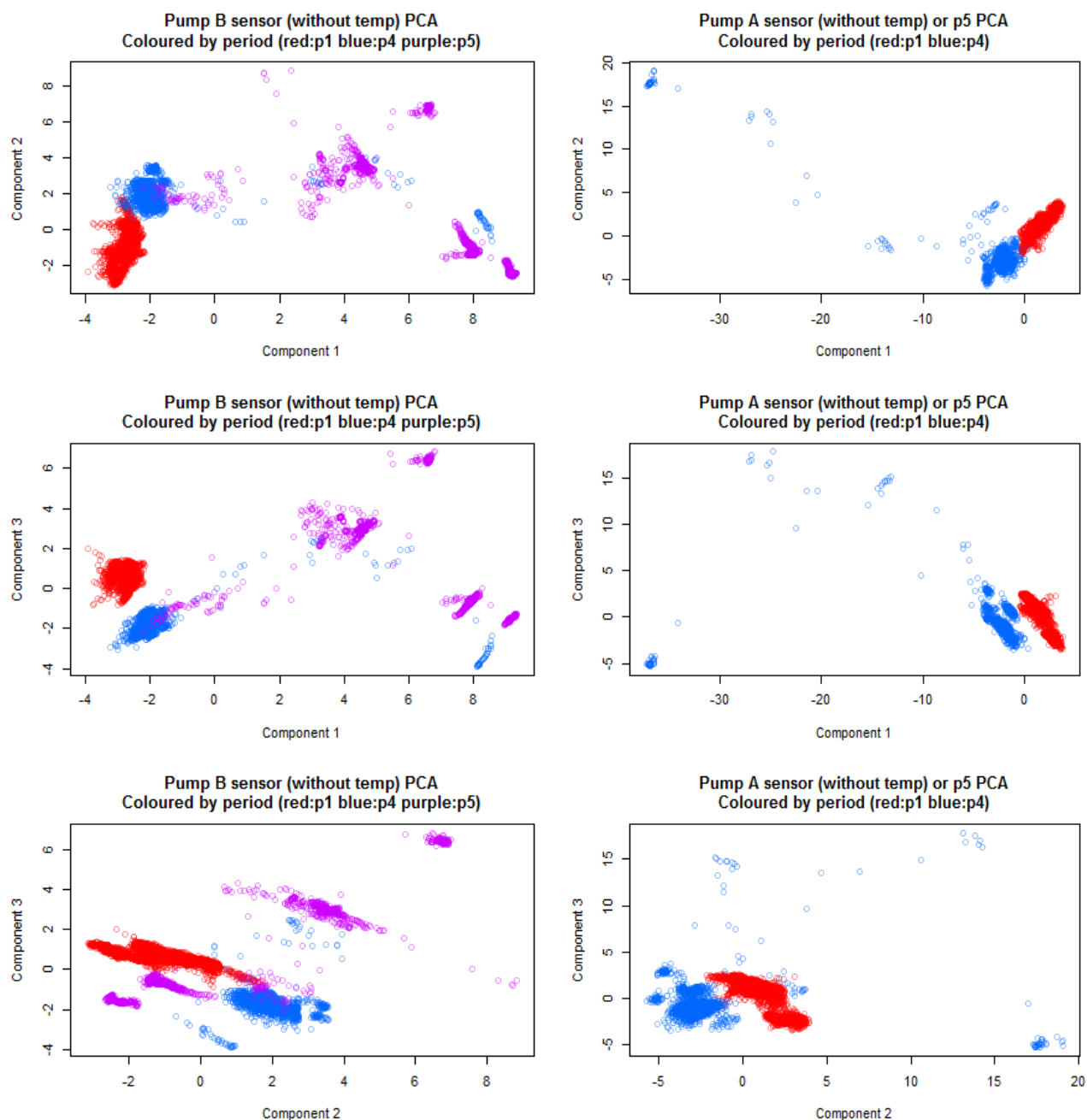


Figure 5-30: Plotting the individual time points by their position each principle component, coloured by the period of origin.

The shutdown in period 4 and the activation in period 5 can clearly be observed affecting component 1 in both analyses. Omission of period 5 does not appear to significantly improve the discriminatory power of the components, and indeed overly weights the shutdown in period 4 on all three components rather than concentrating its loading on component 1. This demonstrates how more data can strengthen PCA analysis.

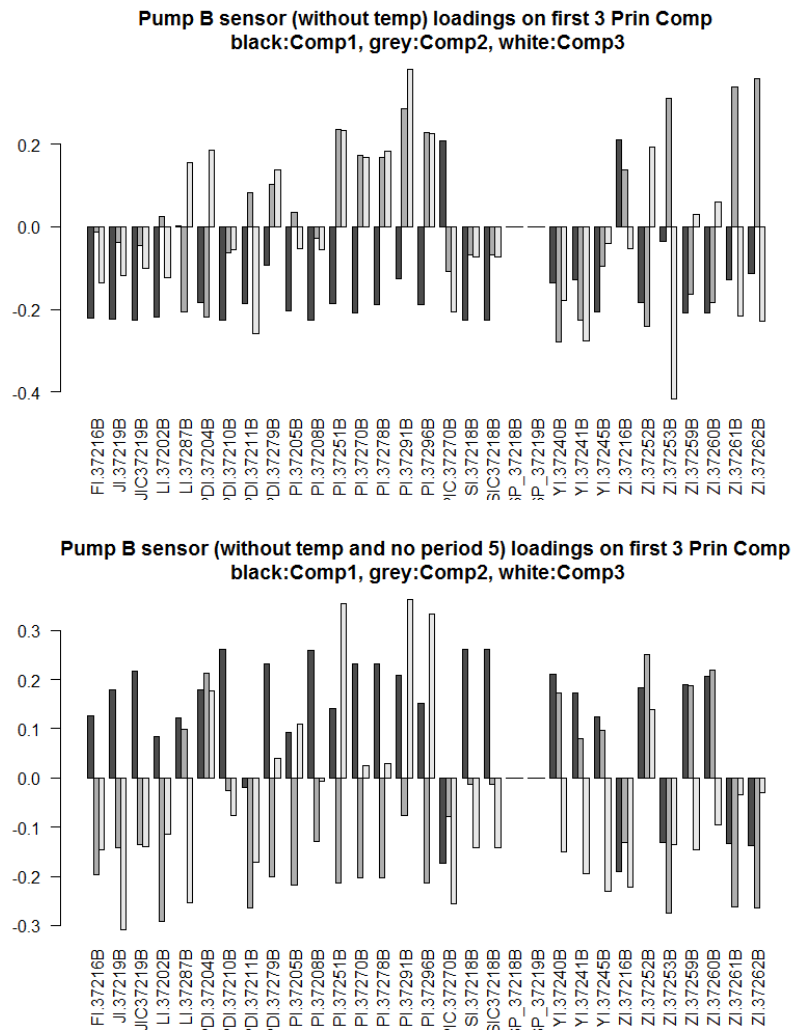


Figure 5-31: Bar plots of how each sensor value contributes to the first 3 principal components in the PCAs where period 5 is included and excluded.

When period 5 is included the first component is much more similar to the first component of the PCA on Pump A than when it is excluded.

It is clear to see that the first principal component of the analysis that included period 5 is driven by the Pump being active or inactive, much like the first component of the PCA for Pump A.

When period 5 is removed from the analysis, several displacement measures join these two variables in loading component 1 – possibly the ‘off’ time at the end of period 4 has this displacement and it is being incorrectly loaded in with the recycle and seal oil. Due to this observation it was decided to continue the process by only looking at the analysis that includes period 5, as it can better be compared with the analysis of pump A.

The second principal component is loaded positively by Non-Driven End axial displacement, Seal Oil pump pressure, Lube Oil pump pressure, and negatively by Seal Oil tank percentage.

This is both overlapping and different to the sensors that load the second component for pump A. It is possible that more data will uncover which are correctly connected to the Non-Driven End axial displacement, though both indicate how the shaft is sitting in the pump.

The third component is also driven by Non-Driven End axial displacement, but instead combined negatively with the driven end motion detectors positively with Lube Oil Pump Pressure, Seal Oil Tank Pressure, and Buffer Tank pressure. This makes the 3rd principal component for pump B most similar to the second principal component for pump A.

5.4.3 *Linking Univariate with Multivariate*

The final and most important use for the PCA aggregate plots is to highlight the position of identified events within that aggregate space. This is critical to develop a solution for the customer because if operating regions can be identified for normal and abnormal operation this can inform customer decisions.

Two events prior to shutdown were identified in univariate analysis for Pump A in period 5, and these are projected in the aggregate space in Figure 5-32 and Figure 5-33. It is clearly shown how these events leave the normal operational region but not towards the shutdown states.

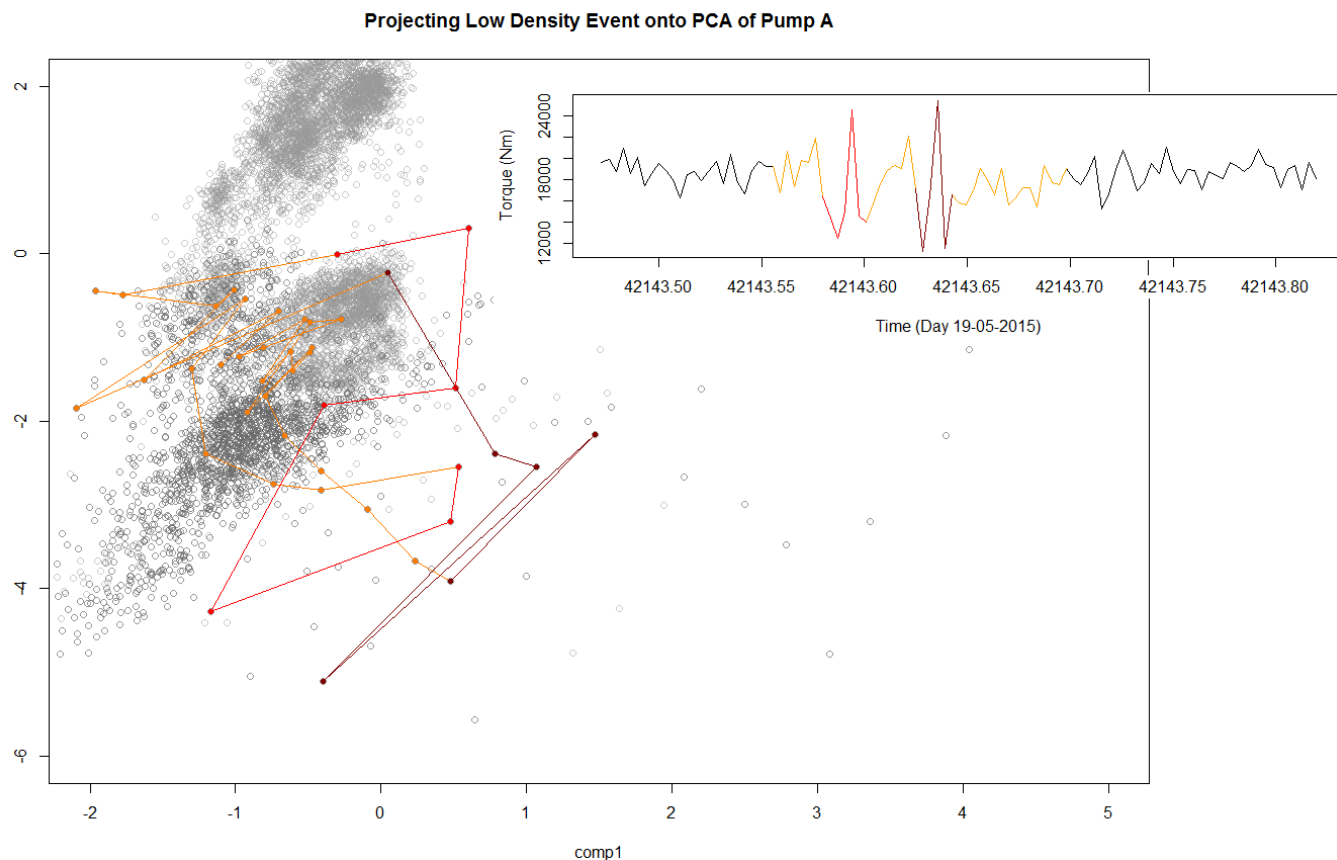


Figure 5-32: Projecting the data values of an event noticed in the technical analysis event 2 in period 5 for Pump A

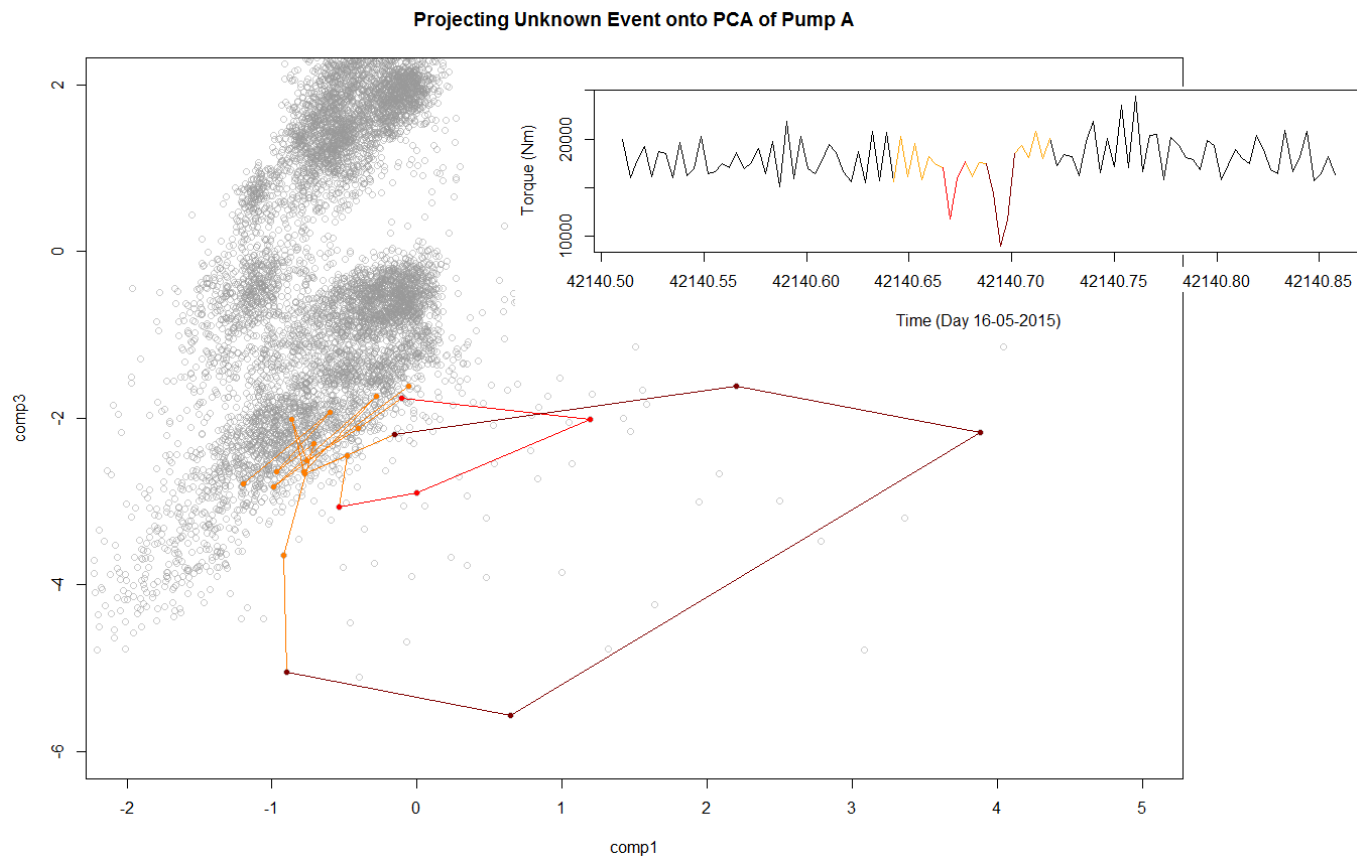


Figure 5-33: Projecting the data values of an event noticed in the technical analysis (event 1 in period 5 for Pump A

5.5 Conclusions

Overall there are number of solid conclusions that can be drawn from the statistical analysis

- a) There are a number of technical issues with the dataset received, both in scope and content.
- b) There are statistically significant relationships between the sensors within and between the two multiphase pumps.
- c) These dependencies can take longer to propagate than the time step of the dataset.
- d) Overall the failure periods for each pump (Pump A – 5 and Pump B -4) prior to failure are statistically different from the non-failure periods of presumed normal operation. (See rate of change and PCA analysis).
- e) Exceptional events occur in the run up to the failure in the failure periods, and do not occur in the periods of presumed normal operation. These exceptional events have similarities with each other but are not identical.
- f) Aggregate plots can be developed to identify regions of normal and abnormal operation which can help provide solutions to customers.
- g) Based on the hypotheses of flow it is suspected that seal failure is caused when high proportions of gas flow through the pump and cause large axial vibration resulting in damage.

5.5.1 *Future directions*

Further work will be dependent on data with both greater scope and types beyond the small number of time periods and sensors provided.

If additional data and resources were available, there are a number of immediate steps to be taken with the aim of producing additional diagnostic tools and operational insight:

- a) With access to the PI historians direct values the analysis can be repeated with greater certainty in the outcome.
- b) Hypotheses can be strengthened or rejected for the operating regions in aggregate space, and better define their borders if they are confirmed.
- c) Furthermore, measures of composition and/or well status would be ideal to align and characterise the sensor data. Compositional data may help to explain the differences over time, and diagnostics may need to vary based on which wells are feeding the pumps.
- d) Additional data could help to test if excursions from presumed normal region do occur prior to failures in a statistically significant manner or not.
- e) Further to (a) and (b) software tools could be developed using existing technology to integrate with the data historian that would identify when excursions are occurring and offer predictive insights into pump failure probability.

Chapter 6:

Conclusions

Chapter 6. Conclusion

The Eng.D project was directed at addressing problems in the hydrocarbon-processing sector, this was undertaken through both the development and implementation of tools to address identified needs. At the start of the thesis a set of objectives for the research were established and now the approaches and solutions developed to address each of these objectives will be examined.

The first two objectives were to develop a methodology for rapid identification of crude oil composition both online and offline and then implement a tool to facilitate optimisation of crude blending performance utilising the information from the first objective.

These objectives 1 were met in case study 1 where the application of chemometric modelling software based on NIR spectra was applied to a major Asian refinery. This was an innovative approach as successful implementation of NIR in a refinery for gasoline blending was well understood (Balabin and Safieva, 2008; Balabin, Safieva and Lomakina, 2010) however crude compositional analysis is not covered in literature sources. This is because of the highly variable nature of crude oil and the difficulty this brings in developing an appropriate chemometric model.

The case study demonstrated that whole crude property measurements (i.e. API gravity and Sulphur) are not a conclusive method of characterising a crude type to give a refinery the real value of each crude delivery, they are also not sufficient to inform blend optimisation decisions. A crude oil family was examined and whole crude property measurements suggested one sample to be of higher value than the rest of the family.

However, implementation of PT5Technology and the chemometric modelling approach allowed the refiner to quickly and easily assess not only API gravity and Sulphur but also the distillation properties for this oil. Application of netback calculations to value this crude oil demonstrated that the refiner was losing >\$1/bbl. on each barrel refined given the deviation in quality.

Using the updated quality information the refinery was able to use the predicted TBP, API gravity, Sulphur, Pour Point and TAN to update the crude blend properties and perform more effective economic optimisation.

The next objective was to develop an approach to characterise the stability and compatibility of blended hydrocarbon streams

To meet this objective a new approach was developed to characterise the stability of blended hydrocarbon streams. Firstly previous work was critiqued, particularly the current ASTM methodologies (D7060, D7112 and D7157) and the work of Wiehe & Kennedy 1999a and Wiehe & Kennedy 1999b. This was deemed to be not fully appropriate to addressing the compatibility issues experienced in blended hydrocarbon streams.

The methodologies use pure materials (such as heptane and toluene) to assess blend stability and do not blend the oils, hence no account is taken for unexpected interactions between crude oils when blended. Another major drawback is there is no provision for time dependent blend stability, which is a well-known phenomenon when dealing with colloidal systems.

The methodology developed was patented and has been granted by the UKIPO. The novel methodology utilises crude oils in the blend to undertake stability assessments and is able to assess any time periods of interest.

The method was applied in two case studies. Firstly for blended Heavy Fuel Oil in a Refinery where observations of stability of HFO blends was undertaken using the proprietary stability methodology developed as part of the Eng.D project. Based on the set of samples studied it was concluded that a change in stability was observed in all blends made from blending 1% Sulphur HFO and 3% Sulphur HFO in the range 1.6% to 2.0% Sulphur.

The change in stability occurred after the time that the HFO was blended and it was shown that although the sample appeared stable initially, the instability worsened over time. This ability to characterise time dependent stability is a key feature of the innovative approach.

It was also suspected that a paraffinic HVN diluent would cause instability problems and indeed increasing the amount of HVN in the blend increased the tendency for instability. The 1.8% Sulphur Used HFO sample (returned by the customer's customer) was the only one exhibiting instability when blended with HVN after 72 hours. Instability with HVN was not observed with 1% Sulphur HFO, 1.8% Sulphur HFO or 3% Sulphur HFO.

Secondly blended marine fuels were assessed for stability which was detected using NIR and microscopy. Once characterised the sample was then additised to assess the effects of additive on sample stability. It was shown that at certain blend ratios the additive was effective and at others it was not. This was the first test of the methodology in blends containing additives.

The final objective was to implement a novel application of data analytics approaches to solve historical hydrocarbon processing issues

This objective was addressed by applying the PT5Technology big data analytics tool to an upstream client experiencing problems with two pumps on an offshore installation. This problem was historic and pump failures had been plaguing the installation for many years.

The Eng.D project was focussed on working as part of an engineering solutions team to identify the root cause of pump failure and thus develop a novel solution which could be implemented to monitor the issue and mitigate the problem to the greatest extent possible.

Through application of data analytics the problem was found to be caused by the ratio of gas:liquids in the stream to the pump, specifically gas slugs hitting the pump caused large axial vibration effects, which would cause cumulative damage to the pumps.

Thus through application of four case studies each of the objectives set out at the start of the thesis were addressed.

Chapter 7:

Future Work

Chapter 7. Future Work

All applications developed as part of the Eng.D project have been commercialised and projects are ongoing in all three areas discussed above. To give an example of an ongoing application of PT5Technology Case Study 5 discussed the application of PT5Technology in the Forties Pipeline System (FPS) for quality bank analysis.

A current application of PT5Technology is on the Forties Pipeline System (FPS) in the North Sea. A map of FPS is shown below. FPS consists of over seventy platforms and hundreds of individual wells with an API gravity range of $\sim 18 - 70$.

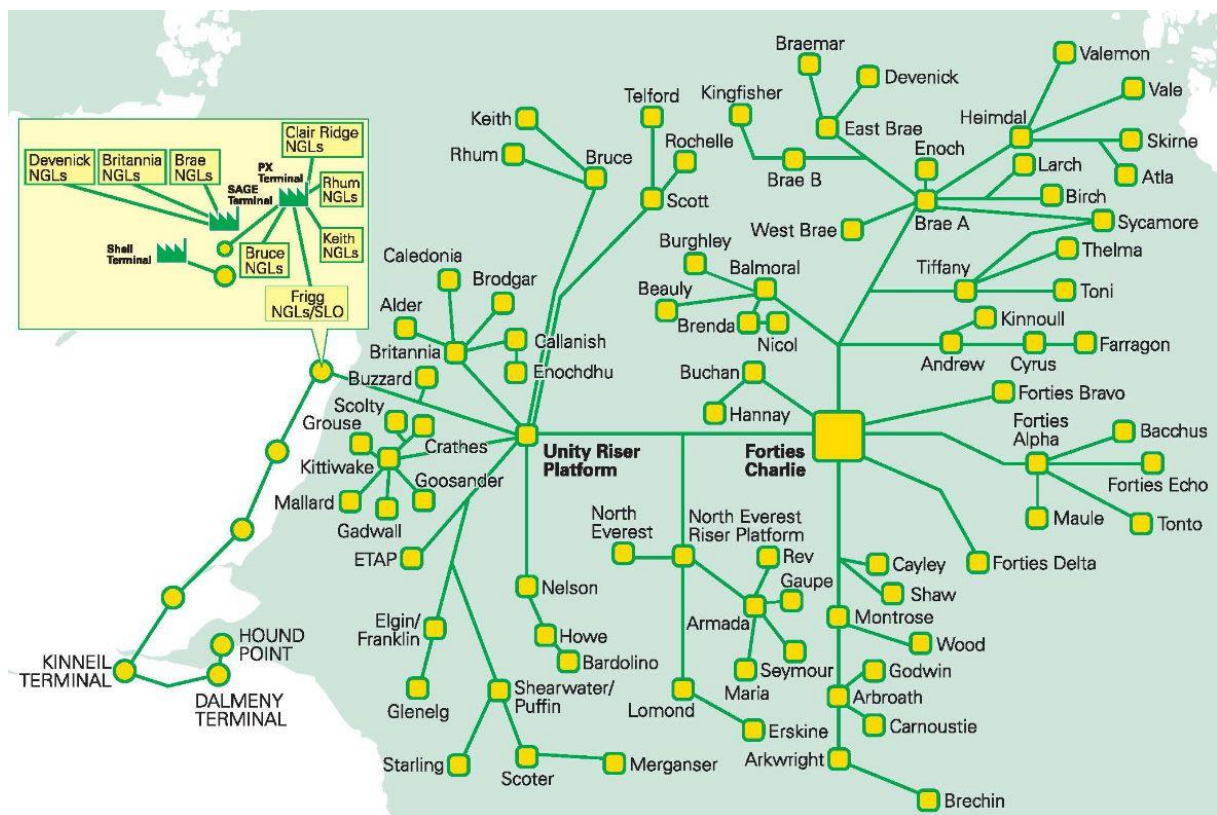


Figure 7-1: Forties Pipeline System (FPS) North Sea taken from Subsea (2017)

FPS is allocated based on the properties and the flow rate of the oil from each platform that each producer puts into the pipeline. Weekly samples are sent from offshore in pressurized piston cylinders and the samples are scanned by NIR at a pressure above the bubble point of the crudes and condensates to ensure no light ends are lost, thus making sure the sample is representative of the production of each platform. Using PT5Technology both the light ends (C1 – C7+) and the full properties (TBP, cut molecular weights and cut densities) are predicted on a weekly basis (Table 7-1) from the NIR scan to give the value of the crude oil from the platform.

Table 7-1: Showing properties measured for the FPS Application on Whole crude (Left) and Light Ends (Right)

Whole Crude Property (Full Analysis)	
Sulphur 350+	
Sulphur 550+	
Viscosity 350+	
Viscosity 550+	
TBP Cut Points (DegC) - Wt% and Vol%, Molecular Weight and SG also Measured for all cuts (NOTE: IBP = Initial Boiling Point)	IBP - 15
	15 - 45
	45 - 60
	60 - 75
	75 - 90
	90 - 105
	105 - 120
	120 - 135
	135 - 150
	150 - 165
	165 - 200
	200 - 250
	250 - 300
	300 - 350
	350 - 400
	400 - 450
	450 - 500
	500 - 550
	550+

Whole Crude Property (Light Ends Analysis)	
	GOR
	Oil Density
	Dry Density
Light Ends Components (Either Wt% or Vol%)	N2
	CO2
	C1
	C2
	C3
	IC4
	NC4
	IC5
	NC5
	C6
	C7+

Using PT5Technology quality tracking functionality, crudes can be quickly assessed and monitored for changing quality using NIR spectra and the PT5 aggregate plot (Figure 7-2). Each point on the plot represents the NIR spectra of an individual sample from a platform. On this plot there are several oil types (indicated by the boxes for crudes 1 – 6) and it can be seen that they are clustered by boxes. From a quality monitoring perspective it would be expected that the crudes always fall in their appointed boxes. If crude falls outside the box the quality has changed and additional analysis must be performed.

If crude 1 is taken as an example it can be seen that this is quite a large box with many samples. This is because this application uses clustering to simplify the analysis. The crude 1 box represents a cluster of fields that have similar properties and are therefore grouped into one

box. This is representative of how the clustering would take place for the Customer application. Other crudes (such as crudes 4 and 5) are relatively new crudes and as such have only a few samples currently in the model. However, as the application progresses these boxes will be built up as more samples are added to the model

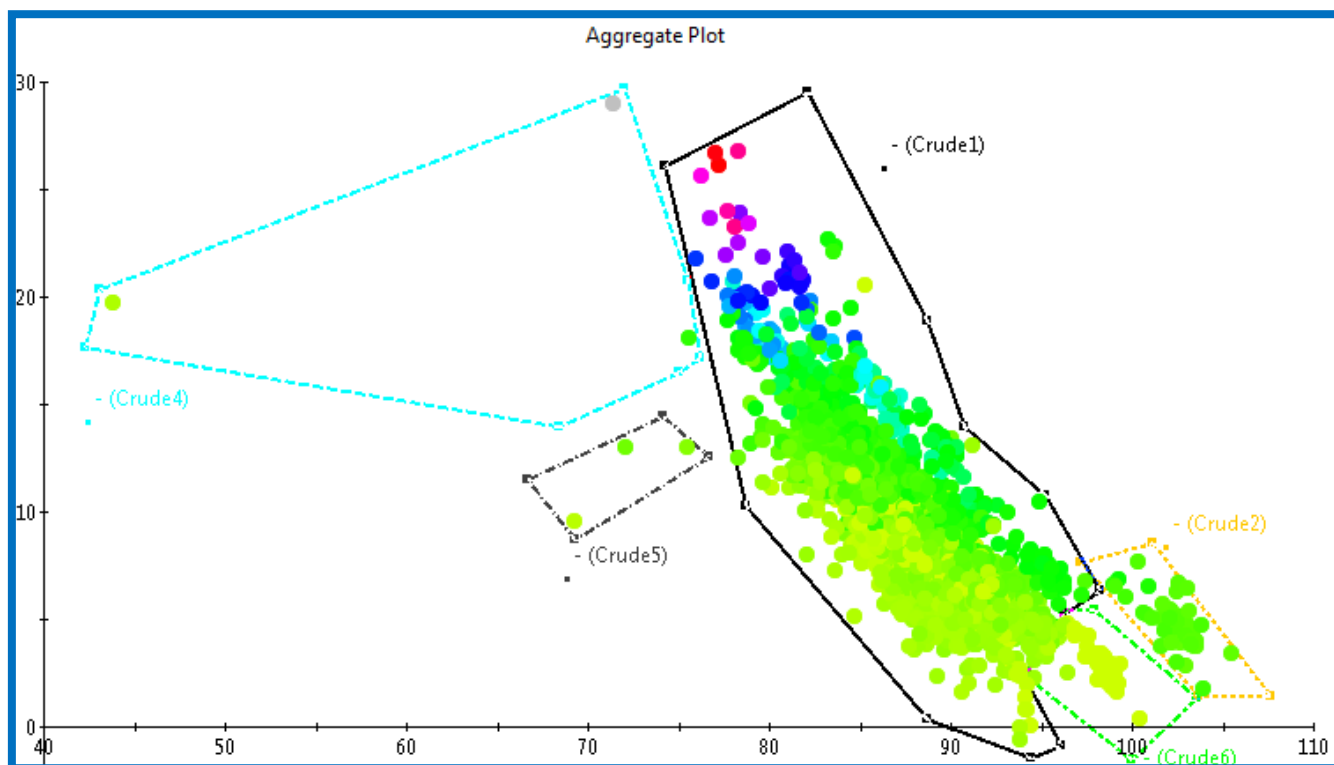


Figure 7-2: North Sea Fields Aggregate Plot

As well as the chemometrics and modelling, the patented approach to assessing stability has been applied with an upstream client bringing online a new well. The well has considerably different properties to the existing crude oil blend and thus the client has concerns about the compatibility of the oils in the process. This concern is further compounded by the fact that the oil is stored on the facility and discharged by tanker every few weeks.

The approach will be applied to assess the stability of the blends of wells at different configuration not only at time 0 but also after 28 days to mimic the time the blend will be stored at the facility. This represents an application where the ASTM methodology could not be applied because of the time dependent requirement.

References

References

- Acevedo, S., Zuloaga, C. and Rodri, P. (2008) 'Aggregation-Dissociation Studies of Asphaltene Solutions in Resins Performed Using the Combined Freeze Fracture-Transmission Electron Microscopy Technique', *Energy & Fuels*, 22(5), pp. 2332–2340.
- Alvarado, V. and Manrique, E. (2010) 'Enhanced oil recovery: An update review', *Energies*, 3(9), pp. 1529–1575. doi: 10.3390/en3091529.
- Ashoori, S. *et al.* (2006) 'Investigation of reversibility of asphaltene precipitation and deposition for an Iranian crude oil', *Iranian Journal of Chemical Engineering*, 25(3), pp. 41–47. Available at: http://www.sid.ir/en/VEWSSID/J_pdf/84320060307.pdf.
- Aske, N. *et al.* (2001) 'Determination of Saturate, Aromatic, Resin, and Asphaltenic (SARA) Components in Crude Oils by Means of Infrared and Near-Infrared Spectroscopy', *Energy & Fuels*, 15(5), pp. 1304–1312. doi: 10.1021/ef010088h.
- Aske, N. *et al.* (2002) 'Asphaltene Aggregation from Crude Oils and Model Systems Studied by High-Pressure NIR Spectroscopy', *Energy & Fuels*, 16(7), pp. 1287–1295.
- Aske, N. (2002a) *Characterisation of crude oil components, asphaltene aggregation and emulsion stability by means of near infrared spectroscopy and multivariate analysis*, *Chemical Engineering*. Thesis. Norwegian University of Science and Technology.
- Aske, N. (2002b) 'Characterisation of Crude Oil Components , Asphaltene Aggregation and Emulsion Stability by means of Near Infrared Spectroscopy and Multivariate Analysis by Narve Aske Department of Chemical Engineering', *Advances in Colloid and Interface Science*, (June), p. 3.
- ASTM (2013) 'D7060 - Standard Test Method for Determination of the Maximum Flocculation Ratio and Peptizing Power in Residual and Heavy Fuel Oils (Optical Detection Method)', pp. 1–12. doi: 10.1520/D7060-12.2.
- Aurdal, T. *et al.* (1998) 'Annual Report Saga Petroleum', *Statoil Research Cooperation on Asphaltenes*, p. 100.
- Balabin, R. M. and Safieva, R. Z. (2008) 'Gasoline Classification by Source and Type based on Near Infrared (NIR) Spectroscopy Data', *Fuel*, 87(7), pp. 1096–1101. doi: 10.1016/j.fuel.2007.07.018.
- Balabin, R. M., Safieva, R. Z. and Lomakina, E. I. (2007) 'Comparison of Linear and Nonlinear Calibration Models Based on Near Infrared (NIR) Spectroscopy Data for Gasoline Properties Prediction', *Chemometrics and Intelligent Laboratory Systems*, 88(2), pp. 183–188. doi: 10.1016/j.chemolab.2007.04.006.
- Balabin, R. M., Safieva, R. Z. and Lomakina, E. I. (2008) 'Wavelet Neural Network (WNN) Approach for Calibration Model Building Based on Gasoline Near Infrared (NIR) Spectra', *Chemometrics and Intelligent Laboratory Systems*, 93(1), pp. 58–62. doi: 10.1016/j.chemolab.2008.04.003.
- Balabin, R. M., Safieva, R. Z. and Lomakina, E. I. (2010) 'Gasoline classification using near infrared (NIR) spectroscopy data: Comparison of multivariate techniques', *Analytica Chimica Acta*. Elsevier B.V., 671(1–2), pp. 27–35. doi: 10.1016/j.aca.2010.05.013.
- Balabin, R. M., Safieva, R. Z. and Lomakina, E. I. (2012) 'Gasoline classification using near infrared (NIR) spectroscopic data: Comparison of multivariate techniques', *Analytica Chimica Acta*, 671, pp. 27–35.
- Bastien, P., Vinzi, V. E. and Tenenhaus, M. (2005) 'PLS Generalised Linear Regression', *Computational Statistics and Data Analysis*, 48, pp. 17–46.
- Berglund, A. and Wold, S. (1999) 'A Serial Extension of Multiblock PLS', *Chemometrics*, 13,

pp. 461–471.

Blanco, A. M. *et al.* (2005) ‘Operational Planing of Crude Oil Processing Terminals’, *European Symposium on Computer Aided Process Engineering*, 15(1).

Blanco, M. *et al.* (2000) ‘Determination of the Penetration Value of Bitumens by Near Infrared Spectroscopy’, *The Analyst*, 125(10), pp. 1823–1828. doi: 10.1039/b004121l.

Braun, R. L. and Burnham, I. K. (1993) *Chemical Model for Oil and Gas Generation from Type I and II Kerogen*. Report. Lawrence Livermore National Laboratory.

Buckley, J. S. *et al.* (1998) ‘Asphaltene Precipitation and Solvent Properties of Crude Oils’, *Petroleum Science and Technology*, 16(3–4), pp. 251–285. doi: 10.1080/10916469808949783.

Buenrostro-Gonzalez, E. *et al.* (2004) ‘Asphaltene Precipitation in Crude Oils: Theory and Experiments’, *AIChE Journal*, 50(10), pp. 2552–2570. doi: 10.1002/aic.10243.

Burg, P., Selves, J. L. and Colin, J. P. (1997) ‘Crude Oils : Modelling from Chromatographic Data- A New Tool for Classification’, *Fuel*, 76(1), pp. 85–91.

Cho, Y. *et al.* (2012) ‘Application of Saturates, Aromatics, Resins, and Asphaltenes Crude Oil Fractionation for Detailed Chemical Characterization of Heavy Crude Oils by Fourier Transform Ion Cyclotron Resonance Mass Spectrometry Equipped with Atmospheric Pressure Photoionizati’, *Energy & Fuels*, 26(5), pp. 2558–2565. doi: 10.1021/ef201312m.

Chung, H. and Ku, M.-S. (2000) ‘Comparison of Near-Infrared, Infrared, and Raman Spectroscopy for the Analysis of Heavy Petroleum Products’, *Applied Spectroscopy*, 54(2), pp. 239–245.

Chung, H., Ku, M.-S. and Lee, J.-S. (1999) ‘Comparison of Near-Infrared and Mid-Infrared Spectroscopy for the Determination of Distillation Property of Kerosene’, *Vibrational Spectroscopy*, 20(2), pp. 155–163.

Cui, H.-F. *et al.* (2012) ‘Automatic and Rapid Discrimination of Cotton Genotypes by Near Infrared Spectroscopy and Chemometrics’, *Journal of Analytical Methods in Chemistry*, p. 7. doi: 10.1155/2012/793468.

Deming, S. M. and Morgan, S. L. (1993) *Experimental Design: A Chemometric Approach*. 2nd edn. Elsevier.

Dinadayalene, T. C., Farag, A. M. and Fujita, N. (2012) ‘Correlation between SARA Fractions, Density and RI to Investigate the Stability of Asphaltene’, *Analytical Chemistry*.

Energia, G. (2010) *Refining Fundamentals*.

Fan, T., Wang, J. and Buckley, J. S. (2002) ‘Evaluating Crude Oils by SARA Analysis’, *Improved Oil Recovery Symposium*. Tulsa, Oklahoma: Society of Petroleum Engineers.

Felicio, C. C. *et al.* (2005) ‘Comparison of PLS algorithms in gasoline and gas oil parameter monitoring with MIR and NIR’, *Chemometrics and Intelligent Laboratory Systems*, 78(1), pp. 74–80. doi: 10.1016/j.chemolab.2004.12.009.

Flumignan, D. L. *et al.* (2012) ‘Multivariate Calibrations on ¹H NMR Profiles for Prediction of Physicochemical Parameters of Brazilian Commercial Gasoline’, *Fuel*. Elsevier Ltd, 99, pp. 180–187. doi: 10.1016/j.fuel.2012.04.037.

Gawrys, K. L. and Kilpatrick, P. K. (2004) ‘Asphaltene Aggregation: Techniques for Analysis’, *Instrumentation Science & Technology*, 32(3), pp. 247–253. doi: 10.1081/CI-120030536.

Gaydou, V., Kister, J. and Dupuy, N. (2011) ‘Evaluation of Multiblock NIR/MIR PLS Predictive Models to Detect Adulteration of Diesel/Biodiesel Blends by Vegetal Oil’, *Chemometrics and Intelligent Laboratory Systems*. Elsevier B.V., 106(2), pp. 190–197. doi: 10.1016/j.chemolab.2010.05.002.

- Gossen, P. D., MacGregor, J. F. and Pelton, R. H. (1993) 'Composition and Particle Diameter for Styrene/Methyl Methacrylate Copolymer Latex Using UV and NIR Spectroscopy', *Applied Spectroscopy*, 47(11), pp. 1852–1870.
- Grace, R. (2007) *Oil - An overview of the petroleum industry*. 6th edn, *Oil - An overview of the petroleum industry*. 6th edn. Edited by R. Grace. Houston: Gulf Publishing Company.
- Graham, B. F., May, E. F. and Trengove, R. D. (2008) 'Emulsion Inhibiting Components in Crude Oils', *Energy & Fuels*, 22(14), pp. 1093–1099. doi: 10.1021/ef700529m.
- Guthrie, V. B. (1960) *Petroleum products handbook*. Edited by V. B. Guthrie. McGraw Hill Book Company Inc.
- Hashmi, S. M. and Firoozabadi, A. (2012) 'Controlling Nonpolar Colloidal Asphaltene Aggregation by Electrostatic Repulsion', *Energy and Fuels*, 26(7), pp. 4438–4444. doi: 10.1021/ef3005702.
- Hidajat, K. and Chong, S. . (2000) 'Quality Characterisation of Crude Oils by Partial Least Square Calibration of NIR Spectral Profiles', *Near Infrared Spectroscopy*, 8(1), pp. 53–59.
- Hsu, C. S. and Robinson, P. (2006) 'Predictions from NIR Data', in *Practical Advances in Petroleum Processing*, pp. 114–115.
- Ibrahim, K. M. (2007) *The Petroleum Engineering Handbook: Sustainable Operation*. Houston: Gulf Publishing Company.
- Intertek (2016) *Intertek Website*.
- Islam, M. R. (2000) 'Emerging Technologies in Subsurface monitoring of Oil Reservoirs', *Canadian International Petroleum Conference*. Calgary.
- Islas-Flores, C. a., Buenrostro-Gonzalez, E. and Lira-Galeana, C. (2005) 'Comparisons Between Open Column Chromatography and HPLC SARA Fractionations in Petroleum', *Energy and Fuels*, 19(5), pp. 2080–2088. doi: 10.1021/ef050148+.
- Jechura, J. (2016) 'Hydroprocessing: Hydrotreating & Hydrocracking'. Colorado School of Mines, p. 5.
- Kardamakis, A. A. and Pasadakis, N. (2010) 'Autoregressive Modeling of Near-IR Spectra and MLR to Predict RON Values of Gasolines', *Fuel*. Elsevier Ltd, 89(1), pp. 158–161. doi: 10.1016/j.fuel.2009.08.029.
- Kelly, J. J. and Callis, J. B. (1990) 'Nondestructive Analytical Procedure for Simultaneous Estimation of the Major Classes of Hydrocarbon Constituents of Finished Gasolines', *American Chemical Society*, 62, pp. 1441–1451.
- Khvostichenko, D. S. and Andersen, S. I. (2010) 'Electrodeposition of Asphaltenes. 2. Effect of Resins and Additives [†]', *Energy & Fuels*, 24(4), pp. 2327–2336. doi: 10.1021/ef900970j.
- Koottungal, L. (2004) '2004 worldwide EOR survey', *Oil and Gas Journal*, 102(14), p. 53.
- Kraus, R. S. (1996) 'Oil and Natural Gas', in *Encyclopaedia of Occupational Health and Safety*. Available at: <http://www.ilocis.org/documents/chpt78e.htm>.
- Lundanes, E. and Greibrokk, T. (1994) 'Separation of Fuels, Heavy Fractions, and Crude Oils into Compound Classes: A Review', *High Resolution Chromatography*, 17, pp. 197–202.
- Marks, D. (2005) 'A Study of CO₂ Induced Asphaltene Precipitation Using NMR', p. 16.
- McLean, J. and Kilpatrick, P. (1997) 'Effects of Asphaltene Aggregation in Model Heptane-Toluene Mixtures on Stability of Water-in-Oil Emulsions', *Journal of colloid and interface science*, 196(1), pp. 23–34. doi: 10.1006/jcis.1997.4807.
- Mercier, S. M. *et al.* (2014) 'Multivariate PAT Solutions for Biopharmaceutical Cultivation: Current Progress and Limitations', *Trends in Biotechnology*, 32(6), pp. 329–336.

- Mouret, S. (2010) 'Optimal Scheduling of Refinery Crude-Oil Operations', *Chemical Engineering*, Doctor of, p. 189.
- Naskar, A. (2015) *Liquid Fuels and their Characteristics*.
- NG, O. (2012) 'The Spectrum of Light'. Edited by spectrum_NG. Oilsensor NG.
- Oh, K., Ring, T. a. and Deo, M. D. (2004) 'Asphaltene aggragation in organic solvents', *Colloid and Interfacial Science*, 271(1), pp. 212–219. doi: 10.1016/j.jcis.2003.09.054.
- Pasikatan, M. C. *et al.* (2003) 'Granulation Sensing of First Break Ground Wheat Using a Near Infrared Reflectance Spectrometer: Studies with Soft Red Winter Wheats', *Journal of the Science of Food and Agriculture*, 83, pp. 151–157.
- PetroleumOnline (2012) *Refining and Product Specification Overview*. Edited by P. Online.
- Poteau, S. *et al.* (2005) 'Influence of pH on Stability and Dynamic Properties of Asphaltenes and other Amphiphilic Molecules at the Oil-Water Interface', *Energy and Fuels*, 19(4), pp. 1337–1341. doi: 10.1021/ef0497560.
- Qiao, Y. and Kempen, T. A. T. G. van (2004) 'Technical note: Comparison of Raman, Mid and Near Infrared Spectroscopy for Predicting the Amino Acid Content in Animal Meals', *Journal of Animal Science*, 82(9), pp. 2596–2600.
- Richardson, M. (2009) 'Principal Component Analysis', p. 23. Available at: <http://www.dsc.ufcg.edu.br/~hmg/disciplinas/posgraduacao/rn-copin-2014.3/material/SignalProcPCA.pdf>.
- Rioloa, D. *et al.* (2017) 'Raman Spectroscopy as a PAT for Pharmaceutical Blending: Advantages and Disadvantages', *Pharmaceutical and Biomedical Analysis*.
- Rohrback, B. G. (1991) 'Computer-assisted rating of gasoline octane', *Trends in Analytical Chemiostry*, 10(9), pp. 269–271.
- Sheffield Hallam (2010) *Gas Chromatography*. Available at: <https://teaching.shu.ac.uk/hwb/chemistry/tutorials/chrom/gaschrm.htm> (Accessed: 8 November 2017).
- Speight, J. G. (2001) *Handbook of Petroleum Analysis*. Edited by J. D. Winefordner. John Wiley & Sons.
- Speight, J. G. (2016) 'Evaluation of Reservoir Fluids', in *Introduction to Enhanced Recovery Methods for Heavy Oil and Tar Sands*. 2nd edn. Cambridge: Elsevier, p. 237.
- Spiecker, P. M. *et al.* (2003) 'Effects of Petroleum Resins on Asphaltene Aggregation and Water-in-oil Emulsion Formation', *Colloids and Surfaces A: Physicochemical and Engineering Aspects*, 220(1–3), pp. 9–27. doi: 10.1016/S0927-7757(03)00079-7.
- Spiecker, P. M., Gawrys, K. L. and Kilpatrick, P. K. (2003) 'Aggregation and Solubility Behavior of Asphaltenes and their Subfractions', *Journal of Colloid and Interface Science*, 267(1), pp. 178–193. doi: 10.1016/S0021-9797(03)00641-6.
- Subsea (2017) *BP Negotiating Sale of Forties Pipeline to Ineos*, *Subsea World News*. Available at: <http://subseaworldnews.com/2017/03/17/bp-negotiating-sale-of-forties-pipeline-to-ineos/> (Accessed: 30 October 2017).
- Tharnivasan, A. K. (2012) *Asphaltene Precipitation from Crude Oil Blends, Conventional Oils, and Oils with Emulsified Water*, *Chemical and Petroleum Engineering*. Thesis. Univeristy of Calgary.
- Wiehe, I. a. and Kennedy, R. J. (2000a) 'Application of the Oil Compatibility Model to Refinery Streams', *Energy and Fuels*, 14(1), pp. 60–63. doi: 10.1021/ef9901342.
- Wiehe, I. a. and Kennedy, R. J. (2000b) 'Oil Compatibility Model and Crude Oil

Incompatibility', *Energy and Fuels*, 14(1), pp. 56–59. doi: 10.1021/ef990133+.

Wiehe, I. A. and Kennedy, R. J. (1999) 'Process for Blending Petroleum Oils to Avoid Being Nearly Incompatible', *US Patent* 5,997,723. Available at: <http://www.google.com/patents/US5997723>.

Wiehe, I. A. and Kennedy, R. J. (1999) 'Process for Blending Potentially Incompatible Petroleum Oils', *US Patent* 5,871,634. Available at: <http://www.google.com/patents/US5871634>.

Wiehe, I. A., Kennedy, R. J. and Dickakian, G. (2001) 'Fouling of Nearly Incompatible Oils', *Energy & Fuels*, 15(5), pp. 1057–1058. doi: 10.1021/ef010063i.

Wood-Mackenzie (2012a) *Refinery Evaluation Model*.

Wood-Mackenzie (2012b) 'The Outlook for Europe's Refining Industry - a changing landscape', (April).

Appendix A

Appendix A - Additional Heavy Fuel Oil Assessment Results

7.1 1% Sulphur HFO

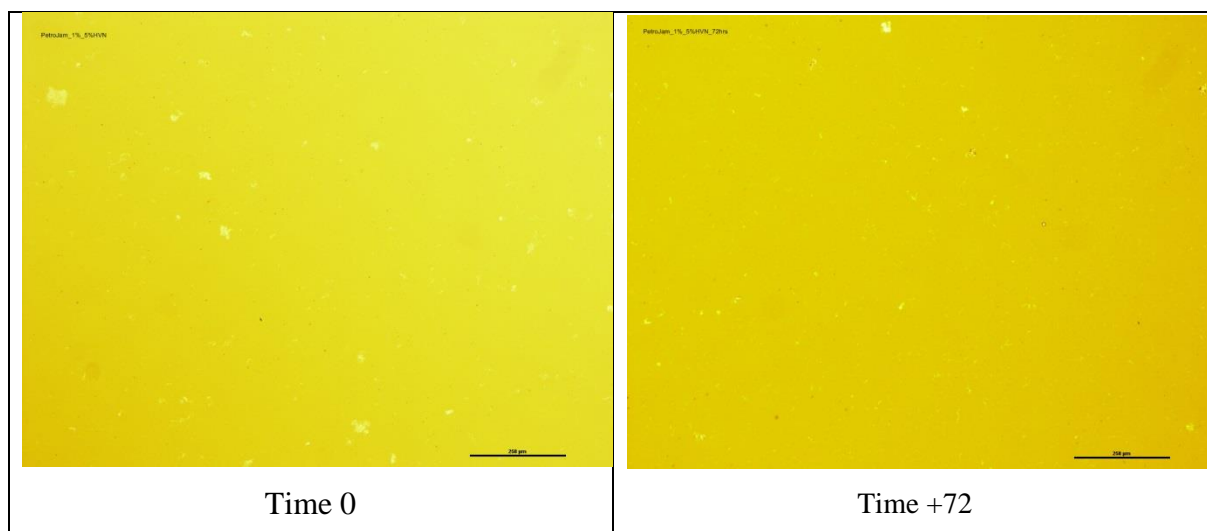


Figure A-1: 1% Sulphur HFO - 5% HVN

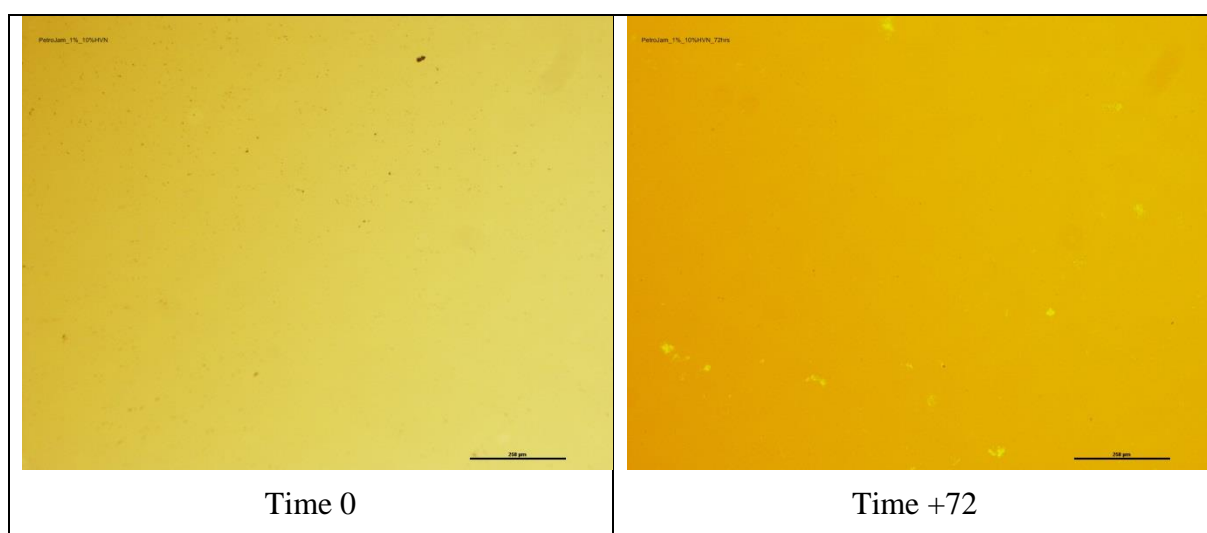


Figure A-2: 1% Sulphur HFO - 10% HVN



Figure A-3: 1% Sulphur HFO - 50% HVN

It can be seen that no bulk organic deposition observed with HVN even at 50% HVN after 72 hours.

7.2 1.8% Sulphur HFO

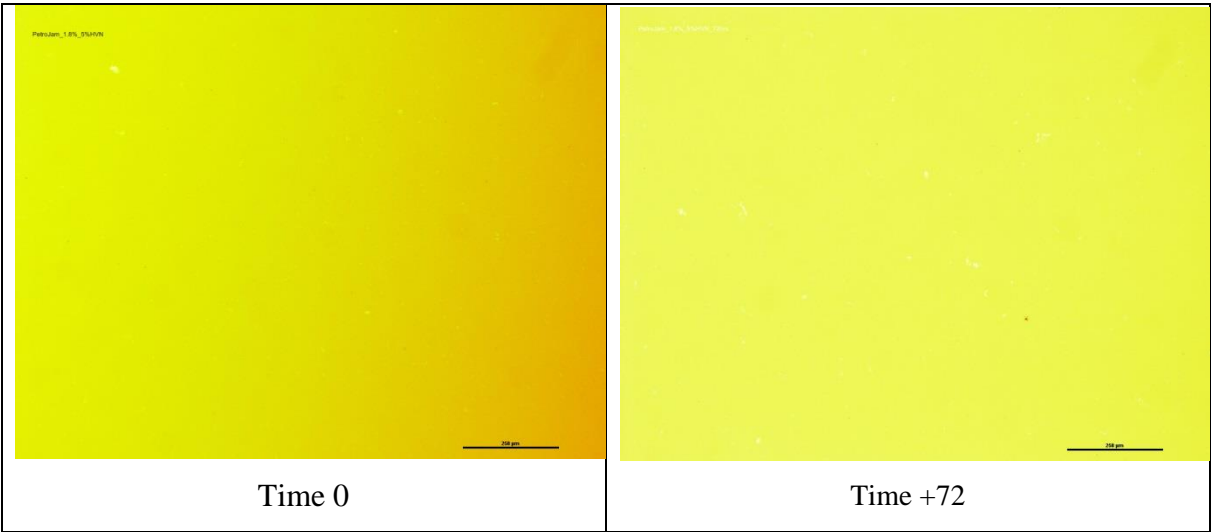


Figure A-4: 1.8% Sulphur HFO - 5% HVN

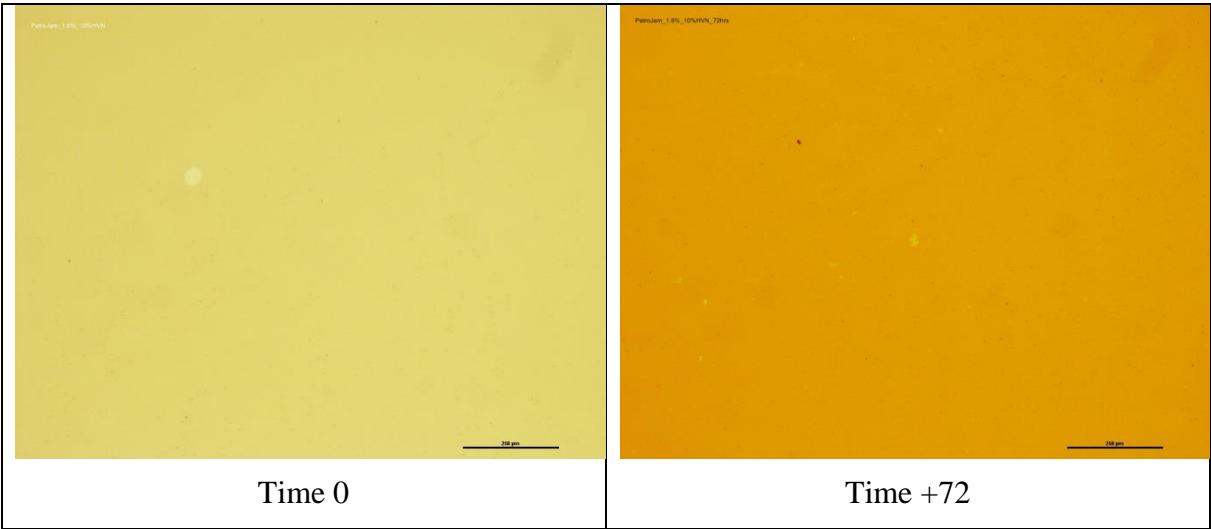


Figure A-5: 1.8% Sulphur HFO - 10% HVN

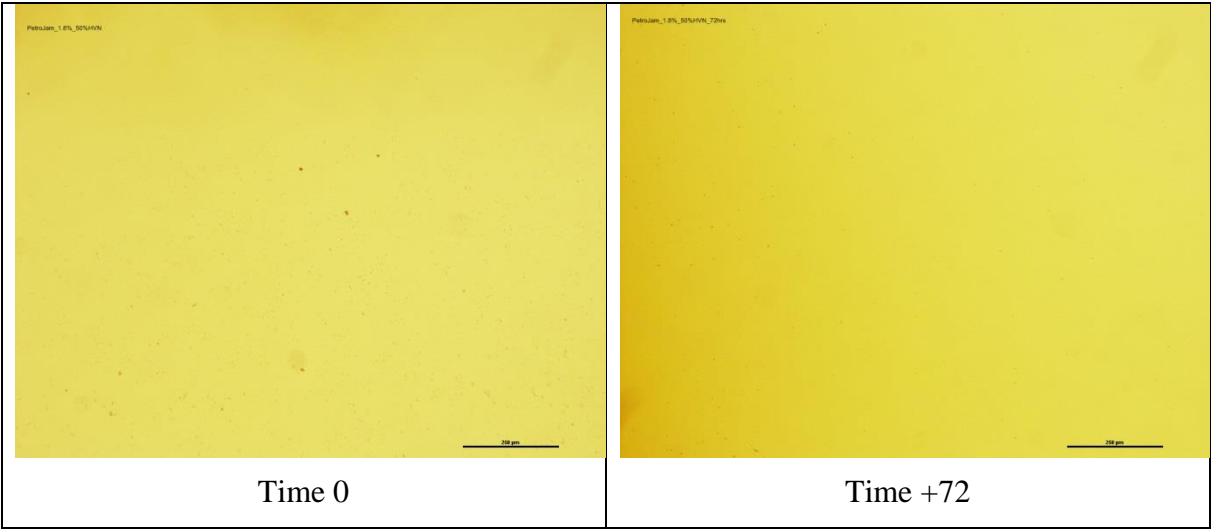


Figure A-6: 1.8% Sulphur HFO - 50% HVN

Once again no bulk organic deposition observed with HVN even at 50% HVN after 72 hours.

7.3 1.8% Used Sulphur HFO

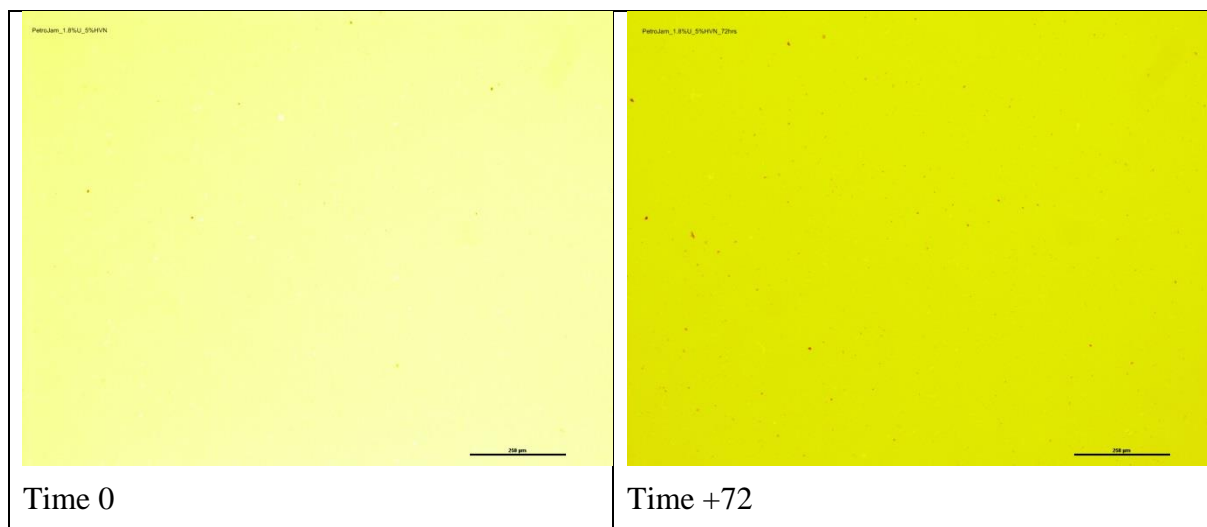


Figure A-7: 1.8% Used Sulphur HFO - 5% HVN

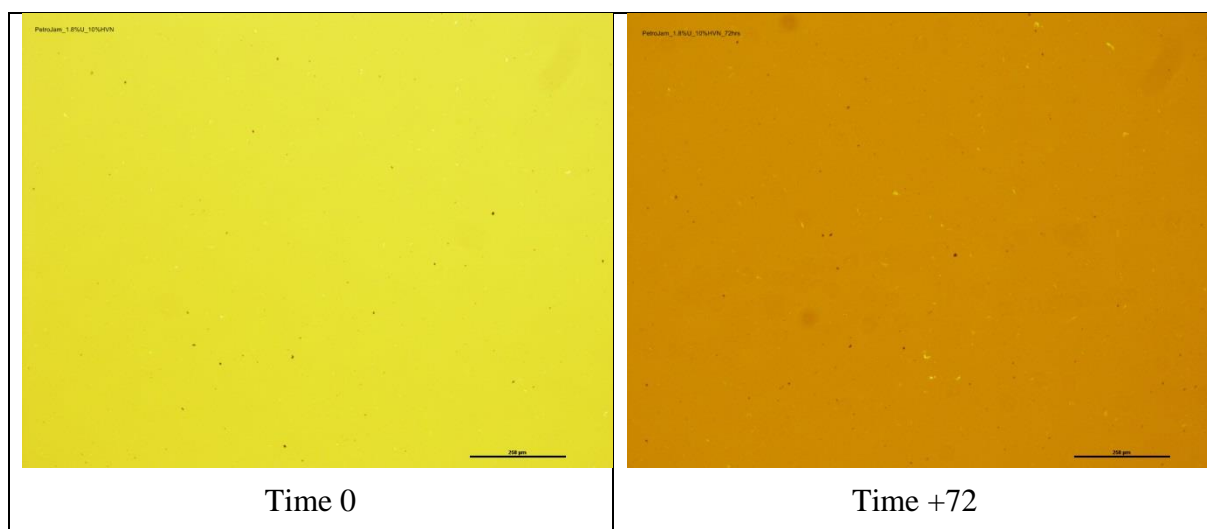


Figure A-8: 1.8% Used Sulphur HFO - 10% HVN (left) and (right)

7.4 3% Sulphur HFO

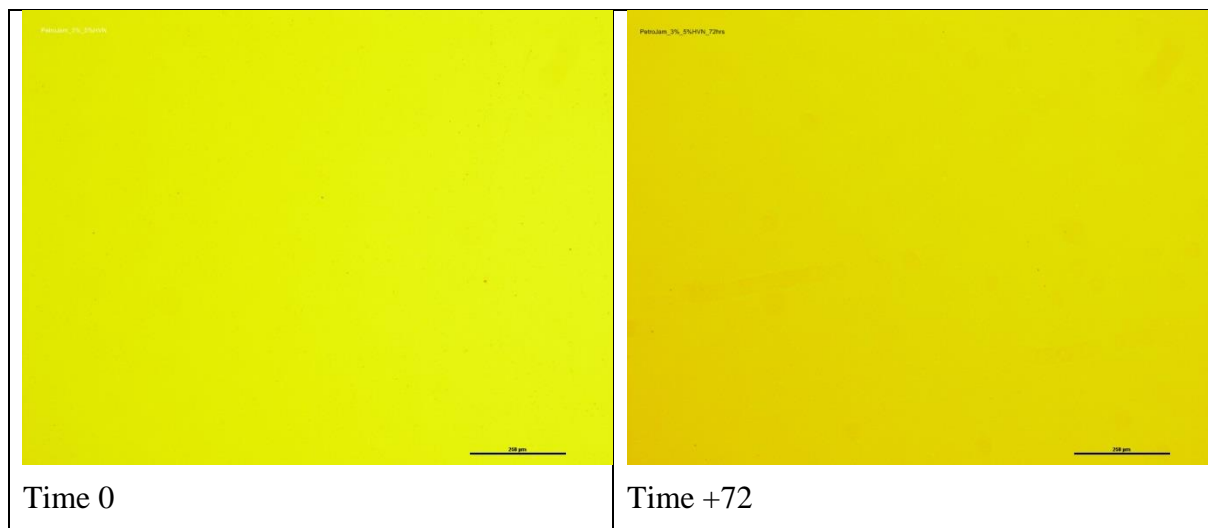


Figure A-9: 3% Sulphur HFO - 5% HVN

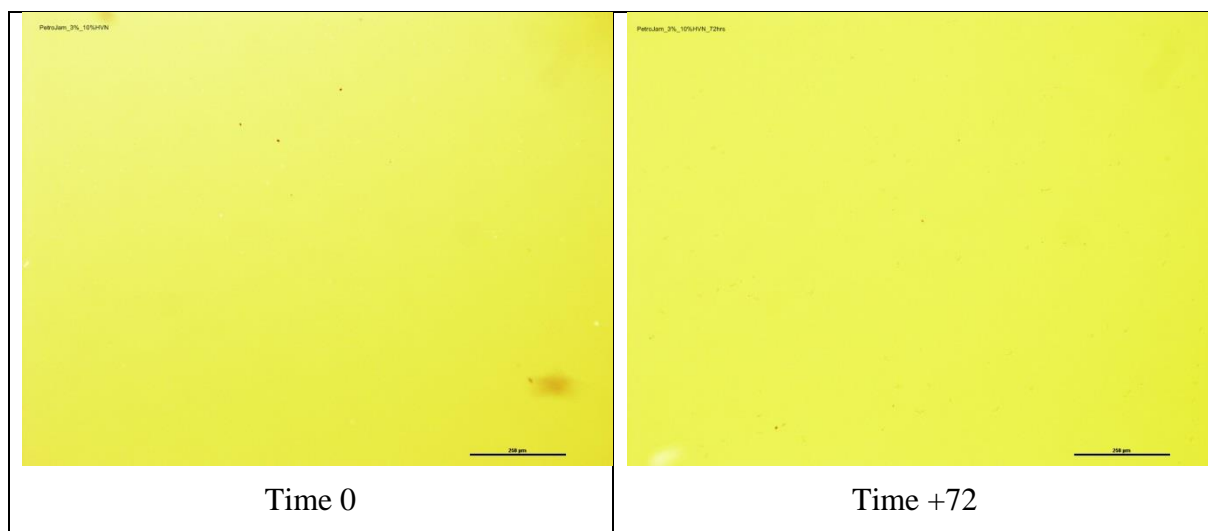


Figure A-10: 3% Sulphur HFO - 10% HVN

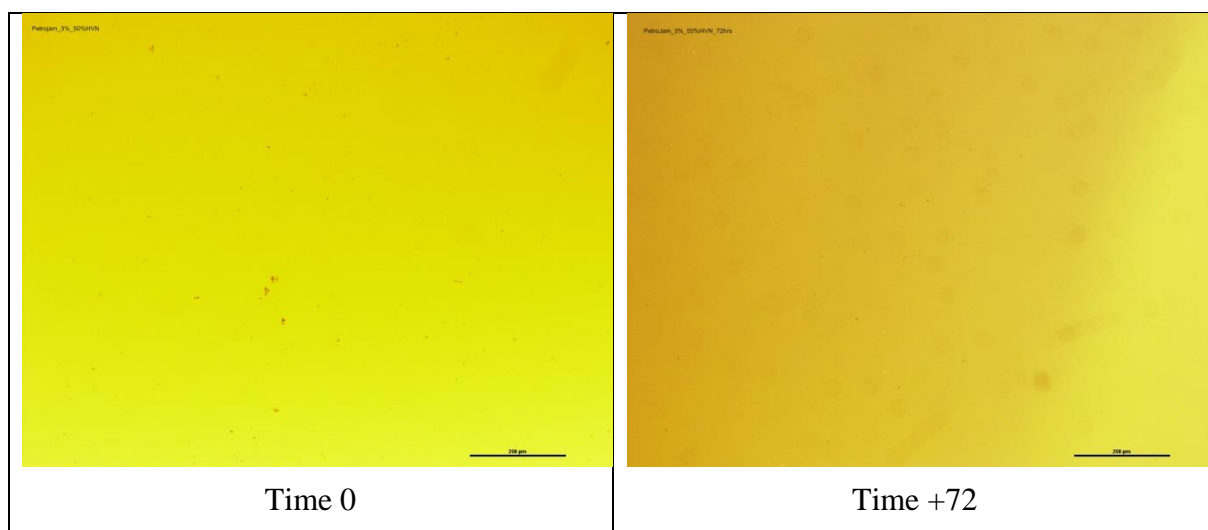


Figure A-11: 3% Sulphur HFO - 50% HVN

Appendix B

Appendix B – Additional Marine Fuel Blending Results

7.5 Blend 3 (DL242837/DL243017)

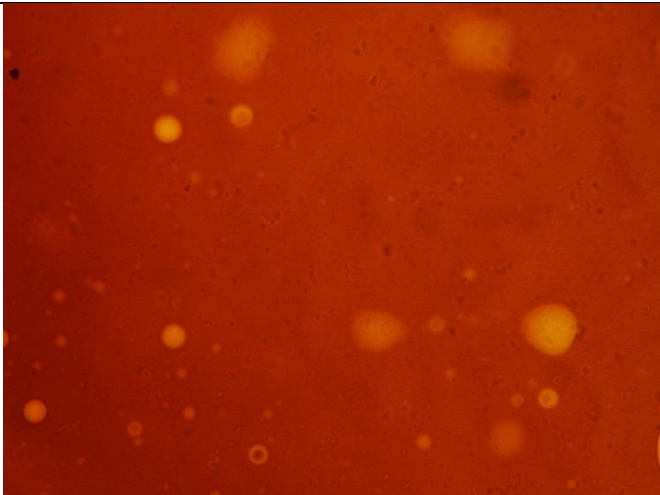
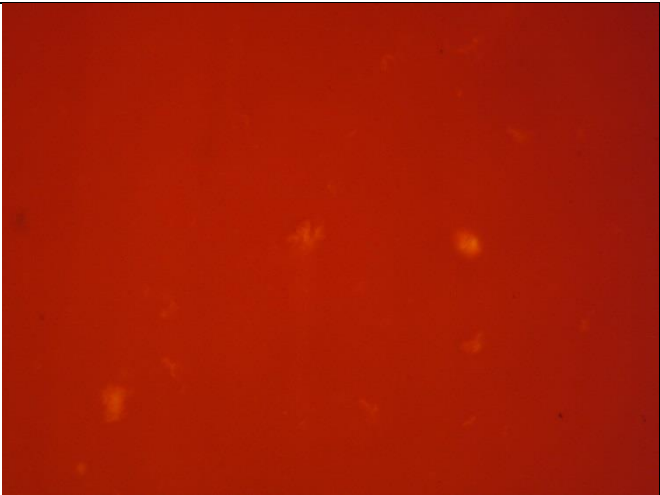
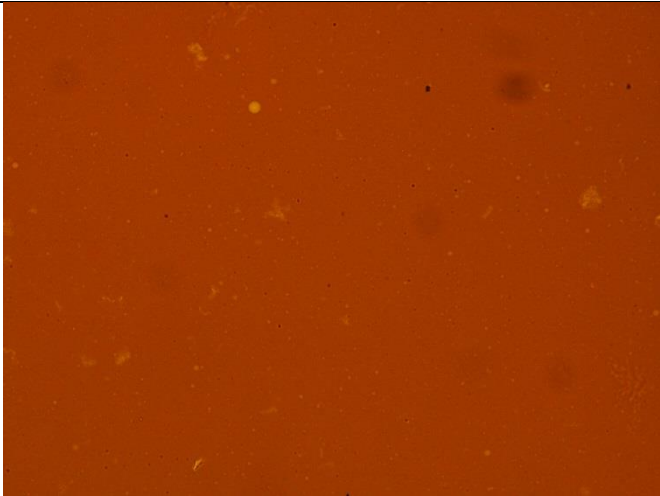

	
Blend 3b (80% HFO/ 20% MDO) With additive	Blend 3b (80% HFO/20% MDO) Without additive
	
Blend 3c (60% HFO/40% MDO) With additive	Blend 3c (60% HFO/40% MDO) Without additive

Figure B-1: Marine Fuel Blends

Appendix C

Appendix C - Algorithms

7.6 Principal Components Analysis

0.	Initialise t_a to some column vector of X_{a-1} , e.g. to the vector corresponding to the variable with the largest variance.	
1.	Estimate the loading vector p_a by regressing the columns of X_{a-1} on the score vector t_a :	$p_a^T = \frac{t_a^T \cdot X_{a-1}}{t_a^T \cdot t_a}$
2.	Scale the loading vector to unit norm	$p_a = \frac{p_a}{\ p_a\ }$
3.	Estimate the score vector t_a by regressing the columns of X_{a-1} on the loading vector p_a :	$t_a = \frac{X_a \cdot p_a}{p_a^T \cdot p_a}$
4.	Check convergence on t_a , if the difference with respect to the previous iteration is larger than a predefined tolerance limit go to step 1 else go to step 5.	
5.	Deflate data matrix X_{a-1} .	$X_a = X_{a-1} - t_a \cdot p_a^T$

7.7 Principal Components Analysis

0	mean centre and scale X and Y	
1	set the output scores u equal to a column of Y	
2	regress columns of X on u	$w^T = \frac{u^T \cdot X}{u^T \cdot u}$
3	normalise w to unit length	$w = \frac{w}{\ w\ }$
4	calculate the input scores	$t = \frac{X \cdot w}{w^T \cdot w}$
5	regress columns of Y on t	$q^T = \frac{t^T \cdot Y}{t^T \cdot t}$
6	normalise q to unit length	$q = \frac{q}{\ q\ }$
7	calculate new output scores	$u = \frac{Y \cdot q}{q^T \cdot q}$
8	check convergence on u : if YES goto 9 ELSE goto 2	
9	calculate the X loadings	$p^T = \frac{t^T \cdot X}{t^T \cdot t}$
10	regress u on t	$b = \frac{t^T \cdot u}{t^T \cdot t}$
11	calculate input residual matrix	$E = X - t \cdot p^T$
12	calculate output residual matrix	$F = Y - b \cdot t \cdot q^T$
13	if additional PLS dimension are necessary then replace X and Y by E and F and repeat steps 1 to 13.	